



UNIVERSIDAD NACIONAL DE COLOMBIA

# **Comparative evaluation of two non-conventional distillation technologies for separation of ethanol water mixtures by extractive distillation**

**Hernán Darío Muñoz Gil**

Universidad Nacional de Colombia  
Facultad de Ingeniería, Departamento de Ingeniería Química  
Bogotá, Colombia  
2018



# **Comparative evaluation of two non-conventional distillation technologies for separation of ethanol water mixtures by extractive distillation**

## ***Evaluación comparativa de dos tecnologías no convencionales para la separación de mezclas Etanol-Agua por destilación extractiva***

**Hernán Darío Muñoz Gil**

Tesis presentada como requisito parcial para optar al título de:  
**Magister en Ingeniería - Ingeniería Química**

Director:

Doctor, Magíster e Ingeniero Químico Iván Darío Gil Chaves

Línea de Investigación:

Diseño de Procesos

Grupo de Investigación:

Grupo de Investigación en Procesos Químicos y Bioquímicos

Universidad Nacional de Colombia

Facultad de Ingeniería, Departamento de Ingeniería Química

Bogotá, Colombia

2018



*A tí, mamá*



## Acknowledgement

This document thesis could not be possible without the continuous contribution of María Fernanda Gutiérrez Sánchez and César Augusto Sánchez. They have given to me generous hours of academic and non-academic talks that were concluded in the most interesting topics compiled in this document. Maria Fernanda has guide me with the used computational tools and Cesar has introduce me to the topology of distillation.

I want to thank to my director, the professor Iván Darío Gil Chaves, for his constant support and patience from the beginning of this work. His experience in the topic of extractive distillation has been a great contribution to the achievement of this thesis. I also want thank to the professor Carlos Arturo Martinez and for giving me the opportunity to participate in the project “Non-conventional column for the improvement of energy efficiency in distillation processes” financed by COLCIENCIAS. Thanks to Diego Mendoza for his contributions to my study of the partial reversible extractive distillation column.

Eternal thanks to my *Alma Mater*, Universidad Nacional de Colombia. It has opened its doors to me and for many good people I have shared with.

I do not find enough words to thank to my mother for been there for me during all these years. She and my brother Juan David are the new day in each day of my life.





## Abstract

In this document, extractive distillation for the separation of Ethanol-Water-ethylene glycol is studied from the conceptual point of view. A methodology for the design of conventional extractive sequences is detailed based on non-linear analysis and the state of the art of extractive distillation. The used methodology can be systematically applied to the design of alternative homogeneous minimum boiling point azeotrope systems. A graphical analysis of extractive distillation sequences is presented by means of the solution of the pinch equations. Obtained pinch branches and column profile maps are analyzed to develop a conceptual based design of an Extractive Dividing Wall Column. This analysis led to reduce the computational effort of designs based on simulation. In order to improve the efficiency of the separation, the obtained designs are studied as a partially diabatic column or a column with Sequential Heat Exchangers (SHE). Finally, an approximation to the application of the results in a pilot scale is made.

**Keywords:** Extractive distillation, Extractive Dividing Wall Columns E-DWC, Bioethanol dehydration, diabatic column, internal Sequential Heat Exchanger SHE.



# Contents

	Pág.
<b>Abstract.....</b>	<b>IX</b>
<b>Contents.....</b>	<b>XI</b>
<b>List of figures.....</b>	<b>XV</b>
<b>List of tables .....</b>	<b>XXI</b>
<b>Introduction .....</b>	<b>1</b>
<b>1. Bioethanol Context .....</b>	<b>5</b>
1.1 World energy consumption .....	6
1.2 World energy policies.....	10
1.3 Renewable Energies.....	12
1.4 Biofuels.....	14
1.5 Bioethanol.....	15
1.6 Bioethanol Market.....	16
1.7 Latin America Context.....	21
1.8 Colombian Context .....	22
1.8.1 Bioethanol in Colombia .....	27
1.8.2 Legal Framework .....	30
1.8.3 Installed Production capacity.....	30
1.9 Bioethanol Production Process .....	32
1.9.1 Sugar production.....	33
1.9.2 Pretreatment of molasses .....	34
1.9.3 Fermentation.....	34
1.9.4 Ethanol recovery .....	35
1.10 Dehydration technologies .....	35
1.10.1 Pressure swing distillation .....	36
1.10.2 Azeotropic distillation.....	37
1.10.3 Extractive distillation.....	38
1.10.4 Adsorption.....	39
1.10.5 Pervaporation.....	40
1.10.6 Comparison of dehydration technologies.....	41
1.11 Conclusions .....	45
<b>2. Conceptual design and tools for extractive distillation design .....</b>	<b>47</b>
2.1 Process Design.....	47
2.2 Conceptual Design .....	48

2.2.1	Process synthesis.....	49
2.2.1.1	Separation process synthesis .....	50
2.2.2	Process analysis.....	51
2.3	Distillation based separation process synthesis.....	52
2.3.1	Ideal case .....	52
2.3.1.1	Solution to the synthesis problem considering energy integration. ....	53
2.3.2	Non-ideal case.....	54
2.4	Azeotropy.....	55
2.5	Thermodynamics in distillation processes.....	57
2.5.1	NRTL activity coefficient model.....	58
2.5.2	Verification of pure component parameters.....	61
2.5.3	Verification of the binary $gE$ model parameters .....	63
2.5.4	Verification of ternary interactions.....	71
2.6	Residue curves.....	71
2.6.1	The equation of simple distillation .....	72
2.6.2	Residue curves equation .....	73
2.6.3	Residue curves for Ethanol-Water-Ethylene glycol system .....	74
2.7	Column profile maps of extractive distillation .....	76
2.8	Conclusions.....	84
<b>3.</b>	<b>Extractive distillation conceptual design.....</b>	<b>85</b>
3.1	Extractive distillation theory .....	87
3.2	Entrainer selection.....	88
3.2.1	Qualitative methods for entrainer selection .....	88
3.2.2	Evaluation of predefined compounds.....	90
3.2.3	Detailed vapor liquid measurements.....	91
3.2.4	Separation simulation .....	92
3.3	Extractive distillation design.....	93
3.3.1	Specifications .....	93
3.3.2	Feasibility.....	99
3.3.3	Reflux ratio and solvent to feed ratio.....	102
3.3.3.1	Bifurcations branches .....	102
3.3.3.2	Minimum entrainer to feed flow ratio .....	109
3.3.3.3	Minimum reflux ratio.....	112
3.3.4	Rigorous simulation .....	116
3.4	Conclusions.....	120
<b>4.</b>	<b>Non-conventional extractive distillation technologies.....</b>	<b>123</b>
4.1	Direct Thermal Integration: Extractive Dividing Wall Column E-DWC .....	124
4.1.1	The dividing wall distillation concept .....	125
4.1.2	Dividing Wall Column DWC .....	130
4.1.2.1	DWC configurations.....	131
4.1.2.2	DWC design .....	133
4.1.2.3	DWC modeling, simulation and optimization .....	134
4.1.3	Conventional extractive distillation sequence to E-DWC. ....	134
4.1.4	E-DWC modeling .....	135
4.1.5	E-DWC conceptual study.....	136
4.2	Indirect Thermal Integration: Sequential Heat Exchangers .....	143
4.2.1	Minimum and real separation work in distillation .....	145
4.2.2	Distillation column entropy mapping.....	146
4.2.3	Distillation column targets .....	148

4.2.4	Column Composite curves .....	151
4.2.5	The ideal distillation column model.....	152
4.2.6	Partially reversible extractive distillation column .....	154
4.2.7	Extractive distillation column with sequential heat exchangers (SHE).....	157
4.2.8	SHE simulation study .....	159
4.3	Conclusions .....	161
<b>5.</b>	<b>Pilot plant non-conventional extractive distillation column.....</b>	<b>163</b>
5.1	Plant location .....	163
5.2	Basis of the design .....	164
5.2.1	Aim of the operation .....	164
5.3	Process variables .....	165
5.3.1	Pressure.....	165
5.3.2	Entrainer .....	166
5.3.3	Heating utility .....	166
5.3.4	Temperature .....	167
5.3.4.1	Feed preheating.....	167
5.3.4.2	Solvent preheating .....	167
5.3.4.3	Reflux ratio.....	167
5.3.4.4	Distillate and bottoms flow.....	168
5.4	Process flow diagram and description.....	168
5.5	Equipment .....	170
5.5.1	Storage tanks.....	170
5.5.2	Preheaters .....	171
5.5.3	Reboiler.....	172
5.5.4	Condenser .....	172
5.5.5	Coolers .....	173
5.5.6	Pumps.....	173
5.5.7	Control valves .....	175
5.5.8	Flow transmitter.....	176
5.6	SHE Column.....	177
5.6.1	Section of heat exchange with cooling service .....	178
5.6.1.1	Top column section .....	178
5.6.1.2	Section of cooling heat exchange stages .....	178
5.6.1.3	Solvent feed stage .....	179
5.6.1.4	Liquid distributor (trays to packing).....	179
5.6.2	Section of glass (packing) .....	180
5.6.3	Section of feed stage.....	180
5.6.4	Section of stainless steel (packing) .....	181
5.6.5	Section of heat exchange with heating service.....	181
5.6.5.1	Liquid distributor (packing to trays).....	181
5.6.5.2	Section with heating heat exchange stages.....	182
5.6.5.3	Bottom column section .....	182
5.6.6	Column support.....	182
5.7	Auxiliary services .....	183
5.7.1	Cooling water .....	183
5.7.2	Steam .....	184
5.7.3	Thermal oil .....	186
5.8	Characteristics of the valves and valve diagram .....	187
5.9	Checking prior to the operation .....	188
5.9.1	Steps of the preliminary checking.....	188

5.10	Detailed preliminary checking.....	189
5.10.1	Preparation of the materials.....	189
5.10.2	Checking of pumps and electrical equipment (Gil, 2006) .....	190
5.10.2.1	Pumps prior to the operation.....	190
5.10.2.2	Pumps during the operation.....	190
5.10.3	Checking of the pipeline loop.....	191
5.10.3.1	Feed pipeline loop.....	191
5.10.3.2	Top pipeline loop.....	192
5.10.3.3	Bottom pipeline loop.....	193
5.10.4	Checking the measurement instruments.....	194
5.11	Conclusions.....	194
<b>6.</b>	<b>Conclusions.....</b>	<b>195</b>
	<b>References.....</b>	<b>199</b>
	<b>Appendix A. Manual of operation of a distillation column with internal Sequential Heat Exchanger (SEH).....</b>	<b>209</b>

## List of figures

<b>Figure 1-1:</b> History and projections of world energy consumption by regions 1990-2040. Adapted from (EIA, 2016a).....	7
<b>Figure 1-2:</b> History and projections of world population projections to 2040. Adapted from (U.S. Census Bureau, 2016).....	8
<b>Figure 1-3:</b> World total gross domestic product (GDP) 1990-2040. adapted from (EIA, 2016a).....	8
<b>Figure 1-4:</b> History and projection of world energy production by end-use sector. Adapted from (EIA, 2016a).....	9
<b>Figure 1-5:</b> History and projection work energy consumption by source. Adapted from (EIA, 2016a).....	10
<b>Figure 1-6:</b> Contribution of renewables to total final energy consumption. From (REN21, 2016).....	12
<b>Figure 1-7:</b> Jobs in renewable energy. From (REN21, 2016). Bioenergy includes biomass, biofuels and biogas. ....	13
<b>Figure 1-8:</b> Contribution of bioenergy to total final energy consumption. From: (REN21, 2016).....	14
<b>Figure 1-9:</b> Biofuels share. From (REN21, 2016). HVO: Hydrogenated Vegetable Oil... ..	15
<b>Figure 1-10:</b> World transport energy consumption by mode. LDV = light duty vehicles. From (WEC, 2011a). ....	17
<b>Figure 1-11:</b> World transport energy consumption by energy source. From (WEC, 2011a). ....	17
<b>Figure 1-12:</b> Global ethanol production in million gallons (RFA, 2016).....	18
<b>Figure 1-13:</b> Ethanol production by country 2009-2015 (IRENA, 2016).....	18
<b>Figure 1-14:</b> Primary energy production in Colombia in 2015, total = 5,96 EJ (UPME, 2016).....	22
<b>Figure 1-15:</b> Final energy consumption in Colombia by source, 2015 (UPME, 2016).....	23
<b>Figure 1-16:</b> Final energy consumption by sector in Colombia in 2015, total = 1,2 EJ (UPME, 2016).....	23
<b>Figure 1-17:</b> Energy consumption in transport by energy mode in Colombia. Total= 0,495 EJ in 2015 (UPME, 2016).....	24
<b>Figure 1-18:</b> Historical gasoline consumption in Colombia (UPME, 2016). ....	24
<b>Figure 1-19:</b> Gasoline trade balance in Colombia (UPME, 2016).....	25
<b>Figure 1-20:</b> Vehicles distribution in Colombia (MINTRANSPORTE, 2015). ....	26
<b>Figure 1-21:</b> Projections of gasoline consumption in Colombia (UPME, 2015b).....	26

<b>Figure 1-22:</b> Historical GHG emission in Colombia due to road transport (IDEAM, 2015). .....	28
<b>Figure 1-23:</b> Reserves of oil in Colombia vs demand, (UPME, 2015a). .....	29
<b>Figure 1-24:</b> Bioethanol balance in Colombia (ASOCAÑA, 2016a).....	32
<b>Figure 1-25:</b> Price of bioethanol in Colombia in 2015-2016 period (ASOCAÑA, 2016a). 32	
<b>Figure 1-26:</b> Stages in a non-autonomous bioethanol production from sugar cane. ....	33
<b>Figure 1-27:</b> Process for sugar production from sugar cane. 1-mill, 2-clarifier, 3- multiple-effect evaporators, 4- vacuum pan, 5- centrifuge and 6- rotatory drum. ....	33
<b>Figure 1-28:</b> Concentration and rectification of bioethanol in culture broths. 1- preheater, 2- concentration column, 3- rectification column, 4- gases washer.....	35
<b>Figure 1-29:</b> Configuration for pressure swing distillation. ....	36
<b>Figure 1-30:</b> Effect of the change of pressure in the azeotrope composition. Data obtained from Aspen plus vapor equilibria simulation.....	37
<b>Figure 1-31:</b> Pseudo diagram vapor liquid equilibrium for extractive distillation with ethylene glycol as solvent. ....	38
<b>Figure 1-32:</b> Extractive distillation scheme for bioethanol dehydration. ....	39
<b>Figure 1-33:</b> Left: Pervaporation Pseudo equilibrium curve of PVA membranes and Vapor liquid equilibrium for ethanol water system, from (Sander & Soukup, 1988). Right: pervaporation mechanism $P1 > P2$ . ....	41
<b>Figure 1-34:</b> Analyze search results in Scopus for ethanol dehydration. ....	43
<b>Figure 1-35:</b> Analyze search results in Scopus for ethanol dehydration by technology... 43	
<b>Figure 1-36:</b> Ten countries with most published documents in Scopus with “extractive distillation” and “ethanol dehydration” as search parameters. 1980 to 2016. ....	44
<b>Figure 1-37:</b> Ten countries with most published documents in Scopus with “adsorption” and “ethanol dehydration” as search parameters. 1980 to 2016.....	44
<b>Figure 2-1:</b> Design = Synthesis + Analysis. Adapted from (Smith, 2005).....	49
<b>Figure 2-2:</b> a) Simple two product column b) column with interheating/intercooling c) column with a side stripper.....	54
<b>Figure 2-3:</b> Verification of vapor pressures for ethanol. Calculated by Aspen plus PLXANT model. Experimental data taken from DDB.....	62
<b>Figure 2-4:</b> Verification of vapor pressure for water. Calculated by Aspen plus PLXANT model. Experimental data taken from DDB. ....	62
<b>Figure 2-5:</b> Verification of vapor pressures for ethylene glycol. Calculated by Aspen plus PLXANT model. Experimental data taken from DDB.....	63
<b>Figure 2-6:</b> Activity coefficient as a function of the liquid composition for the binary system ethanol (1) water (2). Kamihama experimental data (O:1)(Δ:2). Curves predicted with Aspen Plus default parameters. ....	64
<b>Figure 2-7:</b> Activity coefficient as a function of the liquid composition for the binary system water (2) ethylene glycol (3). Kamihama experimental data (O:2)(Δ:3). Curves predicted with Aspen Plus default parameters.....	64
<b>Figure 2-8:</b> Activity coefficient as a function of the liquid composition for the binary system ethanol (1) ethylene glycol (3). Kamihama experimental data (O:1)(Δ:3). Curves predicted with Aspen Plus default parameters.....	65



<b>Figure 2-9:</b> Activity coefficient as a function of the liquid composition for the binary system thanol (1) water (2). Kamihama experimental data (O:1)(Δ:2). Curves predicted with Aspen Plus user parameters from Kamihama. ....	66
<b>Figure 2-10:</b> Activity coefficient as a function of the liquid composition for the binary system water (2) ethylene glycol(3). Kamihama experimental data (O:2)(Δ:3). Curves predicted with Aspen Plus user parameters from Kamihama. ....	66
<b>Figure 2-11:</b> Activity coefficient as a function of the liquid composition for the binary system Ethanol (1) Ethylene Glycol (3). Kamihama experimental data (O:1)(Δ:3). Curves predicted with Aspen Plus user parameters from Kamihama. ....	67
<b>Figure 2-12:</b> composition trajectories of constant volatility (Isovolatility IV) for the system Ethanol-Water-Ethylene Glycol at 1 atm. ....	70
<b>Figure 2-13:</b> Experimental data for ternary interactions reported by (Kamihama et al., 2012) compared with data calculated with Aspen Plus with the parameters reported in <b>Table 2-6</b> . ....	71
<b>Figure 2-14:</b> Simple distillation. ....	72
<b>Figure 2-15:</b> Residue curves for ternary system Ethanol-Water-Ethylene Glycol at 1 atm. (–): Curves calculated by the author (Δ): curves calculated by Aspen Plus. ....	76
<b>Figure 2-16:</b> Scheme of a single feed distillation column. ....	77
<b>Figure 2-17:</b> Typical composition profiles of a single feed distillation column separating ideal mixtures. ....	79
<b>Figure 2-18:</b> Column profiles for a single feed distillation column considering the separation of Ethanol-Water-Ethylene glycol mixtures. ....	80
<b>Figure 2-19:</b> Stripping pinch branches. ....	80
<b>Figure 2-20:</b> Double feed distillation column. ....	82
<b>Figure 2-21:</b> Column profiles for a two feed distillation column used in the separation of Ethanol-Water-Ethylene glycol mixtures. × Middle section; ■ Stripping section; □ Rectifying section. ....	83
<b>Figure 3-1:</b> Seven of the most favorable residue curves that describe the separation of mixtures with minimum binary boiling point azeotropes by adding a separation agent. <i>Figure 7</i> in (Foucher et al., 1991) ....	86
<b>Figure 3-2:</b> Pseudobinary vapor liquid equilibrium diagram for ethanol-water system in presence of different solvents (solvent to feed ratio between 0,2 and 0,3). From (Lee & Pahl, 1985). ....	91
<b>Figure 3-3:</b> Degradation of ethylene glycol solutions. From (Clifton et al., 1985). ....	94
<b>Figure 3-4:</b> Sensitivity of the bottoms temperature in extractive column to the operating pressure. ....	94
<b>Figure 3-5:</b> Sensibility of the equilibrium to pressure change. Red: 0.2 atm. Blue: 1 atm. ....	95
<b>Figure 3-6:</b> Variables of the extractive separation system. ....	96
<b>Figure 3-7:</b> Pseudobinary vapor liquid equilibrium diagram for ethanol-water system in presence of ethylene glycol. ....	100
<b>Figure 3-8:</b> Univolatility curve at 1 atm and 0,2 atm. ....	101
<b>Figure 3-9:</b> Effect of the addition of different quantities of ethylene glycol in the VLE distribution lines. ....	102

<b>Figure 3-10:</b> Column profile map of a extractive distillation column at $Fr = 1$ .....	104
<b>Figure 3-11:</b> Pinch branches of the middle extractive section at $Fr = 1$ and $P = 1 atm.$ .....	105
<b>Figure 3-12:</b> Middle section pinch branches for Ethanol-Water-Ethylene glycol at 1 atm varying the entrainer to feed ratio.....	106
<b>Figure 3-13:</b> Middle section pinch branches for Ethanol-Water-Ethylene glycol at 0.6 atm varying the entrainer to feed ratio.....	107
<b>Figure 3-14:</b> Middle section pinch branches for Ethanol-Water-Ethylene glycol at 0.2 atm varying the entrainer to feed ratio.....	108
<b>Figure 3-15:</b> Qualitative effect of increasing the entrainer to feed flow ratio on the pinch branches.....	109
<b>Figure 3-16:</b> Minimum solvent to feed ratio at 0.2 atm.....	110
<b>Figure 3-17:</b> Unfeasibility of the middle section profile to achieve the rectifying section because of a node pinch branch appearance.....	111
<b>Figure 3-18:</b> Solvent to feed flow rate hysteresis.....	111
<b>Figure 3-19:</b> Extractive distillation profile lines for feasible and unfeasible refluxes at $P=1 atm.$ .....	113
<b>Figure 3-20:</b> Pinch branches for the design conditions.....	113
<b>Figure 3-21:</b> Column profile at $P=0.2$ and $Fr_{design}=1.2145$ ; $R_{op}=0.01$ .....	114
<b>Figure 3-22:</b> Column profile at $P=0.2$ and $Fr_{design}=1.2145$ ; $R_{op}=0.015$ .....	115
<b>Figure 3-23:</b> Intersection stage between middle and rectifying sections as function of reflux.....	115
<b>Figure 3-24:</b> Column profile at 0,2 atm and $Fr_{design}=1,2145$ . The design reflux is $R_{design} = 0,6.$ .....	116
<b>Figure 3-25:</b> Liquid composition column profile of the conventional extractive column. ....	118
<b>Figure 3-26:</b> Temperature column profile of the conventional extractive column. ....	118
<b>Figure 3-27:</b> Liquid composition profiles of the recovery column.....	119
<b>Figure 3-28:</b> Temperature profile of the recovery column.....	120
<b>Figure 4-1:</b> Design variables for an E-DWC.....	124
<b>Figure 4-2:</b> Petlyuk arrangement and typical composition profiles for the middle volatility component.....	125
<b>Figure 4-3:</b> Direct sequence of two simple distillation columns for a ternary ideal separation.....	126
<b>Figure 4-4:</b> Temperature-enthalpy diagrams for a single feed distillation column. a) feed at bubble point temperature and b) at dew point temperature.....	128
<b>Figure 4-5:</b> Temperature-enthalpy diagrams for the separation of a three component mixture. a) conventional direct sequence and b) thermally coupling. From (Smith, 2005) .....	129
<b>Figure 4-6:</b> Prefractionator with sidestream rectifying and sidestream stripping. ....	129
<b>Figure 4-7:</b> Energy requirement of Petlyuk arrangement.....	130
<b>Figure 4-8:</b> Dividing wall distillation column. From (Kiss, 2013).....	130
<b>Figure 4-9:</b> Three products dividing wall columns configurations. From (Yildirim, Kiss, & Kenig, 2011).....	132
<b>Figure 4-10:</b> Possible adaptations of the dividing wall. From (Yildirim et al., 2011).....	132

<b>Figure 4-11:</b> Thermally integration and intensification of an extractive distillation sequence.....	135
<b>Figure 4-12:</b> a) two modules model and b) three modules model .....	136
<b>Figure 4-13:</b> Profile sections in a) conventional extractive sequence and in b) E-DWC.	137
<b>Figure 4-14:</b> Qualitative E-DWC sections profiles for different number of stages in SS1. .....	138
<b>Figure 4-15:</b> Liquid composition profiles of E-DWC for increasing number of SS1 stages. .....	139
<b>Figure 4-16:</b> Liquid composition of an extractive column. ....	140
<b>Figure 4-17:</b> Effect of preheating the feed in the composition of the side stream. ....	141
<b>Figure 4-18:</b> Liquid composition profile of an E-DWC for a feed condition of saturated vapor. ....	142
<b>Figure 4-19:</b> a) Carnot machine and b) distillation column analogy with a Carnot machine. .....	143
<b>Figure 4-20:</b> Reversible distillation column .....	144
<b>Figure 4-21:</b> Entropy generation mapping of extractive and recovery column. ....	147
<b>Figure 4-22:</b> Box representation of the recovery distillation column designed in chapter 3. .....	148
<b>Figure 4-23:</b> Approximation of a real distillation column to the PNMTCC by means of side columns and increasing of stages in a S-H diagram. ....	149
<b>Figure 4-24:</b> T-H grand composite curve for a) the recovery column and b) for the extractive column .....	150
<b>Figure 4-25:</b> S-H grand composite curve for the extractive column designed in <b>Chapter 3</b> . .....	150
<b>Figure 4-26:</b> Column composite curves for the recovery column in <b>Chapter 3</b> .....	151
<b>Figure 4-27:</b> Column composite curves for the extractive column in <b>Chapter 3</b> . ....	151
<b>Figure 4-28:</b> Adiabatic and diabatic distillation column characteristics. From (Kaiser & Gourlia, 1985) .....	152
<b>Figure 4-29:</b> McCabe-Thiele diagram for a) an adiabatic column and b) a diabatic column. ....	154
<b>Figure 4-30:</b> Reversible composition trajectories of an extractive distillation column.....	155
<b>Figure 4-31:</b> Partial reversible composition profile of an extractive distillation column...	155
<b>Figure 4-32:</b> Effect of the reflux in the reduction of irreversibilities .....	156
<b>Figure 4-33:</b> Effect of side exchangers in the extractive distillation column.....	157
<b>Figure 4-34:</b> Extractive distillation column with sequential heat exchangers .....	158
<b>Figure 4-35:</b> Temperature composition diagram for a distillation column where the temperature for heating and cooling is included stage by stage.....	158
<b>Figure 4-36:</b> Column profiles, grand composite curves and loss entropy for a conventional distillation column and a column with SHE.....	160
<b>Figure 5-1:</b> Plot plan of the Chemical Engineering Laboratory building 412 .....	164
<b>Figure 5-2:</b> Process Flow Diagram showing the line numbering. ....	168
<b>Figure 5-3:</b> Storage tanks. ....	171
<b>Figure 5-4:</b> Preheaters.....	171
<b>Figure 5-5:</b> Reboiler of the SHE column. ....	172

<b>Figure 5-6:</b> Condenser of the SHE column.....	172
<b>Figure 5-7:</b> License plate of the pumps. ....	173
<b>Figure 5-8:</b> Pump components. ....	174
<b>Figure 5-9:</b> Damper equipment of pumps.....	175
<b>Figure 5-10:</b> Control valves for the vapor. ....	175
<b>Figure 5-11:</b> Control valves for the water.....	176
<b>Figure 5-12:</b> Feed flow transmitter.....	176
<b>Figure 5-13:</b> Column with sequential heat exchangers SHEC-4001 .....	177
<b>Figure 5-14:</b> System of water supply of the pilot plant of the chemical engineering department UNAL. Taken from (López & Contreras, 2003). ....	183
<b>Figure 5-15:</b> Ambient temperature in Bogotá. Adapted from (IDEAM, 2013) .....	184
<b>Figure 5-16:</b> Boiler for steam generation in the pilot plant of the chemical engineering department UNAL. ....	184
<b>Figure 5-17:</b> Thermal bath with a maximal temperature of 170°C, flow of 15 L/min and pumping pressure of 0,35 bar. ....	186
<b>Figure 5-18:</b> Feed storage pipeline loop. ....	191
<b>Figure 5-19:</b> Top pipeline loop (red closed and blue opened). ....	192
<b>Figure 5-20:</b> Bottom pipeline loop.....	193

## List of tables

<b>Table 1-1:</b> Hypothetical potential for ethanol production from principal raw materials. 2003 petrol use = 1100 billion liters (FAO, 2008).....	19
<b>Table 1-2:</b> Land requirements in bioethanol production (FAO, 2008). ....	20
Table 1-3: Comparison of raw materials for bioethanol production (Balat et al., 2008)....	20
<b>Table 1-4:</b> Policy framework for bioethanol (Mejía, 2010). ....	30
<b>Table 1-5:</b> Bioethanol installed capacity (ASOCAÑA, 2016a).....	31
<b>Table 1-6:</b> Projects of construction to next years (ASOCAÑA, 2016b). ....	31
<b>Table 1-7:</b> Cost comparison for ethanol dehydration by different technological alternatives. Initial composition 11,4%. Taken from (Cardona et al., 2010).....	42
<b>Table 1-8:</b> Energy consumption of some dehydration technologies. Taken from (Gil, 2006).....	42
Table 2-1: Common stages of a process design (Cardona et al., 2010). ....	48
<b>Table 2-2:</b> Values of $q$ , $p$ , $\rho_{ji}$ , and $\alpha_{ji}$ for NRTL from equation (2.7 to (2.9) .....	59
<b>Table 2-3:</b> Analytical solution of equation (2.10) for NRTL method with 3 components. .	60
<b>Table 2-4:</b> Experimental data for verification of PLXANT model from Aspen Plus. ....	62
<b>Table 2-5:</b> Adjusted PLXANT parameters by Aspen Plus.....	63
<b>Table 2-6:</b> Experimental parameters in Aspen Plus Format (Kamihama et al., 2012).....	65
<b>Table 2-7:</b> Equations system for the modeling of the residue curve map.....	75
<b>Table 3-1:</b> Possible entrainers for the extractive distillation of Ethanol-Water mixtures. .	89
<b>Table 3-2:</b> Experimental measurements of the influence of different solvents in the extractive distillation of Ethanol-Water mixtures (Lee & Pahl, 1985). ....	90
<b>Table 3-3:</b> Equation system for the description of the extractive distillation. For details see (Knight, 1987).....	97
<b>Table 3-4:</b> List of specifications.....	98
<b>Table 3-5:</b> Rigorous simulation specifications. ....	117
<b>Table 3-6:</b> Energy requirements.....	120
<b>Table 4-1:</b> Qualitative evaluation of the state of the art for distillation technologies. For details see (Creative Energy, 2008).....	123
<b>Table 4-2:</b> E-DWC energy requirements. ....	142
<b>Table 4-3:</b> Simulation specifications.....	159
<b>Table 5-1:</b> Global mass balance of the extractive distillation separation system to obtain ethanol .....	165
<b>Table 5-2:</b> Specifications of the pumps .....	173
<b>Table 5-3:</b> Boiler specifications .....	185
<b>Table 5-4:</b> Thermal oil specifications.....	186

<b>Table 5-5:</b> Ball valves .....	187
<b>Table 5-6:</b> Globe valves.....	188
<b>Table 5-7:</b> Check list prior to the operation .....	188

# Introduction

The production of biofuels is a topic of growing interest for academy and industry. Among biofuels, bioethanol is known as an energetic substitute of fossil fuels in the transport sector mainly. However, for its use in the current commercial motors, bioethanol should be dehydrated at least until 99% v/v in the Colombian case. The bioethanol dehydration process implies a separation sequence that transforms the diluted ethanol into practically anhydrous bioethanol. The starting diluted solution comes from a fermentation process in which, besides other impurities, the produced bioethanol is mixed with water. Although, there are different alternatives of concentration of bioethanol in mixtures with water, it is common to use a first stage of distillation to remove some impurities that can damage the equipment in the downstream processing, and to decrease the energetic load of heating impurities and water. From this point, bioethanol dehydration has the aim to overcome the azeotrope concentration with the less separation costs. Some technologies proposed to answer this goal are: pressure swing distillation, pervaporation, adsorption with molecular sieves, azeotropic distillation and extractive distillation. This work deals with the extractive distillation technology.

The extractive distillation is the separation of a mixture by means of energy and the use of a separation agent, which has the aim of modify the interactions between the components in the initial mixture. These interactions, between water and ethanol, in the case of bioethanol dehydration, are equalized in the liquid and in the vapor phase, which results in the formation of an azeotrope. The separation agent, known as entrainer, modifies the relative volatility of the liquid mixture and “breaks” the azeotrope. In this study, the entrainer used is ethylene glycol, yet other separation agents can be used. The reason for the selection of this entrainer is that it is a solvent commonly used in the separation of ethanol and water. Therefore, the information about its use in the ethanol dehydration is abundant and can be easily found. Once the entrainer has developed its extraction function, it is mixed with water, which should be removed from the mixture with the aim of recover and recirculate it. This separation is made in a recovery distillation column.

The extractive distillation can have lower thermodynamic efficiencies compared with other dehydration technologies. Moreover, the operational energetic consumptions of the extractive distillation can be higher than those of the adsorption with molecular sieves. Nevertheless, the extractive distillation is a technology commonly validated from the technical point of view of the separation and used for ethanol dehydration in many places over the world. With this technology, higher ethanol concentrations than the required can be obtained with only the addition of a second feed stream, without making substantial structural changes in the conventional distillation columns. The use of extractive distillation columns has less technologic dependence regarding the maintenance of the equipment and the understanding of the phenomena compared with the other technologies, such as the adsorption in molecular sieves.

As most of the separation processes, the extractive distillation has been studied from the energy integration and process intensification point of view. This had led to propose structural modifications of the extractive distillation equipment. Two examples of these modifications are the addition of sequential heat exchangers (SHE) or the use of a dividing wall column (DWC). The use of a DWC allows the integration of the extractive and recovery columns in one equipment reducing the energetic and capital costs of the separation process. However, the use of these technologies has not been deeply studied in the application to the extractive distillation. Therefore, the conceptualization of the non-conventional extractive distillation columns is needed to improve its simulation and design.

In this thesis, two non-conventional distillation arrangements, columns with SHE and extractive distillation columns with DWC (E-DWC), are conceptually studied and designed for its use in the production of bioethanol as biofuel using ethylene glycol as entrainer. The study is divided in six chapters. In the first chapter, the importance of the bioethanol and the existent separation technologies to produce anhydrous ethanol are evaluated. In the second chapter, some tools for the conceptual design of extractive distillation columns are established. In the third chapter, a conceptual methodology for the design of a conventional extractive distillation sequence is applied to the ethanol-water-ethylene glycol system. In the fourth chapter, the study of the use of the dividing wall column technology and the addition of sequential heat exchangers to the conventional separation sequence in the extractive distillation of ethanol is presented. In the fifth chapter, the design of a non-conventional equipment is made, which allows to give continuity to the present work in the future hydraulic studies of the equipment.



This work can be used by the academy because the presented results can contribute to the development and understanding of the dividing wall and sequential heat exchanger technologies. In addition, the bioethanol study case is related with a state policy built with the projection of the country as producer of this biofuel. In this regard, this work can contribute to the improvement of the current processes in the Colombian industries using extractive distillation or in the evaluation of the substitution of these processes with new technologies.



# 1. Bioethanol Context

World population and economy increments in coming years are projected to grow. With this growth, energy offer must also be increased to supply the necessity in buildings, both commercial and living, industry and transport, among others. The main energy source in world are fossil fuels, but many governments are directing their politics to the production of alternative energies. Fluctuation in the oil markets and the geopolitical conflicts between nations affect the energy security of the countries and motivate the interest in alternative energies. Additionally, global warming is a current concern for the international community because of its possible negative impacts in the environmental and its consequences in the stability of the world. These facts have open new politics and markets for alternative energies and stimulate studies and development of more sustainable technologies of energy generation.

Renewables are an alternative option of generation of energy. They have been studied to reduce or replace fossil fuels with more sustainable sources. Gasoline and diesel are two of the most studied conventional fuels to be substituted. Within the proposed alternatives for their substitution, the world is thinking in biofuels, such as bioethanol and biodiesel, obtained from agricultural raw materials. Bioethanol is produced by the fermentation process of different raw materials rich in sugar and/or starches, such as cane, corn, beet and yucca, among others. This biofuel is used in different countries to substitute or oxygenate gasoline used in conventional automobiles. As transport is the second sector of most consumption of energy in the world, the bioethanol production used in mixtures with gasolines requires an agricultural industry of a large scale or, what is equivalent, a big area planted with energy crops. The agroclimatic conditions and the low availability of land hinder the production of bioethanol in developed countries, such as the EU members. In contrast, Latin America countries have high capacities of arable land and optimum climatic conditions that project a promising production of biofuels and market options based on agricultural development.

Colombia is directing its policies in order to establish itself as a bioethanol producer. Some of the reasons to do this are related to environmental and energy security aspects, but also because bioethanol presents an opportunity for the development of the agricultural sector with social and economic benefits. Bioethanol production in Colombia emerges as part of a biofuel program in which ethanol is used to replace the gasoline consumption for transport in 15% in volume. For its use as fuel in vehicles, ethanol needs to have a water content of less than 2%v/v. Nowadays, Colombia has an ethanol production above of 1,6 ML/ day obtained mostly from local sugar cane production. Colombia has six plants for the production of bioethanol each one covering four stages: sugar and molasses production, pretreatment of molasses, fermentation and ethanol recovery.

To be used in mixture with gasoline, bioethanol must undergo a dehydration process before its commercialization as fuel for vehicles. Dehydration of ethanol with conventional distillation is limited by a thermodynamic condition called azeotropy. To overcome this limitation, alternatives to the conventional distillation have been developed, such as extractive distillation, azeotropic distillation, pressure swing distillation, adsorption, pervaporation, among others. Choice between these technologies is not trivial and the final decision depends on the criteria of the engineering to assume the most favorable cost without negatively impacting the environment. The purpose of this chapter is to show a general context around the needs, policies and technologies related to the production of bioethanol that allow to establish the impacts that this document can have.

## 1.1 World energy consumption

World energy consumption has continuously increased and its projections to the coming years show it will continue growing (EIA, 2016a)(IEEJ, 2015)(BP, 2016)(IEA, 2015). Historically, world energy consumption has increased its value by 15% from 1990 to 2000 and by 54% from 2000 to 2012. In year 2016 the world energy consumption is estimated to approximately 618 EJ according to the Energy Administration of United States (EIA), see **Figure 1-1**. Future data are mainly based on historical values and on predictions of geopolitical scenarios. According to these, consumption will arise in 76% at the end of the current decade with respect to 2012 consumption. Long-term projections show that energy consumption will still increase to 2040, when it will be around 859 EJ.

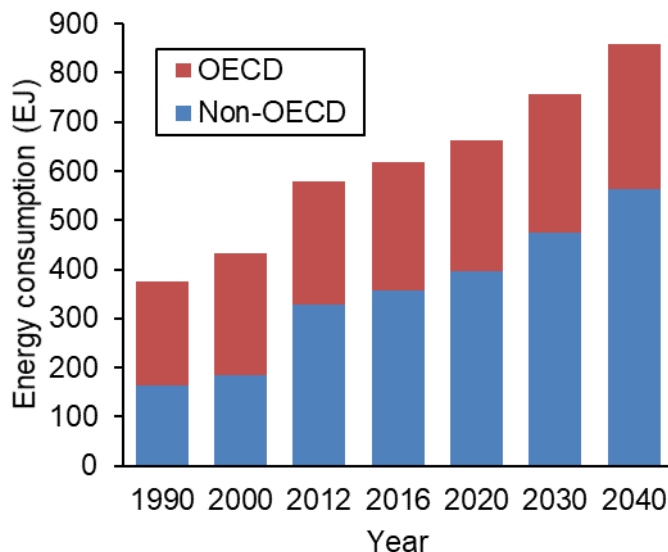


**Figure 1-1:** History and projections of world energy consumption by regions 1990-2040.

Adapted from (EIA, 2016a).<sup>1</sup>

Population and economic growth are two of the principal reasons for the increase in energy consumption. BP company estimates that this increase will be mainly caused by global growth and in a lesser extent due to the population growth (four-fifth and one-fifth respectively) (BP, 2016). In the case of population, a growth of 30% from 7.1 billions in 2013 to around 9 billions in 2040 is projected (~1%/year), see **Figure 1-2**. The main energy consumer driver in the evaluated period is the Non-OECD nations (outside of the Organization for Economic Cooperation and Development). In contrast, a slower consumption in OECD countries, respect to historical values, is expected. On the other hand, global economic growth is projected to increase with an average rate of 3.3%/year from 2012 to 2040. The global domestic product (GDP) in non-OECD countries will growth in average by 4.2%/year and in the case of OECD members the growth will be of 2.0%/year, see **Figure 1-3**. This economy growth will be reflected in more energy consumption in coming years.

---

<sup>1</sup> OECD, the Organization for Economic Cooperation and Development is an intergovernmental organization created in 1961 which group the 35 countries that are together the main drivers of the global economy.

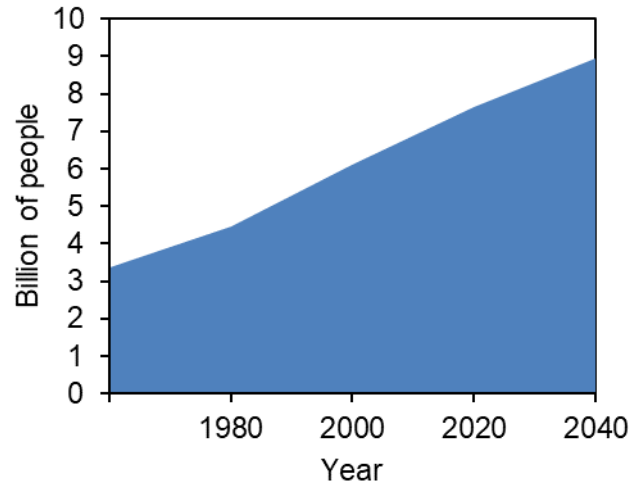


**Figure 1-2:** History and projections of world population projections to 2040. Adapted from (U.S. Census Bureau, 2016)

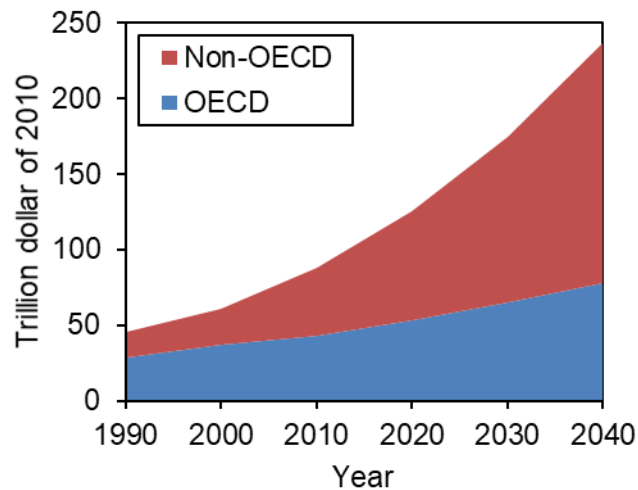


**Figure 1-3:** World total gross domestic product (GDP) 1990-2040. adapted from (EIA, 2016a)

The main end-use sector of energy in the world is industrial sector that covers agriculture, mining, manufacturing and construction, see **Figure 1-4**. 326 EJ of total energy in the world are expected to be consumed by industrial sector in 2040. This is equivalent to a 38% of total consumption in the same year and an increase of 42% related to 2011. Second consumption sector is transportation with 116 EJ consumed in 2016 that represent 25% of the total final energy consumption. In 2040, around 164 EJ will be spent in transportation with a contribution of 19% respect to the total consumption in the same year (24,5% of final consumption as electricity losses are excluded from the total). Respect to 2011, the

transportation sector will increase its consumption by 50% to 2040. Building sector, including residential and commercial sectors, are the less consumer sectors with around 5% of the total energy demand in 2040. Environmental impacts of the energy consumption by these sectors are significant. In sum, industrial, transport and building sectors are the main source of anthropogenic greenhouse gas emissions. A value based on U.S. data estimates that 83,6% of the total anthropogenic greenhouse gas emission in 2014 were due to these sectors.

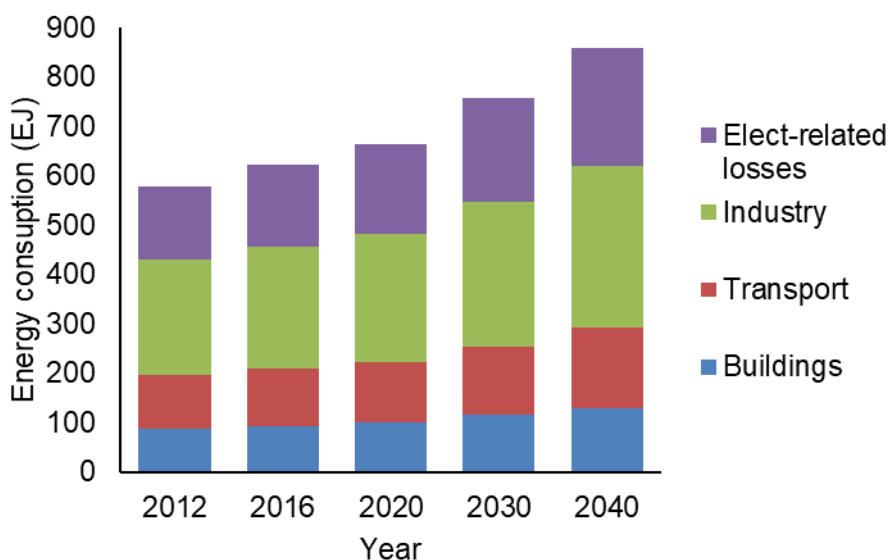


**Figure 1-4:** History and projection of world energy production by end-use sector. Adapted from (EIA, 2016a)

Fossil fuels are and will still be the most popular source of energy to 2040. Liquid fuels, coal, natural gas, renewables and nuclear energy sources are all expected to increase in the next years, see **Figure 1-5**. Projection to 2040 shows liquid fuels as the main energy source with almost 32% contribution to the global consumption. Renewable fuels show the faster growing with almost 98% of increase from 2013 to 2040. In contrast, coal is the slowest growing energy source with a contribution in 2040 of 23% of total energy consumption. Along with natural gas, coal and liquid fuels will contribute with almost the 80% to the total energy sources in 2040.

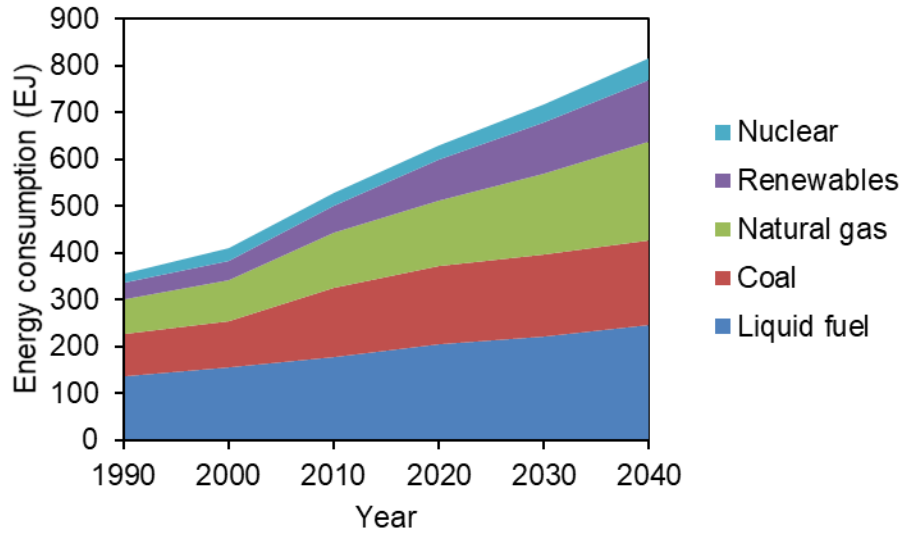


**Figure 1-5:** History and projection work energy consumption by source. Adapted from (EIA, 2016a)

## 1.2 World energy policies

World economy is highly dependent on fossil fuels which is a disadvantage in terms of energy security of the countries and global environmental impact.

The geopolitical world situation, availability of oil producer countries to produce at rational prices and stock exchange speculations are some uncontrollable factors that impact the availability of strategic resources, as oil, in nations around the world. This has led to the countries to think in the concept of energy security defined by International Energy Agency (IEA) as “*uninterrupted physical availability of energy products on the market, at a price which is affordable for all consumers*”. The risks associated to energy security can be categorized in external market instabilities, technical factors as faults in energy supply systems and physical security threat such as terrorism or natural disasters. (Oelz, Sims, & Kirchner, 2007). Each nation has different risk sceneries according to its local circumstances and, in respond to it, different energy policies have been implemented around the world. Some illustrations are the Energy Independence and Security act 2007 of United States, the EU’s Energy Union strategy and the national alcohol program in Brazil (Proálcool) (WEC, 2011b)



Parallel to the risk in energy supply, there is an environmental risk associated to the combustion of fossil fuels that is everyday more latent. Anthropogenic activity has increased the emission of greenhouse gases (GHG) to the highest levels in the human history with implications to the human race as well as natural systems. Intergovernmental Panel on Climate Change (IPCC), which is a scientific body of United Nations (UN), in its Fifth Assessment Report (AR5) establish clearly the influence of the human race on the climate change, its impacts and future risks (IPCC, 2015). As conclusion, the report says that people, societies, economies and environmental are in risk all of them. Climate change is not a hypothesis anymore. This has been understood by 187 countries around the world that have ratified Kyoto protocol in 2009 with the objective of respond to the climate change and its consequences as the global warming. In the last Conference of the Parties (COP21) organized by United Nations Framework Convention on Climate Change (UNFCCC), which was held in Paris in 2015 with 195 countries assistants, the nations agreed to reduce the GHG in order to limit the global temperature increase to 2°C in present century and to make efforts to reduce the temperature to preindustrial levels. However, temperature increase is not the only negative impact of fossil combustion. Pollution, acid rain, water contamination, among others, are additional risks in energy production from fossil fuels.

As environmental and energy security risks are interrelated, policies in these areas are also often interrelated in order to ensure the energy supply with the less environmental impact. World Energy Council (WEC), which is the largest network of energy leaders in the world, analyses the energy policies in terms of energy security, energy equity and environmental sustainability (WEC, 2016). These dimensions of analysis have the objective to facilitate dialogues between nations and the idea of assist policymakers in making decisions about the global, regional and local energy policies. At the same time, United Nations are also interested in driving polices for the future of the energy global scale. Nowadays, near 2 billion of people around the world have not access to modern energy supply which is a factor of inequity. In respond, one of the objectives of the millennium for the United Nations is to promote universal access to sustainable energy that have led to the program Sustainable Energy for All (SE4All).

### 1.3 Renewable Energies

In order to mitigate risks in energy security and environmental impacts, nations can reduce its dependency on fossil fuels by diversification of their energy supply. Since from the 220 oil-consuming countries in the world only 50 are producers and 35 are exporters, access to the oil supply is very limited (Oelz et al., 2007). Diversification means to use local resources to generate energy and reduce imports and external dependences with substitution by native resources. Renewable energy sources are native resources, diverse and widely available and, as their potential is big, they can theoretically displace the use of fossil fuels in a substantial amount.

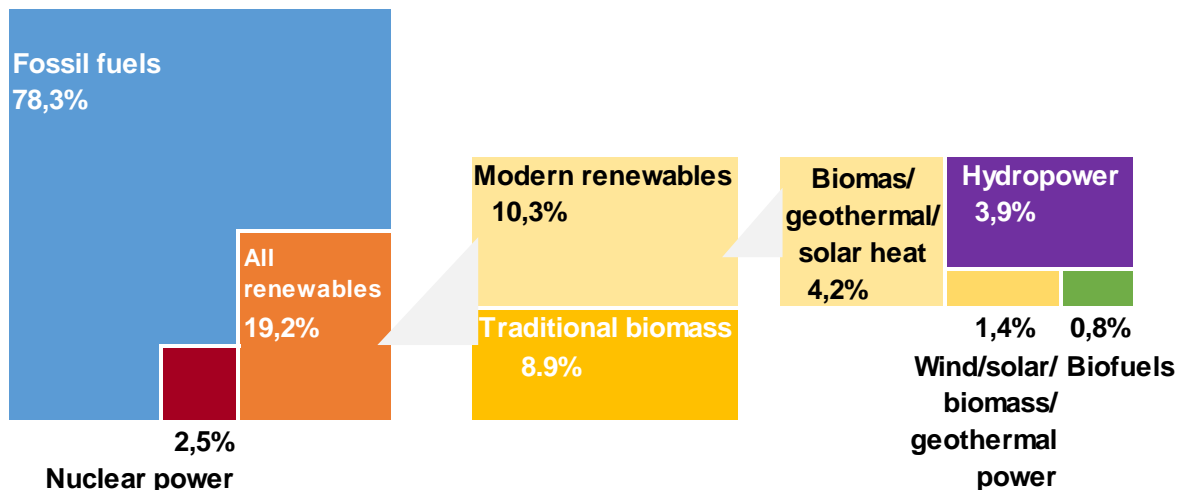


**Figure 1-6:** Contribution of renewables to total final energy consumption. From (REN21, 2016)

To 2014, around 19,2% of the total energy consumption in the world was produced from renewables, according to the “Global Status Report REN21 2016”, see **Figure 1-6**. This scenery is more significant in 2015 as it had the largest addition of global energy capacity seen to date. The year 2015 also had a record of investment of 285,9 thousand million dollar, year in which for the first time developing countries overtook developed countries. These inversions in renewables have an important political support at local level and global level. Today, around 114 countries worldwide have polices related to renewables for electric energy, 66 for transport and 21 for heating and cooling (REN21, 2016). 2015 finished with the assistance of 189 countries to the UNFCCC, where most of them, 147, pledged to implement renewables in order to reduce environmental impacts, which, as it has been

described before, is an actual concern in the global context and is a focus of investment. The 147 countries mentioned renewables to present their Intended Nationally Determined Contributions (INDCs) (REN21, 2016), which not only confirms the commitment of the countries with the renewables, but also drive investors toward developing new markets around more diversified technologies for energy production and efficient transmission. One the more remarkable consequences of the investment in renewables has been the production of jobs which, in spite of the low fossil fuels prices, created 8.1 million of new jobs mainly due to solar and biofuels contribution (REN21, 2016), see **Figure 1-7**.

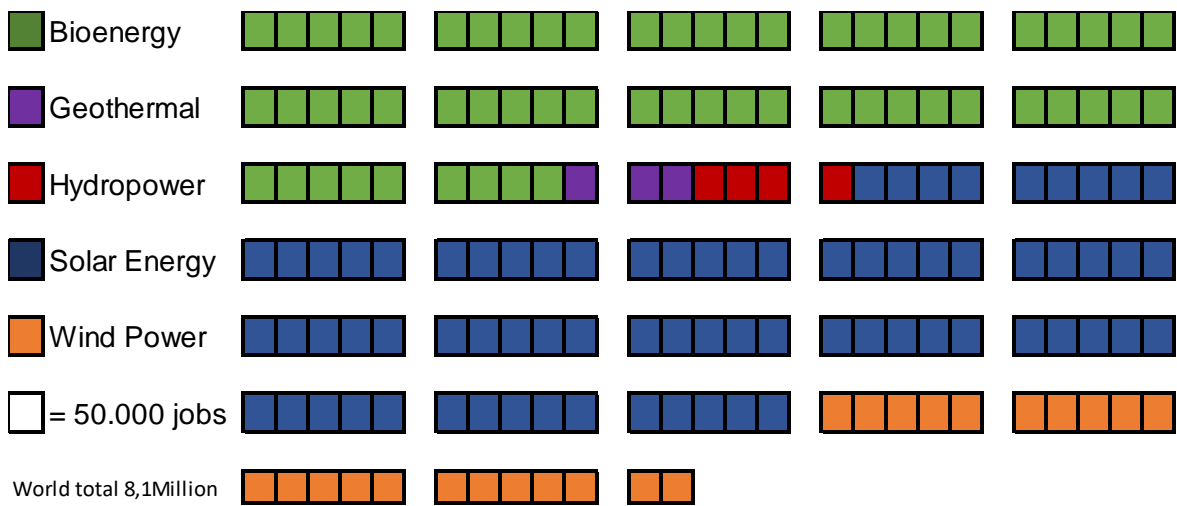


**Figure 1-7:** Jobs in renewable energy. From (REN21, 2016). Bioenergy includes biomass, biofuels and biogas.

Despite its advantages, the future of renewables cannot be predicted because it is a matter of decision, in which several different actors are involved, each one with their own ideas and priorities. However, based on today political scenery of investments, the future of the renewables seems to keep growing every day under more favorable conditions in production cost, mitigation of environment impacts and polices of implementation at local as well as global scale (REN21, 2013).

## 1.4 Biofuels

Bioenergy<sup>2</sup> present the largest renewable contribution to the world total final energy consumption with about a 14% (64 EJ). These quantity is disaggregated in bioenergy for heating 12,6% (57,5 EJ), transport 0,8% (3,7 EJ) and electricity 0,4% (1,8 EJ), see **Figure 1-8**. The sources of bioenergy are commonly known as biofuels. In the case of transport, biofuels refers mainly to biodiesel and bioethanol because of its participation in the market, see **Figure 1-9**. Biofuels have a theoretical potential of displacement significant amounts of fossil fuels in transport with no significant changes in actual engines technologies. However, compared with conventional sources, its use is still very low. One of the disadvantages of biofuels implementations has been the influence of the production cost of fossil fuels in the economic competitiveness of biofuels. These disadvantage led to the need of recognition of no-market benefices around biofuels use, some of which are the reduction of oil demand, reduction in green gas emissions, air quality benefits and waste reduction, vehicle performance and agricultural benefits (IEA, 2004).

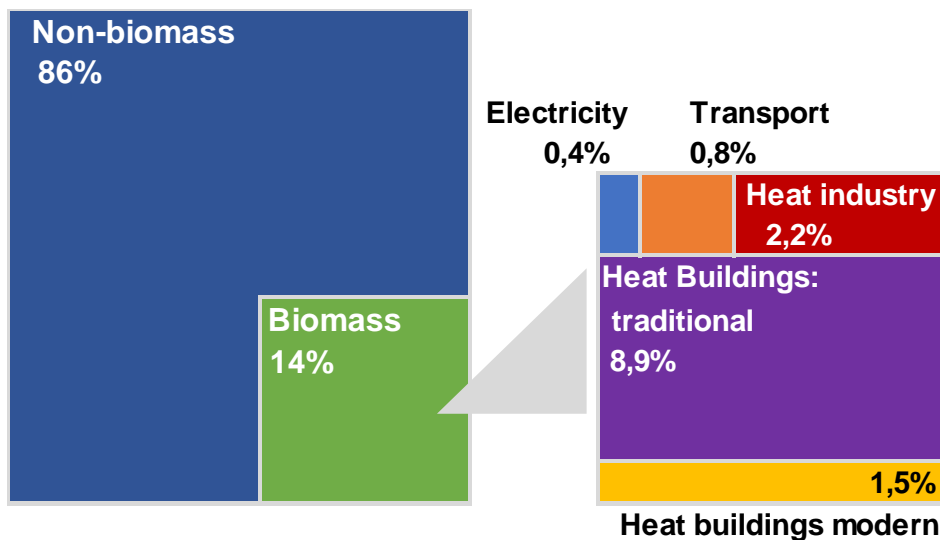


**Figure 1-8:** Contribution of bioenergy to total final energy consumption. From: (REN21, 2016)

<sup>2</sup> Bioenergy refers to a wide range of materials obtained from biological sources and that can be converted with energy purposes. Conversion can be direct combustion or biological conversion as well as thermochemical conversion. It includes forestry, agricultural residues, energy crops, etc.

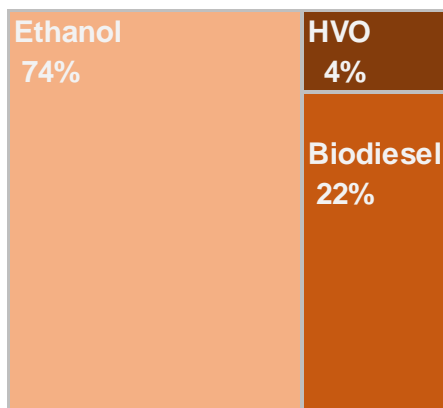


**Figure 1-9:** Biofuels share. From (REN21, 2016). HVO: Hydrogenated Vegetable Oil.

Today is not clear the global potential of production of biofuels but technical sceneries show that, in conservative estimates, around one third of the fossil fuels for road transport can be substituted to 2050-2100 period (IEA, 2004). Nevertheless, market sceneries are uncertain as factors as competence of land, cost of production and social responses, among others, aren't clearly established.

## 1.5 Bioethanol

Bioethanol was discovered in isolated form in 1100 AD as a consequence of the improvements in glass equipment for distillation that lead to the concentration of ethanol from wine. Rapidly this ethanol found uses in the solvent industry, in medicine and recreation (Rasmussen, 2012). To 17<sup>th</sup> century, ethanol was used in lamps and stoves for lighting, heating and cooking. In 1786 a prototype of ignition motor was created by the American Samuel Morey who used alcohol as fuel. Few years after in 1860, the German inventor, Nickolaus Otto, also created an ignition motor with ethanol as fuel (Rothman, 1983). Here after, different social and political scenarios in terms of taxes, uses, production cost and availability of raw materials have influenced the production of ethanol. Today bioethanol is presented as a partial or total substitute of gasoline in compression-ignition engines and is commonly used as additive to oxygenate fossil fuels and to rise the octane number.

Bioethanol is a liquid organic compound obtained by a fermentative process from biomass. Raw materials for its production are classified in sucrose-containing feedstocks, starchy materials and lignocellulosic biomass. Fermentation of sucrose produces ethanol-water

mixtures with a content of bioethanol below 10% in volume. Uses for bioethanol include alcohol beverages, fuels, oxygenates, solvents and some organic compounds. In order to use bioethanol with energy purposes almost all the water must be retired. Two types of bioethanol used as fuel are commonly found: a) hydrous ethanol with a water content of 2-7% v/v and b) anhydrous bioethanol with less than 2% v/v water content depending on local standards (BEST, 2011). Hydrous ethanol is usually used in 100% ethanol engines and anhydrous in low blends with petrol and diesel engines.

The use of bioethanol in mixtures with gasoline above 10% implies modification of the conventional engines that use gasoline because bioethanol is more corrosive than gasoline and generate damages to internal parts of the gasoline engines. Flexible fuel vehicles currently respond to this problem with the use of non-corrosive materials (BEST, 2011). Every day more conventional vehicles are converted to flexible vehicles to work with blends of 85% of biofuel. Bioethanol also has disadvantages in terms of energy content as the energy content of gasoline is 32 MJ/liter and in the case of bioethanol is 21 MJ/liter. This deficiency implies more frequent refueling that is more significant in 85% blends, in which the energy content is 22,7 MJ/L, than in 5% blends, with energy content of 31,5MJ/L (BEST, 2011).

## 1.6 Bioethanol Market

**Figure 1-4** shows that around 25% (116 EJ) of the total finally energy consumption in the world is due to transport. This percentage refers to different transport modes, in which vehicles are the most energy consuming mode with more than half percent of the total consumption followed by trucks mode, see **Figure 1-10**. Gasoline and diesel are the main fuel sources for transport energy, see **Figure 1-11**. 24 million of gasoline barrels/day (44.5 EJ/year) were consumed in 2013 worldwide (EIA, 2016b). To 2016 the gasoline consumption was approximately 46 EJ that fuel around 1300 million of vehicles in use worldwide according to estimates based on (OICA, 2016) reported tendency. This information is relevant in the bioethanol market because, according to the actual energy policies, bioethanol production depends on gasoline used in transport, and this value depends as well on the number of vehicles in the world.

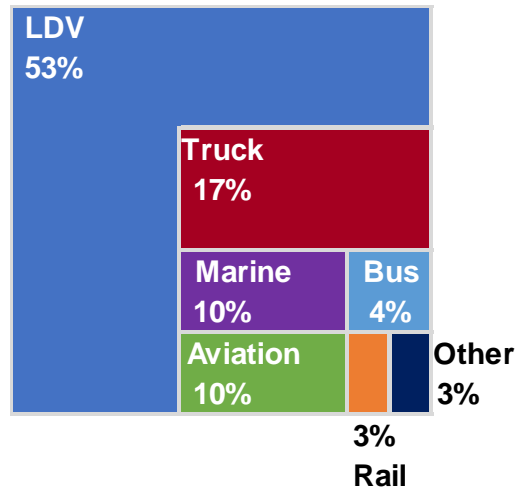


**Figure 1-10:** World transport energy consumption by mode. LDV = light duty vehicles.  
From (WEC, 2011a).

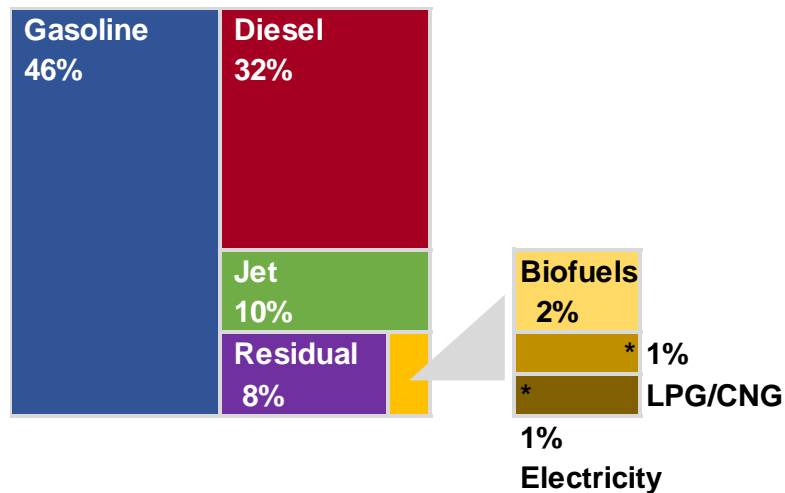


**Figure 1-11:** World transport energy consumption by energy source. From (WEC, 2011a).

The year 2015 finished with a total world production of bioethanol in 25,467 million gallon (2,1 EJ) , see **Figure 1-12**. This production is supported by governments in different countries that have generated mandates in terms of subsidies, credits, tax exceptions and local blends with biofuels. Some of the reasons of the mandates are related with the general concern in the global warming and the energy security. However, especially in developing countries, bioethanol production has additional benefits, impacts and opportunities. As mentioned before, employment generation due to the opening bioethanol markets for farmers can be an important benefit of the establishment an ethanol market, seen in **Figure 1-7**.

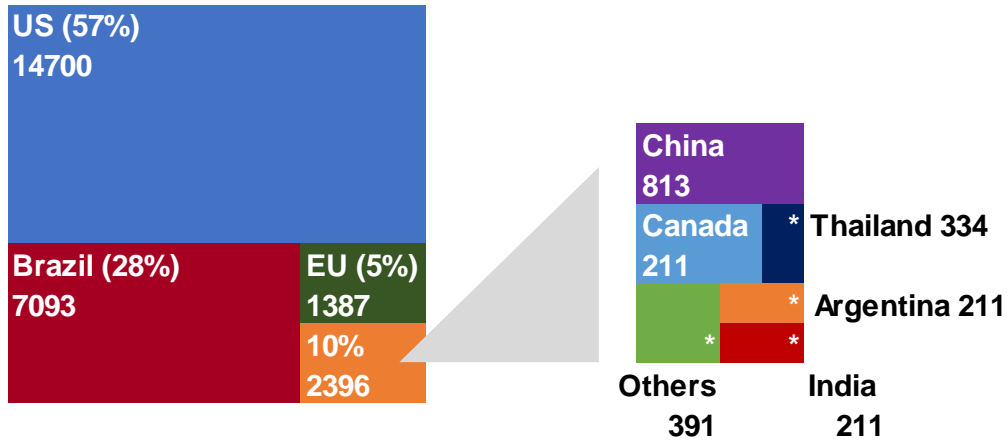


**Figure 1-12:** Global ethanol production in million gallons (RFA, 2016)

Historically, top bioethanol producers in the world are the United States and Brazil, see **Figure 1-13**. They two cover more than 80% of the global bioethanol production. Feed material for US production is mainly corn (around 90%), and almost all of the bioethanol in Brazil is produced from sugar cane (Balat, Balat, & Öz, 2008). In the case of Brazil, almost 80% of its production is spent domestically and the rest 20% is exported to European Union or to United States. Around 199 bioethanol refineries are operating in US to 2016 and 16 more are being installed (RFA, 2016). Brazil had more than 310 refineries in 2013, but its capacity of sugar cane production (around 6,2 million hectares) required the construction of 77 more plants (Macedo, 2007).

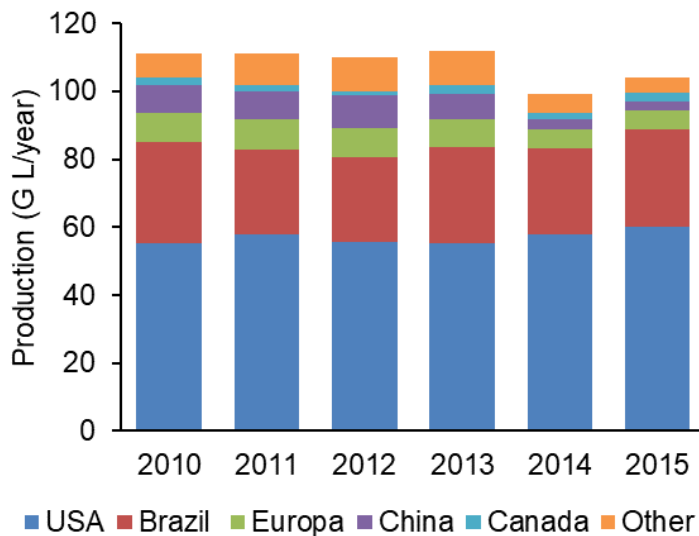


**Figure 1-13:** Ethanol production by country 2009-2015 (IRENA, 2016)



Achieving industrial levels of bioethanol production involves the use of a large amount of arable land, since the production of bioethanol depends of the availability of raw material to produce it. **Table 1-1** shows a hypothetical case where the 42% of the arable land is used to produce crops for biofuels. With this area almost 57% of the global petrol could be supply in 2003. However as have been show previously, the amount of petrol used in the world is growing and in future scenarios this percentage could be lower. In this table is also possible notice the importance of sugar cane as raw material for ethanol production. Sugar is the crop with the highest biofuel yield per hectare along with sugar beet. This is an important advantage since the availability of arable land in the world is limited and biofuels from sugar cane can possibly more sustainable from the food security point of view.

**Table 1-1:** Hypothetical potential for ethanol production from principal raw materials. 2003 petrol use = 1100 billion liters (FAO, 2008).

Crop	Global area (M ha)	Global production (M t)	Biofuel yield (l/ha)	Maximum ethanol (G l)	Petrol equivalent (G l)	Supply as share of 2003 global petrol use %
Wheat	215	602	952	205	137	12
Rice	150	630	1 806	271	182	16
Maize	145	711	1 960	284	190	17
Sorghum	45	59	494	22	15	1
Sugar cane	20	1 300	4 550	91	61	6
Cassava	19	219	2 070	39	26	2
Sugar beet	5.4	248	5 060	27	18	2
<b>Total</b>	599	...	...	940	630	57

A more realistic estimation of land use for energy proposes can be seen in **Table 1-2** where three scenarios are projected to 2030. The reference scenario states an increase of the percent of land in the world used to produce biofuels to 2,5% respect to the 1% presented in 2004. The second scenario states the implementation of policies to increase in 2,5% the use of land for biofuels. The third scenery is based on an eventual development of second generation bioethanol produced from lignocellulosic materials. Based on the data available in **Table 1-1** and **Table 1-2** the base scenario can produce less than 2% of the petrol in the same year. In the reference case it percentage could be increased to 3,2% and in the alternative police scenario the increase could be to 5,5%. With a gross estimate based on these tables the necessity of land to produce enough ethanol for substitute 10 of petrol should be 105 Mha equivalent to almost 7,6% of the world arable land.

**Table 1-2:** Land requirements in bioethanol production (FAO, 2008).

Country grouping	2004		2030					
			Reference scenario		Alternative policy		Second-generation	
	M ha	% Arable land	M ha	% Arable land	M ha	% Arable land	M ha	% Arable land
Africa and Near East	–	–	0.8	0.3 %	0.9	0.3 %	1.1	0.4 %
Developing Asia	–	–	5.0	1.2 %	10.2	2.5 %	11.8	2.8 %
European union	2.6	1.2 %	12.6	11.6 %	15.7	14.5 %	17.1	15.7 %
Latin America	2.7	0.9 %	3.5	2.4 %	4.3	2.9 %	5.0	3.4 %
OECD pacific	–	–	0.3	0.7 %	1.0	2.1 %	1.0	2.0 %
Transition economies	–	–	0.1	0.1 %	0.2	0.1 %	0.2	0.1 %
United States of America and Canada	8.4	1.9 %	12	5.4 %	20.4	9.2 %	22.6	10.2 %
World	13.8	1.0 %	34.5	2.5 %	52.8	3.8 %	58.5	4.2 %

**Table 1-3** lists different types of raw materials for production of bioethanol with their estimated production cost and crop yield. The production cost of bioethanol is not constant in the practice, it depends on the behavior of different variables of its production chain. In Brazil, ethanol is produced at the lowest price, which is calculated in 0,68-0,95 \$US/gal. Brazil's ethanol is cost competitive when oil prices are above US\$30 per barrel, while U.S's and EU's ethanol are competitive when oil barrel price is above US\$60 and US\$70, respectively (Balat et al., 2008).

**Table 1-3:** Comparison of raw materials for bioethanol production (Balat et al., 2008).

Type	Yield (t/ha/year)	Conversion rate to sugar or starch (%)	Conversion rate to Bioethanol (l/ton)	Bioethanol yield (l/ha/year)	Cost (US\$/m <sup>3</sup> )
Sugar Cane	70	12.5	70	4900	160
Cassava	40	25	150	6000	700
Sweet Sorghum	35	14	80	2800	200-300
Corn	5	69	410	2050	250-420
Wheat	4	66	390	1560	380-480

## 1.7 Latin America Context

Some fundamental aspects have been taken into account in the bioethanol production in Latin America countries (Mejía, 2010). The first one is the possibility of expanding the agricultural capacity by the focus of Latin American countries on the generation of crops for the production of biofuels. This expansion can occur given that the Latin American countries have a high availability of cultivable land compared to other geographic areas such as Europe. The second one is the establishment of global markets by countries around the world that have found themselves adept to diversify their energy supply by introducing biofuels into their energy mixes. Another reason is related to the opportunity of increase the local infrastructure of the Latin American countries and the possibility of innovate in agricultural and industrial sectors if an agro-export policy is implemented.

Bioethanol production in Latin America has focused mainly in sugar cane as raw material with Brazil as the main producer. The actual target market of interests is mainly local with an important projection to supply European and United States requirements. Public policies are the main factor to develop the production, as well as the fact that the governments have implemented obligations of bioethanol consumption mainly in E10 mixtures. From the producers points of view inversions are based on the commitment of the governments to ensure a local demand with a regulated price and incentives to the production. In order to promote collaboration between countries public institutions as universities, research centers and ministries have been directed by the *Comisión Interamericana de Etanol (CIE)*, which was created in 2006. Bioethanol producers in Latin America also works in alliance with the *Instituto Interamericano de Cooperación Agrícola (IICA)* that advises the region in production and consumption of biofuels through documents as “*Atlas de la agroenergía y los biocombustibles en las Americas*” (IICA, 2007).

Main achievement of the region in recognition of bioethanol potential in the economy of the country members has been “*La Declaración de Margarita*” signed in Venezuela in 2017. This declaration, which establishes the liabilities of the countries to promote bioethanol production, has had different criticism based on the lack of a previously analysis of the impacts that the bioethanol industry can potentially have. The *Comisión Económica para América Latina y el Caribe (Cepal)* has made a report about the contribution of the biofuels in Latin America and Caribbean in which alerts about the lack of studies supporting bioethanol development in terms of its implications to the agriculture, use of the natural

resources, mitigation of the hunger and impacts in the food cost. The present document doesn't deep in opposition to bioethanol industry because this debate is out of the scope of this text. More detailed analysis can be find in (Mejía, 2010).

## 1.8 Colombian Context

Colombia is a country with around 48 million inhabitants and a GDP of 292 billion dollar to 2015 according to The World Bank. Its primary energy production is based predominantly on oil and coal sources as it can be seen in **Figure 1-14**. Energy contribution to the GDP is approximately 10% and oil sales cover almost the half part of this percentage. Colombia exports a big part of its energy production. 65% of the total primary energy production, estimated in 5,96 EJ, is exported mainly as coal and oil, the rest 35% is offered in the local market. In Colombia, the total final energy consumption is near to 1,2 EJ, distributed by source as shown in **Figure 1-16**, with liquid biofuels included in oil percentage as mixture with diesel and gasoline.

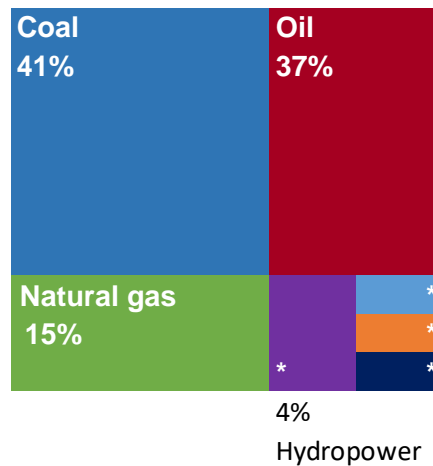


**Figure 1-14:** Primary energy production in Colombia in 2015, total = 5,96 EJ (UPME, 2016).

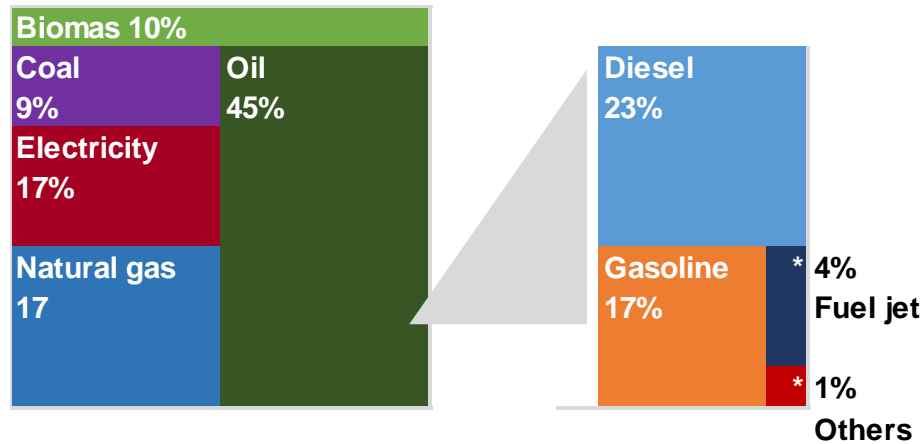


**Figure 1-15:** Final energy consumption in Colombia by source, 2015 (UPME, 2016).

The sector with the biggest final energy consumption in Colombia is transport, followed by industry and residential sectors, see **Figure 1-16**. The total energy consumption for transport, which includes marine, air, train and road modes, was 0,5 EJ in 2015, see **Figure 1-17**. In the case of road transport, the demand of fuels was 0,43 EJ in 2015 distributed in 47% of gasoline, 46% of diesel and 7% of gas. Data about electric energy for transport is not reported in the official energy balance of the country.

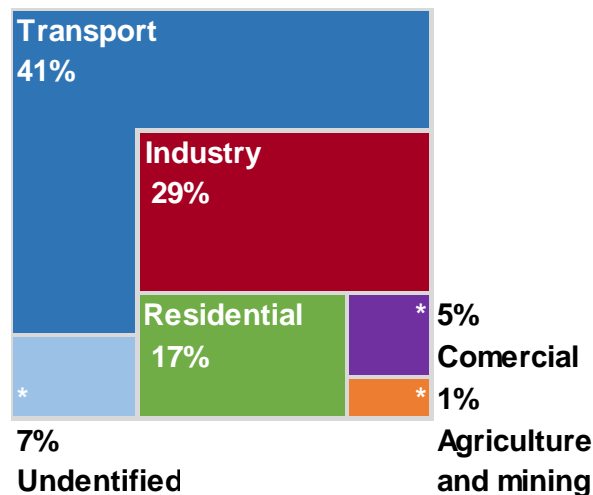


**Figure 1-16:** Final energy consumption by sector in Colombia in 2015, total = 1,2 EJ (UPME, 2016).

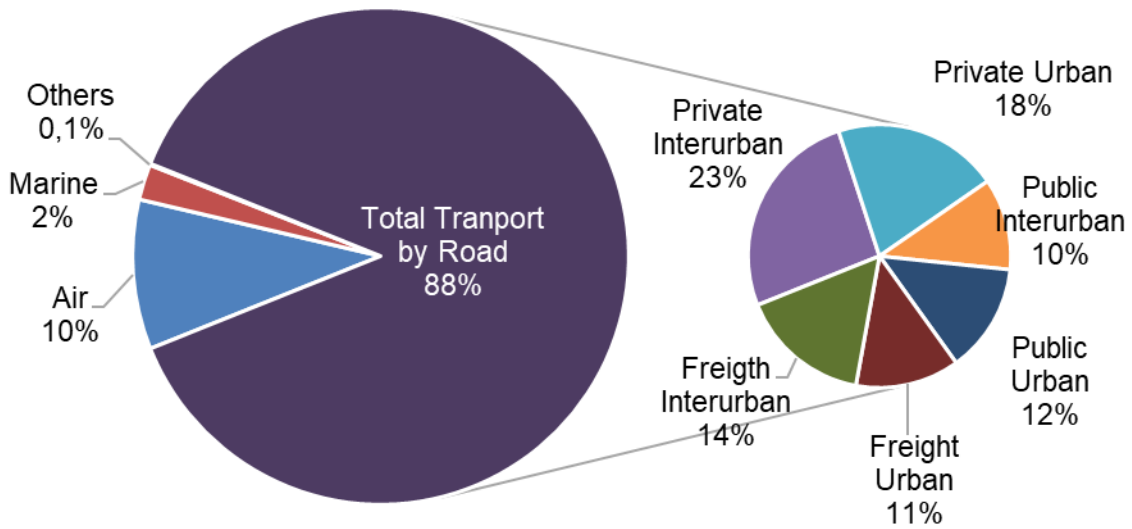


**Figure 1-17:** Energy consumption in transport by energy mode in Colombia. Total= 0,495 EJ in 2015 (UPME, 2016).

Gasoline consumption in Colombia has growth in the last years, see **Figure 1-18**. Most of this consumption is used in the transport sector and the rest is used essentially in the industry sector. Actual gasoline imports relative to the total demand are between 15% and 20% with a growing tendency in contrast to the decreasing in exports that led to a negative trade balance, see **Figure 1-19**.

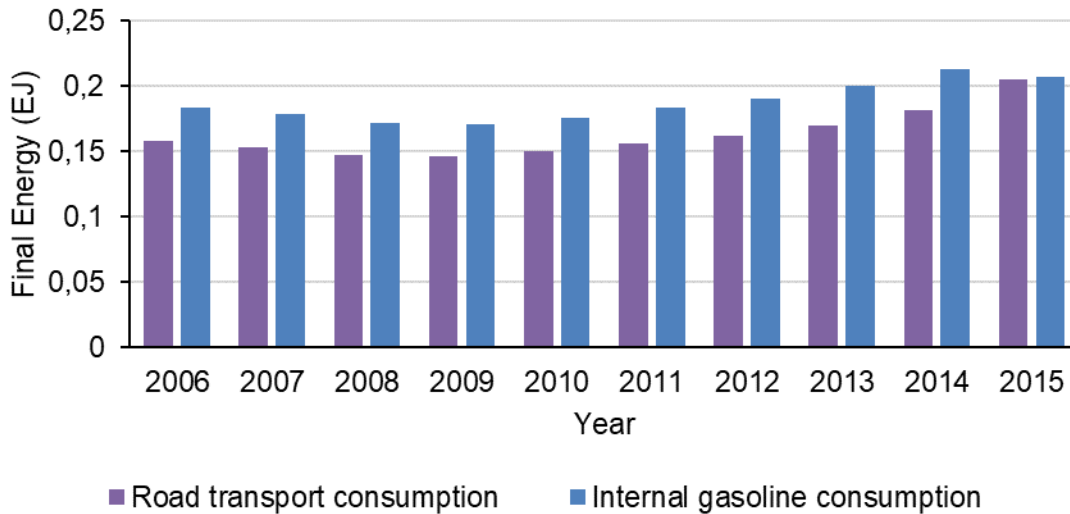


**Figure 1-18:** Historical gasoline consumption in Colombia (UPME, 2016).

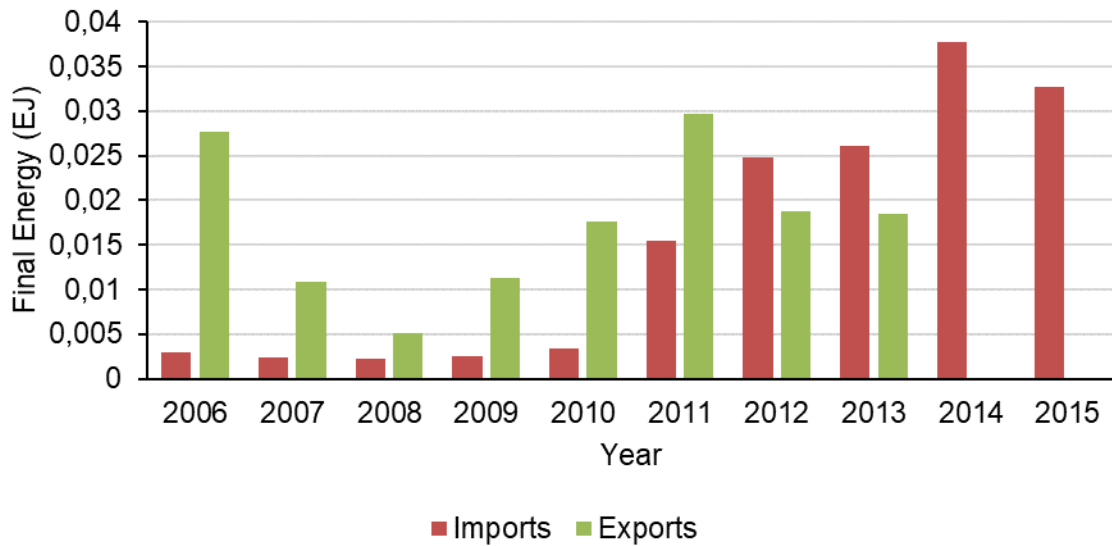


**Figure 1-19:** Gasoline trade balance in Colombia (UPME, 2016).

Last decade was a time of important economic growth in the country oil market but the economic future is not clear because of the dollar prices, geopolitical situation of the world and the local availability of oil. According to the national energy plan to 2050 (UPME, 2015a), the oil reserves available in the country are enough to guaranty the self-supply to 2018. From 2020 the energy supply will decently on the discovery of new hydrocarbon fields or on the change in the local politics to promote alternative energy sources to ensure the local demand. Independent of the source of energy, the demand for transport in the next years is expected to increase continuously. According to the Ministry of Transport in Colombia there were 4,9 million of cars and 6,5 million of motorcycles registered in 2015 with an average annual market from 2000 to 2015 of 300.000 new vehicles and a projection to 2030 of 21,3 million vehicles (UPME, 2015b), see **Figure 1-20**. Projections of the annual trips, based on the population growth, led to annual gasoline future consumptions as reported in **Figure 1-21**. Even in the low scenario, the demand is expected to growth more than 40% to 2025.

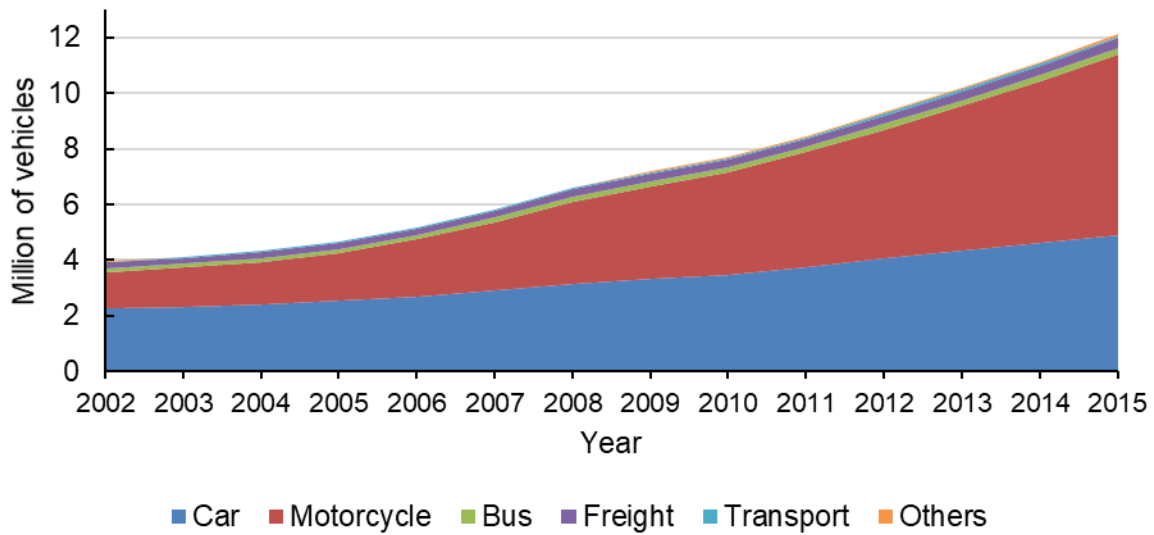


**Figure 1-20:** Vehicles distribution in Colombia (MINTRANSPORTE, 2015).

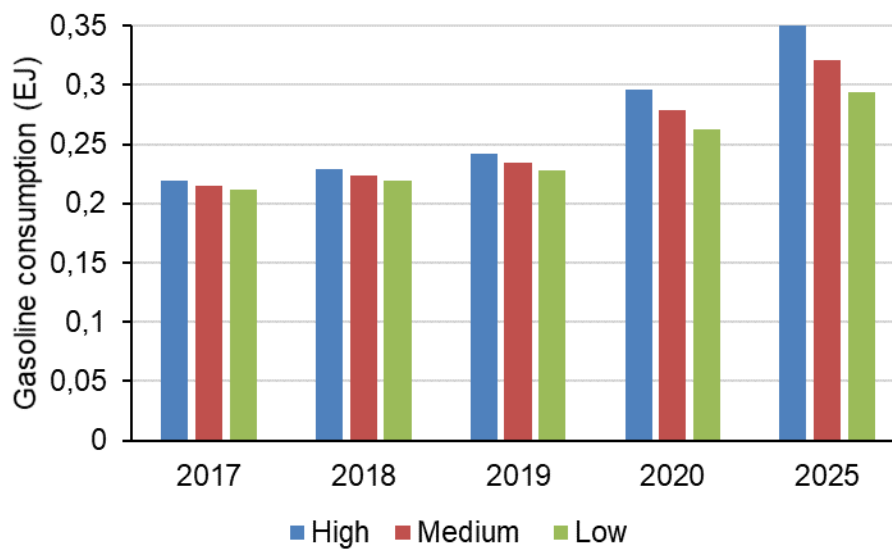


**Figure 1-21:** Projections of gasoline consumption in Colombia (UPME, 2015b).



### 1.8.1 Bioethanol in Colombia

The reasons why Colombia started a program in biofuels production is not clear (Ariel & Alzate, 2009). Three possible reasons could explain the origin of the biofuels program: a) to ensure the energy balance consumption, b) as an answer of the government to pressure done by economic groups with particular interests of in participating in a big market and c) as agricultural impulse with environmental advantages. Nowadays, after 16 year of the start of the bioethanol program, the country is more mature in terms of policies, objectives and industry decision for the promotion of bioethanol production and the establishment of a potential market. According to the National Federation of Biofuels, Fedebiocombustibles, there are two main reasons for produce bioethanol in Colombia (Fedebiocombustibles, 2016):

- a) *Concern about the environment because the cars thrown into the air large amounts of gases that cause diseases to the people and conduce warming the world. The use of bioethanol helps to reduce these gases*

Colombia was country added to the Kyoto protocol in 2001 and has taken part of the UNFCCC with the idea of establishing alternatives to contribute to the mitigation of the climate change. The country periodically publishes the document “*Comunicación del Cambio Climático*” that have the objective of informing the world about the advances in terms of the UNFCCC objectives. The document also presents the inventory of greenhouse gases of Colombia that according to the Ministry of Environment and Sustainable Development (MADS) are calculated in 177 Mt CO<sub>2</sub> eq to 2012, year in which the total GHG emissions due to road transport mode were 25,4 Mt CO<sub>2</sub> eq, see **Figure 1-22**.

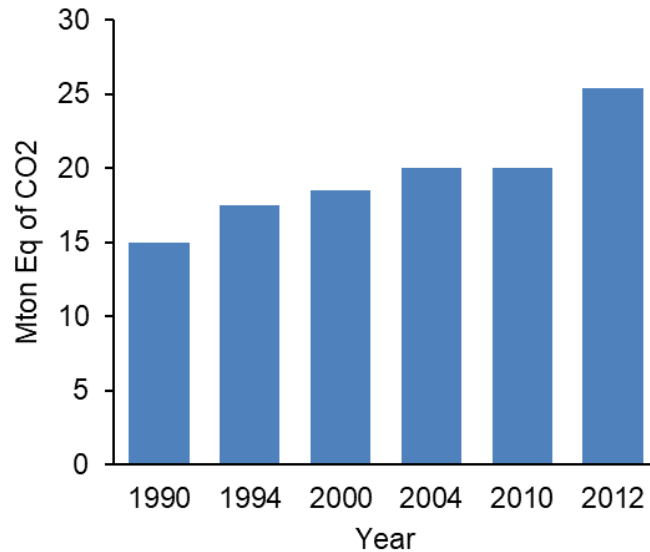


**Figure 1-22:** Historical GHG emission in Colombia due to road transport (IDEAM, 2015).

The effects of the climate change in Colombia are different in each region. Island and coastal areas are susceptible of the worst impacts. As an example, the risk of flooding of San Andres Island is 17% of its total area with complicated consequences like the salinization of 80% of drinking water. On the other hand, the consequences in interior regions of the country include the increasing of desertification in around 3,6 Mhe, flooding affecting almost 2% of the total population of the country to 2030 and modification of the rivers and watercourse in a 50% (MADS, 2016). In order to mitigate the effects of the climate change, Colombia has established the “*Estrategia Colombiana de Desarrollo Bajo en Carbono (ECDBC)*”. This strategy recognized the transport sector as one of the largest emitters of GHG and proposed a plan of mitigation called “*Plan de Acción Sectorial (PAS)*”. The PAS for transport sectors established as one of its politics of action the amount of ethanol in mixture with gasoline up to 10% (MINTRANSPORTE, 2014). Recently, Colombia has committed to the COP21 to reduce its greenhouse gases by 20% to 2030. Bioethanol contribution currently with 12,5% of the GHG reduction target.

The use of fossil fuel not only generates GHG but also generates other pollution materials such a particle matter, sulfur dioxide, carbon monoxide and ozone. These emissions have negatively impact the health of Colombian people with annual expenses of 5700 billion pesos with 5000 early deaths and 4700 new cases of chronic bronchitis. The use of bioethanol in transport helps to mitigate these effects, since it reduce the emissions of particulate matter PM10 in 9%, sulfur dioxide in 26%, carbon monoxide in 11% and ozone in 12% (ASOCAÑA, 2016a).

b) *The fuel comes from oil, which is a non-renewable source of energy and is gradually depleted.*

Colombian energy plan to 2050 states that there are enough oil reserves to meet the domestic demand until 2018. Including non-proved reserves in the projection, the supply can be extended to 2020 without imports, see **Figure 1-23**. A more recent document (García & Camacho, 2016) conclude that in medium term the country will need to adequate its infrastructure to import gas since 2018, and gasoline and diesel since 2020. In the case of transport sector, biofuels as bioethanol and biodiesel can help to mitigate the dependence of the imports that supply the local consumptions and can even be enough to establish an export industry. However, the success of the implementation of biofuel in Colombia must first accomplish goals in terms of vehicle technologies as flex-fuel vehicles, availability of the land to guaranty the production of energy crops, cost of production of the biofuel and other social challenges as the competition of land for food production.

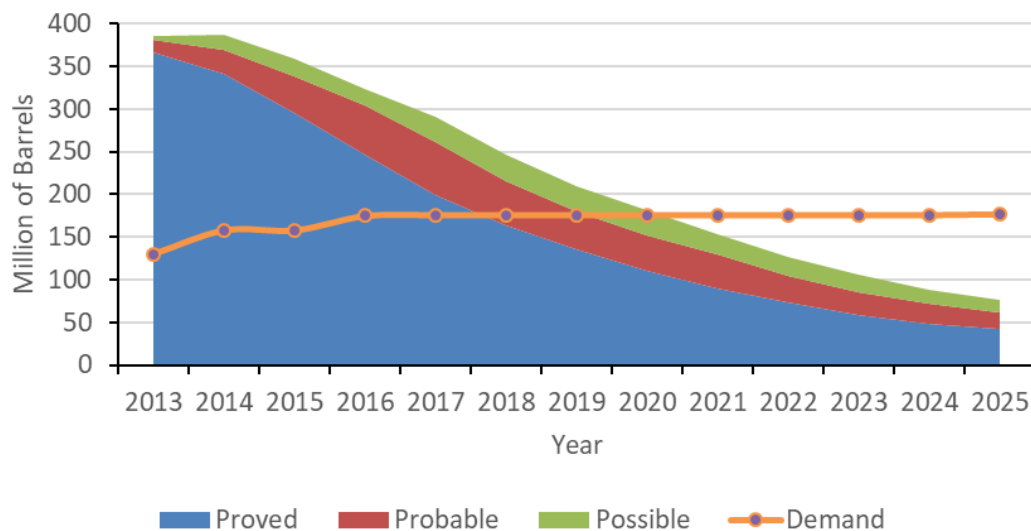


**Figure 1-23:** Reserves of oil in Colombia vs demand, (UPME, 2015a).

The introduction of flexible-fuel vehicles in Colombia is regulated by the decree 1135 of 2009 (MINIMINAS, 2009a). The document decrees that from 2012 gasoline vehicles must adapt their engines to run with mixtures E85. Also it decrees that new vehicles marketed in the further years in Colombia must be of flexible-fuel technology. The objective was to migrate to 100% of this technology in the country market to 2016. However, to 2018 this objective has not been achieved.

## 1.8.2 Legal Framework

Colombia started a policy of biofuels by adoption of the law 693 of 2001 which regulates the use of biofuels of vegetable sources (Congreso de Colombia, 2001). The legal framework of biofuels in the country has focused on promoting the cultivation materials by expanding energy crops, stimulate the production and commercialization of biofuels through tax incentives and regulation of domestic consumption of ethanol by setting of mixtures percent with fossil fuels. **Table 1-4** resume the policy framework of bioethanol in Colombia.

**Table 1-4:** Policy framework for bioethanol (Mejía, 2010).

<b>Regulation</b>	<b>Content</b>
Ley 639 September, 2001	Obligatory use if alcohol fuels
Res. No. 0447 April, 2003	Quality of fuels
Res. No. 180687 June, 2003	Established the mixtures E10
Decreto 2629 July, 2007	Dispositions to promote the use of biofuels in the country
Ley 939, 2004	Stimulate the production of biofuels
Conpes 3510 March, 2008	Policy guidelines for promoting sustainable production of biofuels in Colombia

## 1.8.3 Installed Production capacity

Colombia has 114 Mhe of land area and 98 Mhe of sea. Total area available to agriculture in 2015 was 21,5 Mhe but only 4,9 Mhe are used today. Sugar cane fields in Colombia cover 232 khe of plantation with a possible expansion to 3,9 Mhe (MINIMINAS, 2009b). Colombia has the highest productivity of the world in terms of crops and sugar with 122 ton/he of cane and around 15,5 ton/he, respectively. Total bioethanol production in 2011 in the country used 41 khe of sugar cane crops as raw materials for its production, distributed as can be seen in **Table 1-5**.

**Table 1-5:** Bioethanol installed capacity (ASOCAÑA, 2016a).

No.	Region	Investor	Capacity (L/Day)	Raw sugar (T/year)	Planted area (he)	Direct jobs	Indirect jobs
1	Miranda, Cauca	Incauca	350.000	97.690	11.942	2.171	4.342
2	Palmira, Valle	Ingenio Providencia	300.000	65.126	9.287	1.688	3.376
3	Palmira, Valle	Manuelita	250.000	81.408	8.721	1.586	3.172
4	Candelaria, Valle	Mayagüez	250.000	48.845	6.587	1.198	2.396
5	La Virginia, Risaralda	Ingenio Risaralda	100.000	32.563	3.004	546	1.092
6	Zarzal, Valle	Riopaila Castilla	400.000				
<b>TOTAL</b>			<b>1.650.000</b>	<b>366.632</b>	<b>40.741</b>	<b>7.429</b>	<b>14.858</b>

Colombia has six distilleries in which has invested around 225 million dollars until today. The installed capacity of the distilleries is 165000000 L/day of bioethanol with a production of 456 million of liters in 2015. Currently the construction of six new distilleries is planed which would increase the total production of the country in 1.500.000 L/day, see **Table 1-6**.

**Table 1-6:** Projects of construction to next years (ASOCAÑA, 2016b).

Region	Investor	Capacity (L/Day)
Puerto López – Puerto Gaitán, Meta	Bioenergy	300.000
Tuta, Boyacá	Malquitec *	300.000
Pivijay, Magdalena	Agrifuels S.A.	300.000
Barbosa, Santander	Alcohol del rio Suarez	300.000
Valle R. La Vieja, Quindío	AQA S.A.	150.000
Candelaria, Valle	Ingenio Mayagüez (expansion)	150.000
<b>Total Production</b>		<b>1.500.000</b>

\*bitter yucca.

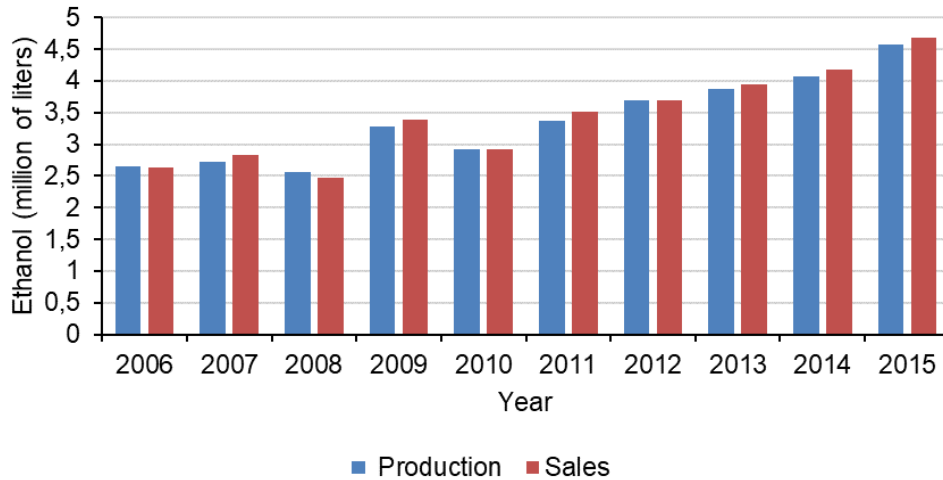


**Figure 1-24:** Bioethanol balance in Colombia (ASOCAÑA, 2016a).

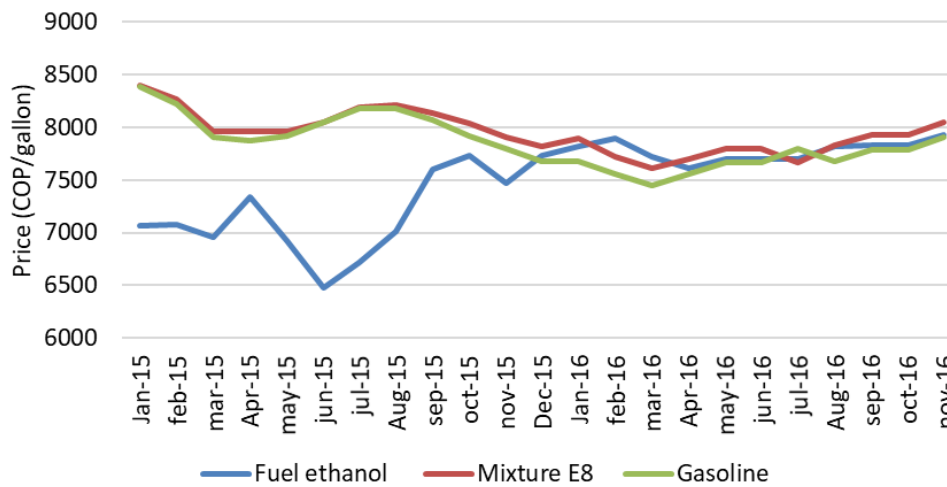


**Figure 1-25:** Price of bioethanol in Colombia in 2015-2016 period (ASOCAÑA, 2016a).

## 1.9 Bioethanol Production Process

There are different bioethanol production processes depending on the raw materials from which it is obtained (Cardona, Sánchez, & Gutiérrez, 2010). One of the most important configurations is based on sucrose-containing materials as sugar cane. The process of obtaining bioethanol from sugar cane can be autonomous or non-autonomous depending on whether it is obtained directly from sugar cane juice or whether it is obtained from its secondary products of industrial sugar production. In Colombian case the production process of bioethanol is made in non-autonomous plants, the bioethanol is produced mostly from molasses resulting from the industrial sugar production. A typical non-autonomous configuration for bioethanol production from sucrose-containing materials comprises the steps shown in **Figure 1-26**.

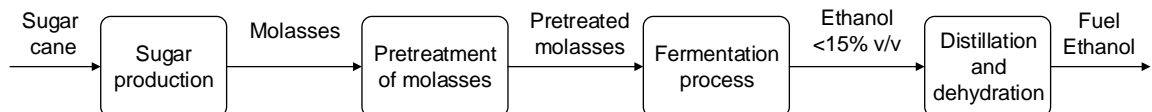


**Figure 1-26:** Stages in a non-autonomous bioethanol production from sugar cane.

### 1.9.1 Sugar production

Sugar production from sugar cane consists of the steps shown in **Figure 1-27**. The process starts with an extraction of sugar juice from the sugar cane in the mill. The bagasse obtained as by-product is dried and used as fuel for generation of electricity for the operation of the sugar plant. The raw juice is sent to the clarifier where it is added sulfur dioxide in order to clarify the juice and destroy the microorganisms carried in it. Then, it is necessary to add lime to neutralize the juice and to avoid the hydrolysis of sucrose to glucose and fructose. The unwanted materials precipitates allowing the separation of the caned juice and a solid material that is used as animal feed. Clarified juice is sent to a multiple-effect evaporator where the juice is concentrated by removing of water until obtain a liquid of around 60° Brix called syrup.

Syrup is clarified by addition of sulfur dioxide, phosphoric acid and lime and then is sent to the vacuum pan. In the pan stage sucrose contained in syrup is crystallized by evaporation at vacuum conditions. The crystals obtained are separated from mother liquor, called molasses, by centrifugation. Molasses are the raw material for the fermentative production of ethanol in this document.

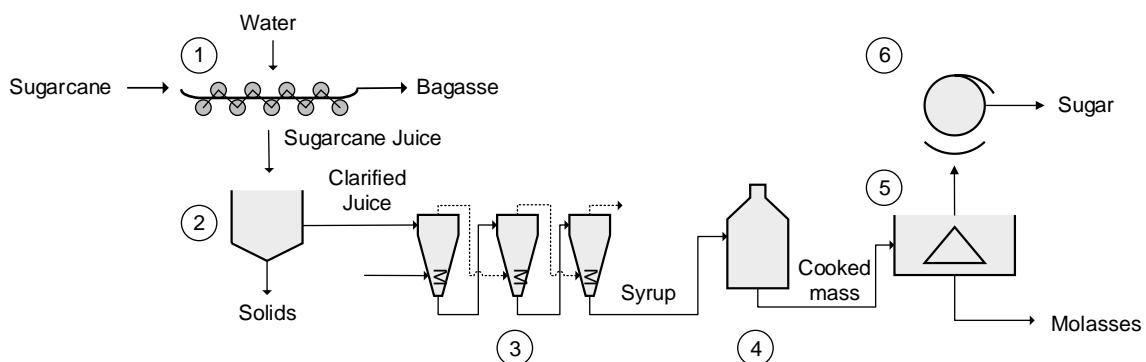


**Figure 1-27:** Process for sugar production from sugar cane. 1-mill, 2-clarifier, 3- multiple-effect evaporators, 4- vacuum pan, 5- centrifuge and 6- rotatory drum.

### 1.9.2 Pretreatment of molasses

The pretreatment of molasses, before being brought to a fermentative process by yeast metabolism, consists of some steps to know: dilution of molasses, acidification of diluted molasses, addition of nutrients for the growth of yeast and removal of ashes in the solution. In the dilution step molasses are brought from a solid content of 80° Brix to a concentration of 25° brix in order to avoid the inhibition of the yeast used in the fermentative process (Cardona et al., 2010). Inhibition is caused by the osmotic pressure that molasses exert on yeast cells due to their high sugar and salt content and dilution reduce this pressure.

Once the molasses has been diluted, sulfuric acid is added to the dilution. Sulfuric acid modifies the pH of the substrate in which the yeast growth with the advantage of facilitating the hydrolysis of sucrose to fructose and glucose. In the fermentation step the yeast synthesizes the enzyme invertase to convert sucrose in their components glucose and fructose. The addition of sulfuric acid reduces the metabolic load of the yeast improving the process. An acid pH also influences the growth of undesirable microorganisms reducing the development of bacteria in the molasses.

Yeast needs nutrients to grow. Even when the molasses is a substrate rich in nutrients, substances as urea and diammonium phosphate are required and are added to the dilution in small amounts. The molasses rich in nutrients are sent to the fermentative step.

### 1.9.3 Fermentation

In the fermentative stage a microorganism consumes a substrate and transform it into bioethanol by means of metabolic processes. In the case of materials rich in sucrose the microorganism most used for the production of ethanol is the yeast *Saccharomyces Cerevisiae*. This yeast can grow in both aerobic and anaerobic environments. However, in aerobic environments its metabolic route is oriented to the production of carbon dioxide preferentially. Under anaerobic conditions the yeast produces ethanol along with byproducts like butanol, isobutanol and isoamyl alcohol. The initial process of reproduction of the yeast, is carried out under aerobic conditions, and after that, the fermentation process is done under anaerobic conditions. Fermentation is made in a controlled system typically at 30°C, a pH range of 4,0 to 4,5, yeast concentration between 0,8-1% by dry weight and continuous agitation (Gil, 2006).



### 1.9.4 Ethanol recovery

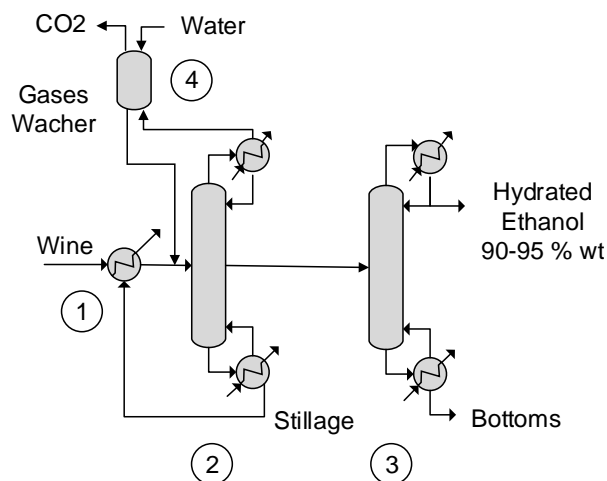


**Figure 1-28:** Concentration and rectification of bioethanol in culture broths. 1- preheater, 2- concentration column, 3- rectification column, 4- gases washer.

To use ethanol as fuel, the content of water must be less than 2% v/v. Culture broths obtained in fermentation oscillates between 3% and 10% v/v of ethanol, which means that a high percent of water must be removed. The stages involved in the pursuit of this objective are shown in **Figure 1-28**. Culture broths from fermentation (wine) are preheated and feed to the concentration distillation column (sometimes called bear column) from where ethanol is obtained as side stream at 35-50% v/v. Higher concentration is achieved in a second column called rectification column. Maximum concentration obtained in this column is limited by a thermodynamic condition called azeotropy. In this condition, separation by conventional distillation is not possible, since the concentration of the components in the liquid phase and vapor phase in equilibrium are similar (a concentration of 96% v/v of ethanol).

## 1.10 Dehydration technologies

In order to obtain ethanol of a concentration up to 96 % v/v. special dehydration technologies must be used. These technologies can be classified in general separation processes, that include pressure swing distillation, pervaporation and adsorption, and entrainer addition distillation methods.

The addition of a third component to a liquid mixture forming an azeotrope can change the physicochemical behavior of the vapor liquid equilibrium VLE and can offer different opportunities for separation of the original mixture. The additional component is called as entrainer in this document, but some other terms, as solvent, separation agent or extractants, among others, are used. Based on the role and properties of the entrainer, the most common distillation separation methods for separation of azeotropic mixtures by entrainer addition are: homoazeotropic distillation, heteroazeotropic distillation and extractive distillation. Some less common entrainer methods that are not discussed in this document are reactive distillation, chemical drying and distillation in presence of salts.

### 1.10.1 Pressure swing distillation

The composition of an azeotrope in a mixture varies with the pressure of the system. In the case of ethanol water mixtures, the azeotrope changes as shown in **Figure 1-30**. Pressure swing distillation technology uses this change to overtake the azeotrope. The process configuration to do it is shown in **Figure 1-29**. Ethanol of concentration near to the azeotrope is feed to column I that works at 1 atm. Column I separate the feed F1 in two streams B1 that is basically water and D1 of concentration in the azeotrope at 1 atm. D1 is feed to column II that works at 10 atm, and is separated in distillate D2 of azeotropic composition at 10 atm and the bottoms B2 of ethanol fuel grade.

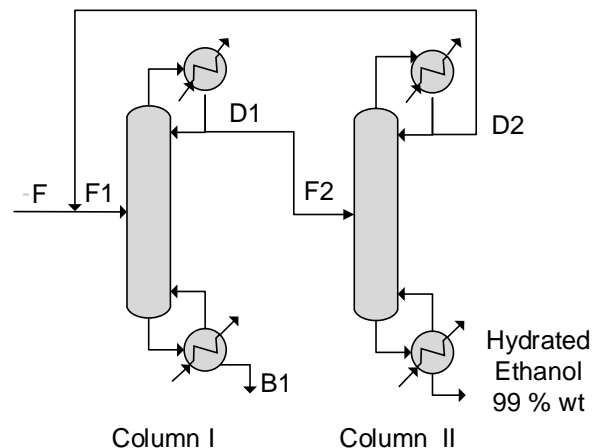


**Figure 1-29:** Configuration for pressure swing distillation.

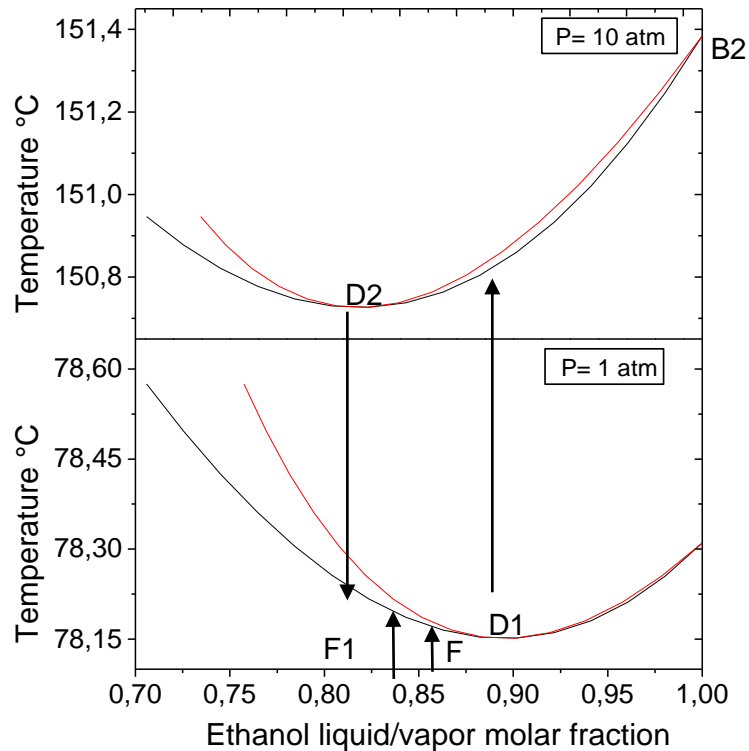


**Figure 1-30:** Effect of the change of pressure in the azeotrope composition. Data obtained from Aspen plus vapor equilibria simulation.

### 1.10.2 Azeotropic distillation

The azeotropic distillation is a separation process that consists of the addition of an entrainer to the ethanol water mixture with the formation of a new azeotrope. Azeotropic distillation can be of one of two types depending on if the new azeotrope is a homoazeotrope or is a heteroazeotrope. In the homogeneous azeotropic distillation the entrainer is completely miscible with the original mixture, as well as with the new formed azeotrope. As the azeotrope is miscible in the solution, the separation is carried out in a single distillation column. The new azeotrope formed in heterogeneous azeotropic distillation generates a new liquid phase and its separation is carried out by a combined column and decanter configuration.

### 1.10.3 Extractive distillation

The extractive distillation is a separation process based on the addition of a separation agent that is miscible with the mixture to be separated. The separation agent has a higher boiling point than the other species in the mixture and doesn't form azeotropes with them. Extractive distillation of bioethanol uses a large amount of the entrainer that modifies the activity coefficient of the mixture ethanol-water, and consequently, modifies the relative volatility of the ethanol, as can be seen in **Figure 1-31**. When there is not solvent, the vapor-liquid equilibrium line touches the 45° line indicating an azeotropy. While the amount of entrainer (in this case ethylenglycol) is increased, the pseudo equilibrium line moves away from the 45° line without azeotrope formation as in the 30% line. If more solvent is added the relative volatility of the ethanol in the mixture increases and the separation process becomes easier.

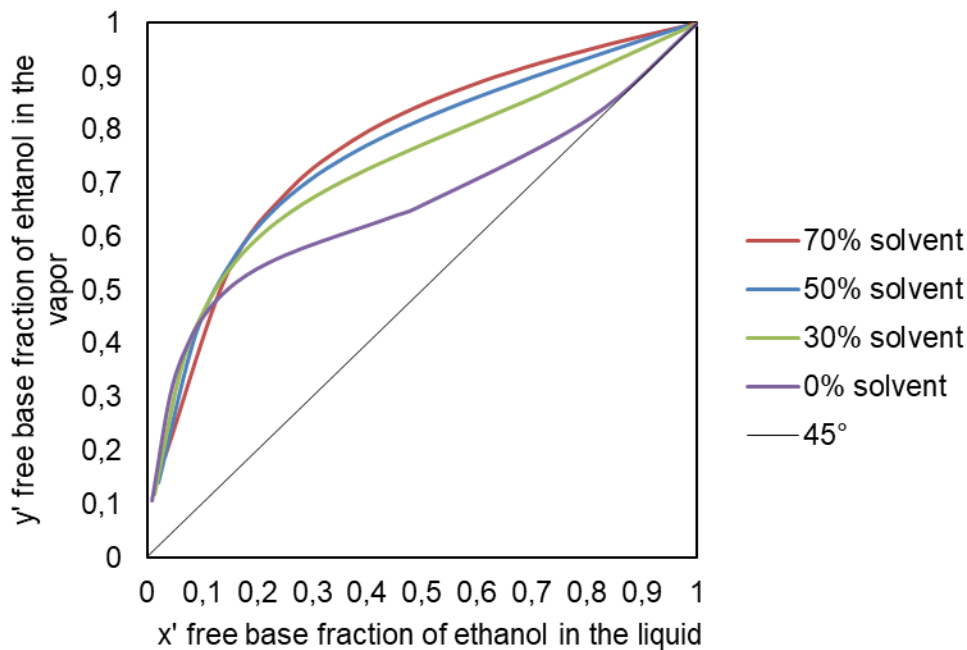


**Figure 1-31:** Pseudo diagram vapor liquid equilibrium for extractive distillation with ethylene glycol as solvent.

The scheme for dehydration of bioethanol by extractive distillation is shown in **Figure 1-32**. The separation equipment consists of a first two-feed column called extractive column and a second single-feed column called recovery column. The feed stream coming from the rectification train is fed to an intermediate stage of the extractive column and the entrainer is fed to an upper stage near to the top of the column. The distillate product of the extractive

column is rich in ethanol and the bottom product is a water-entrainer mixture that is fed to the recovery column. The objective of the recovery column is to recover the entrainer in order to recirculate it, and thus, to reduce the capital cost of the separation process. The distillate product of the recovery column is mostly water and the bottom product is the entrainer.

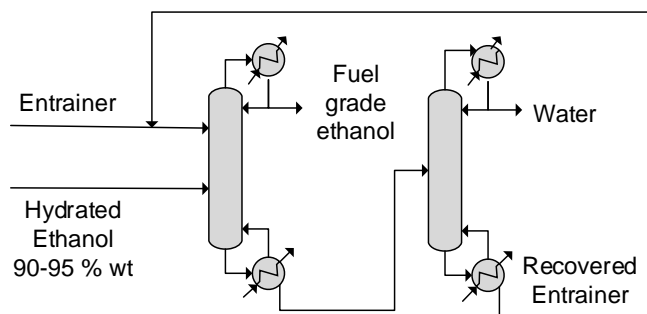


**Figure 1-32:** Extractive distillation scheme for bioethanol dehydration.

### 1.10.4 Adsorption

The adsorption is a separation process based on a solid agent that sorbs certain species from a liquid or vapor phase to its surface area. In the case of ethanol dehydration, sorption refers to the selectively transfer of water molecules from the ethanol-water mixture to an insoluble solid called adsorbent. Common adsorbents for ethanol dehydration in liquid phase are zeolites of type A and cellulose based materials. In the case of vapor phase some inorganic adsorbents such as zeolite molecular sieves 3A and 4A are commonly used as well as lithium chloride and silica gel (Frolkova & Raeva, 2010).

Industrial dehydration of ethanol by adsorption implies the pass of ethanol water mixture through an equipment containing the adsorbent material. The equipment can be one of the three types: stirred-tank, cyclic fixed-bed or continuous countercurrent operation. As the ethanol water mixtures is feed to the adsorption equipment, water molecules (adsorbate) remain in the solid agent by one of two types of adsorption: chemisorption or physical adsorption depending on whether chemical bounds are formed or if the attraction is due to Van der Waals interactions respectively. The output of the equipment is a concentrated ethanol that can overcome the azeotrope composition and can be used as fuel ethanol.

As the adsorbent material is now saturated, a recover procedure must be established in order to reuse the solid agent and reduce the capital investment of the dehydration plant.

There are five methods to regenerate the saturated adsorbent material: thermal swing adsorption (TSA), pressure swing adsorption (PSA), vacuum swing adsorption (VSA), inter purge swing and displacement purge (Seader, Hendley, & Roper, 2011). The regeneration of the adsorbent material implies a dead time of the equipment for the dehydration of ethanol, and in order to avoid this disadvantage, it is common to use two adsorption equipment in parallel that helps to operate the plant in continuous.

### 1.10.5 Pervaporation

The pervaporation is a separation process through the use of membranes. The word pervaporation is a contraction of permeability and evaporation. Permeability refers to the preferential pass of molecules from a liquid mixture through membranes without modifying altering the internal structure of the membrane. **Figure 1-33** right shows a diagram for separation of an ethanol-water liquid mixture in which the dark spots represent water molecules and the light spots represent ethanol molecules. In the equipment shown, the points pass through the membrane due to a pressure difference between both sides of the membrane  $P_1 > P_2$ . The transport mechanism through the membrane consists of three stages: absorption of the components of the liquid mixture in the walls of the membrane, diffusion of the molecules absorbed by the membrane from the high pressure section  $P_1$  towards the side of low pressure ( $P_2$ ) and desorption of the molecules on the surface of lower pressure  $P_2$ . In the right side of the membrane the low pressure leads to a calorific effect of evaporation in which the molecules in the surface are removed instantaneously. Pervaporation can be plotted on a vapor-liquid diagram, as shown in **Figure 1-33** left. The pseudo equilibrium curve for the membrane separation shows a good selectivity to water with feed composition greater than 0,8 mol fraction of ethanol. Below this composition the selectivity of the membrane decrease and more molecules of ethanol can pass through the membrane. In order to avoid this, the pervaporator with PVA membranes must be fed with a composition near to the azeotrope.

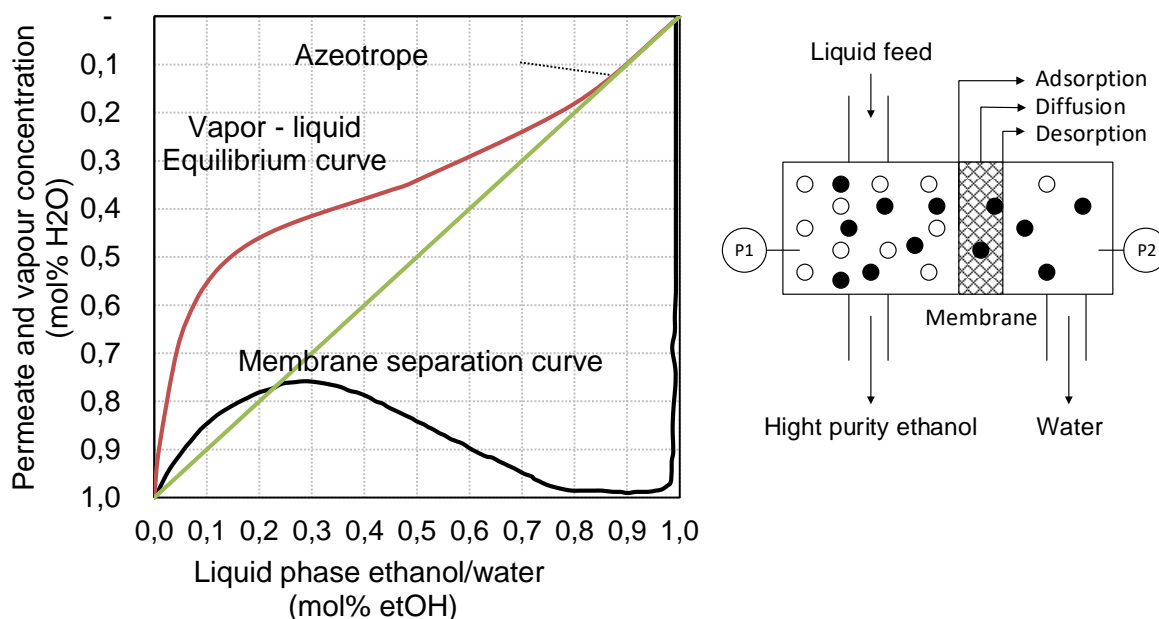


**Figure 1-33:** Left: Pervaporation Pseudo equilibrium curve of PVA membranes and Vapor liquid equilibrium for ethanol water system, from (Sander & Soukup, 1988). Right: pervaporation mechanism  $P1 > P2$ .

### 1.10.6 Comparison of dehydration technologies

The selection among ethanol dehydration technologies is an open-ended problem in which chemical engineers usually want to find the alternative with the lowest cost. However, in the practice it is not common to find two engineers doing the same comparison based on equivalent process circumstances, and consequently, their decisions do not necessarily lead to the selection of the same dehydration technology. The reason for this is easy to understand, since the engineers are immersed in a social context that requires them to think in aspects related to safety and environmental restrictions while ensuring the operability and profitability that investors want. To help themselves, engineers use different selection tools, such as heuristics, the criteria of an expert designer, a selection matrix, etc. However, in many cases it is necessary to design different alternatives and to decide based on an economic criterion. **Table 1-7** shows a cost comparison of technologies for dehydration of ethanol. The assumptions for the comparison are reported in (Cardona et al., 2010). Obtained results show a cost disadvantage in the case of vacuum PSD compared to the other technologies. Molecular sieves have the lowest operating costs but its capital cost gives a disadvantageous weight in the total cost calculation, in comparison with azeotropic and extractive distillation. Extractive distillation is the lowest cost technology

in the study case reported and has advantages in terms of safety and environmental impacts because the entrainer, ethylene glycol, in extractive distillation is less toxic than, in azeotropic distillation.

**Table 1-7:** Cost comparison for ethanol dehydration by different technological alternatives. Initial composition 11,4%. Taken from (Cardona et al., 2010).

Item	Units	Vacuum PSD	Azeotropic Distillation	Extractive Distillation	Molecular Sieves
<b>Ethanol produced</b>	kg/yr	141.560.084	142.609.349	141.897.940	142.726.998
<b>Total capital costs</b>	US\$	14.156.063	9.547.963	9.525.920	12.809.706
<b>Total operation costs</b>	US\$/yr	11.539.808	8.943.642	8.023.714	7.730.563
<b>Utilities</b>	US\$/yr	9.063.508	7.113.850	6.266.715	53.821.429
<b>Labor</b>	US\$/yr	600.000	600.000	600.000	600.000
<b>Maintenance costs</b>	US\$/yr	381.000	78.000	75.100	191.000
<b>Other</b>	US\$/yr	1.495.300	1.151.592	1.081.899	1.118.134
<b>Unit capital costs</b>	US\$/kg	0,1000	0,0670	0,0671	0,0897
<b>Unit operation costs</b>	US\$/kg	0,0815	0,0627	0,0565	0,0542
<b>Unit total costs</b>	US\$/kg	0,1815	0,1297	0,1236	0,1439

A similar study, but now considering energy rather than cost, give a analogous idea of the advantages of extractive distillation in comparison with other cited dehydration technologies, see **Table 1-8**.

**Table 1-8:** Energy consumption of some dehydration technologies. Taken from (Gil, 2006).

Technology	Feed composition	KJ/kg ethanol
Azeotropic distillation with benzene	85% molar ethanol	4853
Azeotropic distillation with benzene	85% molar ethanol	4188
Azeotropic distillation with hexane	85% molar ethanol	6063
Azeotropic distillation with cycle hexane	85% molar ethanol	6037
Azeotropic distillation with toluene	85% molar ethanol	8114
Extractive distillation with potassium acetate	60% molar ethanol	9270
Extractive distillation with calcium chloride	20% molar ethanol	1998*
Extractive distillation with ethylene glycol	85% molar ethanol	1760
Extractive distillation with gasoline	85% molar ethanol	3180
Pervaporation	8% peso ethanol	4602
Molecular sieves	Azeotropic composition	1430

A review of the bibliographic data base *Scopus*, using “ethanol dehydration” as search parameter, shows a year by year growing tendency in the study of dehydration of ethanol,



see **Figure 1-34**. Including the name of each technology as a search parameter, together with “ethanol dehydration”, it is possible to obtain the number of documents related to each technology of dehydration of ethanol, see **Figure 1-35**. The fields of search in both cases were “Article title, abstract, keywords”. The results show pervaporation as the technology with more documents published with the selected parameters, followed by adsorption, and extractive and azeotropic distillation covering the third place.

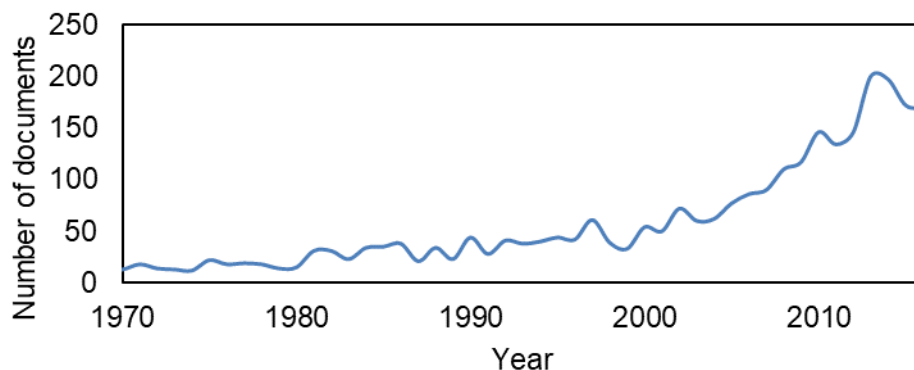


**Figure 1-34:** Analyze search results in Scopus for ethanol dehydration.

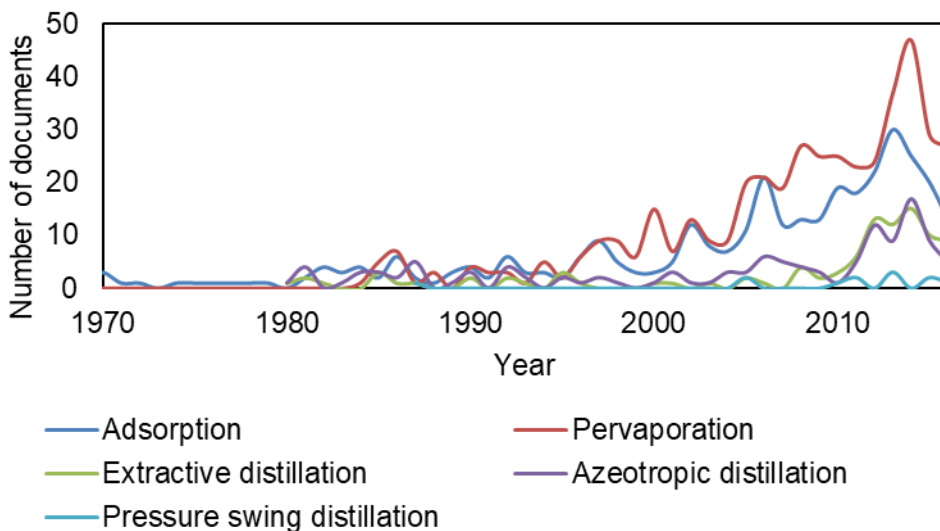


**Figure 1-35:** Analyze search results in Scopus for ethanol dehydration by technology.

Even when extractive distillation is not the most studied technology, it is still a technology of interest in the world. But, ¿who is interested in this technology? **Figure 1-36** shows the ten countries with more published documents about extractive distillation according to Scopus analysis. It is remarkable the presence of Latin American countries in the study of this technology, in comparison with the data shown in **Figure 1-37** for adsorption documents producers.

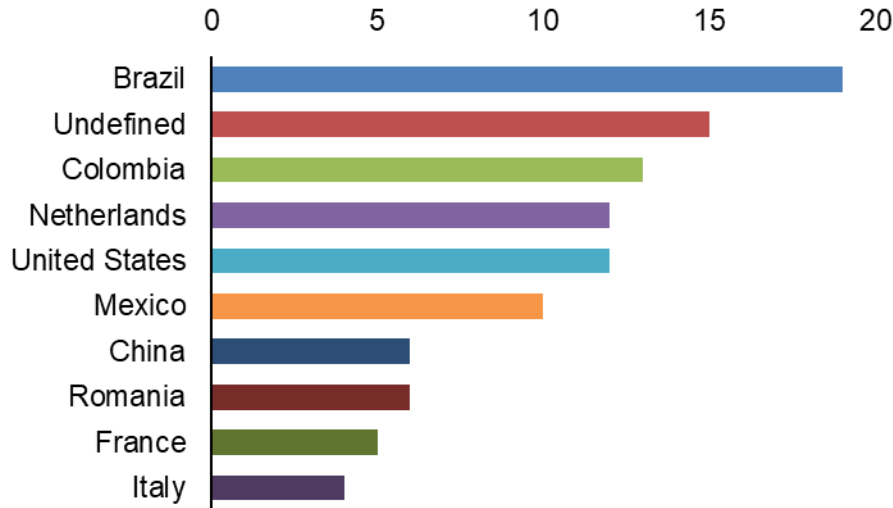


**Figure 1-36:** Ten countries with most published documents in Scopus with “extractive distillation” and “ethanol dehydration” as search parameters. 1980 to 2016.

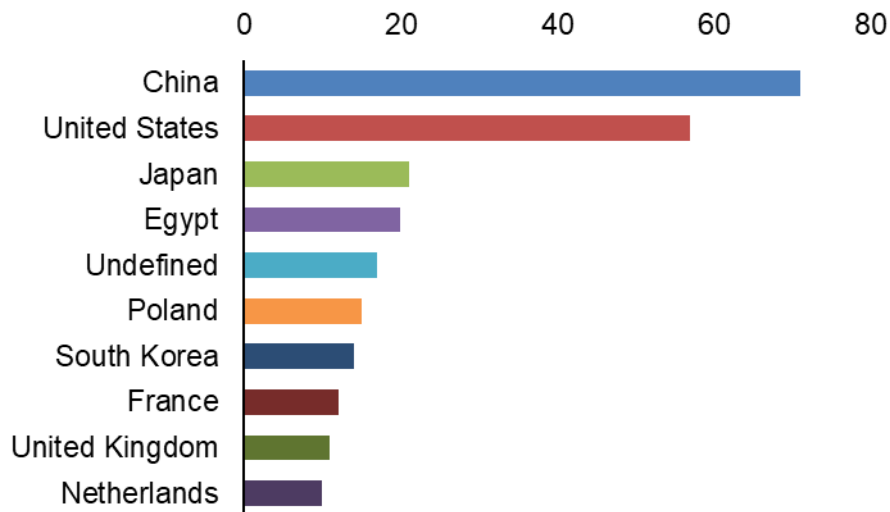


**Figure 1-37:** Ten countries with most published documents in Scopus with “adsorption” and “ethanol dehydration” as search parameters. 1980 to 2016.

Ethanol dehydration in Colombia is made by adsorption with molecular sieves. However the technology used comes from India and has clauses that limit the country’s knowledge used in its ethanol dehydrating plants (Guerrero, 2014). On the other hand, extractive distillation has some advantages for Colombia as it is a technology based on a well-known knowledge of the conventional distillation. Moreover, the construction, operation and maintenance of the hardware used in this technology is better understood by the technical and professional personnel available in the country.

## 1.11 Conclusions

Bioethanol importance was studied from an international geopolitical point of view, regional point of view and national point of view. It was concluded that there will be a continuous growing in the demand of this biofuel in future years as consequence of growing population and economy and as consequence of the risk for the energy security of the countries that implies the dependence in fossil fuels.

It was found that an important investment in renewables sources of energy that is motivated by world energy policies for mitigation of the global climate change and the actual situation of different geopolitical scenarios. However, future predictions consider an energy supply predominantly based on fossil fuels.

It is concluded that renewables not only have advantages in substituting fossil fuels but they also represent an important source of jobs and ensure the energy risk of the countries as they are based on indigenous sources.

The analysis the available of arable land, crops yield and climate advantages, it is concluded the importance of Latin American countries as source of liquid biofuels for the global energy demand of transport media.

It was not possible to clarify how the bioethanol policy in Colombia emerged. However, it was shown that the actual development of this market and industry by means of the analysis of installed capacity and capacity in construction, labor force and employment generation, local policy, local consumption and market.

A review of technologies involved in dehydration is made. By means of technological surveillance, it is concluded that developed countries have a preference for adsorption based dehydration technologies and developing countries as Latin countries prefer distillation based dehydration technologies.

This chapter led to recognize the relevance of the study case presented in this thesis for the conceptual design of conventional and non-conventional extractive distillation sequences.



## 2. Conceptual design and tools for extractive distillation design

Design research is often identified as the developing of theories to support computational methods used in design calculations (Westerberg, 1981). In this way, the present chapter introduces the theories of synthesis and analysis for the conceptual design of extractive distillation systems. As extractive distillation is highly influenced by vapor liquid equilibrium, this chapter presents some ideas for its calculation. Finally, computational tools based on nonlinear analysis of distillation are also described and applied to the study of the Ethanol-Water-Ethylene Glycol system.

### 2.1 Process Design

Chemical process design is a creative and complex process of which the objective is, in a simple way, the definition and selection between different process configurations that makes possible the conversion of feedstocks into a valuable product. To achieve this objective, chemical engineering tries to establish systematic procedures that are commonly guided by the stages listed in **Table 2-1**. Depending on the nature of the design problem, the stages listed can be carried out under different engineering perspectives such as sequential engineering, reverse engineering, reengineering and concurrent engineering (Dhillon, 1998). Once the design has been established, it can be evaluated based on technical, techno-economic, financial, environmental and/or other criteria. This evaluation is concluded in a decision between possible designs.

**Table 2-1:** Common stages of a process design (Cardona et al., 2010).

Stages
Analysis of the chemical reaction
Conceptual process design
Process development
Process assessment
Detailed engineering
Plant operation
End Cycle of life

In the case of bioethanol process design, the first stage in **Table 2-1**, “analysis of the chemical reaction”, is commonly assumed to be clearly established as bioethanol is a commodity product. The second stage, “conceptual process design”, is the stage of interest studied in this chapter. Some approximations to the “process development”, “process assessment” and “detailed engineering” are given in this and future chapters and appendix.

Conceptual design is applied for new designs (grassroot design). It is used in chapter 3 for the design of conventional extractive distillation. In chapters 4 and 5, the study of dividing wall column DWC and sequential heat exchanger column SHEC will be presented. These technologies are not necessarily new designs but retrofit designs. A retrofit design is a physical modification of an existing plant. This thesis presents a retrofit study of the conventional extractive distillation design described in chapter 3. The retrofit design (as well as this document) is motivated by, among others reasons, the reduction of operation and capital costs as the use of existing equipment is maximized.

## 2.2 Conceptual Design

Conceptual process design stage involves two terms called synthesis and analysis, see **Figure 2-1**. Synthesis represents an open-ended activity of which the objective is to compare different alternative processes in order to identify feasible flowsheets and ranges of operating conditions of the process. Analysis is an activity that categorizes the alternative flowsheets and ranges based on a defined criterion, for example economic cost. Process synthesis starts from the definition of individual transformations units and then interconnects them to produce global processes represented graphically in process flow diagrams (flowsheets). In analysis, these processes are modeled mathematically and

varied between the selected ranges in order to define equipment sizes, process configurations and operations conditions. The answer of the mathematical model of the process is used then to evaluate it.

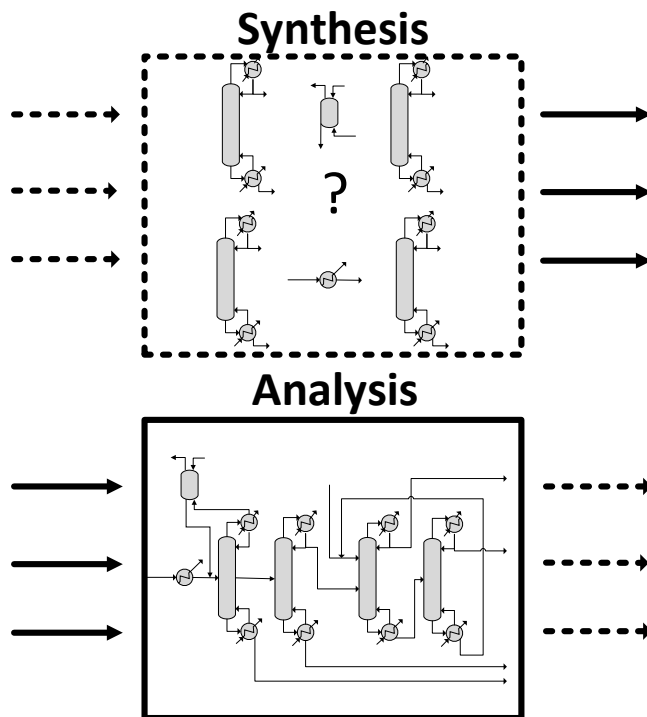


**Figure 2-1:** Design = Synthesis + Analysis. Adapted from (Smith, 2005)

### 2.2.1 Process synthesis

The synthesis and analysis of an entire chemical process is commonly a complex activity. For this reason, the design problems are often broken down in subtasks. Bioethanol production process, introduced in chapter 1, is an example of complexity and its design is not a trivial activity as can be deduced from (Cardona et al., 2010). To better understand this process, it was broken down into four subtasks shown in **Figure 1-26**. Each one of these subtasks, as well as the heat exchanger network, the complete flowsheet and the control system of the process, can be subject of synthesis in a separated but interrelated form (Nishida, Stephanopoulos, & Westerberg, 1981). (Douglas, 1988) has established a way to do this that is recognized as a hierarchy decomposition approach to design. For the production of bioethanol, the hierarchy approach starts with the synthesis of the fermentation process, which is the core of the entire process, and is followed by synthesis of the separation train or the separations process subtask. The synthesis of the

fermentation process is out of the scope of this document. On the other hand, in this thesis, the study of the separation train is reduced to the single study of the azeotropic separation system as the rest of separation is based on clear knowledge of conventional distillations columns.

### **2.2.1.1 Separation process synthesis**

The synthesis of separation processes deals with two main problems: 1) finding the optimum sequence of separations and the nature of each separator and 2) finding the optimal design values for each separator (sizes, operating conditions) (Nishida et al., 1981). Several approaches have been established in the case of the first problem (Li & Kraslawski, 2004). The most clearly established are (Barnicki, Hoyme, & Siirola, 2006) :

- a) Superstructure optimization: in this approach a superstructure containing as much as possible of the applicable separation alternatives is created and then the less desirable alternatives of the superstructure are systematically discarded. Superstructure optimization method usually employs mixed integer nonlinear programming.
- b) Evolutionary modification: this method starts with an initial separation sequence for a similar separation, identify evolutionary rules and finely determine the evolutionary strategy. Evolutionary method usually employs flowsheets in patents or encyclopedias for the process synthesis as well as different design heuristics. A typical example of this method is the synthesis based on standard flowsheets for azeotropic and extractive distillation.
- c) Systematic generation: in this method, a portfolio of basic separators is available and some of them are sequentially selected to solve the separation problem. This method uses heuristics rules and physicochemical properties to solve the synthesis problem. Heuristics can be restricted to ideal distillation sequences or generalized to include other separation methods as extractive distillation, absorption, pervaporation among others. Some properties of importance in the systematic generation method of synthesis are molecular properties (as molecular weight, Van der Waals volume, dipole moment) and thermodynamics properties (vapor pressure, adsorptivity, solubility, diffusivity).



The second problem of the separation process synthesis involves a routinary design. As the routinary design is highly analytical, it depends on a large and extent understanding of specific separation units. An introduction to the understanding of different separation process is given by (Seader, Ernest, & Henley, 2006). These authors conveniently established that a separation process can be based on a phase addition (or creation), on a barrier (by a solid agent and by an external field) and on a gradient (for example of velocity). However, a better solution to the problem of the routinary design will need specialized literature in order to find the better specifications and operation parameters of the selected separation unit.

### **2.2.2 Process analysis**

Process analysis refers to the application of scientific methods to the recognition and definition of problems and their solving procedure. It means, to establish the physical phenomena in mathematical terms, formulate detailed mathematical models based on analysis of the problem and obtaining results to ensure the understanding of the process (Himmelblau & Bischoff, 1968). The process analysis allows to evaluate the process in global terms and to compare it with other processes or configurations. The comparison is usually made in terms of cost but can also be made based on technical, mathematical, phenomenological and/or physicochemical aspects.

Process analysis have a great importance in both design and operation of plants. In the case of operation, it works mainly in the field of optimization and control of operating variables. It also leads to study changes in operation conditions which may not be possible by direct manipulation on plant. In design, process analysis could help the designer to support his ideas and to give him bases of comparison and selection based on established criteria. In both cases, operation and design, analysis requires modeling tools such as mathematical models, physical models, analogical models, among others. In most cases, process analysis uses conceptual models based on mathematical expressions. In the case of chemical engineering there are three common types of models: models of transport phenomena, population balance models and empirical models (Himmelblau & Bischoff, 1968). The evaluation of these models requires of the collection of experimental data and comparison with the model results. If the agreement of the model with the data is acceptable the model is used. If not, it must be modified.

Analysis made in this document is based on simulation. The objective is to test basic parameters of the studied systems in terms of technical and economic comparison criteria. Simulations are carried out in Aspen Plus software of Aspen technology, Inc. Used thermodynamic and equipment models are explained in later sections of the document giving the great importance of physical property on process analysis.

## 2.3 Distillation based separation process synthesis

Distillation is commonly described as the most important separation process in the chemical industry. Distillation consists of the successive evaporation and condensation of a liquid mixtures with preferential enrichment of the vapor phase in the more volatile component. Conceptual explanation of distillation is based on the behavior of the vapor phase equilibrium. The separation principle in this operation is the difference in volatilities of the components in a liquid mixture, and the separation agent is heat transfer. Several processes have put into practice the knowledge of distillation with good performance. Most of the separation processes for liquid mixtures in the world are related to distillation. The study of distillation based separation process is commonly divided in two cases: the distillation of thermodynamically ideal systems and the distillation of thermodynamically non-ideal systems. Synthesis of both cases is described below.

### 2.3.1 Ideal case

The synthesis problem in distillation based separation processes consists of a systematic synthesis of a process that is able to separate the desired products from a feed stream of known conditions (Nishida et al., 1981). Section 2.2.1.1 showed that the first question that it can be made is ¿how to find the optimum sequence of separators?. A question that may arise immediately after this is how many sequences can there be for the separation into pure components of a mixture of  $N$  species? (Thompson & King, 1972) proposed the next equation to answer this question in the case of ideal mixtures:

$$R = \frac{[2(N - 1)]!}{N!(N - 1)!} M^{N-1} \quad (2.1)$$

Where:  $R$ : is the number of sequences  
 $N$ : is the number of components  
 $M$ : is the number of different types of separators

As the number of possible sequences for the separation of  $N$  components to its pure products can be enormous ( $R=1430$  for  $N=9$ ), the selection between all the possible sequences is not a trivial decision. The approaches shown in section 2.2.1.1 can be applied here for making the decision. In the case of distillation based separation synthesis, these approaches usually start with ranking the components based on the relative volatilities, and then reducing the problem as much as possible with heuristic rules before developing the chosen methodology.

### 2.3.1.1 Solution to the synthesis problem considering energy integration.

The optimal sequential column configuration for the separation of ideal mixtures has also been studied from the point of view of heat integration. **Figure 2-2a** shows a simple two product distillation column. As distillation columns require heat at high temperature in the reboiler and release heat at low temperature from the condenser, the synthesis of distillation process can include the problem of to find the optimal conditions to degrade heat in order to achieve the separation of a mixture. Two approaches have been developed to solve this problem (Biegler, Grossmann, & Westerberg, 1999):

The first approach is shown in **Figure 2-2b** where part of the heat needed for the separation is added into the column in down stages (interheating) and a part of the heat is removed from the top stages of the column (intercooling). A column with interheating/intercooling spends the same energy than a column with heat transfer only in the boiler and condenser and as the heat transfer is made in indirect form, more investment in capital cost of the column is required. However, interheating/intercooling have some cost advantages if the separation is analyzed from the plant point of view. In Chapter 4 this idea is further developed.

The second approach is based on heat transfer due to direct mixture of streams with different temperature. One example of this configuration is shown in **Figure 2-2c**. Side stripper showed is considered an alternative that reduces the heating and cooling requirements of a column. If the side column has a condenser instead of a reboiler the configuration is called side enricher. Both side enricher and side column seems to have

reductions in energy costs of around 20-40% and similar savings in capital investment. In Chapter 3 the ideas of this integration approach are further developed.

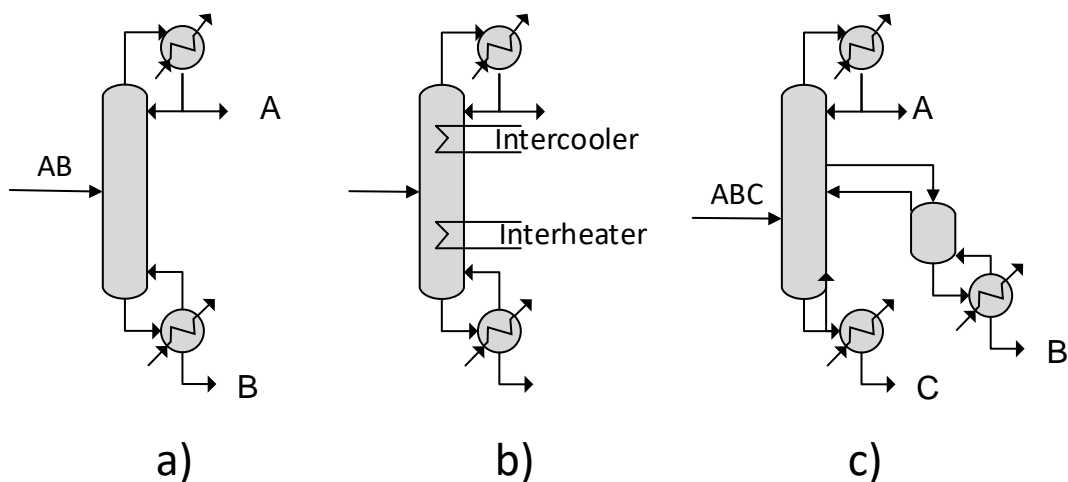


**Figure 2-2:** a) Simple two product column b) column with interheating/intercooling c) column with a side stripper.

### 2.3.2 Non-ideal case

Distillation separation based process synthesis for non-ideal behavior is less understood than the separations of mixtures with ideal behavior. The presence of azeotropes makes impossible to obtain pure components by ordinary distillation and there are no clear globally accepted rules for the sequencing of the separation columns. One of the differences of azeotropic distillation separation sequences with respect to zeotropic distillation is that in the azeotropic distillation the top and bottom products are constrained by the feed composition whereas in zeotropic distillation they don't. For zeotropic distillation of binary mixtures, the top product and bottom product can be respectively the most and less volatile components. In azeotropic distillation one of the products (top or bottom) can be one of the components in the mixture and the other product is the azeotrope. The definition of which one of the components or azeotropes comes from the top (bottoms) depends on the feed condition (Doherty & Caldarola, 1985). Without a priori knowledge of the azeotropic distillation boundaries of the system it is not possible to develop the synthesis of the separation train for these mixtures.

To solve the synthesis problem of the separation train for non-ideal systems with presence of azeotropes, (Westerberg & Wahnschafft, 1996) established an analysis-driven synthesis approach. In this approach, the synthesis process begins with a pre-synthesis analysis (pre-analysis) which characterizes the behavior of the species in the feed mixture and then, in a post-synthesis stage, a specific equipment is chosen and evaluated to determine the better configuration between different options. This means that post-synthesis analysis implies the column design: the estimation of the reflux ratio, number of stages and feed location.

There are two types of pre-analyses in the approach shown by (Westerberg & Wahnschafft, 1996): one based in the equilibrium phase behavior of the species in the feed mixture (e.g. finding azeotropes, liquid-liquid behavior, pressure dependences), and another based on the behavior of a piece of separation equipment (in this case, the distillation column). Both types of pre-analyses use the thermodynamic topology that, once is understood, allows establishing infeasible specifications and alternative distillation sequences without trial and error. Thermodynamic topological analysis of distillation (in Russian literature) or residue curve maps (in other literature) are graphical tools for the visualization of the phase equilibrium that are especially useful in the representation of material balance lines, operating lines and distillation composition trajectories for non-ideal and azeotropic mixtures. A brief introduction to this tool is given in chapter 3. Before analyzing this graphical tool it is convenient to introduce the concept of azeotropy.

## 2.4 Azeotropy

An azeotrope is a compound word from greek language that means “nonboiling by any means”. This term was first introduced by (Wade & Merriman, 1911) to designate a mixture characterized by the formation of one minimum or maximum boiling point under isothermal conditions. However, these author were not the first to report the phenomenon of azeotropy. Dalton at the beginning of 20<sup>th</sup> century was the first to report this it when he was distilling a mixture of hydrochloric and nitric acids.

Nowadays, it is common to find different suffixes accompanying the word azeotrope as the prefix hetero or “*heteroazeotrope*” to designate the formation of more than one liquid phase in the azeotropic state and the prefix homo or “*homoazeotrope*” to designate only one liquid phase formation. Also it is common to find adjectives highlighting the characteristics of the

azeotrope as in “reactive azeotrope” in which, a boiling state of constant temperature and composition is simultaneously in both phase and reaction equilibrium (Song, Huss, Doherty, & Malone, 1997). But, what is interesting here is that there is one definition general enough to involve all the possible connotations that the word azeotrope can have (Doherty & Malone, 2001):

*“An azeotropic state is defined as a state in which mass transfer occurs between phases while the composition of each phase remains constant but not necessary equal”*

From the separation process point of view, an azeotrope means that a complete separation of a mixture is not possible to be achieved by simple distillation. Then, the importance of studying azeotropy from this point of view has to do with the fact that industry process frequently deals with mixtures forming azeotropes. In fact, according to the azeotropic data book by Gmehling, which compiles some information of the data available in the Dortmund Data Bank, almost half percent of the 18800 reported binary systems are azeotropic. The occurrence of azeotropes of minimum boiling point per azeotropes of maximum boiling point is 9 to 1 and most of the total binary azeotropic systems are homogeneous mixtures (~80%) (Hilmen, 2000).

The phenomenon of azeotropy occurs because it exists a strong molecular interaction of the components in the mixture which affects its vapor liquid equilibrium. This molecular interaction refers to forces of attraction and repulsion between molecules that usually are associated to hydrogen type interactions. In the case of Ethanol-Water mixture, the components dislike each other and the attraction between molecules ethanol-ethanol is stronger than the attraction between molecules ethanol-water. This conduces to a positive deviation of the Raoult’s law which generates the minimum boiling azeotrope characteristic of the binary system Ethanol-Water. As azeotropy is due to molecular interactions, it is important to obtain information of this interaction at molecular level in order to improve our capacity and the knowledge in the field of separation processes.

An example of the molecular study of the azeotrope ethanol-water is given in (Mejia, Espinal, & Mondragón, 2006). These authors studied the azeotrope by molecular simulation using the density functional theory. As a conclusion, they suggested that the molecular

interaction that mainly stabilizes the azeotrope Ethanol-Water is the formation of a hydrogen bound of C-H-O type.

## 2.5 Thermodynamics in distillation processes

The fundamental thermodynamics that involves the description of the Vapor Liquid Equilibrium (VLE) are of relevant importance in the understanding of distillation based separation processes. VLE exists for any mixture of  $c$  components if they show identical fugacities in the vapor and liquid phase:

$$f_i^L = f_i^V \quad (2.2)$$

Where:

$f_i^L$ : is the fugacity of component  $i$  in liquid phase, and

$f_i^V$ : is the fugacity of component  $i$  in vapor phase.

Fugacity  $f$  is commonly known as an “escaping tendency” or as thermodynamic pressure that not necessary has a physical significance. This means that equation (2.2) describes an equilibrium where the “escaping tendency” in vapor and liquid phases are similar for each component.

Fugacity in vapor and liquid phase can be described in terms of their fugacity coefficients of which definitions are given by equations (2.3) and (2.4). A third definition that is also commonly used in VLE is the definition of the activity coefficient expressed by equation (2.5):

$$f_i^V = y_i \phi_i^V P_T \quad (2.3)$$

And,

$$f_i^L = x_i \phi_i^L P_T \quad (2.4)$$

Also,

$$f_i^L = x_i \gamma_i f_i^o \quad (2.5)$$

Where:

$\phi_i^V$ : is the vapor phase fugacity coefficient

$\phi_i^L$ : is the liquid phase fugacity coefficient

- $y_i$  : is the mole fraction of component  $i$  in vapor phase  
 $x_i$  : is the mole fraction of component  $i$  in liquid phase  
 $P_T$  : is the pressure of the system  
 $\gamma_i$  : is the liquid phase activity coefficient for component  $i$   
 $f_i^o$  : is the fugacity of component  $i$  at standard state

If the system is at moderate conditions,  $f_i^o$  can be approximated by the saturation pressure of the pure component  $i$ ,  $P_i^{sat}$ . Then, replacing equations (2.3) and (2.5) in (2.1) gives:

$$x_i \gamma_i P_i^{sat} = y_i \phi_i^V P_T$$

or

$$y_i = \frac{x_i \gamma_i P_i^{sat}}{\phi_i^V P_T} \quad (2.6)$$

Equation (2.6) relates the mole fraction of component  $i$  in the vapor phase with its mole fraction in the liquid phase. This expression is the base for the calculation of VLE, together with sum equations  $\sum_{i=1}^{i=c} x_i = 1$  and  $\sum_{i=1}^{i=c} y_i = 1$  and with the thermodynamic model for the calculation of the activity coefficient and the fugacity coefficient.

For moderate pressures (less than 10 bar) vapor phase can be considered as ideal and the fugacity coefficient can be equal to 1. As the pressure of the studied system in this research is near to 1 bar, it is assumed that the vapor phase is ideal.

The calculation of  $\gamma_i$  requires the use of an activity coefficient model. This kind of models are commonly used when polar molecules are present in the mixture, which is in here the case. Three of the most used activity coefficient models are Wilson, Non-Random Two Liquid (NRTL) and Universal Quasi Chemical (UNIQUAC). For the here referenced case of study the recommended coefficient model is NRTL.

### 2.5.1 NRTL activity coefficient model

NRTL is an activity coefficient model that correlates the activity coefficient of a compound with the mole fraction of the component in the liquid mixture. This model comes from the generalized excess Gibbs energy equation for a multicomponent system expressed in (Renon & Prusnitz, 1968) as follows:



$$\frac{g^E}{RT} = -q \sum_{i=1}^N x_i \ln \left( \sum_{j=1}^N G_{ij} x_j \right) + p \sum_{i=1}^N x_i \frac{\sum_{j=1}^N \tau_{ji} G_{ji} x_j}{\sum_{k=1}^N G_{ki} x_k} \quad (2.7)$$

$$\tau_{ji} = \frac{(g_{ji} - g_{ii})}{RT} \quad (2.8)$$

$$G_{ji} = \rho_{ji} \exp(-\alpha_{ji} \tau_{ji}) \quad (2.9)$$

Where:

- N: number of components in the system
- $\tau_{ji}$ : is the temperature dependence parameter of the NRTL model
- $g_{ji}, g_{ij}$ : are the energy interactions between molecules  $j$  and  $i$
- $\alpha_{ji}$ : characterizes the tendency of molecule  $i$  and molecule  $j$  to be distributed in a random fashion
- $q, p$ : are the values which the equations of Wilson, Heil and NRTL can be obtained. These values are reported in **Table 2-2**

**Table 2-2:** Values of  $q$ ,  $p$ ,  $\rho_{ji}$ , and  $\alpha_{ji}$  for NRTL from equation (2.7 to (2.9

Equation	$p$	$q$	$\rho_{ji}$	$\alpha_{ji}$
NRTL	1	0	1	$\alpha_{ji} = \alpha_{ji}$

From equation (2.7) and **Table 2-2**, the activity coefficient is obtained by appropriate differential equations:

$$\ln \gamma_i = p \left[ \frac{\sum_{j=1}^N \tau_{ji} G_{ji} x_j}{\sum_{k=1}^N G_{ki} x_k} + \sum_{j=1}^N \frac{G_{ij} x_j}{\sum_{k=1}^N G_{kj} x_k} \left( \tau_{ij} - \frac{\sum_{l=1}^N \tau_{lj} G_{lj} x_l}{\sum_{k=1}^N G_{kj} x_k} \right) \right] \quad (2.10)$$

For a system of three components the equation (2.10 is solved analytically as it is listed in **Table 2-3**.

**Table 2-3:** Analytical solution of equation (2.10) for NRTL method with 3 components.

For	For	Equation
i=1	A1	$\frac{\tau_{11}G_{11}x_1 + \tau_{21}G_{21}x_2 + \tau_{31}G_{31}x_3}{G_{11}x_1 + G_{21}x_2 + G_{31}x_3}$
i=1	j=1	B1 $\left[ \frac{G_{11}x_1}{G_{11}x_1 + G_{21}x_2 + G_{31}x_3} \right] * \left[ \tau_{11} - \frac{\tau_{11}G_{11}x_1 + \tau_{21}G_{21}x_2 + \tau_{31}G_{31}x_3}{G_{11}x_1 + G_{21}x_2 + G_{31}x_3} \right]$
i=1	j=2	C1 $\left[ \frac{G_{12}x_2}{G_{12}x_1 + G_{22}x_2 + G_{32}x_3} \right] * \left[ \tau_{12} - \frac{\tau_{12}G_{12}x_1 + \tau_{22}G_{22}x_2 + \tau_{32}G_{32}x_3}{G_{12}x_1 + G_{22}x_2 + G_{32}x_3} \right]$
i=1	j=3	D1 $\left[ \frac{G_{13}x_3}{G_{13}x_1 + G_{23}x_2 + G_{33}x_3} \right] * \left[ \tau_{13} - \frac{\tau_{13}G_{13}x_1 + \tau_{23}G_{23}x_2 + \tau_{33}G_{33}x_3}{G_{13}x_1 + G_{23}x_2 + G_{33}x_3} \right]$
i=1	A2	$\frac{\tau_{12}G_{12}x_1 + \tau_{22}G_{22}x_2 + \tau_{32}G_{32}x_3}{G_{12}x_1 + G_{22}x_2 + G_{32}x_3}$
i=2	j=1	B2 $\left[ \frac{G_{21}x_1}{G_{11}x_1 + G_{21}x_2 + G_{31}x_3} \right] * \left[ \tau_{21} - \frac{\tau_{11}G_{11}x_1 + \tau_{21}G_{21}x_2 + \tau_{31}G_{31}x_3}{G_{11}x_1 + G_{21}x_2 + G_{31}x_3} \right]$
i=2	j=2	C2 $\left[ \frac{G_{22}x_2}{G_{12}x_1 + G_{22}x_2 + G_{32}x_3} \right] * \left[ \tau_{22} - \frac{\tau_{12}G_{12}x_1 + \tau_{22}G_{22}x_2 + \tau_{32}G_{32}x_3}{G_{12}x_1 + G_{22}x_2 + G_{32}x_3} \right]$
i=2	j=3	D2 $\left[ \frac{G_{23}x_3}{G_{13}x_1 + G_{23}x_2 + G_{33}x_3} \right] * \left[ \tau_{23} - \frac{\tau_{13}G_{13}x_1 + \tau_{23}G_{23}x_2 + \tau_{33}G_{33}x_3}{G_{13}x_1 + G_{23}x_2 + G_{33}x_3} \right]$
i=3	A3	$\frac{\tau_{13}G_{13}x_1 + \tau_{23}G_{23}x_2 + \tau_{33}G_{33}x_3}{G_{13}x_1 + G_{23}x_2 + G_{33}x_3}$
i=3	j=1	B3 $\left[ \frac{G_{31}x_1}{G_{11}x_1 + G_{21}x_2 + G_{31}x_3} \right] * \left[ \tau_{31} - \frac{\tau_{11}G_{11}x_1 + \tau_{21}G_{21}x_2 + \tau_{31}G_{31}x_3}{G_{11}x_1 + G_{21}x_2 + G_{31}x_3} \right]$
i=3	j=2	C3 $\left[ \frac{G_{32}x_2}{G_{12}x_1 + G_{22}x_2 + G_{32}x_3} \right] * \left[ \tau_{32} - \frac{\tau_{12}G_{12}x_1 + \tau_{22}G_{22}x_2 + \tau_{32}G_{32}x_3}{G_{12}x_1 + G_{22}x_2 + G_{32}x_3} \right]$
i=3	j=3	D3 $\left[ \frac{G_{33}x_3}{G_{13}x_1 + G_{23}x_2 + G_{33}x_3} \right] * \left[ \tau_{33} - \frac{\tau_{13}G_{13}x_1 + \tau_{23}G_{23}x_2 + \tau_{33}G_{33}x_3}{G_{13}x_1 + G_{23}x_2 + G_{33}x_3} \right]$

$$\ln \gamma_1 = A1 + B1 + C1 + D1 \quad (2.11)$$

$$\ln \gamma_2 = A2 + B2 + C2 + D3 \quad (2.12)$$

$$\ln \gamma_3 = A4 + B4 + C4 + D4 \quad (2.13)$$

Equations (2.11) to (2.13) and sum equations (2.15) to (2.16) can be numerically solved for different compositions at a given temperature once the parameters of the model are experimentally obtained. For common systems these parameters are reported in articles or data bases as the Dortmund Data Bank.

$$\sum_{i=1}^N x_i = 1 \quad (2.14)$$

$$\sum_{i=1}^N y_i = 1 \quad (2.15)$$

## 2.5.2 Verification of pure component parameters

One of the most important pure component parameter that must be verified for calculations related to distillation is the vapor pressure of pure components. For a given temperature, the vapor pressure corresponds to the boundary between the vapor and liquid equilibrium that is established by a curve line from the triple point to the critical point in a temperature pressure diagram. When the vapor pressure corresponds to 1 atm the correlated temperature is the normal boiling point of the pure component. One of the simplest equations used for determining vapor pressures is the Clausius-Clapeyron equation. However, this equation is applicable only over a small temperature ranges. For an extended range it is more accurate to use the expression of Antoine shown in equation (1.16).

$$\ln p^{vap} = A - \frac{B}{C - T} \quad (2.16)$$

In the previous equation, A, B and C are parameters obtained by correlation of experimental data. These parameters must be verified for the range of temperatures over which the proposed model will be evaluated. For the here studied case, the range of temperature that will be used in the distillation model is 300-480 K.

Aspen Plus uses by default an extended Antoine vapor pressure method called PLXANT, which is shown in equation (1.17).

$$\ln p^{vap} = C_{1i} + \frac{C_{2i}}{T + C_{3i}} + C_{4i}T + C_{5i} \ln T + C_{6i}T^{C_{7i}} \quad (2.17)$$

In Equation (2.17), pressure is in kPa and temperature is in K. For a short temperature range, this model can be compared with the experimental data available in the Dortmund Data Bank. For a more extended range, new versions of Aspen plus use extended data bases from NIST. In the case of ethanol, the PLXANT method uses parameters from more than 2000 experimental temperature-vapor pressure data which cover a temperature range between 200 K and 515 K. Available data can be accepted or rejected according to a table reported in aspen. Uncertainty of the data is also reported with its cited article (In Aspen plus >> Components >> find >> ethanol >>run property analysis>> HOME menu >> NIST >> Pure component >> Ethanol >> Evaluate now>> Properties for ethanol >> Vapor

pressure >> Experimental data). **Figure 2-3**, **Figure 2-4** and **Figure 2-5** show a comparison between the model PLXANT and experimental data reported in NIST and references.

**Table 2-4:** Experimental data for verification of PLXANT model from Aspen Plus.

Temperature K	A	B	C	Reference
364,8	513,91	4,92531	1432,526	-61,819 (Ambrose, Sprake, & Townsend, 1975)
292,77	366,63	5,24677	1598,673	-46,424 (Ambrose & Sprake, 1970)
273,77	351,7	5,37229	1670,409	-40,191 (Kretschmer & Wiebe, 1949)

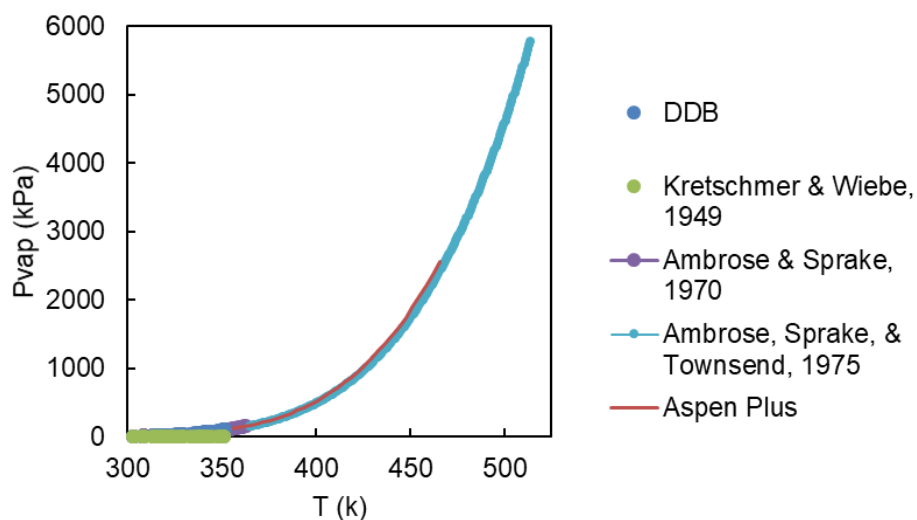


**Figure 2-3:** Verification of vapor pressures for ethanol. Calculated by Aspen plus PLXANT model. Experimental data taken from DDB.

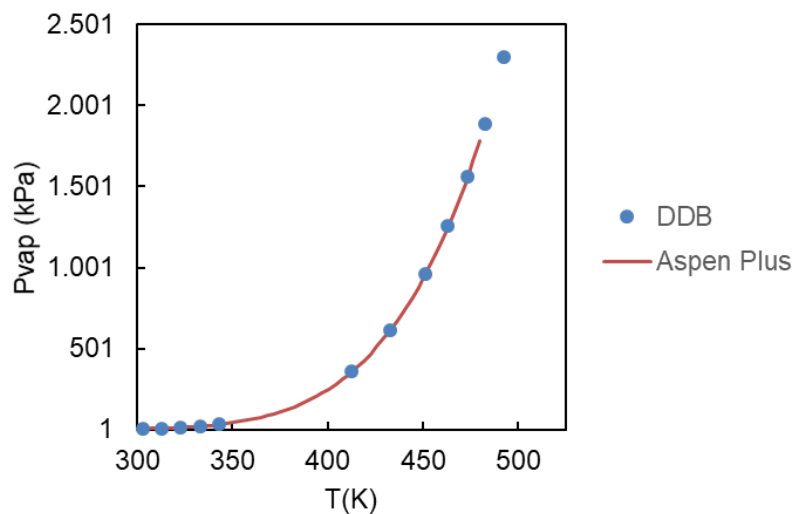


**Figure 2-4:** Verification of vapor pressure for water. Calculated by Aspen plus PLXANT model. Experimental data taken from DDB.

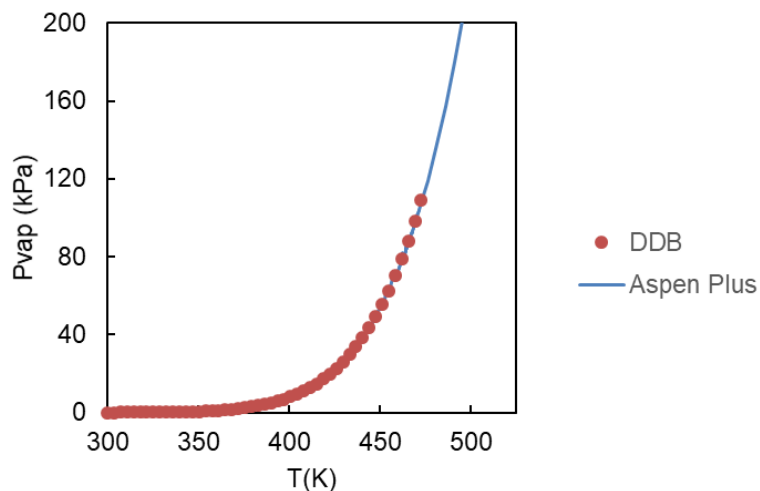


**Figure 2-5:** Verification of vapor pressures for ethylene glycol. Calculated by Aspen plus PLXANT model. Experimental data taken from DDB.

**Table 2-5:** Adjusted PLXANT parameters by Aspen Plus.

Parameters	C1	C2	C3	C4	C5	C6	C7	C8	C9
Ethanol	66,3962447	-7,12E+03	0	0	-7,1424	2,89E-06	2	159,05	514
Water	66,7412447	-7,26E+03	0	0	-7,3037	4,17E-06	2	273,16	647,1
Ethylen Glycol	77,1822447	-1,04E+04	0	0	-8,1976	1,65E-18	6	260,15	720

### 2.5.3 Verification of the binary $g^E$ model parameters

The number of theoretical stages of a distillation column involves the calculation of the so called MESH equations. The solution of these equations uses, in an implicit way, binary parameters of the thermodynamic VLE model. If the number of stages or height of a column is calculated with the MESH equations, an incorrect selection of the binary parameters of the  $g^E$  model will generate questionable results. On the other hand, a good selection of the binary parameters leads to a good approximation of the mathematical model to the physical behavior and therefore, more reliable results are obtained. Then, the VLE model must be evaluated with experimental data and its parameters must be adjusted.

Simulators as Aspen Plus use default binary parameters for the solution of the VLE model. The default parameters of the NRTL model in Aspen Plus were used to predict the ternary system Ethanol-Water-Ethylene Glycol. Constituent binary mixtures were analyzed in graphical form by means of activity coefficient vs composition diagrams as shown in **Figure**

**2-6, Figure 2-7 and Figure 2-8.** Obtained results were compared with experimental data reported by (Kamihama, Matsuda, Kurihara, Tochigi, & Oba, 2012) (also corroborated by (Pla-Franco, Lladosa, Loras, & Montón, 2013)). It can be seen that even when the default parameters of Aspen Plus are used, the model fit to the experimental data with a good accuracy for Ethanol-Water subsystem. However, the two remaining subsystems Ethanol-Ethylene glycol and Water-Ethylene glycol are not well predicted.

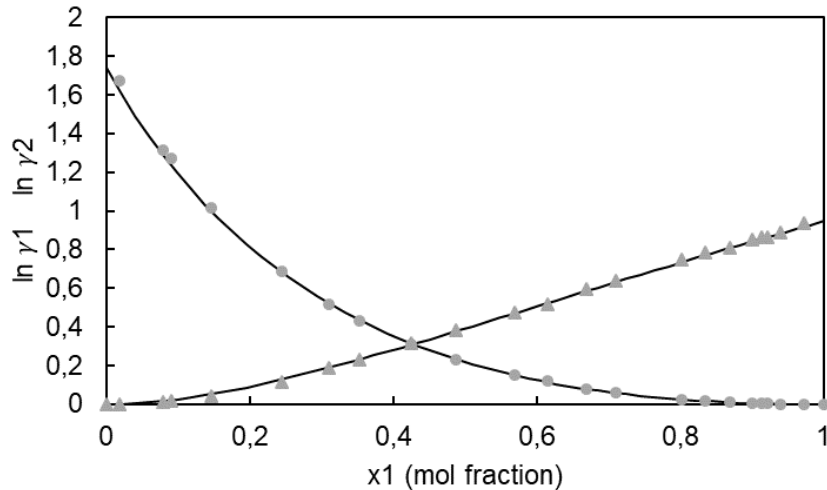


**Figure 2-6:** Activity coefficient as a function of the liquid composition for the binary system ethanol (1) water (2). Kamihama experimental data (O:1)(Δ:2). Curves predicted with Aspen Plus default parameters.

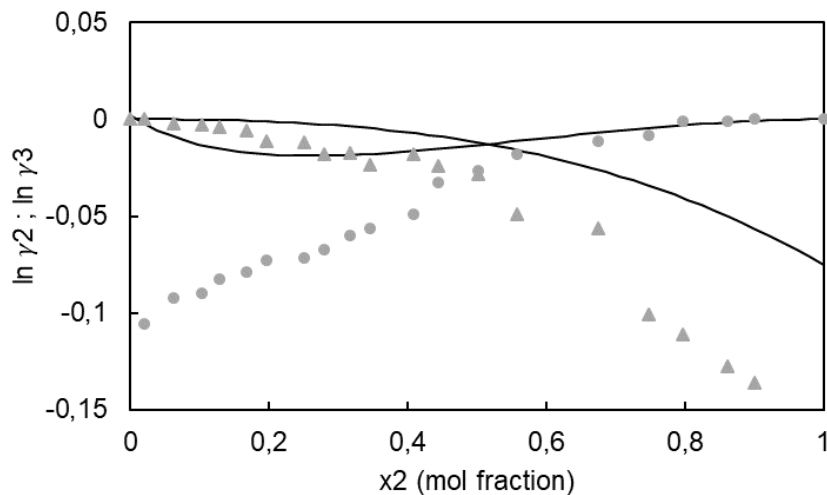


**Figure 2-7:** Activity coefficient as a function of the liquid composition for the binary system water (2) ethylene glycol (3). Kamihama experimental data (O:2)(Δ:3). Curves predicted with Aspen Plus default parameters.

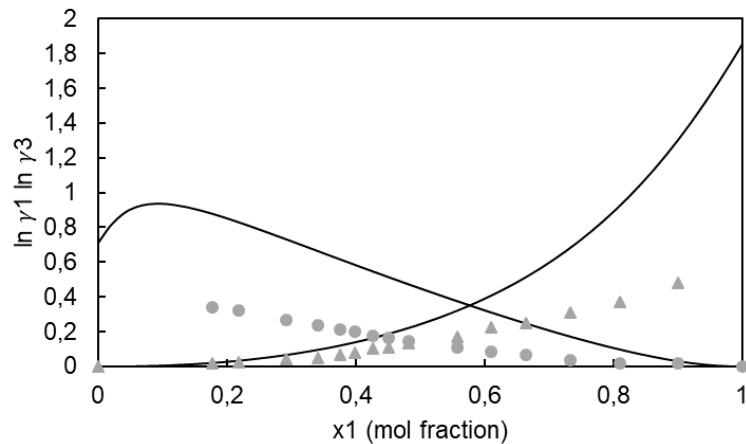


**Figure 2-8:** Activity coefficient as a function of the liquid composition for the binary system ethanol (1) ethylene glycol (3). Kamihama experimental data (O:1)(Δ:3). Curves predicted with Aspen Plus default parameters.

A better fit between the VLE model available in the simulator and the cited experimental data is possible to obtain by replacing the default parameters with the parameters reported by Kamihama. In Aspen Plus, this is possible to do in Properties >>Methods >>Parameters >>Binary Interaction >> NRTL>>DECHEMA, see **Table 2-6**. The adjustment can be seen graphically in **Figure 2-9**, **Figure 2-10** and **Figure 2-11**.

**Table 2-6:** Experimental parameters in Aspen Plus Format (Kamihama et al., 2012).

Component i	ETHAN-01	ETHYL-01	WATER
Component j	WATER	ETHAN-01	ETHYL-01
Temperature units	K	K	K
Source	USER	USER	USER
Property units			
AIJ	0	0	0
AJI	0	0	0
BIJ	27,36	85,19	-301,88
BJI	625,04	124,55	328,50
CIJ	0,4	0,23	0,33
DIJ	0	0	0
EIJ	0	0	0
EJI	0	0	0
FIJ	0	0	0
FJI	0	0	0
TLOWER	0	0	0
TUPPER	1000	1000	1000

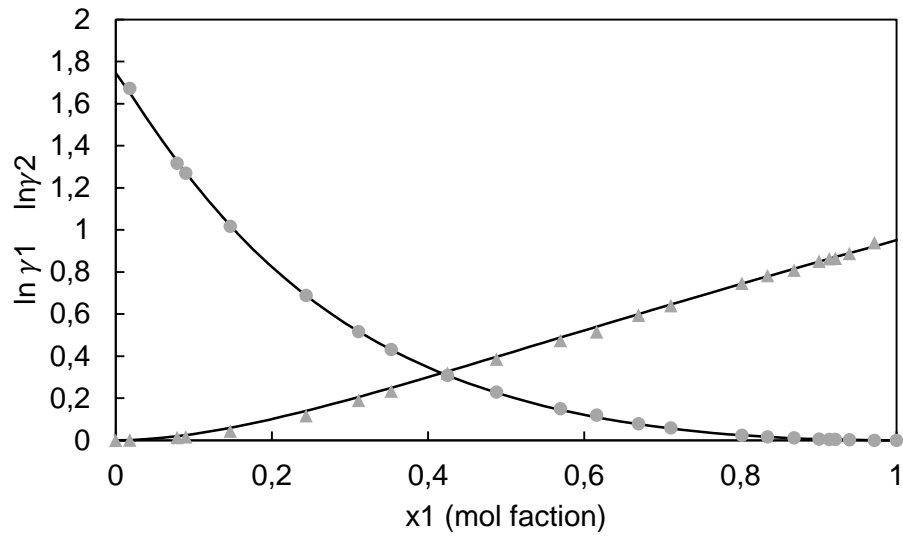


**Figure 2-9:** Activity coefficient as a function of the liquid composition for the binary system thanol (1) water (2). Kamihama experimental data (O:1)(Δ:2). Curves predicted with Aspen Plus user parameters from Kamihama.

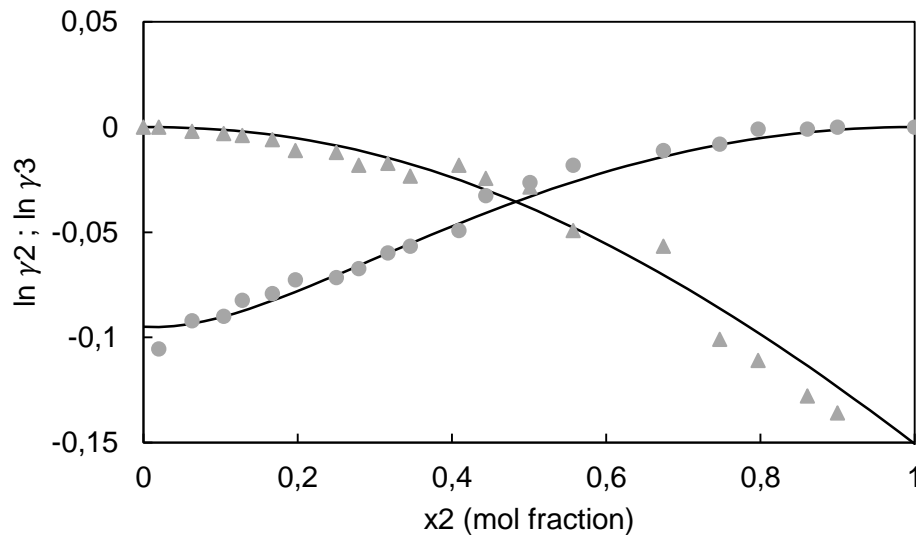


**Figure 2-10:** Activity coefficient as a function of the liquid composition for the binary system water (2) ethylene glycol(3). Kamihama experimental data (O:2)(Δ:3). Curves predicted with Aspen Plus user parameters from Kamihama.



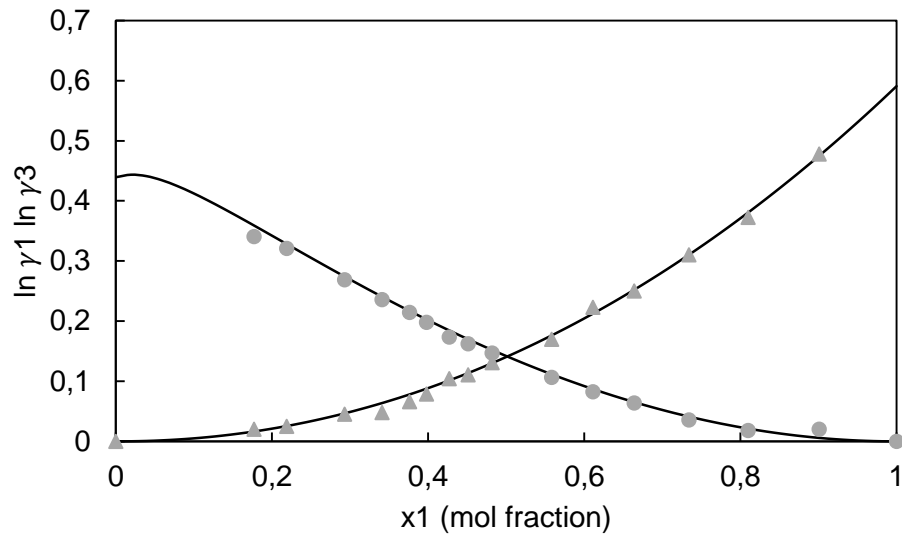


**Figure 2-11:** Activity coefficient as a function of the liquid composition for the binary system Ethanol (1) Ethylene Glycol (3). Kamihama experimental data (O:1)(Δ:3). Curves predicted with Aspen Plus user parameters from Kamihama.

NRTL parameters are dependent on the composition of the species involved in the ternary system but they are also dependent on temperature. In distillation process, this dependency can seriously impact the calculation of the activity coefficients and, as a consequence, a correct adjustment of the activity model parameters influences the capital investment and operation of final distillation column designed. In the case of ethanol-water system, a positive deviation of Raoult's law is observed and for this kind of deviations a separation problem often occurs: in the top of the column, where the less boiling component has to be removed, the most unfortunate separation factors are obtained (Gmehling, Kolbe, Kleiber, & Rarey, 2012). Equation (2.18) shows this mathematically by displaying the equation to calculate the separation factor. In the top of the column with infinity dilution, as the activity coefficient increases (positive deviation  $\gamma_i > 1$ ) the separation factor decreases, see equation (2.19). The separation factor is a measure of the degree of enrichment or the ease of separation, therefore, a decreasing value means a difficulty for separation. In bottoms of the column at infinite dilution equation (2.20) is employed but in this case positive deviation increases the separation factor.

Relative volatility or separation factor definition:

$$\alpha_{12} = \frac{\gamma_1 P_1^s}{\gamma_2 P_2^s} \quad (2.18)$$

Separation factor at the top of the column ( $x_1 \rightarrow 1$ ):

$$\alpha_{12}^\infty = \frac{P_1^s}{\gamma_2^\infty P_2^s} \quad (2.19)$$

Separation factor at the bottom of the column ( $x_2 \rightarrow 1$ ):

$$\alpha_{12}^\infty = \frac{\gamma_2^\infty P_1^s}{P_2^s} \quad (2.20)$$

In order to verify the temperature dependence of the parameters for the VLE model, it is common to appeal to draw lines of constant volatility in composition space diagram (Gmehling et al., 2012). Isovolatility curves are formed by a set of points representing the composition of different mixtures boiling with same relative volatility. To trace the isovolatility curves, (Sanchez, Estupiñan, & Salazar, 2010) describe a numerical method based on the homotopy continuation method proposed by Davidenko. Authors first write the VLE equations with equation (2.18) as discrepancy functions:

$$h_i = y_i - K_i x_i, \quad i = 1, 2, 3 \quad (2.21)$$

$$h_4 = 1 - y_1 - y_2 - y_3 \quad (2.22)$$

$$h_5 = 1 - x_1 - x_2 - x_3 \quad (2.23)$$

$$h_6 = \frac{K_i}{K_j} - \alpha_{ij} \quad (2.24)$$

Equations 2.25 correspond to the VLE for a defined pressure. Equation 2.24 is the restriction of constant volatility, in this case between ethanol and water only. Therefore, there are only one 2.24 equation. The system corresponds to six equations with nine intensive variables.:

$$\lambda = [x_1, x_2, x_3, y_1, y_2, y_3, T, p, \alpha_{ij}]^T \quad (2.26)$$

Then, the three obtained degrees of freedom are reduced by specifying the system pressure and the value of the constant relative volatility. Last degree of freedom is used in order to specify the natural parameter of the equations system. This can be the liquid mole

fraction of one of the three species in mixture. By thermodynamic homotopy, based on the component ethanol, the equation system (2.21) to (2.24) can be written in similar terms of the Davidenko equation:

$$H(X(x_1), x_1) = 0 \quad (2.27)$$

$$X = [x_2, x_3, y_1, y_2, y_3, T]$$

By derivation of equation (2.27) and rearranging it in the form  $AX=B$  next equations are obtained:

$$dH = \frac{\partial H}{\partial X} \frac{\partial X}{\partial x_1} \partial x_1 + \frac{\partial H}{\partial x_1} \partial x_1 \quad (2.28)$$

$$\frac{\partial H}{\partial X} \frac{\partial X}{\partial x_1} = - \frac{\partial H}{\partial x_1} \quad (2.29)$$

$$\frac{\partial X}{\partial x_1} = \left( \frac{\partial H}{\partial X} \right)^{-1} \left( - \frac{\partial H}{\partial x_1} \right) \quad (2.30)$$

Equation (2.30) can be approximated by finite differentiation as follows:

$$\frac{X(x_1 + \Delta x) - X(x_1)}{\Delta x} = \left( \frac{\partial H}{\partial X} \right)^{-1} \left( - \frac{\partial H}{\partial x_1} \right) \quad (2.31)$$

Where  $\left( \frac{\partial H}{\partial X} \right)$  is the 6X6 jacobian matrix for equations system (2.21) to (2.24) and  $-\frac{\partial H}{\partial x_1}$  is a vector 1X6:

$$\left( \frac{\partial H}{\partial X} \right) = \begin{bmatrix} \frac{\partial h_1}{\partial x_2} & \frac{\partial h_1}{\partial x_3} & \frac{\partial h_1}{\partial y_1} & \frac{\partial h_1}{\partial y_2} & \frac{\partial h_1}{\partial y_3} & \frac{\partial h_1}{\partial T} \\ \frac{\partial h_2}{\partial x_2} & \frac{\partial h_2}{\partial x_3} & \frac{\partial h_2}{\partial y_1} & \frac{\partial h_2}{\partial y_2} & \frac{\partial h_2}{\partial y_3} & \frac{\partial h_2}{\partial T} \\ \frac{\partial h_3}{\partial x_2} & \frac{\partial h_3}{\partial x_3} & \frac{\partial h_3}{\partial y_1} & \frac{\partial h_3}{\partial y_2} & \frac{\partial h_3}{\partial y_3} & \frac{\partial h_3}{\partial T} \\ \frac{\partial h_4}{\partial x_2} & \frac{\partial h_4}{\partial x_3} & \frac{\partial h_4}{\partial y_1} & \frac{\partial h_4}{\partial y_2} & \frac{\partial h_4}{\partial y_3} & \frac{\partial h_4}{\partial T} \\ \frac{\partial h_5}{\partial x_2} & \frac{\partial h_5}{\partial x_3} & \frac{\partial h_5}{\partial y_1} & \frac{\partial h_5}{\partial y_2} & \frac{\partial h_5}{\partial y_3} & \frac{\partial h_5}{\partial T} \\ \frac{\partial h_6}{\partial x_2} & \frac{\partial h_6}{\partial x_3} & \frac{\partial h_6}{\partial y_1} & \frac{\partial h_6}{\partial y_2} & \frac{\partial h_6}{\partial y_3} & \frac{\partial h_6}{\partial T} \end{bmatrix} \quad \left( \frac{\partial H}{\partial x_1} \right) = \begin{bmatrix} \frac{\partial h_1}{\partial x_1} \\ \frac{\partial h_2}{\partial x_1} \\ \frac{\partial h_3}{\partial x_1} \\ \frac{\partial h_4}{\partial x_1} \\ \frac{\partial h_5}{\partial x_1} \\ \frac{\partial h_6}{\partial x_1} \end{bmatrix}$$

Finally, the procedure to find the composition points of the isovolatility curve is as follow:

- Initialization: an initial point from the composition space must be selected ( $x_1 = a$ ). With selected point at defined pressure, the temperature and activity coefficient can be calculated.
- Prediction: Equation (2.31) is used to predict the second point by defining a size of step  $\Delta x$ . The terms of this equation are calculated by evaluating the matrix H at  $x_1$  and  $x_1 + \Delta x$  and by obtaining its derivative by numerical differentiation. The replacement of the known values in equation (1.30) gives a new value for  $X(x_1 + \Delta x)$ .
- Correction: the new value  $X(x_1 + \Delta x)$  is evaluated in equation (2.27) and corrected. If it is necessary, a method of correction by curve length is used.

The procedure results are graphically shown in **Figure 2-12**. These results are thermodynamically consistent as the isovolatility values of the curves have a growing increment in all composition space moving from the less volatile component to the heaviest component.

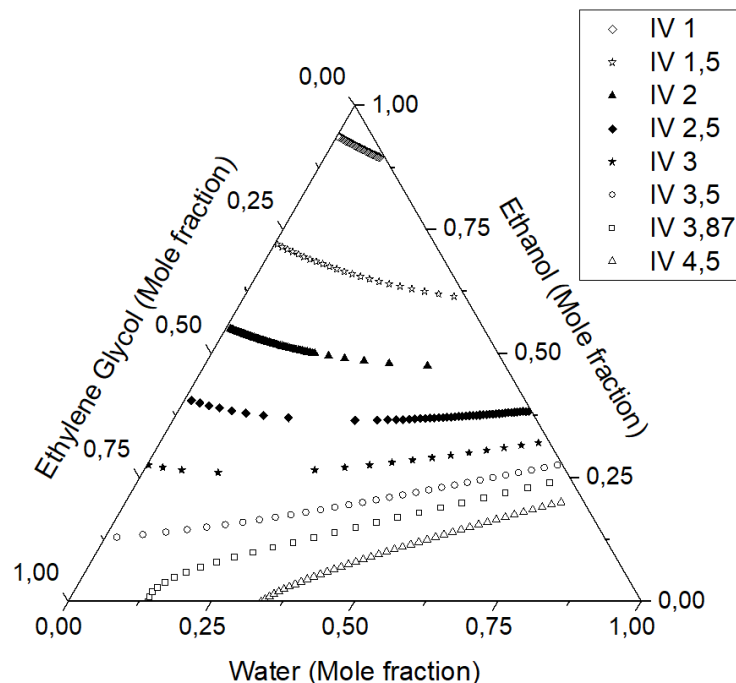


**Figure 2-12:** composition trajectories of constant volatility (Isovolatility IV) for the system Ethanol-Water-Ethylene Glycol at 1 atm.

### 2.5.4 Verification of ternary interactions

(Kamihama et al., 2012) also report the experimental ternary interactions for the system ethanol-water-ethylene glycol. Their activity coefficient results are graphically compared with modeled predictions in order to verify the accuracy of the model, see **Figure 2-13**. In view of obtained results, parameters in **Table 2-6** are used in this document.

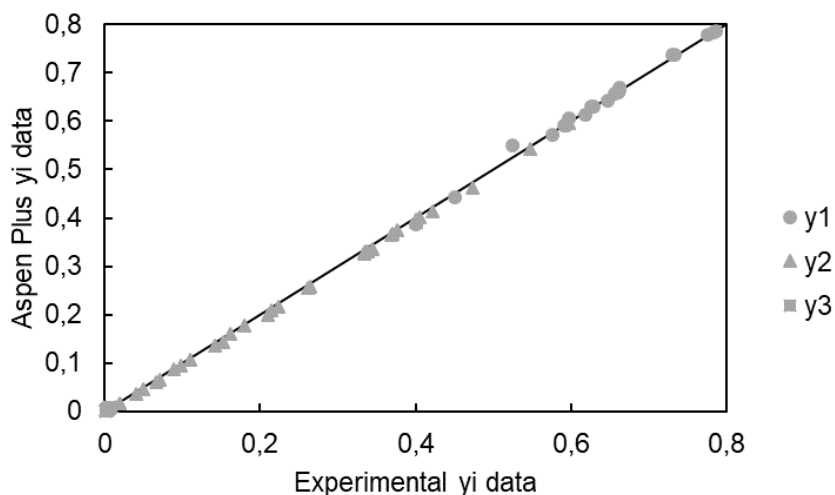


**Figure 2-13:** Experimental data for ternary interactions reported by (Kamihama et al., 2012) compared with data calculated with Aspen Plus with the parameters reported in **Table 2-6**.

## 2.6 Residue curves

Graphical representations of VLE are powerful tools for synthesis, analysis and operation of distillation columns. For binary systems, Ponchon-Savarit and McCabe-Thiele diagrams are commonly introduced in undergraduated courses of chemical engineering for the study of binary distillation columns. For ternary mixtures, graphical representation of VLE is also possible in the so called composition space. Residue curve maps, distillation lines, condensation lines, isobaric-isotherm lines, among other, are examples of these representations. Residue curve (or topological analysis in Russian literature) is the most used tool for the VLE description of azeotropic mixtures. A brief description of them is made in this section.

### 2.6.1 The equation of simple distillation

Simple distillation is the most basic form of distillation, see **Figure 2-14**. In this type of unit, a multicomponent mixture is slowly boiled in an open vessel and the vapor formed is continuously removed as fast as it is formed. Ideally, three characteristics of simple distillation can be experimentally observed:

- The vapor mixture is in equilibrium with its liquid at any instant of time
- The vapor mixture is always richer in the most volatile component than the liquid phase.
- The liquid phase is always richer than the vapor phase in the less volatile component. As consequence, the remained liquid in the pot becomes more concentrate in the less volatile component with the time.

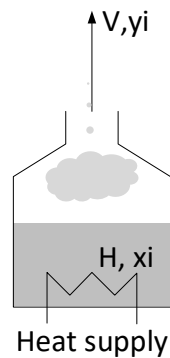


**Figure 2-14:** Simple distillation.

Mathematical description of simple distillation is obtained by a mass balance for the component  $i$  as follows:

$$\frac{d(Hx_i)}{dt} = -Vy_i, \quad i = 1; c \quad (2.32)$$

$$x_i \frac{dH}{dt} + H \frac{dx_i}{dt} = -Vy_i, \quad i = 1; c \quad (2.33)$$

Where:

- $V$ : is the molar flow rate of escaping vapor  
 $H$ : is the molar liquid holdup in the still

Overall mass balance gives:

$$\frac{dH}{dt} = -V \quad (2.34)$$

Substituting (2.34) in (2.32) we get:

$$\begin{aligned} x_i(-V) + H \frac{dx_i}{dt} &= -Vy_i, \quad i = 1; c \\ \frac{dx_i}{dt} &= \frac{-V}{H}(y_i - x_i), \quad i = 1; c \end{aligned} \quad (2.35)$$

Equation (2.35) is known as Rayleigh equation.

## 2.6.2 Residue curves equation

The concept of residue curve was first introduced by Schreinemakers at the beginning of 20<sup>th</sup> century (Beneke, Peters, Glasser, & Hildebrandt, 2013). A residue curve is the trajectory of compositions that describes the remaining liquid composition in the pot of a simple distillation unit (Doherty & Malone, 2001). A mathematical development of this trajectories was developed by (Doherty & Perkins, 1978). Following the treatment of the authors, equation (2.35) can be written as an autonomous set of equations parametrized by an arbitrary variable  $\xi$ :

$$\frac{dx_i(\xi)}{d\xi} = x_i(\xi) - y_i(x_i(\xi)), \quad i = 1; c - 1 \quad (2.36)$$

It can be noticed that only  $c-1$  differential equations are needed for the description of the  $c$  components systems as liquid composition and vapor are related by the sum equations (2.14) and (2.15). As  $y_i$  is a function of  $x_i(\xi)$ , an equilibrium model must be used to solve the system. The mathematical model is completed by specification of the initial liquid composition condition of  $c-1$  components. With numerical methods as Euler it is possible to draw the total trajectory of the curve by rewriting equation (2.36) as finite differences and solving it for  $x_i(\xi + \Delta\xi)$ :

$$\frac{x_i(\xi + \Delta\xi) - x_i(\xi)}{\Delta\xi} = x_i(\xi) - y_i(x_i(\xi)), \quad i = 1; c - 1 \quad (2.37)$$

$$x_i(\xi + \Delta\xi) = \Delta\xi[x_i(\xi) - y_i(x_i(\xi))] + x_i(\xi), \quad i = 1; c - 1 \quad (2.38)$$

### 2.6.3 Residue curves for Ethanol-Water-Ethylene glycol system

Residue curves for Ethanol-Water-Ethylene Glycol can be calculated by the use of the equations developed above. **Table 2-7** summarize the system equations needed for the calculation of the variables that are involve. Based on **Table 2-7** the degrees of freedom (DOF) analysis can be done as follows:

$$DOF = \# \text{ variables} - \# \text{ equations}$$

$$DOF = 16 - 13$$

$$DOF = 3$$

As there are more variables than equations, three specifications should be established to solve the system. From the numerical method a step size  $\Delta\xi$  must be defined. The two remaining variables are defined by the initial conditions for the calculation.

$$x_{EtOH}(\xi) = x_{EtOH}(0)$$

$$x_{water}(\xi) = x_{water}(0)$$

Applying the numerical method of Euler for the integration of the differential residue curve equation, it is possible to find a graphical solution as shown in **Figure 2-15**.

The residue curves in **Figure 2-15** perform together the residue curve map for the ternary system. A minimum boiling point azeotrope exists on the mass balance line between pure ethanol and pure water (shown as a blue point). The residue curves are originated from the azeotrope point and end in the entrainer corner. Technically it means that the entrainer is a *stable node*, the azeotrope is an *unstable node* and the ethanol and water vertices are *saddle nodes*. These concepts are the base for the qualitative drawing of the curves. (Foucher, Doherty, & Malone, 1991) discuss this in deep by the use of the topological analysis and by developing an algorithm based on 8 main steps for the determination of the structure of residue curve maps in ternary mixtures.



**Table 2-7:** Equations system for the modeling of the residue curve map.

<b>Mass balance equations</b>		
<b>1</b>	$x_{EtOH}(\xi + \Delta\xi) = \Delta\xi [x_{EtOH}(\xi) - y_{EtOH}(x_{EtOH}(\xi))] + x_{EtOH}(\xi)$	$x_{EtOH}(\xi + \Delta\xi)$ $x_{EtOH}(\xi)$ $y_{EtOH}$ $\Delta\xi$
<b>2</b>	$x_{water}(\xi + \Delta\xi) = \Delta\xi [x_{water}(\xi) - y_{water}(x_{water}(\xi))] + x_{water}(\xi)$	$x_{water}(\xi + \Delta\xi)$ $x_{water}(\xi)$ $y_{water}(\xi)$
<b>Sum equations</b>		
<b>3</b>	$1 = x_{EtOH}(\xi) + x_{water}(\xi) + x_{EtGly}(\xi)$	$x_{EtGly}(\xi)$
<b>4</b>	$1 = y_{EtOH}(\xi) + y_{water} + y_{EtGly}$	$y_{EtGly}(\xi)$
<b>Equilibrium equations</b>		
<b>5</b>	$y_{EtOH} = \frac{x_{EtOH} \gamma_{EtOH} P_{EtOH}^S}{1 * P_T}$	$\gamma_{EtOH}$ $P_{EtOH}^S$
<b>6</b>	$y_{water} = \frac{x_{water} \gamma_{water} P_{water}^S}{1 * P_T}$	$\gamma_{water}$ $P_{water}^S$
<b>7</b>	$y_{EtGly} = \frac{x_{EtGly} \gamma_{EtGly} P_{EtGly}^S}{1 * P_T}$	$\gamma_{EtGly}$ $P_{EtGly}^S$
<b>Auxiliary equations</b>		
<b>8</b>	$\gamma_{EtOH} = f(x_{EtOH}, x_{water}, x_{EtGly}, T)$ from equation (2.11)	
<b>9</b>	$\gamma_{water} = f(x_{EtOH}, x_{water}, x_{EtGly}, T)$ from equation (2.12)	
<b>10</b>	$\gamma_{EtGly} = f(x_{EtOH}, x_{water}, x_{EtGly}, T)$ from equation (2.13)	
<b>11</b>	$P_{EtOH}^S = f(T)$ from equation (2.17)	
<b>12</b>	$P_{water}^S = f(T)$ from equation (2.17)	
<b>13</b>	$P_{EtGly}^S = f(T)$ from equation (2.17)	

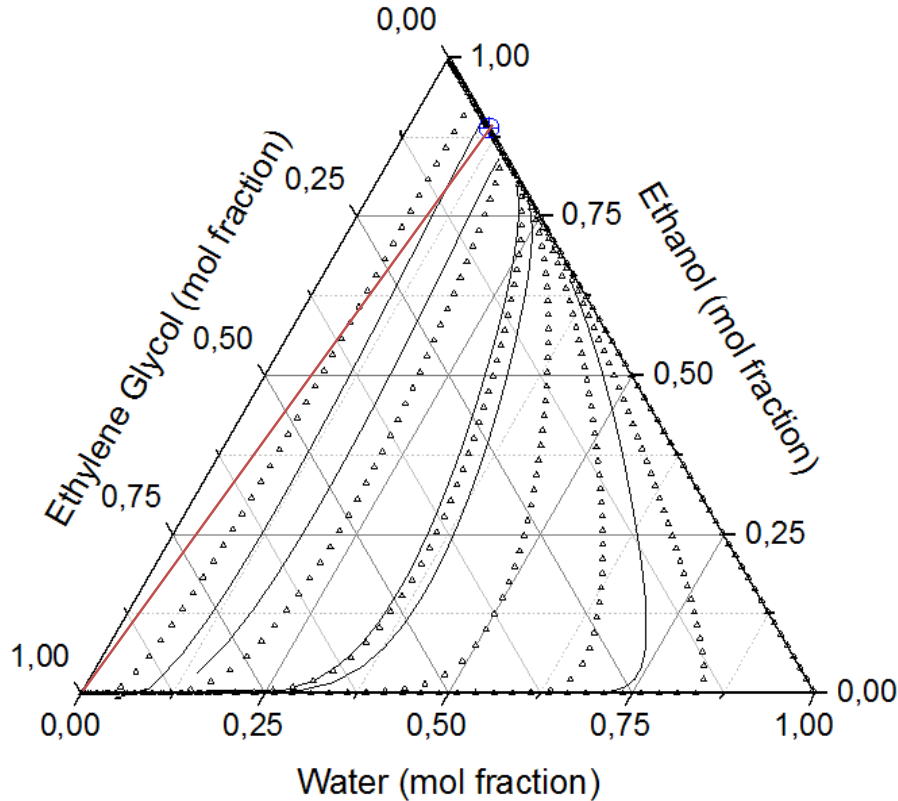


**Figure 2-15:** Residue curves for ternary system Ethanol-Water-Ethylene Glycol at 1 atm.  
 (–): Curves calculated by the author (Δ): curves calculated by Aspen Plus.

## 2.7 Column profile maps of extractive distillation

Distillation operations are carried out in an equipment called distillation column. In this equipment a liquid phase is formed at top in a condenser and is put in contact with a vapor phase coming up from a bottom reboiler where it is formed. The purpose of the equipment is to put in contact liquid and vapor phase in successive stages in order to achieve a thermodynamic equilibrium. The contact can be carried out by means of plates or by different types of packing. A typical single feed distillation column with stages is shown in **Figure 2-16**. The feed stream (F) is fed to an intermediate stage as saturated liquid. The product stream from condenser is called distillate (D) and product stream from reboiler is called bottoms (B).

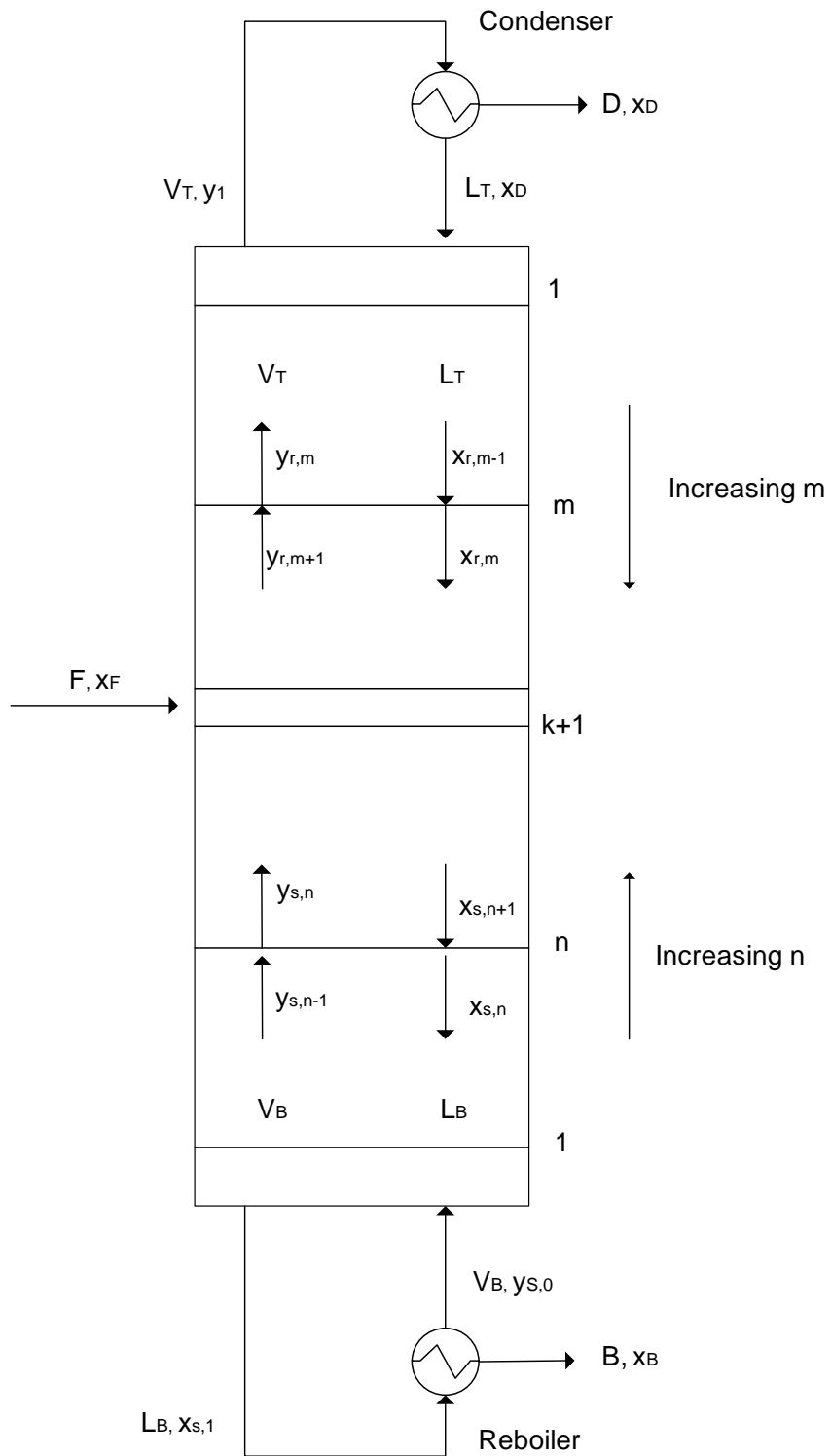


**Figure 2-16:** Scheme of a single feed distillation column.

The section above of the feed plate is called rectifying section and the section below is called stripping section. For each stage inside the distillation column, it is convenient to assume that the liquid leaving the stage is in thermodynamic equilibrium with the vapor leaving the stage. It is also assumed negligible heat effect in each stage (constant molar overflow). Based on these assumptions and on (Julka & Doherty, 1990), it is possible to deduce an equation that describes the liquid composition in each stage of the rectifying section (2.39 a) and other that describes the liquid composition in stripping section (2.40):

Rectifying section:

$$y_{m+1}^r = \frac{r}{r+1} x_m^r + \frac{1}{r+1} x_D \quad (m = 0, 1, 2 \dots) \quad (2.39 \text{ a})$$

$$x_0^r = x_D \quad (2.39 \text{ b})$$

$$r = \frac{L_T}{D} \quad (2.39 \text{ c})$$

$$r + 1 = \frac{V_T}{D} \quad (2.39 \text{ d})$$

Stripping section:

$$x_{n+1}^s = \frac{s}{s+1} y_n^s + \frac{1}{s+1} x_B \quad (n = 0, 1, 2 \dots) \quad (2.40 \text{ a})$$

$$x_0^s = x_B \quad (2.40 \text{ b})$$

$$s = \frac{V_B}{B} \quad (2.40 \text{ c})$$

$$s + 1 = \frac{L_B}{B} \quad (2.40 \text{ d})$$

Once the composition of the distillate and bottoms are specified, operation equations (2.39) and (2.40) can be computed stage by stage for a defined reflux. **Figure 2-17** shows the typical column profile lines of the stripping and rectifying sections of a single feed distillation column used for the separation of a ternary ideal mixture. It is interesting to notice the formation of pinch points on the profile lines. The *pinch points* are points where the composition does not vary between stages. Pinch points where the profile line has an asymptotic behavior are called *saddle* and pinch point that appear at the end of the profile lines are called *nodes*. The behavior of the pinch points is important for the definition of

minimum reflux and solvent to feed ratio in extractive distillation, which will be detailed in next chapter.

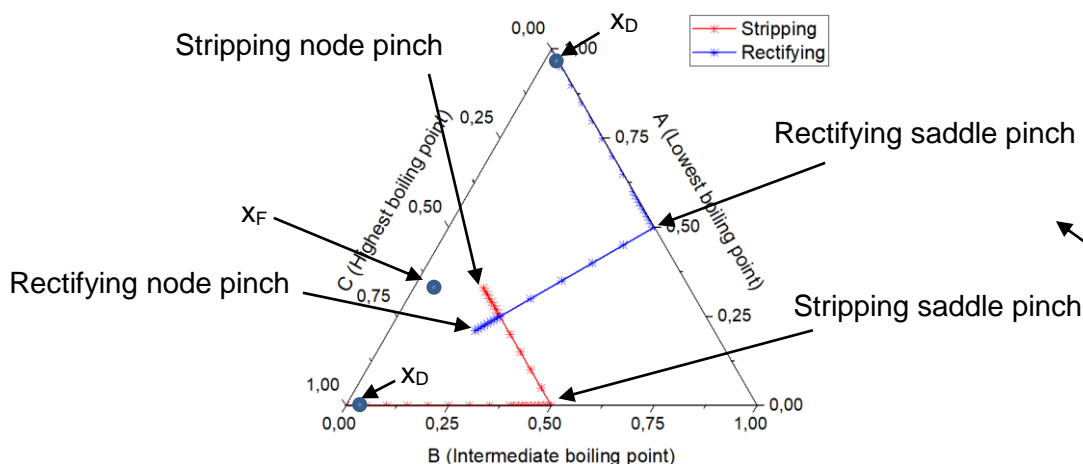


**Figure 2-17:** Typical composition profiles of a single feed distillation column separating ideal mixtures.

When the single feed configuration shown in **Figure 2-16** is used for the separation of Ethanol-Water-Ethylene glycol mixtures, it is possible to use equation (2.39) and (2.40) in order to compute the stage to stage composition of the column. **Figure 2-18** shows two column profiles for a solvent to feed ratio ( $Fr$ ) of 1 and a variable reflux ratio ( $R$ ). It can be noticed that the stripping profile ends in a node pinch, which corresponds to the most upper stage composition of the stripping section. According to the observation, the separation is not feasible in a single feed column because the stripping profile does not reach the rectifying profile due to a limiting node pinch. If more column profiles are plotted, a node line can be obtained by joining the node pinch points of each stripping profile. Similarly, a saddle pinch line can be plotted by joining the saddle pinch points of each profile. These lines are called node and saddle *pinch branches*, see **Figure 2-19**. The presence of stripping node branches makes unfeasible the separation of Ethanol-Water-Ethylene glycol in a single feed distillation column. Fortunately, it is possible to create a bridge between the rectifying and stripping profiles by means of a two-feed column, the extractive distillation.

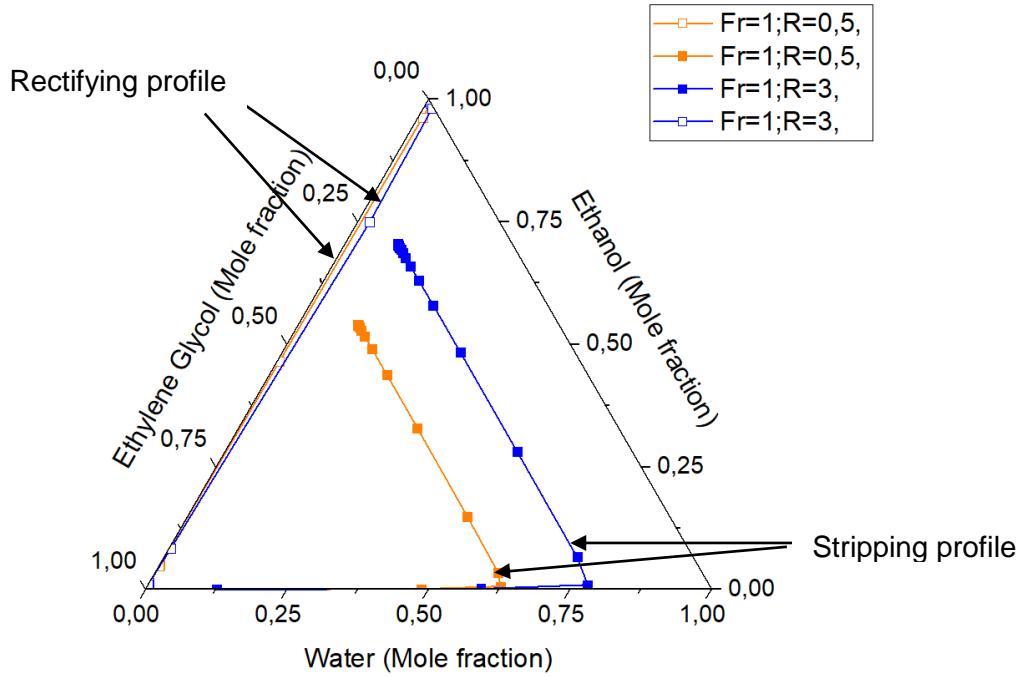


**Figure 2-18:** Column profiles for a single feed distillation column considering the separation of Ethanol-Water-Ethylene glycol mixtures.

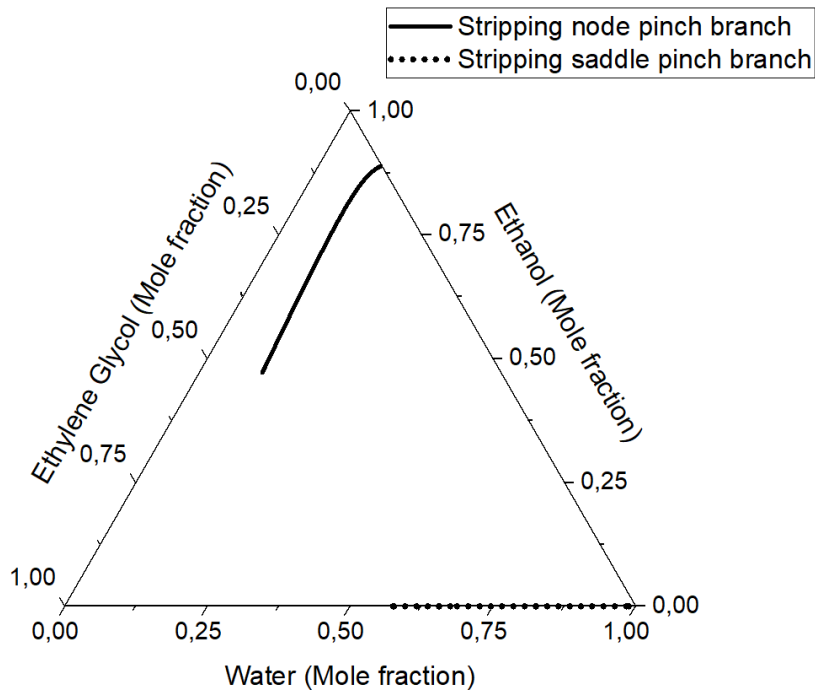


**Figure 2-19:** Stripping pinch branches.

**Figure 2-20** shows a two-feed distillation column for extractive distillation. The upper feed to the column is nearly pure entrainer and the lower feed is an Ethanol-Water mixture of composition near to the binary azeotrope shown in **Figure 2-15**. The addition of a new feed generates a new section. This section is called middle section as it is located between the rectifying and stripping sections. The new configuration with two feeds has the advantage that the equations that describe a single feed column, equations (2.39) and (2.40), are also applicable here (Julka & Doherty, 1990). Therefore, the total column profile is defined if the middle section equations are defined. According to (Knight, 1987), these equations can be described in terms of either reflux or reboil ratio, but the natural form of the middle section is based on the reflux ratio. For middle section calculations, the stages are counted up from the lower feed tray, which corresponds to the upper tray of the stripping section. A deduction of these equation is reported in (Knapp & Doherty, 1994). See equations (2.41):

Middle section:

$$x_{k+1}^m = \left[ \frac{r + 1 + (q_U - 1)h(Fr, w)}{r + q_U h(Fr, w)} y_k^m \right] + \left[ \frac{h(Fr, w)x_{FU} - x_D}{r + q_U h(Fr, w)} \right] \quad (2.41a)$$

$(k = 0, 1, 2 \dots)$

The initial conditions for the computation of the middle section are based on the last stage of the stripping section.

$$x_0^m = x_N^s \quad (2.41b)$$

In order to close the equation system, the reboil and reflux ratios must be related with equation (2.42).

$$s = (r + 1) \frac{D}{B} + \frac{F_L}{B} [h(Fr, w) + (q_U - 1)] \quad (2.42)$$

where

$$h(Fr, w) = \frac{Fr(x_{D,i} - x_{B,i})}{Fr(x_{FU,i} - x_{B,i}) + x_{FU,i} - x_{B,i}} \quad (2.43)$$

and:

- $Fr$ : feed ratio FU/FL
- $w$ : is a vector of feed and product mole fractions
- $q_U$ : is upper feed quality

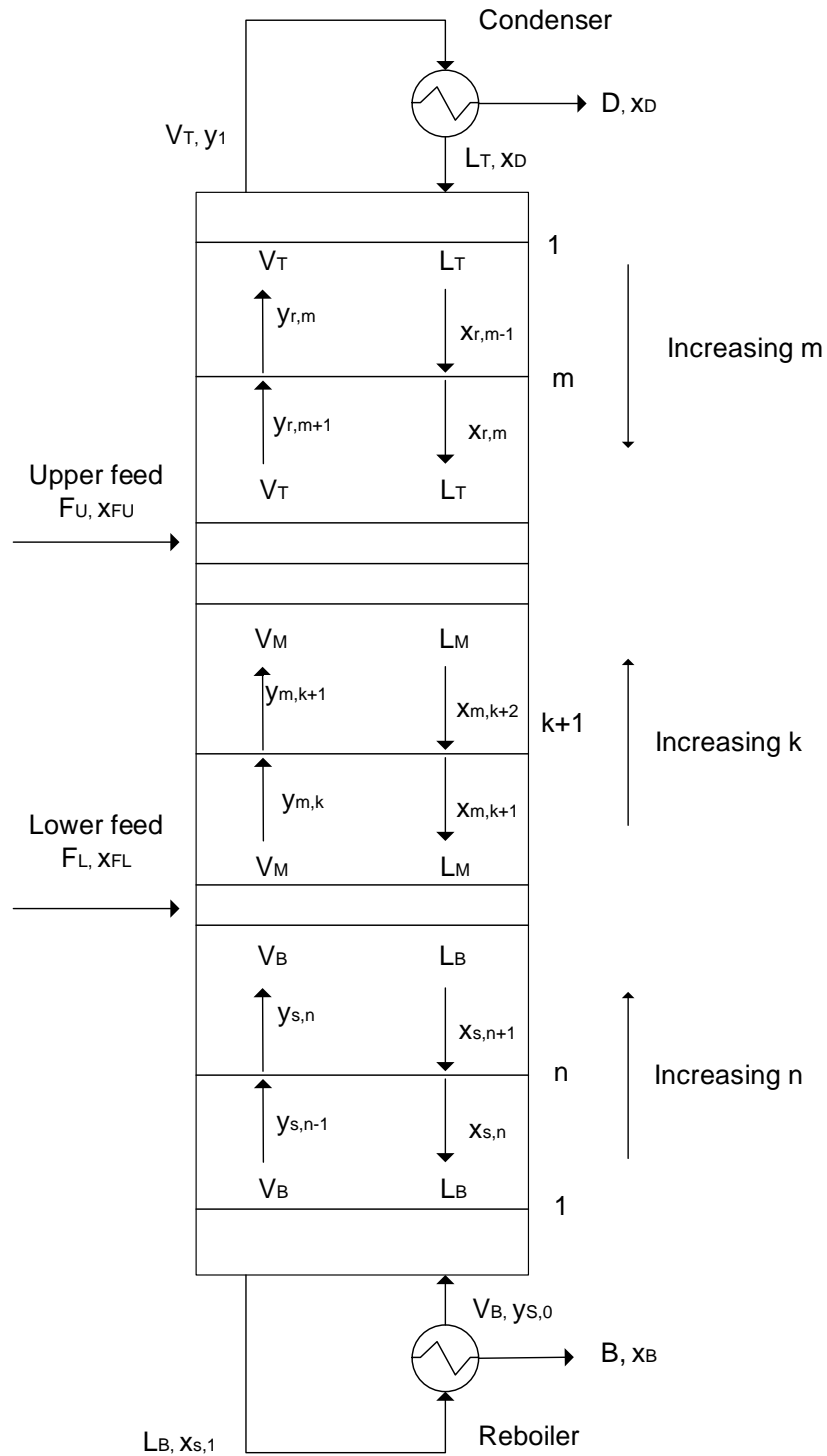


**Figure 2-20:** Double feed distillation column.



Complete two feed column profiles for the extractive distillation of ethanol-water using ethylene glycol as entrainer are shown in **Figure 2-21**. It can be noticed that the middle section joins the stripping and rectifying profiles at its ends. The middle section profile also reaches a node pinch near to the rectifying section and presents a saddle pinch near to the upper stages of the stripping section. If more column profiles are plotted the result is called Column Profile Map and, if the node and saddle pinch points for each profile are plotted, the formed line are called *pinch branches*. This will be studied again in next chapter for determination of the solvent to feed ration and reflux ratio.

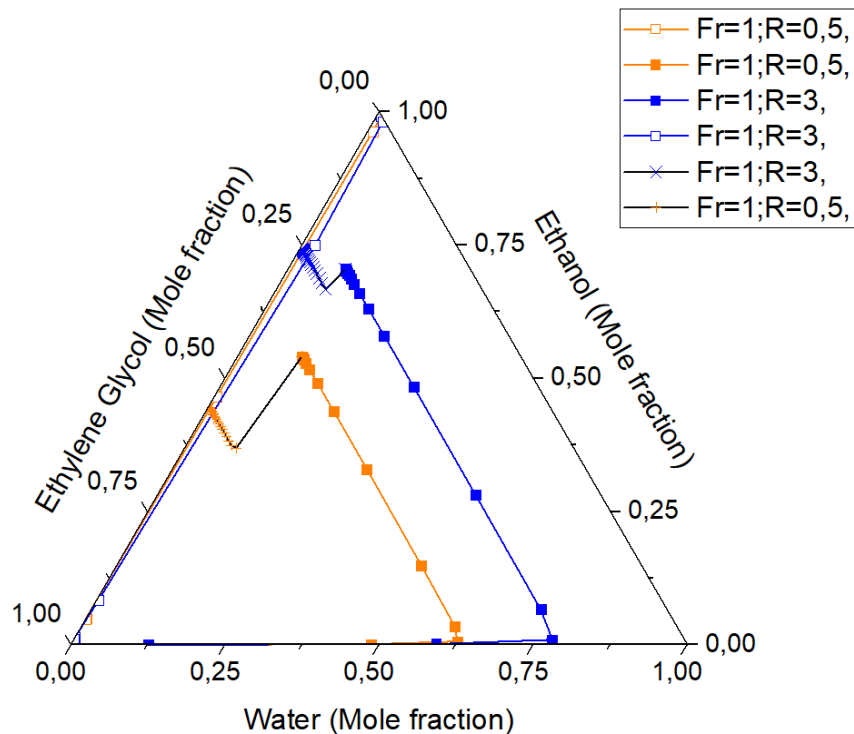


**Figure 2-21:** Column profiles for a two feed distillation column used in the separation of Ethanol-Water-Ethylene glycol mixtures.  $\times$  Middle section;  $\blacksquare$  Stripping section;  $\square$  Rectifying section.

## 2.8 Conclusions

In this chapter a detailed study of conceptual design for distillation based separation processes is developed. The definition of this conceptual design has led to define the methodology of this work.

The review of the literature related to the design of distillation based separations has contextualized the synthesis problems for the extractive separation sequence. These are: 1) finding the optimum sequence of separations and the nature of each separator and 2) finding the optimal design values for each separator (sizes, operating conditions). This has led to propose the first synthesis problem from the point of view of direct and indirect thermal integration. It means, improvements by extractive dividing wall distillation and internal sequential heat exchangers.

Verification of thermodynamic equilibrium parameter led to conclude that the default parameters available in Aspen Plus do not adjust the equilibrium experimental data. This values need to be changed. In contrast, the default parameters of the vapor pressure generate satisfactory adjustment.

Generated isovolatility curves allowed to analyze in graphical form the thermodynamic consistence of the activity model based on the tendency behavior of the curves.

The residue curve equations were solved by means of Matlab and Excel. The results were mapping in the composition space. The three results had a similar behavior taking into the count the use of different numerical method in their solution.

It was shown graphically the unfeasibility of the separation of the Ethanol-Water-Ethylene Glycol mixture in a single feed column. A feasible column was proposed by means of a second upper feed that generates an intermediate profile that connect the stripping profile with the rectifying profile in a two feed column.

### 3. Extractive distillation conceptual design

Some distillation based separation processes use a mass agent in liquid phase to influence the relative volatility of the mixture and improve its separation. This agent is commonly known as entrainer and depending on its effect on the separation of the mixture, it can be distinguished between three types of azeotropic distillation: a) homogeneous azeotropic distillation, b) heterogeneous azeotropic distillation and c) extractive distillation. From the graphical point of view, it is possible to differentiate each one of these types of distillations using residue curve maps. The total number of residue curve maps structures that can be obtained from ternary combinations of the available components in the world is enormous. However, all these possible structures can be classified in 113 characteristic residue curve maps defined with the topological index theory by (Matsuyama & Nishimura, 1977). From the total, 87 characteristic residue curve maps can have at least one azeotrope. Doherty and coworkers made a graphical representation of these 87 maps (Doherty & Caldarola, 1985). A sample is shown in **Figure 3-1**.

From all 113 characteristic maps, there is one residue curve map named as 100 in the Matsuyama nomenclature (one azeotrope in L-L, non-azeotrope in I-H and non-azeotrope in H-L), see **Figure 3-1**. This is the characteristic structure of the extractive distillation defined by Benedict as follows:

*“Distillation in the presence of a substance which is relatively non-volatile compared to the components to be separated and which therefore, is charged continuously near the top of distillation column so that an appreciable concentration is maintained on all plates of the column”.* (Benedict & Rubin, 1945)

(Doherty & Caldarola, 1985) conclude that this definition is too restrictive and analyzed a more general concept. However, in this document the definition of Benedict is used as its author considers that it applies enough for the studied system Ethanol-Water-Ethylene Glycol.

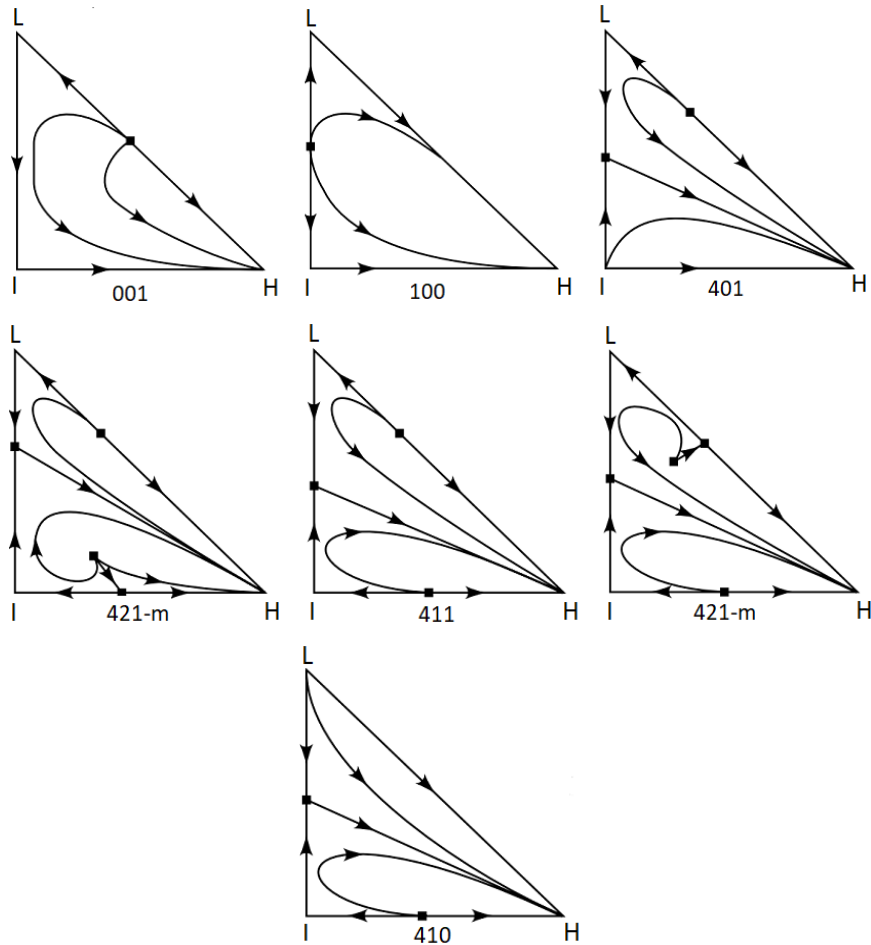


**Figure 3-1:** Seven of the most favorable residue curves that describe the separation of mixtures with minimum binary boiling point azeotropes by adding a separation agent.

*Figure 7 in (Foucher et al., 1991)*

Also based on the Benedict definition, Doherty established three categories of extractive distillation: a) extractive distillation for separation of minimum boiling azeotropes, b) extractive distillation for separation of maximum boiling azeotropes, and c) extractive distillation for separation of low relative volatility non-azeotropic mixtures (Doherty & Knapp, 2004). The present study focuses only on the first category: a non-ideal mixture with non-reactive, non-heterogeneous, minimum boiling point azeotrope.

### 3.1 Extractive distillation theory

It is not common to find quantitative theories to explain the extractive distillation. However, at least two theories exist related to extractive distillation. The first one was published by (Prausnitz & Anderson, 1961) and gave a semi-quantitative theory for the separation of hydrocarbon mixtures by addition of an entrainer. This theory tries to explain the solvent selectivity in hydrocarbon separations by using the definition of chemical and physical forces. In their article, the authors provide an equation that associates the selectivity (see **section 3.2.1**) with three separated contributions of the physical force. Among these, the polarity of the molecules is the measure that more affects the selectivity of non-ideal interactions. In contrast, for ideal mixtures, there is no polarity contribution, and the selectivity is affected mainly by chemical forces.

The second theory is the Scaled Particle Theory and is completely quantitative (Li, Lei, Ding, Li, & Chen, 2005). This theory tries to interpret the effect of solid salts on the relative volatility of the components to be separated. It means that the solid salt is diluted in the liquid entrainer in order to improve the separation. The advantage of the Scaled Particle Theory is that it is based on thermodynamics and statistical physics, and, therefore, it requires only molecular parameters that are readily available. Other particle theories can be found in the literature, but they are based mainly on experimental measurements.

In contrast to quantitative theories, qualitative analysis of extractive distillation is mainly based on the concepts of relative volatility, selectivity and Raoult's law deviations. These analyses have the advantage that they provide initial arguments for the selection of possible entrainers despite the lack of theoretical information or experimental data. An example of this is the work of (Doherty & Knapp, 2004), which describes some characteristics of the entrainers that, based on a qualitative analysis, can be used to select between possible candidates (e.g. chemical homologues, polarity of functional groups and hydrogen-bonding tendencies).

## 3.2 Entrainer selection

Entrainer selection is a crucial decision in the development, design and operation of a feasible extractive distillation process. According to (Doherty & Knapp, 2004) the entrainer selection is carried out by next steps:

- Use of qualitative methods for the identification of general classes of compounds or functional compounds that make the entrainer effective for the separation.
- The pre-defined compounds are evaluated individually and ranked to identify the most promising candidates.
- Detailed vapor liquid equilibrium measurements are made for the top candidates.
- The separation is simulated using chemical process simulation software.
- The separation is evaluated in lab equipment.
- The solvent selection is made.

### 3.2.1 Qualitative methods for entrainer selection

Qualitative methods are based on the qualitative characteristics of the possible entrainers and its effect on the relative volatility of the mixture to be separated. From the binary distillation theory, it is well known that the separation of a two-components mixture is favored as the relative volatility, expressed in equation (2.18), moves away from the unity. For the extractive distillation theory, the relative volatility is also important in order to explain the influence of the entrainer in the separation of the components in the original binary mixture. This influence is commonly measured by means of the so-called selectivity  $S$ . For a given entrainer the selectivity respect to the ethanol water system is defined as follows:

$$S_{EtOH,Water} = \frac{\alpha_{EtOH,water|E}}{\alpha_{EtOH,water}} \quad (3.1)$$

Equation (3.1) expresses the ratio of relative volatilities of the key components with and without solvent. Assuming that for small temperature changes, the ratio  $\frac{P_1^s}{P_2^s}$  is approximately constant, it could be noticed that the relative volatility is mainly affected by the ratio of activity coefficients of ethanol and water with and without entrainer. In addition, as the denominator in equation (3.1) is always the same for different entrainers, it is common to find an expression of selectivity as equation (3.2) (Gerbaud & Rodriguez, 2014).

$$S_{EtOH,Water} = \frac{\gamma_{EtOH|E}}{\gamma_{water|E}} \quad (3.2)$$

If it is not possible to have access to experimental data, a good approximation that can be implemented based on computation of thermodynamic model is the selectivity at infinite dilution of the entrainer, which is shown in equation (3.3).

$$S_{EtOH,Water}^{\infty} = \frac{\gamma_{EtOH|E}^{\infty}}{\gamma_{water|E}^{\infty}} \quad (3.3)$$

Some entrainers enhance the selectivity and others reduce it. Heuristically, for extractive distillation purposes it is preferred to use entrainers that enhance the selectivity ( $S_{EtOH,Water} > 1$ ), and, therefore, that cause the more volatile component to distill overhead. In practice this means that the solvent should have an ideal behavior with the intermediate component and a positive deviation of Raoult's law with the most volatile component. For the Ethanol-Water-Entrainer system, (Lee & Pahl, 1985) proposed ten candidates as entrainer for the extractive distillation, as shown in **Table 3-1**.

**Table 3-1:** Possible entrainers for the extractive distillation of Ethanol-Water mixtures.

Proposed entrainers
Tetraethyleneglycol
Triethylene Glycol
Trimethylene Glycol
Diethylene Glycol
Ethylene Glycol
1,4-Butanediol
Glycerin
n-Methylpyrrolidone
Phenylthioethanol
Di-n-Propyl Sulfone

As there are thousands of different substances that can be studied as entrainers for a given system, it is convenient to reduce the number of possible candidates to a few ones. For this purpose, calculation methods as Computer-Aided Molecular Design (CAMD) can reduce the number of experiments for the screening of substances. CAMD has also the advantage of being used to identify new possible candidates. As example, according to CAMD

simulation, it was found that a very well performing solvent for extractive distillation for the Ethanol-Water system is Hexachlorobutadiene. This solvent has a calculated relative volatility of 8.41 in contrast to the calculated 2.58 for ethylene glycol at similar additions (Dyk & Nieuwoudt, 2000). However, it has been noticed that entrainers with high selectivity usually have low capacities (Gerbaud & Rodriguez, 2014). In this way, the selection of the solvent usually must take into account both selectivity and capacity in order to optimize the decision. *Capacity* of a solvent is its ability to solubilize the components to be separated. Equation (3.4) evaluates the capacity of the entrainer with respect to component  $i$ .

$$C_i^\infty = \frac{1}{\gamma_i^\infty} \quad (3.4)$$

### 3.2.2 Evaluation of predefined compounds

In (Lee & Pahl, 1985), the pre-defined compounds in **Table 3-1** were individually evaluated and ranked to identify the most promising candidate. This evaluation was done using experimental methods. Some results obtained by the authors are shown in **Table 3-2**.

**Table 3-2:** Experimental measurements of the influence of different solvents in the extractive distillation of Ethanol-Water mixtures (Lee & Pahl, 1985).

Proposed entrainers	Ethanol to water relative volatility with 35%wt of solvent
Tetraethyleneglycol	2.33
Triethylene Glycol	1.88
Trimethylene Glycol	1.92
Diethylene Glycol	1.69
Ethylene Glycol	1.68
1,4-Butanediol	1.45
Glycerin	3.23
n-Methylpyrrolidone	1.30
Phenylthioethanol	1.22
Di-n-Propyl Sulfone	0.78

From **Table 3-2** it is noticed that initially the possible candidates Tetraethyleneglycol and glycerin could have the most promising performances for the separation. In contrast, Phenylthioethanol, n-Methylpyrrolidone and Di-n-Propyl Sulfone should be initially discarded.



### 3.2.3 Detailed vapor liquid measurements

Vapor liquid equilibria calculation brings not only a qualitative measurement of influence of different solvents in the separation of azeotropic mixtures, but it also brings a quantitative tool for the rapid screening of the solvents by means of their graphic performance.

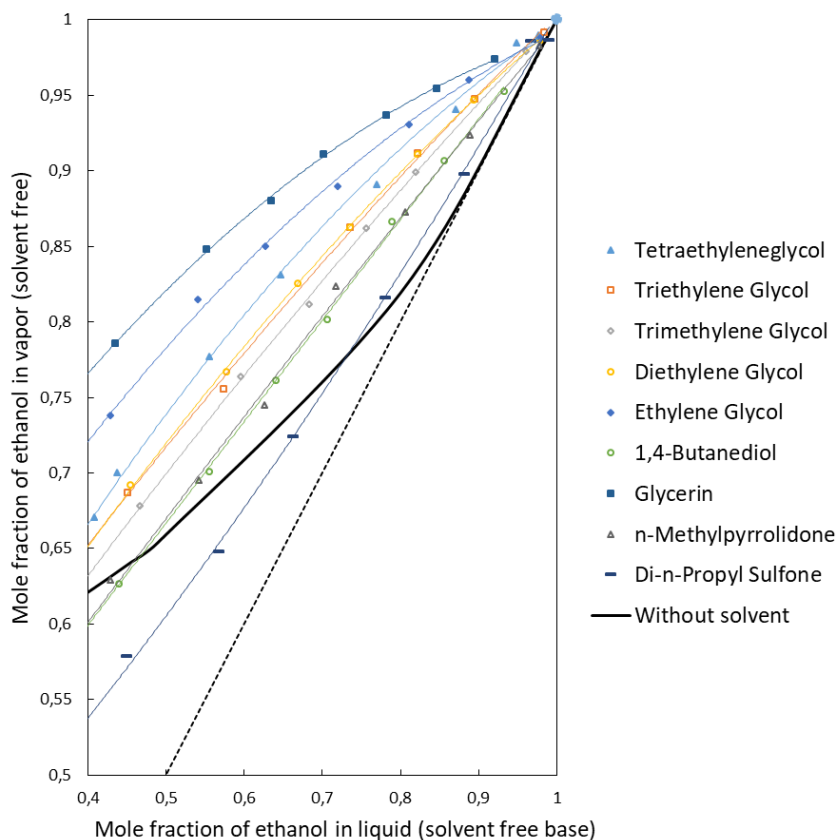


**Figure 3-2:** Pseudobinary vapor liquid equilibrium diagram for ethanol-water system in presence of different solvents (solvent to feed ratio between 0,2 and 0,3). From (Lee & Pahl, 1985)

**Figure 3-2** shows the influence of the entrainers listed in **Table 3-2** on the equilibrium of the Ethanol-Water system. The compositions of ethanol in liquid and vapor phase are plotted in a free basis of entrainer. The compositions of the equilibrium without solvent are also plotted in order to visualize the azeotrope formation. The deviation of the equilibrium from the dotted line of 45° in the presence of each solvent is a qualitative measurement of the facility of the separation. The more deviated the line is, the easier the separation. With this in mind, the two entrainers that have the most positive effect in the separation of ethanol water mixtures are Glycerin and Ethylene glycol.

### 3.2.4 Separation simulation

In chapter 1, a scheme of the characteristic column sequence for the separation of ethanol water by extractive distillation was described, see **section 1.10.3**. Probably the earliest reported case of separation of Ethanol-Water mixtures by extractive distillation was the patent of (Schneible, 1922), which uses glycerin as separation agent. On the other hand, one of the earliest patents using ethylene glycol entrainer was reported by (Washall, 1969). Both patents describe the separation process used that is shown in **Figure 1-32**, in a simple way. In this work, this scheme is used for simulation in Aspen Plus with Radfrac models.

Several studies in the simulation of extractive distillation have been made for both ethylene glycol and glycerin. In case of ethylene glycol, (Black & Ditsler, 1974) and (Meirelles, Weiss, & Herfurth, 1991) are two of the earliest studies with this solvent. A more recent reference is the document by (Kiss & Ignat, 2012). On the other hand, the study of glycerin based on simulation is reported by (Gil, Aguilar, & Caicedo, 2006).

Ethylene glycol is maybe the most used entrainer in extractive distillation of ethanol water system. However, it was noticed from **Figure 3-2** that glycerin produces a better relative volatility than ethylene glycol. Consequently, from the referenced article (Gil et al., 2006), it was concluded that glycerin also has advantages in terms of energy consumption respect to the process with ethylene glycol. As glycerin is a byproduct of biodiesel production, there is a growing supply of glycerin in the world that leads to economic and environmental advantages of the use of glycerin as entrainer. However, glycerin has the disadvantage of its high viscosity, which limits the operation of extractive distillation process and increases the pump work. This disadvantage can be overcome by the use of mixtures ethylene glycol – glycerin. (Gil, García, & Rodríguez, 2014) report a simulation based study in this way.

In the present document, ethylene glycol is chosen as entrainer taking into account that it has been subject of several conceptual, computational and experimental studies. Moreover, ethylene glycol has proven to be a suitable entrainer for the separation of Ethanol-Water mixtures in industrial applications. In contrast, more studies in glycerin performance are required for its use at industrial scale.

### 3.3 Extractive distillation design

The design of a distillation column for extractive distillation is conveniently categorized in two stages of design (Sánchez, 2011). The first stage consists in the conceptualization of the design based on input specifications, and the second stage consists on hardware specifications and requirements. The results of the first stage are the feasibility analysis of the separation and definition of the minimum and maximum reflux ratio and solvent to feed ratio. Hardware requirements for the design are e.g. column diameter, definition of tray or packing, and prediction of the column performance. The first stage is developed here after.

#### 3.3.1 Specifications

The first specification that must be established in design of extractive distillation is the pressure at which the equilibrium will be evaluated. In absence of restrictions, related to the degradation of the components or operation conditions, this pressure is preferred to be atmospheric. This is not the case of the Ethanol-Water-Ethylene glycol separation system where the pressure must be adjusted to avoid the entrainer degradation. There is reported evidence of the degradation of ethylene glycol as the temperature increases (Clifton, Rossiter, & Brown, 1985). The degradation of this compound leads to the formation of different organic acids that corrodes the equipment used in industrial processes (Wheeler, 2002). As a consequence, an increasing maintenance and operation cost is expected if the degradation is not avoided.

**Figure 3-3** shows the effect of the temperature on the degradation of ethylene glycol. This degradation is measured in terms of pH as the glycol forms acids in presence of water and heat. It can be seen that, for temperatures over 100 °C, the rate of degradation of the glycol is significantly increased with respect to temperatures below 100°C. In fact, the time that it takes for the glycol to achieve the pH=4 at 86°C is four times larger than the time that it takes at 101°C. In the case of the separation of Ethanol-Water mixtures with ethylene glycol, a similar degradation can be produced as a consequence of the boiling in the reboiler of both extractive and recovery columns.

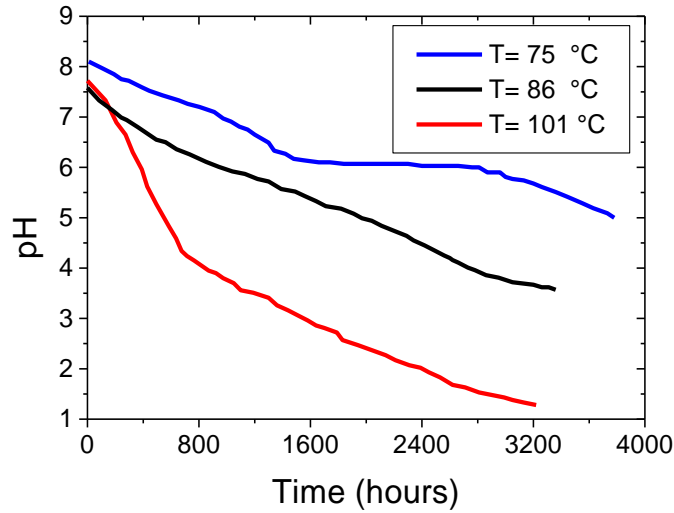


**Figure 3-3:** Degradation of ethylene glycol solutions. From (Clifton et al., 1985)

In order to avoid the degradation of the entrainer in an extractive distillation of Ethanol-Water system, the temperature in the warmest place of the column (the reboiler) should not reach 150°C (Meirelles et al., 1991). In the practice it means that the operation pressure of the column should be fixed under 0.2 bar, see **Figure 3-4**.

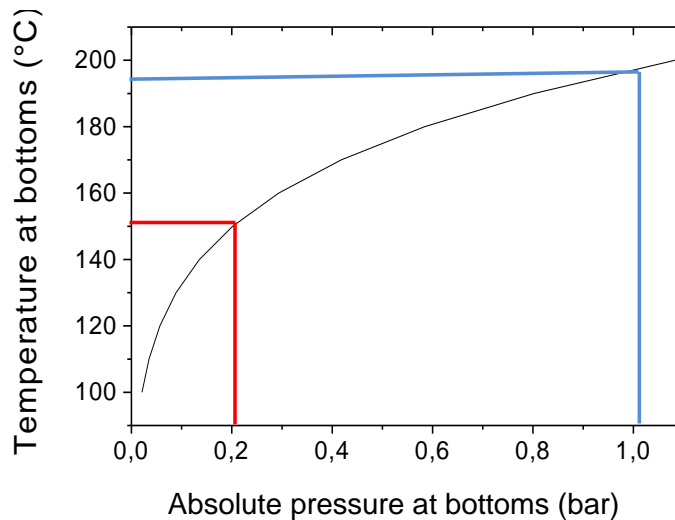


**Figure 3-4:** Sensitivity of the bottoms temperature in extractive column to the operating pressure.

On the other hand, as pressure changes, the performance of the equilibrium also changes, see **Figure 3-5**. Therefore, the composition of the azeotrope deviates from its value of 0.8889 ethanol mol fraction at 1 atm to 0.9081 mol fraction at 0.2 atm.

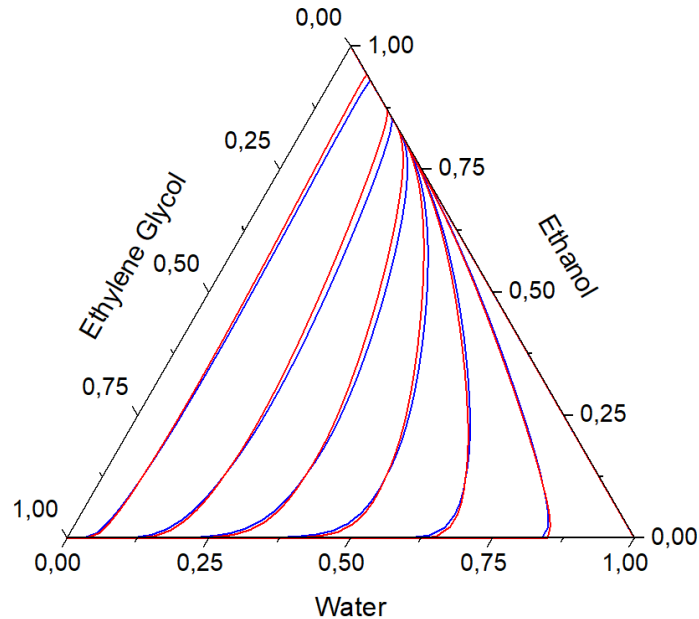


**Figure 3-5:** Sensibility of the equilibrium to pressure change. Red: 0.2 atm. Blue: 1 atm.

After the pressure of the calculation of the equilibrium has been specified, the next step is to define the total number of variables that are involved in the system. Based on **Figure 3-6**, the **Table 3-3** shows the equations for mass and energy calculations. It can be noticed that the total number of equations is 18 and the number of variables is 39. It means that at least the 21 variables shown in **Table 3-4** must be specified for the solution of the system (Knight & Doherty, 1989).

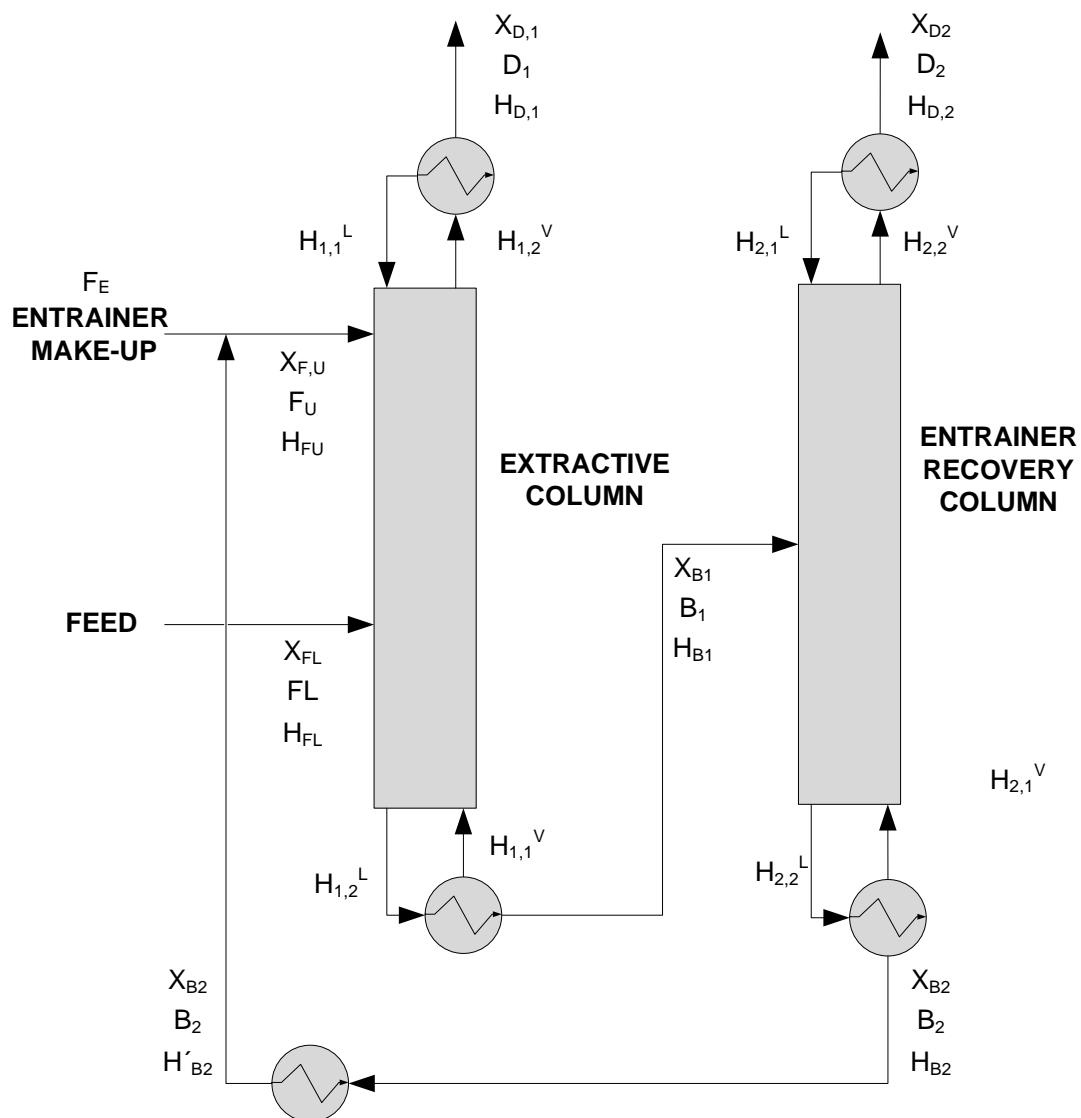


**Figure 3-6:** Variables of the extractive separation system.

**Table 3-3:** Equation system for the description of the extractive distillation. For details see (Knight, 1987).

<b>Mass balance equations</b>		
1	$F_E + F_L = D_1 + D_2$	$F_E$ $F_L$ $D_1$ $D_2$
2	$x_{F_E,EtOH}F_E + x_{F_L,EtOH}F_L = x_{D_1,EtOH}D_1 + x_{D_2,EtOH}D_2$	$x_{F_E,EtOH}$ $x_{F_L,EtOH}$ $x_{D_1,EtOH}$ $x_{D_2,EtOH}$
3	$x_{F_E,water}F_E + x_{F_L,water}F_L = x_{D_1,water}D_1 + x_{D_2,water}D_2$	$x_{F_E,water}$ $x_{F_L,water}$ $x_{D_1,water}$ $x_{D_2,water}$
4	$F_L + F_U = D_1 + B_1$	$B_1$ $F_U$
5	$x_{F_E,EtOH}F_L + x_{F_U,EtOH}F_U = x_{D_1,EtOH}D_1 + x_{B_1,EtOH}B_1$	$x_{F_U,EtOH}$ $x_{B_1,EtOH}$
6	$x_{F_E,water}F_E + x_{F_U,water}F_U = x_{D_1,water}D_1 + x_{B_1,water}B_1$	$x_{F_U,water}$ $x_{B_1,water}$
7	$B_1 = D_2 + B_2$	$B_2$
8	$x_{B_1,EtOH}B_1 = x_{D_2,EtOH}D_2 + x_{B_2,EtOH}B_2$	$x_{B_2,EtOH}$
9	$x_{B_1,water}B_1 = x_{D_2,water}D_2 + x_{B_2,water}B_2$	$x_{B_2,water}$
<b>Energy balance equations</b>		
10	$h_{F_E}F_E + h_{F_L}F_L + Q_{ex} + B_1(h_{B_1} - Q_{reb,1}) + B_2(h_{B_2} - Q_{reb,2}) = D_1Q_{cond,1} + D_2Q_{cond,2}$	$H_{F_E}$ $H_{F_L}$ $Q_{ex}$ $H_{B_1}$ $H_{B_2}$ $Q_{reb,1}$ $Q_{reb,2}$ $Q_{cond,1}$ $Q_{cond,2}$
11	$h_{F_U}F_U + h_{F_L}F_L - B_1Q_{reb,1} = D_1Q_{cond,1}$	$H_{F_U}$
12	$h_{B_1}B_1 - B_2Q_{reb,2} = D_2Q_{cond,2}$	
13	$h_{B_2}B_2 = h'_{B_2}B_2 + Q_{ex}B_2$	$H'_{B_2}$
14	$Q_{cond,1} = (r_{ext,1} + 1)h_{1,2}^V - r_{ext,1}h_{1,1}^L$	$r_{ext,1}$
15	$Q_{cond,2} = (r_{ext,2} + 1)h_{2,2}^V - r_{ext,2}h_{2,1}^L$	$r_{ext,2}$
16	$S_{ext,1} = \frac{\left[ \frac{x_{B_1,EtOH} - x_{F,EtOH}}{x_{F,EtOH} - y_{D_1,EtOH}} \right] (Q_{cond,1} - h_F) - h_F + h_{1,2}^L}{h_{1,1}^V - h_{1,2}^L}$	$(h_{1,1}^V; h_{1,2}^L; y_{D_1,EtOH}) \rightarrow h_{D1}$ $S_{ext,1}$
17	$S_{ext,2} = \frac{\left[ \frac{x_{B_2,EtOH} - x_{B_1,EtOH}}{x_{B_1,EtOH} - y_{D_2,EtOH}} \right] (Q_{cond,2} - h_F) - h_{B_1} + h_{2,2}^L}{h_{2,1}^V - h_{2,2}^L}$	$(h_{2,1}^V; h_{2,2}^L; y_{D_2,EtOH}) \rightarrow h_{D2}$ $S_{ext,2}$
18	$F_r = F_U/F_L$	$F_r$

The feed composition for the extractive column is defined to be near to the azeotrope with a molar flow of 100 kmol/h. The condition of this stream saturated liquid. Upper feed is mainly ethylene glycol. As some of this entrainer is lost in the out streams of the system, it is necessary to use a make-up with a high purity entrainer. The top composition of extractive column is defined by the legal framework reported in Chapter 1. In here case, 99 %vol of ethanol purity is required with 99,9% of ethanol recovery. The top composition of the recovery column is defined to be higher than 0.999 mol fraction of water with high recovery in order to ensure high purity of the recycled entrainer. **Table 3-4** lists these and other variables specified for the solution of the mathematical model of the system.

**Table 3-4:** List of specifications.

DESIGN VARIABLE	SYMBOL	SPECIFIED	DESCRIPTION
<b>Etrainer make-up</b>			
Composition	$x_{F_E,EtOH}$	1	Both specified as 0. Mol fraction of entrainer equal to 1
	$x_{F_E,water}$	2	
Enthalpy	$H_{F_E}$	3	Liquid at ambient temperature
Flow rate	$F_E$	4	Calculated by material balance
<b>Column 1</b>			
<b>Lower feed</b>			
Composition	$x_{F_L,EtOH}$	5	Based on: 0,8564 mol/mol 0,1436 mol/mol
	$x_{F_L,water}$	6	
Enthalpy	$H_{F_L}$	7	Saturated liquid
Flow rate	$F_L$	8	100 kmol/h (~37kTon/year; ~53x10 <sup>6</sup> L/year)
<b>Upper feed</b>			
Composition	$x_{F_U,EtOH}$	9	0 mol/mol 1,716x10 <sup>-3</sup> mol/mol 0,9983 mol/mol
	$x_{F_U,water}$	10	
	$x_{F_U,Glycol}$		
Enthalpy	$H_{F_U}$	11	Liquid at 80 °C
Flow rate	$F_U$		Calculated, $F_U = F_r * F_L$
<b>Feed ratio</b>	$F_r$		Defined in <b>section 3.3.3.1</b>
<b>Distillate</b>			
Composition	$x_{D_1,EtOH}$	12	>99 %vol (with 99,9% recovery) <1 %vol
	$x_{D_1,water}$	13	
Enthalpy	$H_{D_1}$	14	Liquid at specified temperature
Flow rate	$D_1$		Calculated by material balance
<b>Bottoms</b>			
Composition	$x_{B_1,EtOH}$		7,3x10 <sup>-5</sup> mol/mol 0,1436 mol/mol
	$x_{B_1,water}$		



DESIGN VARIABLE	SYMBOL	SPECIFIED	DESCRIPTION
Enthalpy	$H_{B_1}$	15	Saturated liquid
Flow rate	$B_1$		Calculated by material balance
<b>Reflux ratio</b>	$r_{ext_1}$		Defined in <b>section 3.3.4</b>
<b>Reboil ratio</b>	$s_{ext,1}$		Calculated by energy balance
<b>Condenser difference point</b>	$Q_{cond_1}$		Calculated with equation 14 in <b>Table 3-3</b>
<b>Reboiler difference point</b>	$Q_{reb,1}$		Calculated with equation 15 in <b>Table 3-3</b>
<b>Column 2</b>			
<b>Distillate</b>			
Composition	$x_{D_2,EtOH}$	16	0,0000 mol/mol
	$x_{D_2,water}$	17	0,9994 mol/mol Glycol by balance
Enthalpy	$H_{D_2}$	18	Vapor at ~100°C
Flow rate	$D_2$		Calculated by material balance
<b>Bottoms</b>			
Composition	$x_{B_2,EtOH}$	19	0,000 mol/mol
	$x_{B_2,water}$	20	<0,0001 mol/mol Glycol > 0,999 mol/mol
Enthalpy	$H_{B_2}$	21	Saturated liquid
Flow rate	$B_2$		Calculated by material balance
<b>Reflux ratio</b>	$r_{ext_2}$		$r_{ext_2} = 1,2 r_{min}$
<b>Reboil ratio</b>	$s_{ext,2}$		Calculated by energy balance
<b>Condenser difference point</b>	$Q_{cond_2}$		Calculated with equation 14 in <b>Table 3-3</b>
<b>Reboiler difference point</b>	$Q_{reb,2}$		Calculated with equation 15 in <b>Table 3-3</b>
<b>Recycle stream</b>			
<b>Exchanger heat duty</b>	$Q_{ex}$		Calculated by energy balance
<b>Enthalpy</b>	$H'_{B_2}$		Calculated by energy balance

### 3.3.2 Feasibility

The feasibility is related to the question of it is possible to overcome the composition of the azeotrope, and, if it is possible, what must be the requirements to do it. The answer to these questions deals with the nonlinear analysis of the system with the tools developed earlier in chapter 2: residue curve maps, isovolatility lines and vapor liquid equilibrium. It also implies the characterization of the separation (specifications) and establishment of the minimum reflux, the solvent to feed ratio and the reflux ratio.

From **Figure 3-2** it is observed that the addition of the entrainer to the azeotrope mixture Ethanol-Water affects positively the equilibrium, making the separation feasible. In the specific case of ethylene glycol as entrainer, there is a formation of azeotrope of minimum temperature boiling point. **Figure 3-7** shows that the addition of the entrainer displaces this azeotrope to higher compositions until it is overcome and the equilibrium line is deviated from the 45° line.

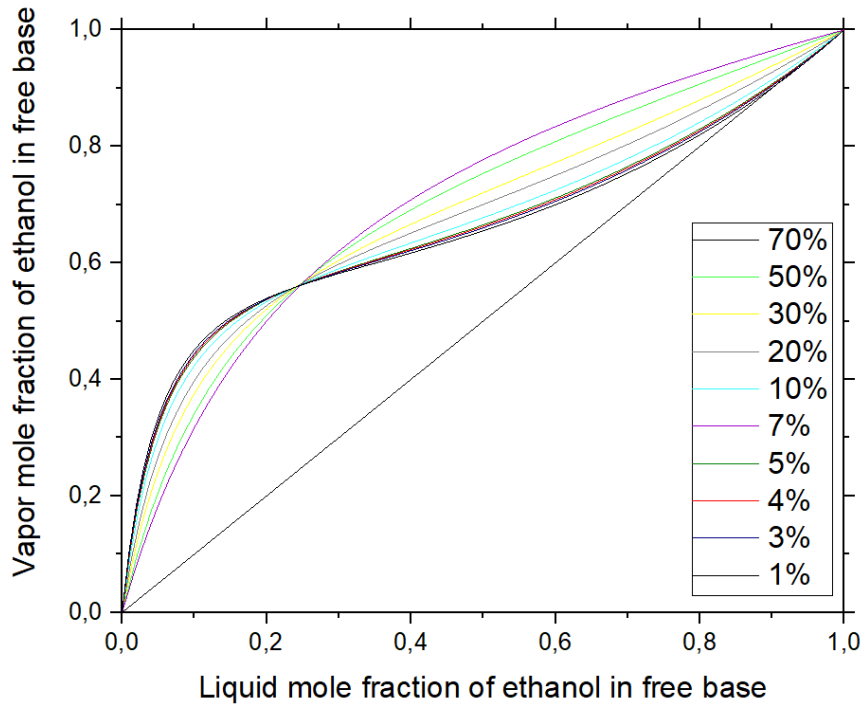


**Figure 3-7:** Pseudobinary vapor liquid equilibrium diagram for ethanol-water system in presence of ethylene glycol.

All the possible pseudobinary azeotropes shown in **Figure 3-7** belong to one point on the curve of univolatility  $\alpha = 1$  on the composition space, shown in **Figure 3-8**. The curve starts at the composition of the azeotrope and finishes on the binary composition line Ethylene glycol-water. In consequence, the curve divides the composition triangle in two regions: one with relative volatility  $\alpha_{ethanol-water}$  higher than unity and other with relative volatility lower than unity. The point of maximum ethylene glycol composition on the univolatility curve ( $x_p$ ) defines the minimum solvent required to overcome the azeotrope. For ethylene glycol this point is  $x_p = \sim 0.0603$  at 1 atm and  $x_p = \sim 0.0438$  at 0.2 atm, see **Figure 3-8**.

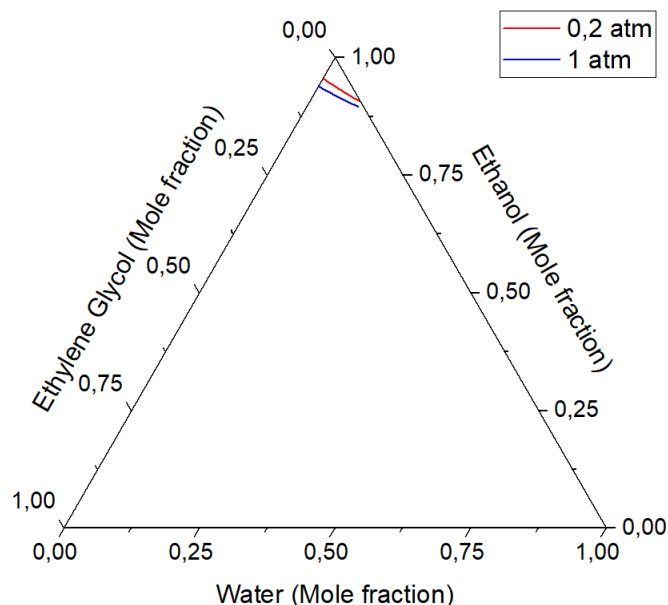


**Figure 3-8:** Univolatility curve at 1 atm and 0,2 atm.

As comparison, the end point in the univolatility curve with glycerol as entrainer is  $x_p = \sim 0.028$  at 1 atm (based on NRTL model with default parameters in Aspen Plus). This means that ethylene glycol has a minimum requirement of entrainer that is higher than the minimum entrainer requirement for glycerol. On the other hand, the isovolatility at infinite dilution for ethylene glycol is  $\sim 1,688$  and for glycerol is  $\sim 7,99$  at 1 atm. According to equation (3.3), this means that glycerol has a better selectivity than ethylene glycol and is a better candidate for the separation. However, despite its advantages in selectivity, the entrainer capacity of the glycerol is lower than the entrainer capacity of the ethylene glycol (see equation (3.4)). This shows that the selection between solvents is not trivial. Furthermore, the optimal selection could be a mixture of ethylene glycol – glycerol instead of the use of a single component as entrainer (Gil et al., 2014). Complementary studies will be required in this aspect. In the present document, glycerol is initially discarded because despite of its advantages, this entrainer has a high viscosity that could make unfeasible its use at industrial scale. On the other hand, the use of ethylene glycol has been widely validated in laboratories and industries as can be found in different patents and articles.

**Figure 3-9** shows the effect of the solvent addition in the VLE distribution lines. Empty symbols represent the composition in liquid phase that are in equilibrium with the vapor phase composition represented by filled symbols. For a defined amount of solvent, the distance between vapor and liquid composition points is a measure of the easiness of the separation. This is analogous to the separation of the bubble line from the dew line in a T-

x binary vapor liquid equilibrium diagram. Based on this observation, it is noticed that the consequence of the addition of entrainer is the increasing of the potential of separation which increases the feasibility of the separation.

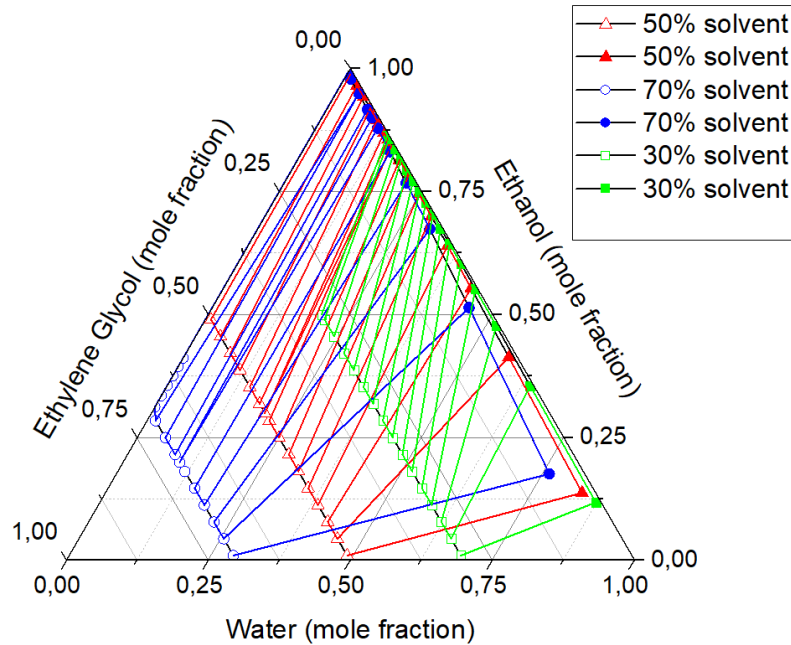


**Figure 3-9:** Effect of the addition of different quantities of ethylene glycol in the VLE distribution lines.

### 3.3.3 Reflux ratio and solvent to feed ratio

From the binary distillation theory its well known that the existence of a minimum reflux below which the separation of zeotropic and azeotropic mixtures is not possible. In addition to that limitation, the extractive distillation exhibits a maximum reflux above which the separation is also impossible. The range between minimum and maximum reflux ratio in extractive distillation depends on the entrainer to feed flow ratio ( $Fr$ ). For feasible entrainer additions, if  $Fr$  is reduced, the range of feasible reflux ratio decreases. This can be shown through the construction of the bifurcation branches based on the pinch equations of the middle section of an extractive distillation column.

#### 3.3.3.1 Bifurcations branches

In chapter two, the equations describing the composition profiles of the rectifying, stripping and middle section of a double feed extractive distillation column were presented. These equations were plotted in the composition space and interpreted as the column profile for

the ternary system Ethanol-Water-Ethylene glycol, see **Figure 2-18**. A larger number of column profiles were plotted in **Figure 3-10** at constant  $Fr$  for different reflux ratios. This collection profile is known as the column profile map of the system at a defined entrainer to feed flow ratio.

From **Figure 3-10** it can be noticed that the column profiles of the middle section present some points at which the composition does not change from stage to stage (the scatter symbols concentrate in a composition point). These points are known as fixed points and its composition location (pinch point) govern the liquid phase composition profile of the double feed column in extractive distillation. According to (Knapp & Doherty, 1994) the fixed points of and extractive distillation column can be located by means of the so called pinch equations as follows:

Rectifying section:

$$\frac{r}{r+1}x^r - y^r + \frac{1}{r+1}x_D = 0 \quad (3.5)$$

Stripping section:

$$\frac{s}{s+1}y^s - x^s + \frac{1}{s+1}x_B = 0 \quad (3.6)$$

Middle section:

$$\left[ \frac{r+1+(q_U-1)h(Fr,w)}{r+q_U h(Fr,w)} y^m \right] - x^m + \left[ \frac{h(Fr,w)x_{F_U} - x_D}{r+q_U h(Fr,w)} \right] = 0 \quad (3.7)$$

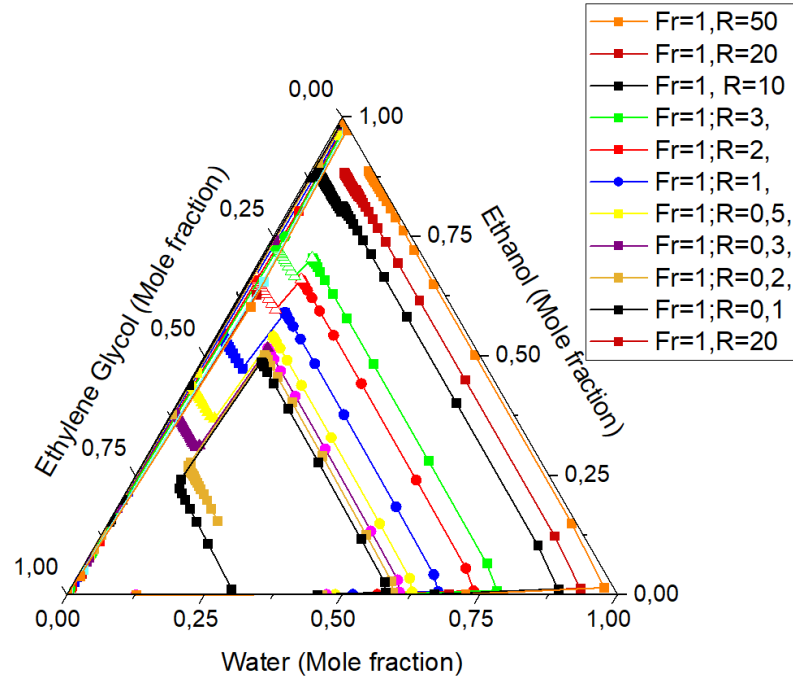


**Figure 3-10:** Column profile map of an extractive distillation column at  $Fr = 1$

For a fixed value of the entrainer to feed flow ratio, the pinch equations are one-dimensional functions of the reflux ratio. The loci of these solutions are called pinch branches and are shown in **Figure 3-11** for a solvent to feed flow ratio of 1. It can be noticed that there are two types of pinch branches: node pinch branches (continuous lines) and saddle pinch branches (dotted lines). Node pinch branches can be stable or unstable being differentiated by a stability criterion using the eigenvalues and eigenvectors at the pinch (Julka & Doherty, 1990). Based on the mathematical description in (Knapp & Doherty, 1994), the node pinch branch originated in the azeotrope is a stable node pinch branch, which is opposite to the unstable node of the residue curve of the system.

The points where the stability of the branches change from saddle to node are called saddle-node bifurcation points (red points). These points are of interest in the definition of the minimum entrainer to feed ratio and also for establishing a range of feasible refluxes. The bifurcation points location in the composition space depends on the entrainer to feed flow ratio used in the separation system. If no solvent is used, a bifurcation point appears in the binary composition ethanol-water edge between the azeotrope and the water component, see **Figure 3-12a** and **Figure 3-12b**. In this case, the node branch and the saddle branch represent the loci of the all possible unstable node pinches and saddle pinches in the binary separation of the azeotrope as distillate product and the water as

bottoms product. At infinite reflux the node and pinch points on the pinch branches are located in the azeotrope and in the water vertex. As the reflux of the column is reduced, the node and saddle pinches point approximate to the bifurcation point ( $r=1.34$ ) in which they cancel each other. If a little amount of solvent is added to the separation, the bifurcation point moves inside the ternary composition space. In **Figure 3-12c** and **Figure 3-12d**, a entrainer to feed flow ratio of 0.4 was used to calculate the pinch branches of the middle section by means of the pinch equations. The bifurcation point was also plotted but now it falls on a ternary composition. The node branch is generated from the azeotrope and the saddle branch from water vertex. The effect of more solvent addition is shown in **Figure 3-12e** and **Figure 3-12f** with a more near approximation of the branches to the ethanol-glycol edge.

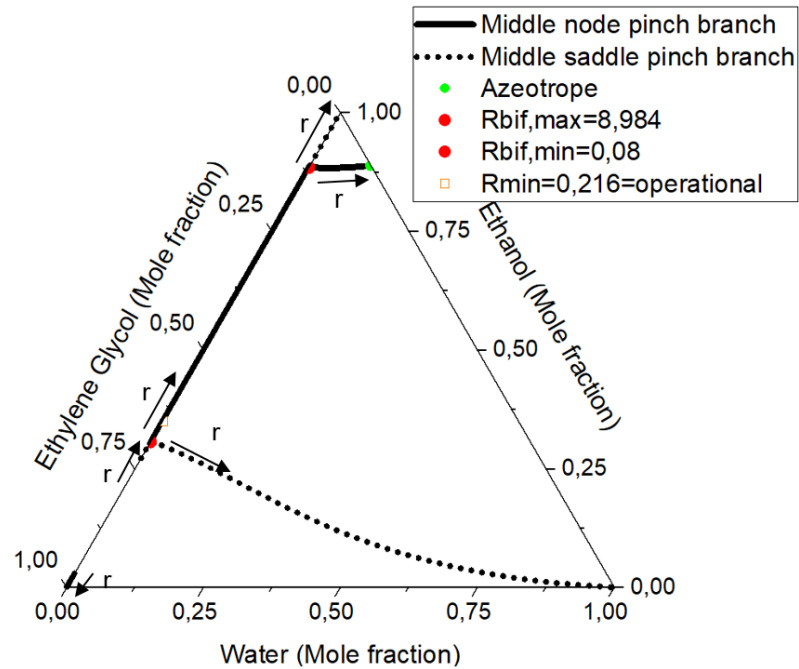


**Figure 3-11:** Pinch branches of the middle extractive section at  $Fr = 1$  and  $P = 1 \text{ atm}$ .

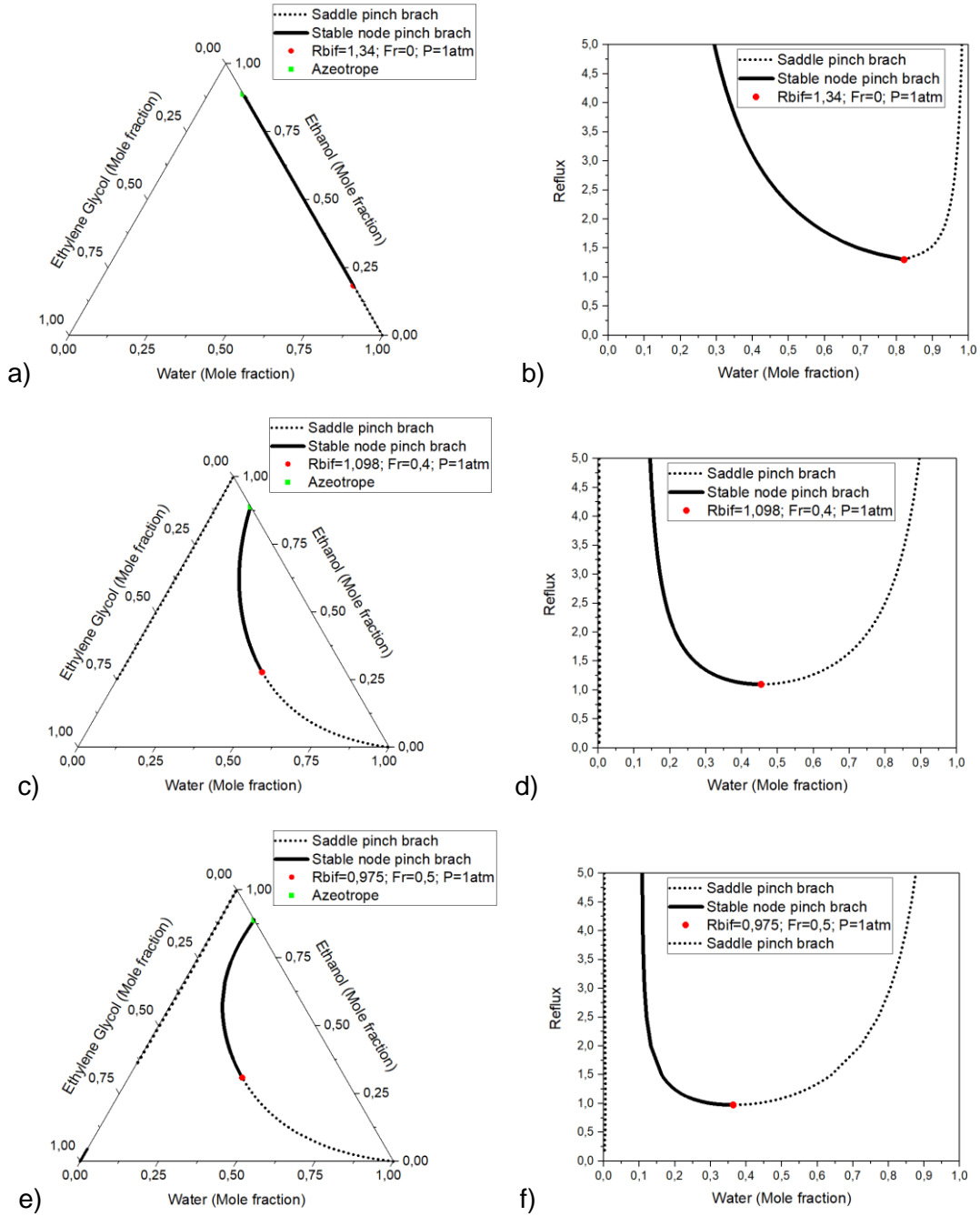
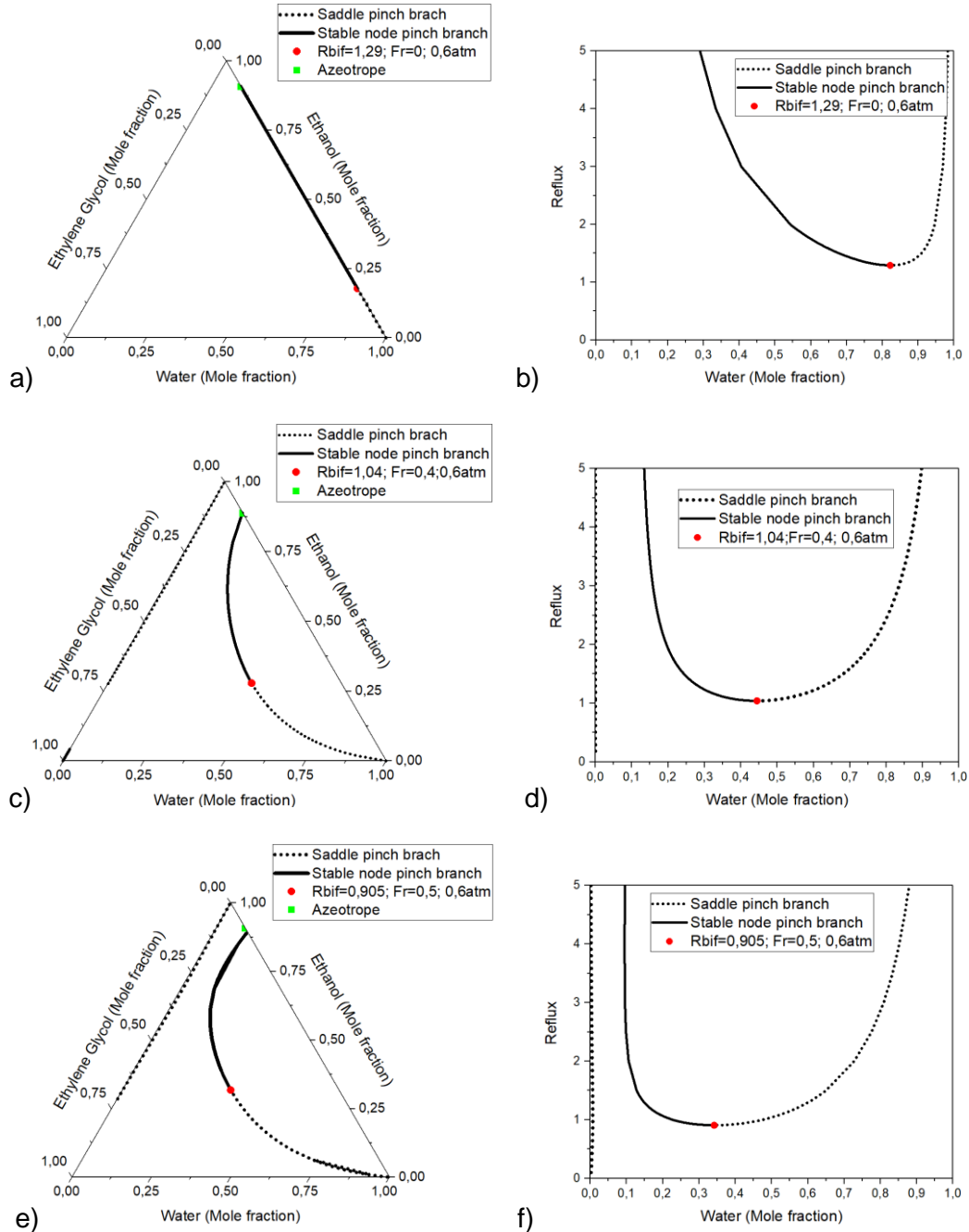


Figure 3-12: Middle section pinch branches for Ethanol-Water-Ethylene glycol at 1 atm varying the entrainer to feed ratio.



In order to see the effect of the pressure on the position of the bifurcation points for the same amount of entrainer, **Figure 3-15** and **Figure 3-14** show the tendency of **Figure 3-12** for 0.6 and 0.2 atm.



**Figure 3-13:** Middle section pinch branches for Ethanol-Water-Ethylene glycol at 0.6 atm varying the entrainer to feed ratio.

Note that for **Figure 3-14e** and **Figure 3-14f** there is a formation of three bifurcation points that do not exist for the same entrainer to feed flow ratio at 1 atm. The additional bifurcation points are important for the design as it is explained in the next section.

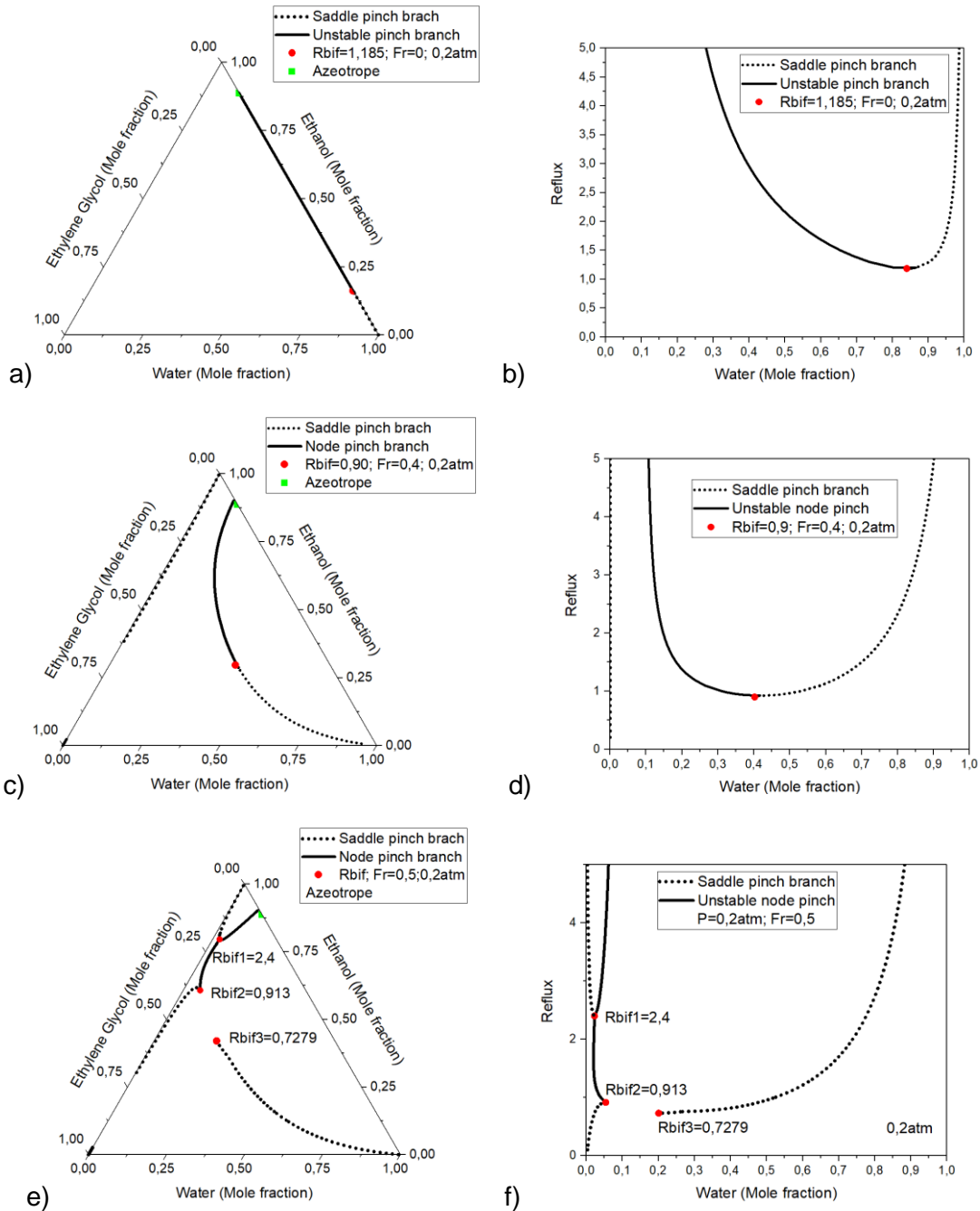


**Figure 3-14:** Middle section pinch branches for Ethanol-Water-Ethylene glycol at 0.2 atm varying the entrainer to feed ratio.

### 3.3.3.2 Minimum entrainer to feed flow ratio

From **Figure 3-14a** to **Figure 3-14d** it was shown that the addition of entrainer separates the bifurcation point from the ethanol-water edge. However, for a solvent to feed flow ratio of 0.4, every reflux higher than 0.9 will make that the node pinches and saddle pinches fall on the node branches and saddle branches, respectively. In the case of total reflux, the node pinch falls on the azeotrope composition and the saddle pinch falls on the water vertex. It means that at this solvent to feed ratio or less it is not possible to obtain pure ethanol as there is no branch originating from the ethanol vertex. However, increasing the solvent to feed ratio approximates the node branch originated at azeotrope to the saddle branch originating at the ethanol vertex. This is qualitatively shown in **Figure 3-15**. Note that as the solvent to feed ratio increases, the saddle branch approximates the azeotrope node branch. At some solvent to feed ratio the saddle branch originated from ethanol vertex intersects the azeotrope node branch, and this is the minimum solvent to feed ratio for the separation.

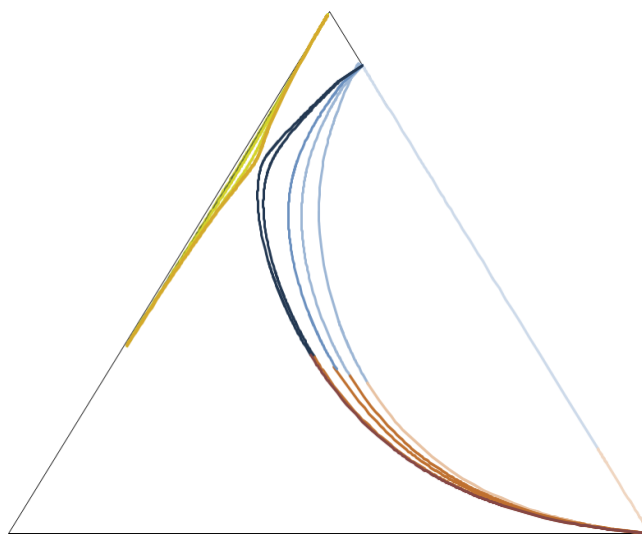


**Figure 3-15:** Qualitative effect of increasing the entrainer to feed flow ratio on the pinch branches.

**Figure 3-16** shows the pinch branches for the minimum solvent to feed flow ratio ( $F_{r,min} = 0,4858$ ). The intersection point between the azeotrope node branch and the saddle branch originated from ethanol vertex is located in a ternary point of reflux  $R_{bif1} = R_{bif2} = 1,48$ . At this location there are two bifurcation points (named 1 and 2) which have the same

composition and the same reflux, therefore they are overlapping. The saddle branch originated at water vertex end in a bifurcation of reflux  $R_{bif3} = 0,7435$ .

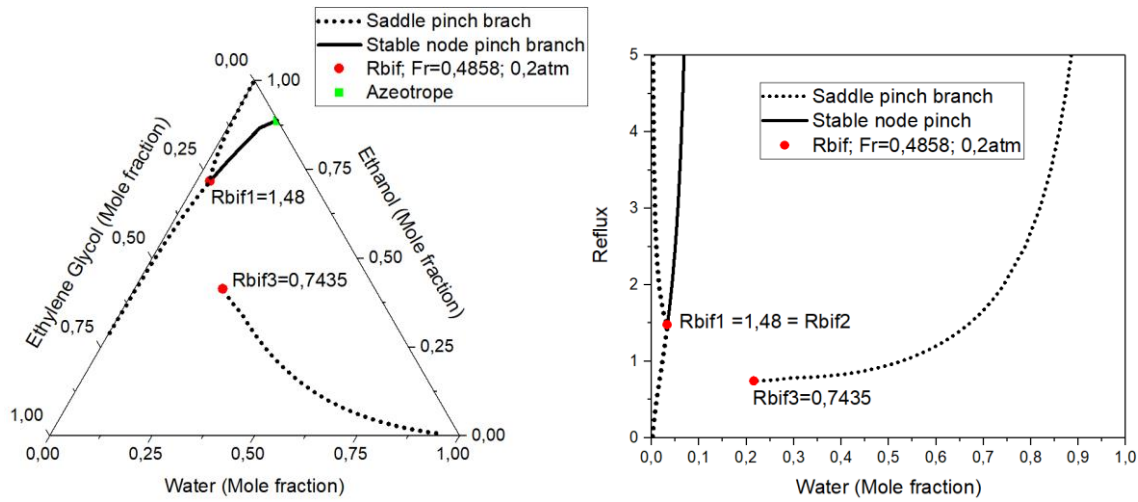


**Figure 3-16:** Minimum solvent to feed ratio at 0.2 atm

Larger additions of entrainer deals with the separation of bifurcation point 1 and bifurcation point 2 with formation of a stable node pinch branch between them, see **Figure 3-14e** and **Figure 3-14f**. These bifurcation points now have different reflux ratios and compositions. On the now formed node pinch branch, the reflux grows up from the bifurcation point 2,  $R_{bif2} = 0,913$ , to bifurcation point 1,  $R_{bif1} = 2,4$ . Intermediate composition points of the branch correspond to stable pinch points of the middle section of the extractive column. It means that this branch represents a barrier for the middle section to achieve the rectifying column section as it can be seen in **Figure 3-17**. Therefore, even when the entrainer to feed flow ratio is above the minimum, the separation is still unfeasible. If more entrainer is added, some points compositions of the stable node branch fall outside the ternary composition space until the branch breaks from the saddle branch originated at glycol vertex, see **Figure 3-18**. The entrainer to feed ratio that produces this break is called hysteresis solvent to feed flow rate  $Fr_H$  by (Knapp & Doherty, 1994). Simultaneously, a continuous saddle pinch branch originated from water vertex is formed. This topology opens a way for middle section profile to reach the rectifying section profile. This middle section profile now ends in a stable node pinch branch outside of the composition space where the behavior of the pinches has not physical meaning.

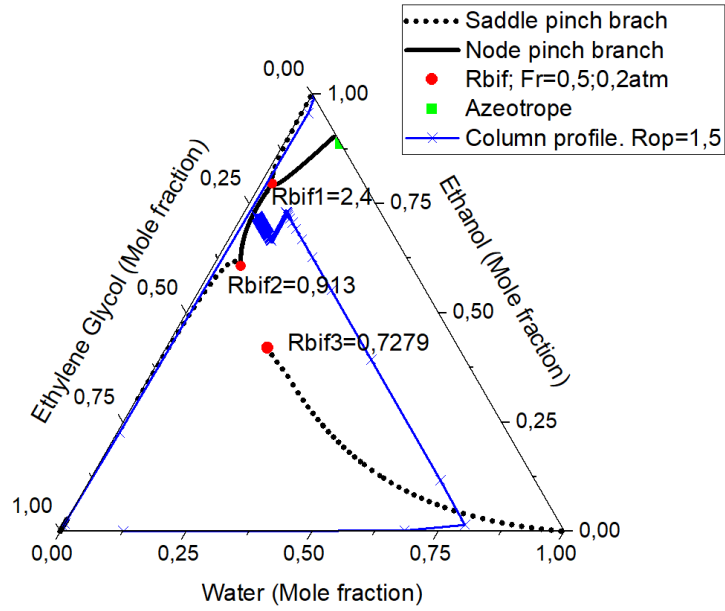


**Figure 3-17:** Unfeasibility of the middle section profile to achieve the rectifying section because of a node pinch branch appearance.

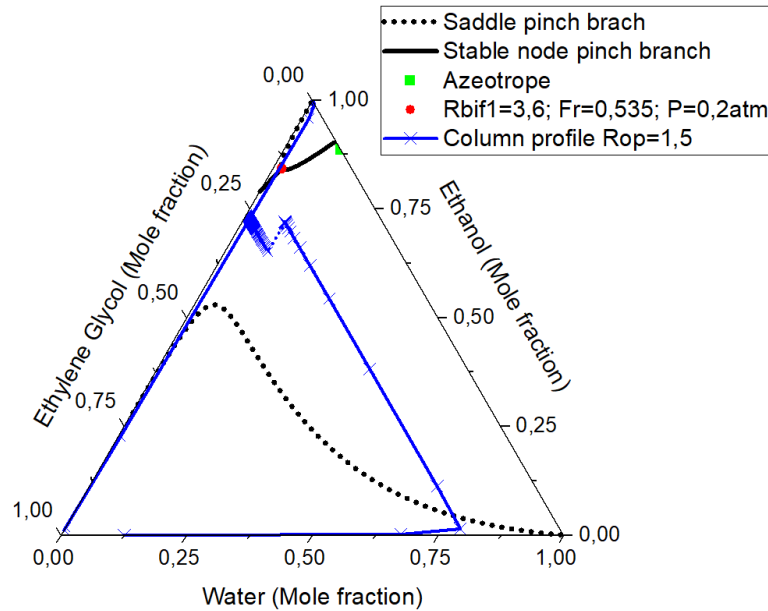


**Figure 3-18:** Solvent to feed flow rate hysteresis.

The solvent to feed flow rate for the design  $Fr_{min}$  can be heuristically obtained as a factor of the minimum entrainer to feed flow ratio (Doherty & Knapp, 2004):

$$2Fr_{min} < Fr_{design} < 4Fr_{min}$$

The optimal value between this range is the topic for future work. The design value used in this document has been fixed in  $2,5 Fr_{min}$ :

$$Fr_{design} = 2,5Fr_{min} = 2,5 * 0,4858 = 1,2145$$

With this entrainer to feed ratio the design is based on two times  $Fr_H$ .

### 3.3.3.3 Minimum reflux ratio

In chapter 2 it was noticed that the separation in a single-feed distillation column as well as in a tow-feed distillation column is feasible only if there is a continuity in the global profile line of the column. In **Figure 3-19**, for a reflux of 0.2, the middle section profile crosses the stripping section profile but does not cross the rectifying section. In fact, the middle section profile deviates from the rectifying section as a consequence of the presence of a saddle pinch. For an increased reflux of 2, the middle section connects to the stripping section at one of its ends and the rectifying section at the other end. Then, the global column profile is continuous and therefore the separation with this column is feasible. Finally, if the reflux is increased to 20, the middle section joins the stripping section but do not join the rectifying profile. In contrast to the 0,2 reflux, the middle section profile for a reflux of 20 does not deviate from the rectifying section, it ends in a node pinch. These observations show that two unfeasible regions can be distinguished: one of unfeasible low refluxes and other of unfeasible high refluxes. Between both unfeasible regions there is a region of feasibility where the operation reflux can be chosen.

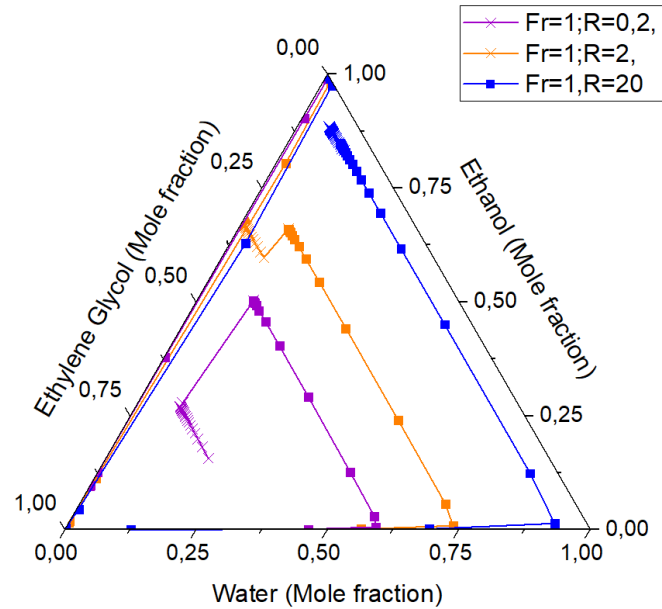


**Figure 3-19:** Extractive distillation profile lines for feasible and unfeasible refluxes at  $P=1\text{atm}$ .

**Figure 3-20** shows the topology of the middle section profile for the entrainer to feed flow rate design condition. There is one bifurcation point at  $R_{bif} = 15$ . This point marks the higher reflux ratio where extractive column can be ideally operating, but where infinite stages would be required. The geometric minimum reflux in this case is zero as the pinch branches end in points of zero reflux,  $R = 0$ .

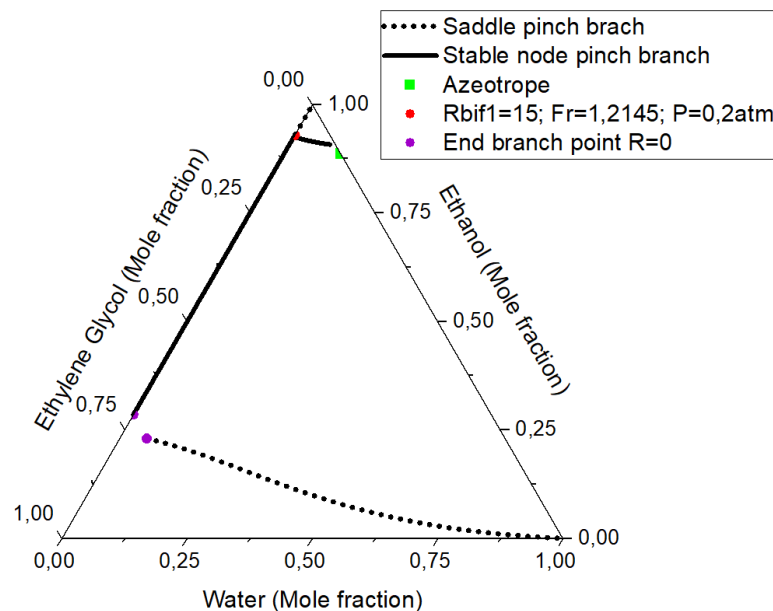


**Figure 3-20:** Pinch branches for the design conditions

A minimum reflux ratio with zero value does not mean an optimal value for the reflux but an extreme value. This zero reflux was obtained from the middle section analysis. However, the stripping and rectifying profiles are also affected by the reflux. If the reflux used for the design is not high enough for a defined pressure and  $Fr_{design}$ , the stable node pinch of the rectifying section falls on a point that does not cross the middle section, see **Figure 3-21**.

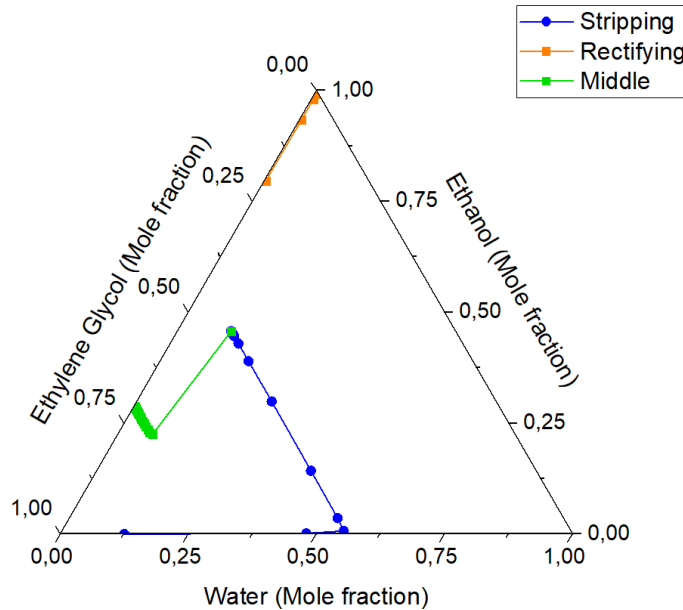


**Figure 3-21:** Column profile at  $P=0.2$  and  $Fr_{design}=1.2145$ ;  $Rop=0.01$

A feasible minimum reflux should ensure that the rectifying stable pinch point crosses the middle section profile as is shown in **Figure 3-22**. In this crossing point, the rectifying section presents a pinch and the number of rectifying stages is high (18 aprox). Heuristically it is known that the feed entrainer should be in a near stage to the top of the column (Company et al., 1985). The number of the stages where rectifying and middle section intersects is shown in **Figure 3-23** for different reflux ratios. Below a reflux of 0.6 the number of stages in the rectifying increases exponentially. However, higher reflux ratios do not change the number of stages (refluxes below the maximum). Then, for the design of the separation column, a reflux of 0.6 is used with a entrainer to feed ratio of 1.2145. The total number of stages used under these conditions are counted from the total column profile shown in **Figure 3-24**. There are 27 stages: 1 for the condenser, 3 for the rectifying section, 9 for the middle section, 13 for the stripping section and 1 for the reboiler. With these values a simulation based design can be made in next section.



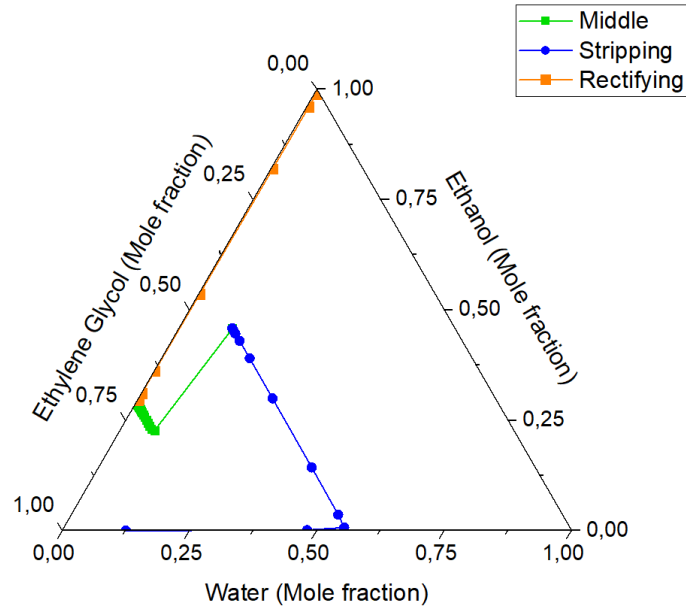


Figure 3-22: Column profile at  $P=0.2$  and  $Fr_{design}=1.2145$ ;  $Rop=0.015$

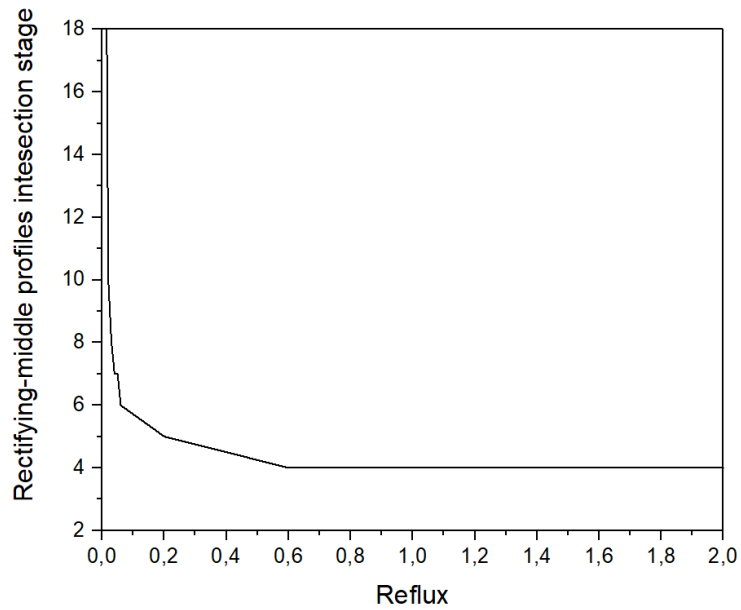
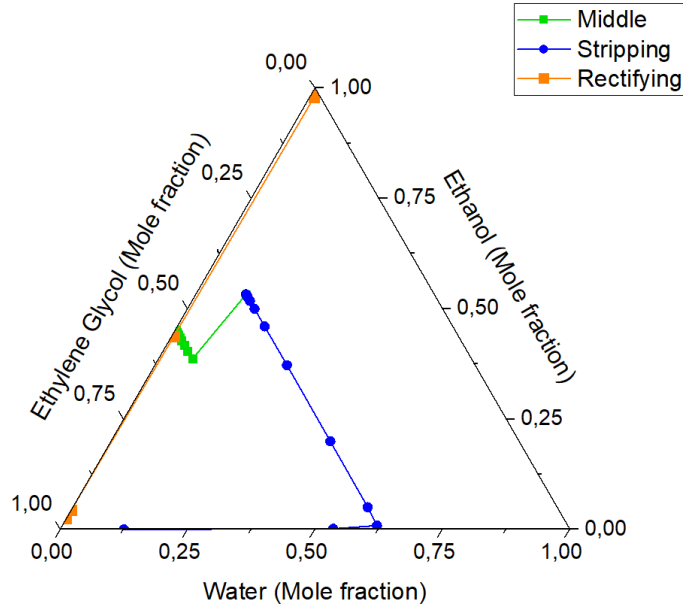


Figure 3-23: Intersection stage between middle and rectifying sections as function of reflux.



**Figure 3-24:** Column profile at 0,2 atm and  $Fr_{design}=1,2145$ . The design reflux is  $R_{design} = 0,6$ .

### 3.3.4 Rigorous simulation

Once the entrainer to feed flow ratio, the reflux ratio and the number of stages have been conceptually determined, the next step in the design is to make rigorous simulations of the extractive system. With this purpose, a rigorous simulation was made with the Aspen plus software. The NRTL thermodynamic model used was verified as was described in the previous chapter. The mathematical column model used was RADFRAC with the equilibrium calculate type, and total condenser was assumed. The feed streams were fed to the extractive column at atmospheric pressure in concordance to the upstream processes described in chapter 1. The specifications for the simulation of the extractive column are given in **Table 3-5**. The recovery column specifications were obtained based on a shortcut model.

The extractive column composition and temperature profiles are given in **Figure 3-25** and **Figure 3-26** respectively. Stages are counted according to Aspen Plus nomenclature that is inverse to the counting procedure derived from profile equations used above.

**Table 3-5:** Rigorous simulation specifications.

<b>Specification</b>	<b>Extractive column</b>	<b>Recovery column</b>
<b>Condenser pressure (bar)</b>	0,20265	0,20265
<b>Theoretical stages</b>	27	8
<b>Condenser stage</b>	1	1
<b>Upper feed</b>	5	--
<b>Lower feed</b>	14	6
<b>Reboiler</b>	27	8
<b>Entrainer to feed ratio (FU/FL)</b>	1,2145	--
<b>Reflux ratio</b>	0,6	0,36
<b>Distillate to feed ratio</b>	0,858	0,136
<b>Distillate mole fractions</b>		
Ethanol	0,998	0
Water	0,002	0,9994
Ethylene glycol	0	0,0006
<b>Upper feed mole fractions</b>		
Ethanol	0	--
Water	$1,7 \times 10^{-3}$	--
Ethylene glycol	0,9983	--
<b>Lower feed mole fractions</b>		
Ethanol	0,8564	0
Water	0,1436	0,1258
Ethylene glycol	0	0,8742
<b>Bottom mole fractions</b>		
Ethanol	$7,3 \times 10^{-5}$	0
Water	0,1257	$1,16 \times 10^{-3}$
Ethylene glycol	0,8742	0,9983
<b>Upper feed quality</b>	1,2769	
<b>Upper feed temperature °C</b>	50	
<b>Lower feed quality</b>	1	

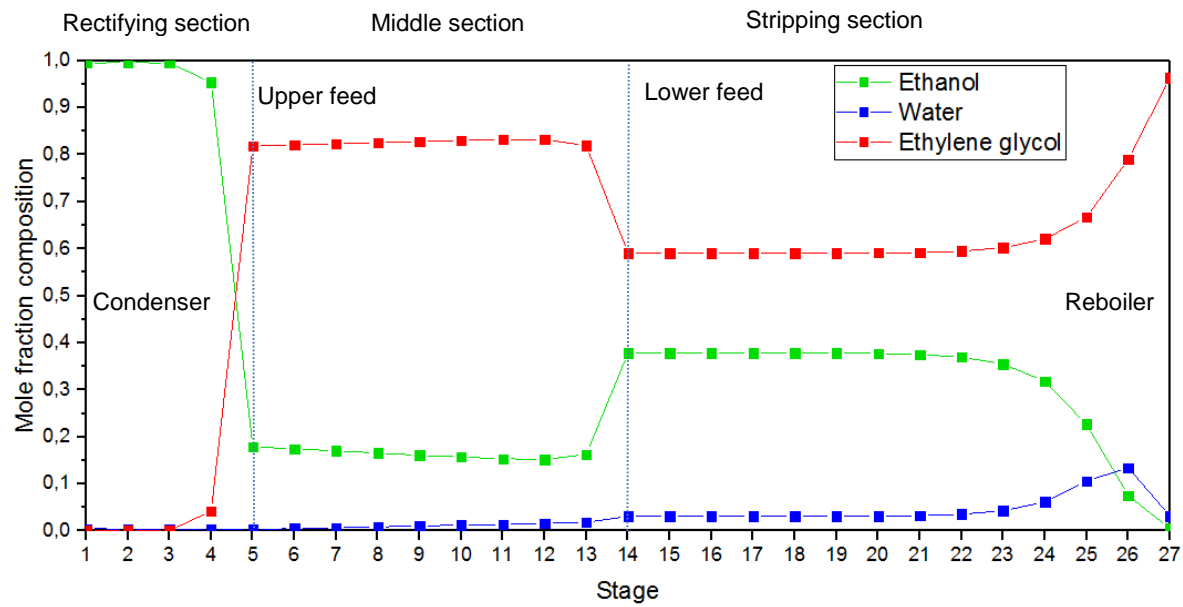


Figure 3-25: Liquid composition column profile of the conventional extractive column.

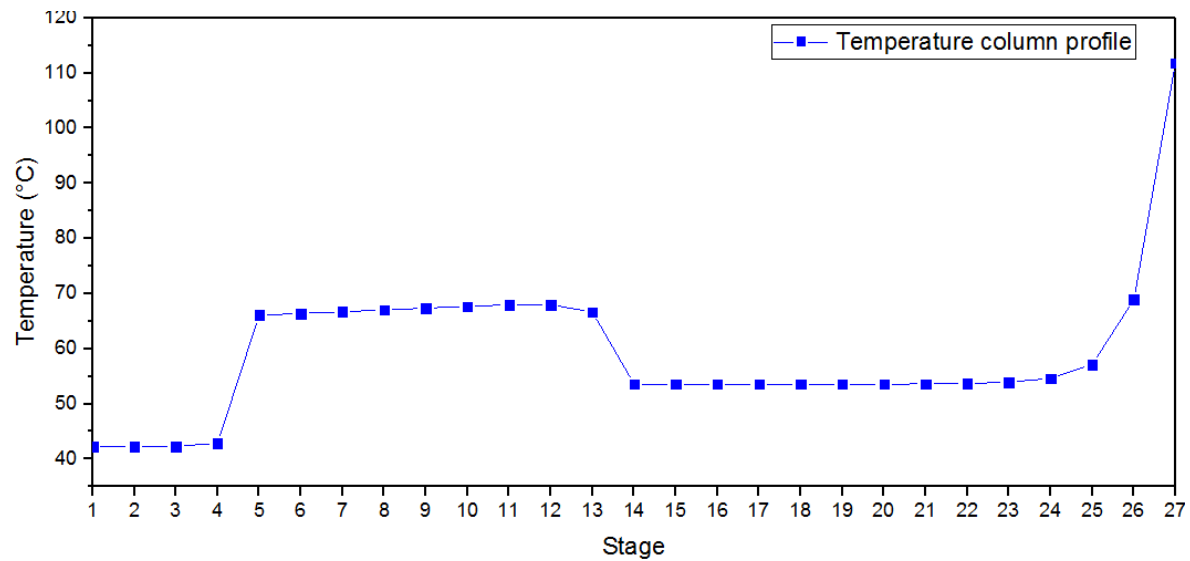
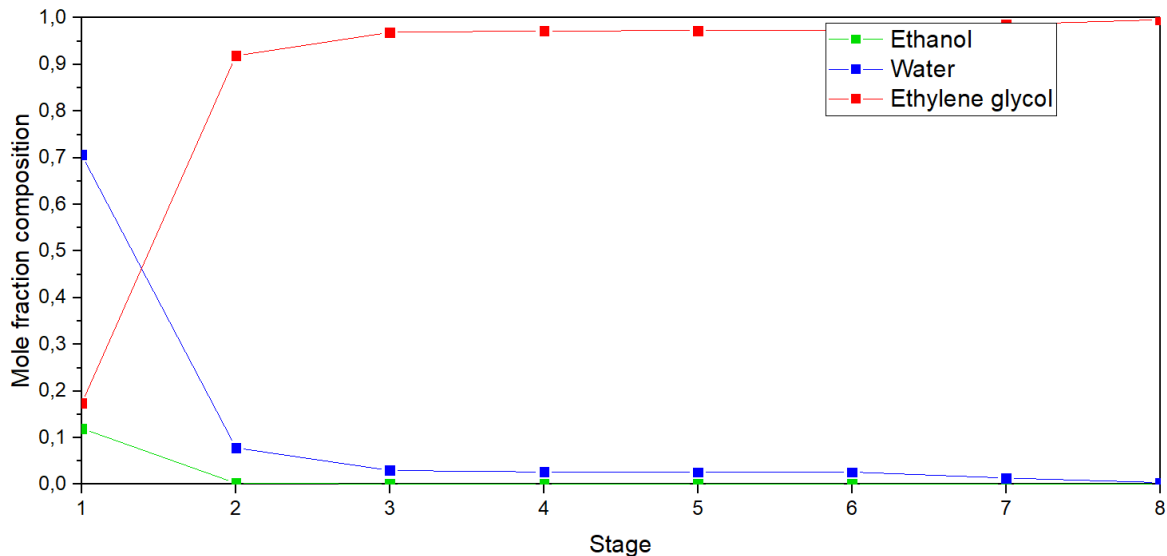


Figure 3-26: Temperature column profile of the conventional extractive column.

In **Figure 3-25**, the middle section has a zone of high entrainer liquid composition. This is due to the fact that the effect of the solvent is carried out mainly in the liquid phase and in order to maximize their influence on the relative volatility it must be as constant as possible. **Figure 3-25** also allows to observe that the separation can be possibly made in a column with less stages because between stages 15 and 20 there is no appreciable composition change. This could mean that these stages do not make a net separation and then the capital costs of the separation are reduced by using of less stages. However, a reduction in the number stages could require a larger reflux ratio that increases the operation costs of the separation. To find the better design an optimization problem should be considered. This will be a topic of future work.

It is interesting to notice that, near the bottoms column, the water profile shown in **Figure 3-25** evidences a remix effect. For example, in stage 20 the water profile has a composition near zero, but in stage 26 it grows above 0,1 and then, it falls to a composition near to zero at the bottoms. It means that some energy was used for the separation and then it was lost in the re mixing. As a consequence more energy than necessary was required. This is one of the reasons why the conventional distillation arrangement has a low energy efficiency. In the next chapter this idea is considered.



**Figure 3-27:** Liquid composition profiles of the recovery column

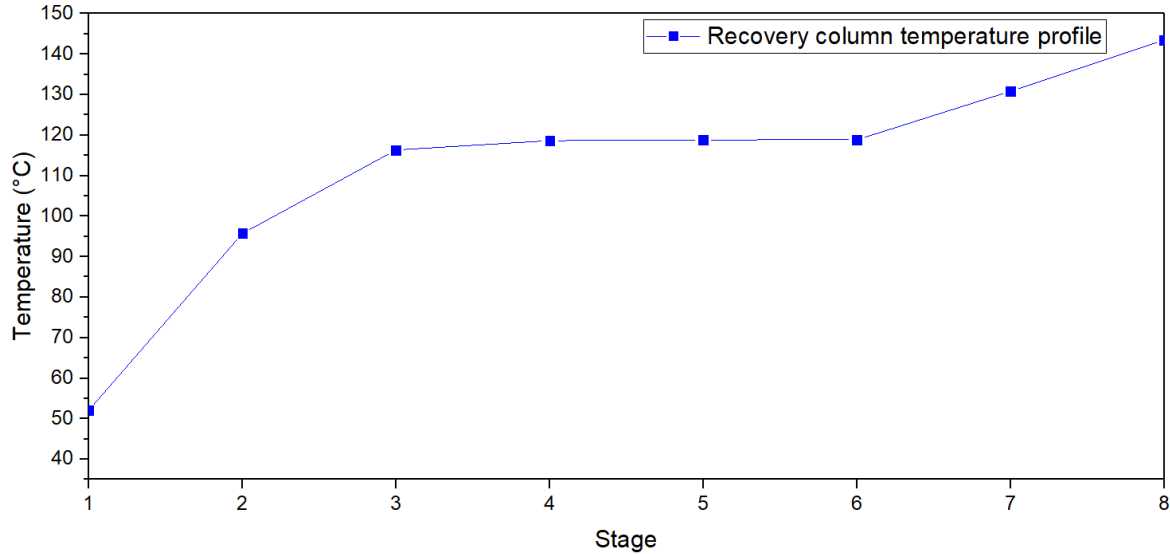


**Figure 3-28:** Temperature profile of the recovery column

**Figure 3-27** and **Figure 3-28** show the column profiles of the recovery column. The energy consumption of this column and the extractive column are listed in **Table 3-6**. Based on the distillate stream, an energy requirement relative to ethanol flow is reported.

**Table 3-6:** Energy requirements.

<b>Extractive column</b>	<b>kJ/s</b>	<b>1591</b>
<b>Recovery column</b>	kJ/s	399,1
<b>Total energy</b>	kJ/s	1990,1
<b>Extractive column distillate flow</b>	kg/s	1,09
<b>Energy requirement</b>	kJ/kg	1824,9

### 3.4 Conclusions

Review of literature allowed to propose different candidates to entrainer in the separation of Ethanol-Water mixtures. This was concluded in the selection of Ethylene Glycol and Glycerol as the most promising entrainers based on selectivity and capacity criteria. Ethylene Glycol was concluded to be the better candidate based on reported advantages in terms of hydrodynamic properties.

Degradation of the Ethylene Glycol at high temperatures represents a restriction in the design and operation of the used extractive separation sequence. Therefore, the process must be design for vacuum pressure.

It was concluded that the form of the residue curve maps does not change appreciably for a reduction of the pressure above 0,2 atm. However, in the vicinity of the azeotrope point this could not be totally true.

The feasibility of the separation was evaluated by means of pseudo binary and ternary diagrams. It was shown that the addition of solvent can overtake the azeotrope and that the easiness of the separation increases as the solvent increases. In addition, generated isovolatility curves allowed to analyze in graphical form the possible composition space zones for a feasible separation. Specifically, the univolatility line allowed to measure qualitatively the minimum solvent to feed ratio and the infinite dilution isovolatility line allowed to measure qualitatively the selectivity of the solvent.

A detailed analysis of the construction of pinch branches was generated for the Ethanol-Water-Ethylene Glycol mixture. This allowed to identify limiting ranges of the design variables reflux ratio and solvent to feed ratio. The analysis was made for pressure of 0,2 atmospheres and compared with 1 atmosphere. At vacuum, the minimum bifurcation point of the pinch branches is reached in a zero reflux ratio.

A minimum solvent to feed flow ratio was obtained as well as a hysteresis solvent to feed flow ratio. Operational feed flow rate was calculated by means of a heuristic factor. Maximum reflux ratio  $R_{bif,1}$  and minimum reflux ratio also were calculated for the defined operational entrainer to feed flow ratio.

The used conceptual design method results in the successful definition of the variables of design for the extractive sequence. These values were analyzed by means of simulation and the required number of theoretical stages and energy composition were reported.





## 4. Non-conventional extractive distillation technologies.

Chemical engineering is a well delimited knowledge branch in the field of engineering. It is represented by four paradigms that resume its evolution: a) Unit operations, b) Transport phenomena, c) Chemical product engineering, and d) Sustainable chemical engineering. These paradigms have converged in novel equipment and techniques with potential to transform the actual plant design concept. This potential is focused on Process Intensification (PI). The aim of PI is to generate a “drastic improvement of equipment and process efficiency” (Van Gerven & Stankiewicz, 2009). To that end, several technologies have emerged in the last decades. Most of them are listed in (Creative Energy, 2008) and are categorized in process intensification of methods and process intensification of equipment. This chapter refers to last category. Specifically this document refers to the class of hybrid non-reactive technologies “2.1.3 Extractive Distillation” and “2.1.4 Heat-integrated distillation” (only Dividing Wall Columns), reported in the *Appendix 1* in (Creative Energy, 2008). **Table 3-2** shows the evaluation of the projection perspectives of these technologies.

**Table 4-1:** Qualitative evaluation of the state of the art for distillation technologies. For details see (Creative Energy, 2008).

Evaluated technology	Extractive distillation	Dividing wall columns
Potential for energy savings	Medium	High
Potential for eco impact CO <sub>2</sub>	low	High
Potential to improve cost competitiveness	low	High
Ripeness of application in X years	5-10	
Ripeness of related technology fields	Medium	High
Likelihood of overcoming barriers	Medium	High
Potential for innovative high quality products	Medium	Low
Character of required R&D	Fundamental	Applied

## 4.1 Direct Thermal Integration: Extractive Dividing Wall Column E-DWC

The conventional extractive distillation presents a relative high energy cost due to the typical inefficiencies that this distillation separation has, see (King, 1979). To avoid this disadvantage some authors have proposed advanced distillation technologies based on process intensification and integration (Kiss, 2013). Among these alternatives, the Dividing Wall Columns have shown to be a good improvement of conventional sequences (Olujić, Jödecke, Shilkin, Schuch, & Kaibel, 2009). Dividing wall columns are an implementation of the totally thermally coupled distillation Petlyuk arrangement in one single shell. Partial integrations of ternary separation sequences can be based also on a side rectifier or side stripper configuration. The extractive dividing wall column is the implementation of a side rectifier in one single shell with two feeds. Some simulation based studies of this technology have been reported for the separation of Ethanol-Water mixtures with Ethylene glycol (Kiss & Suszwalak, 2012). In this section, some conceptual analysis about the behavior behind this technology is carried out. The aim at the end of the section is to bring some ideas that led to improve the methodology for the convergence of the design. It means to delimit the domain of the variables established in **Figure 4-1**

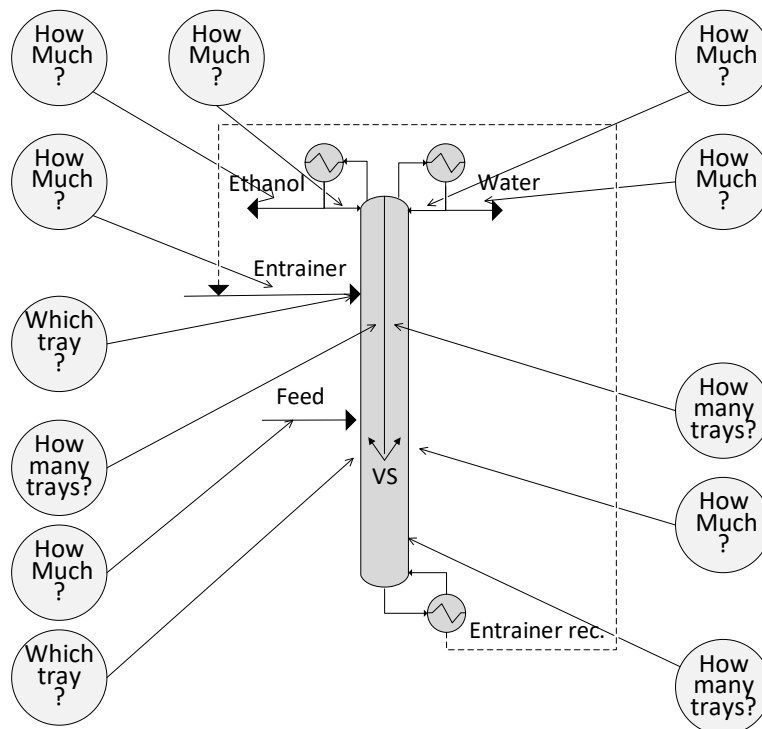


**Figure 4-1:** Design variables for an E-DWC

### 4.1.1 The dividing wall distillation concept

Modern distillation technologies for separation of multicomponent mixtures are based on thermal integration of columns, as the arrangement shown in **Figure 4-1**. This configuration was first reported by (Wright, 1949) and later developed Petlyuk in the second half of the XX century. The main concepts of this kind of integration are described in (Petlyuk, 1965) and (Kaibel, 1987). A Petlyuk arrangement can be defined as:

*“A column arrangement separating three or more components using a single reboiler and a single condenser, in which any degree of separation (purity) can be obtained by increasing the number of stages (provided the reflux is above a certain minimum value)”* (Christiansen, Skogestad, & Lien, 1997)

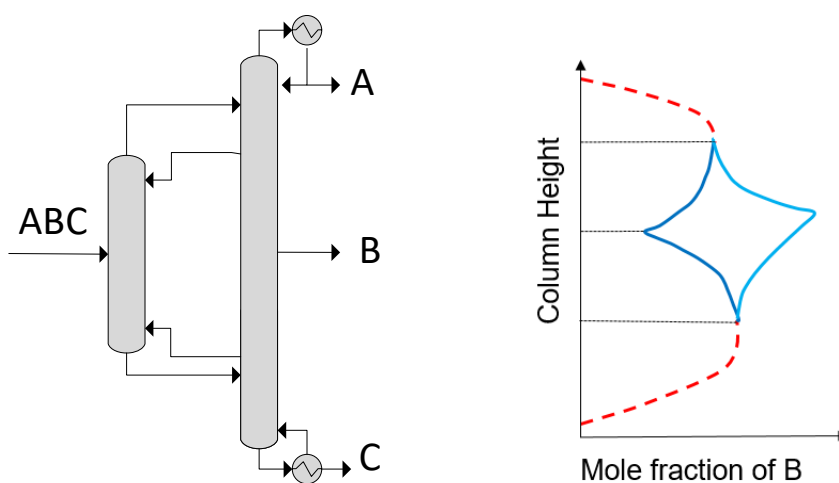


**Figure 4-2:** Petlyuk arrangement and typical composition profiles for the middle volatility component.

The Petlyuk arrangement for the separation of three components is composed of a pre-fractionator module and a main column, as shown in **Figure 4-2**. The pre-fractionator separates the more volatile component A entirely at the top of the column and the less volatile component C at the bottoms. The intermediate component B is distributed between the two output streams of the pre-fractionator, in combination with A at the top and with C at the bottoms. It means that an AB vapor mixture is fed to the main column on an upper stage, and a CB liquid mixture is fed to the main section on a down stage. In order to avoid the drying of the pre-fractionator, a side liquid stream from the main column is returned to pre-fractionator at the top, and a side vapor streams is returned at the bottoms. The products of the Petlyuk

arrangement are: near pure A at the top of the main column, near pure C at the bottoms and near pure B at the side stream product.

One of the most important advantages of the Petlyuk arrangement is the fact of that A and C components are efficiently separated in the pre-fractionator. This early separation avoids the remixing of non-identical streams inside the column, and therefore, a higher efficiency than conventional arrangements is obtained (Dejanović, Matijašević, & Olujić, 2010). This is explained as follows.

Suppose that a three-component mixture is going to be separated by means of simple columns. The only two possible sequences that can be used to do this are the direct A/BC and indirect AB/C configurations. The direct separation is shown in **Figure 4-3** together with a typical column composition profile for middle-boiling point component B. According to this profile, the B component has a composition near to zero at the top of the column 1. While the column height decreases, the mole fraction of the middle component composition increases until it reaches a maximum. After that, the middle component composition is reduced to the bottoms composition. This is due to a remixing of the separated components. As the separation requires energy to be made, the remixing means a loss of energy that makes inefficient the separation.

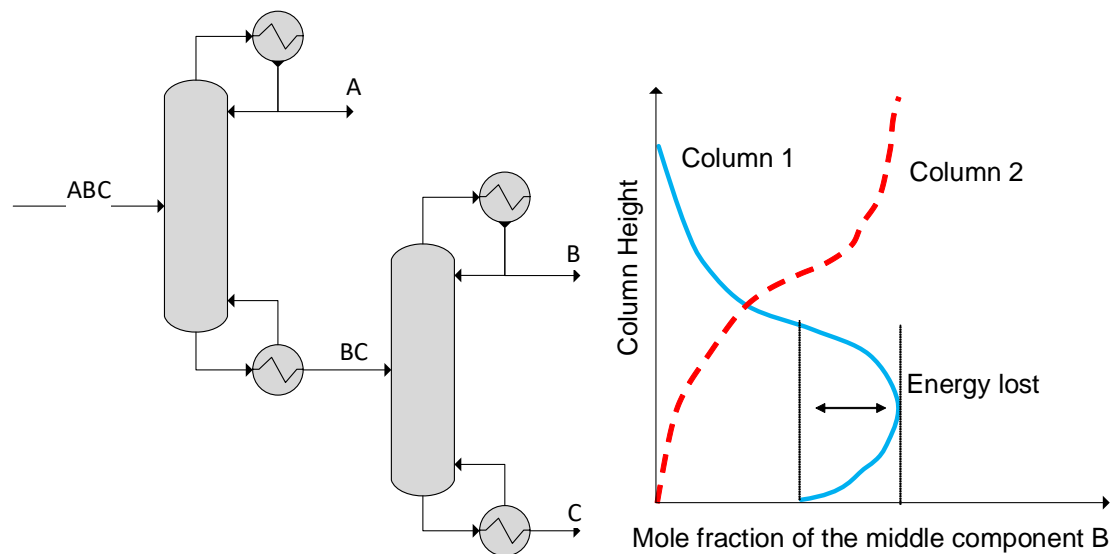


**Figure 4-3:** Direct sequence of two simple distillation columns for a ternary ideal separation.

The remixing inefficiency can be reduced by means of the Petlyuk arrangement. If instead to obligate the first column in **Figure 4-3** to separate the most volatile component A, the intermediate component B is distributed in the column, the profile does not reach a maximum in the down stages. The Petlyuk arrangement does this. Note that according to the profile shown in **Figure 4-2**, the Petlyuk arrangement reaches a maximum B composition at the top and the bottom of the pre-fractionator. From these compositions, a top and bottom product are taken and fed as side feed in the main column, which concentrates B component to almost pure composition. In consequence, with this configuration the remixing of B is avoided.

From the energy point of view, a series of articles published by (Terranova & Westerberg, 1989)(Carlberg & Westerberg, 1989a)(Carlberg & Westerberg, 1989b) analyze the remixing problem and the coupling of columns for the deduction of the Petlyuk arrangement. This requires the assumption of that the feed and products are liquids at the bubble point temperature. It also assumes that the internal remixing in the cooler and reboiler are high in comparison to the feed and product flows (Caballero, 2008). A global energy balance of this column is gives:

$$h_F(T_{F,bubble})F + Q_{reb} = h_D(T_{D,bubble})D + h_B(T_{B,bubble})B + Q_{cond} \quad (4.1)$$

If sensible heat of the streams is neglected with respect to the heat in the cooler and the reboiler, equation (4.1) is reduced to:

$$Q_{reb} = Q_{cond} \quad (4.2)$$

This is represented in a temperature-enthalpy diagram in **Figure 4-4**. If the feed is preheated, the first term in equation (4.2) has a reduction equivalent to the heat used for the preheater. In that case the reboiler requires less energy:

$$Q_{reb} = Q_{cond} - Q_{feed} \quad (4.3)$$

For a sequence of two single distillation columns, a temperature diagram that describes this configuration is shown in **Figure 4-5a**. Note that in the second column, the reboiler is at higher temperature than the reboiler in the first column. This is because in a direct sequence the two heaviest components are separated in the second column.

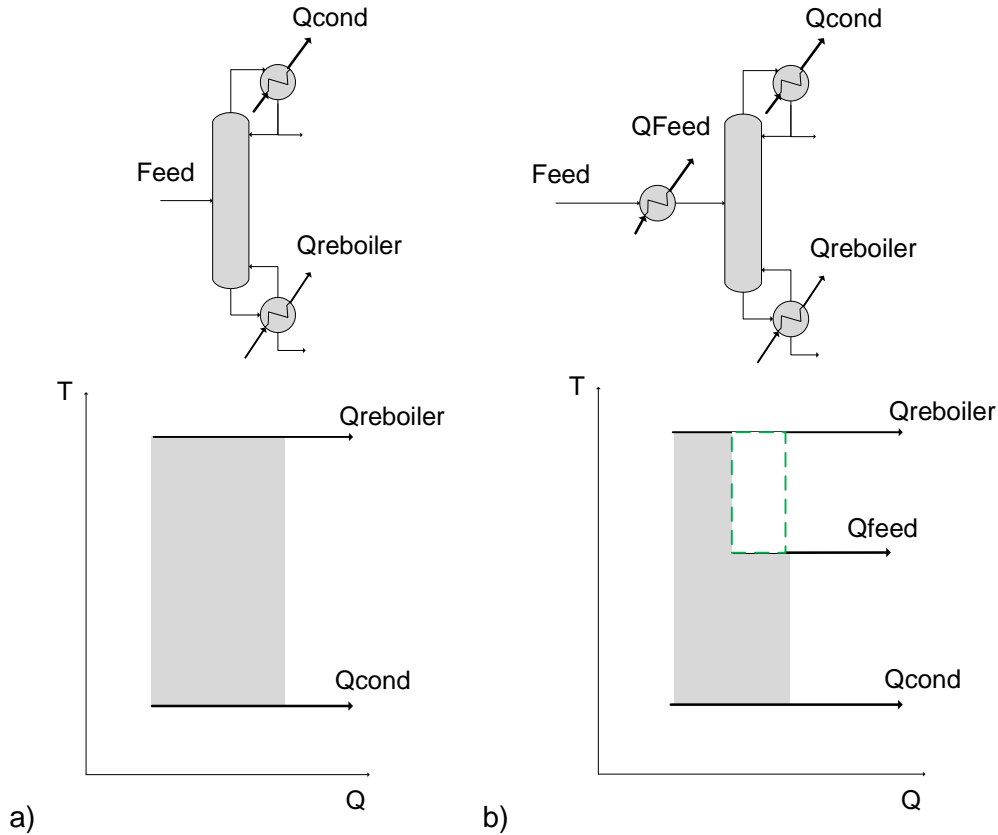


**Figure 4-4:** Temperature-enthalpy diagrams for a single feed distillation column. a) feed at bubble point temperature and b) at dew point temperature.

**Figure 4-5b** shows a thermal coupling of the direct sequential configuration. This column arrangement is known as side-rectifying coupling. This coupling has two condensers, and only one reboiler. The absence of the reboiler in the first column implies that all the energy required for the separation must be supplied only by the second column reboiler. This reduces the global energy required in the overall separation system with respect to the conventional configuration. However, as only one reboiler is used, only one service temperature is used. This means that the quality of the heat service must be higher than the quality of the service used in the first reboiler of the direct conventional sequence. Analogous analyses for the indirect sequence gives equivalent results.

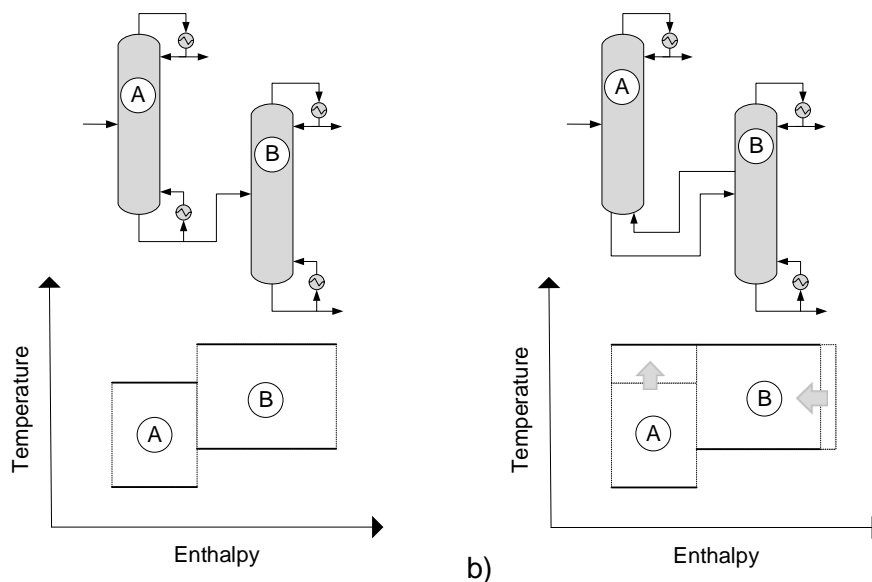


**Figure 4-5:** Temperature-enthalpy diagrams for the separation of a three component mixture. a) conventional direct sequence and b) thermally coupling. From (Smith, 2005)

The Petlyuk arrangement is originated from a prefractionator with a sidestream rectifying and a sidestream stripping, see **Figure 4-6**. If additional thermal integrations are made between the sidestream rectifying reboiler and the sidestream stripping condenser, the result is the Petlyuk arrangement shown in **Figure 4-7**. The energy requirements for this arrangement are less than those for the conventional separation. The capital costs are also reduced because only one reboiler and condenser are required for the separation. More capital reductions can be made by implementing the so called dividing wall column.

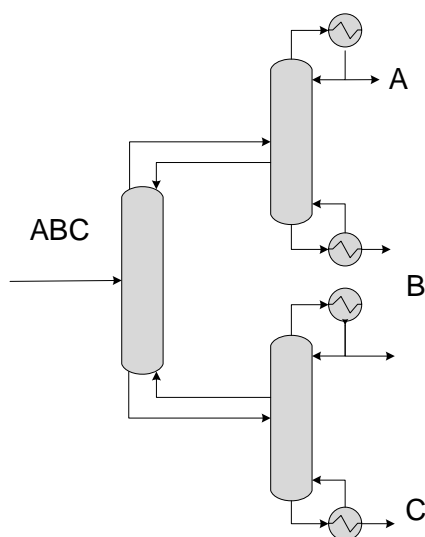


**Figure 4-6:** Prefractionator with sidestream rectifying and sidestream stripping.

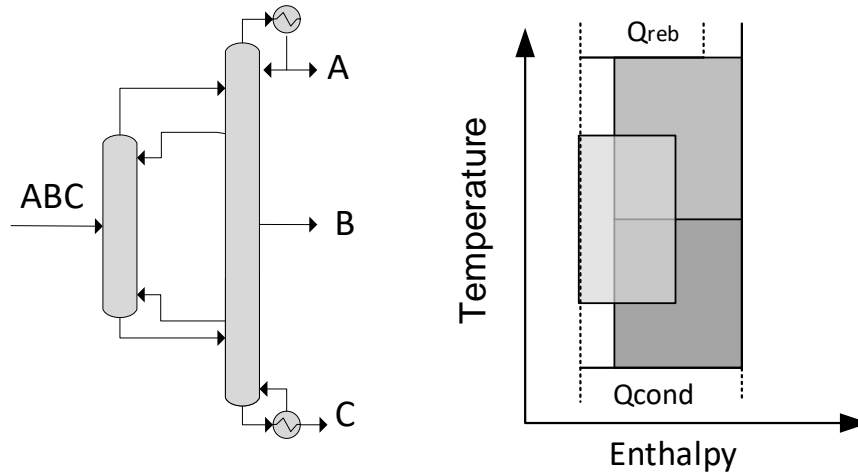


**Figure 4-7:** Energy requirement of Petlyuk arrangement.

#### 4.1.2 Dividing Wall Column DWC

The dividing wall column (DWC) shown in **Figure 4-8** is an implementation of the Petlyuk arrangement in a single shell divided longitudinally by a wall that separates the pre-fractionator zone from the main zone. Dividing wall columns are thermodynamically equivalent to the Petlyuk columns but with an additional reduction in capital costs and space in the plant. Operation costs savings with respect to the conventional sequences are between 30% and 50%. Capital savings have a similar interval (Kiss, Flores Landaeta, & Infante Ferreira, 2012). These savings depend on the composition system to be separated.

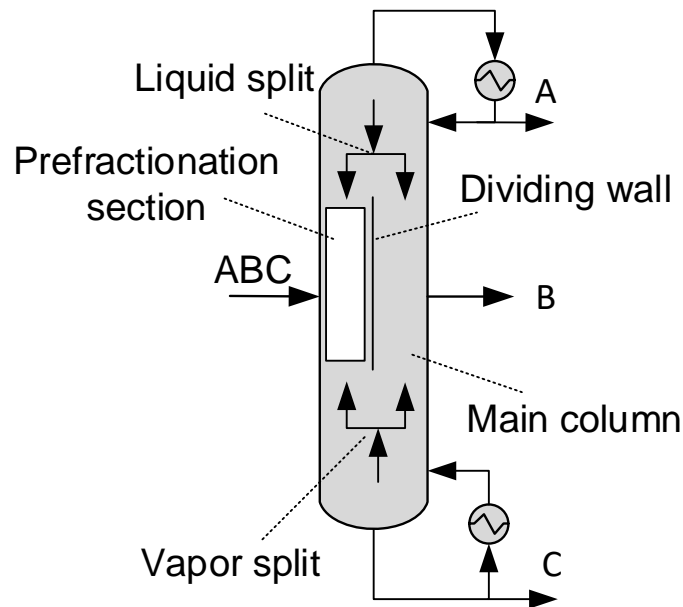


**Figure 4-8:** Dividing wall distillation column. From (Kiss, 2013)



The dividing wall columns are not new in the world. BASF has built more than 70 columns of this type with diameters of more than 4 m and height over 80 m (Dejanović et al., 2010). However, the knowledge about this technology is not totally reported in the open literature. The scientific community has made efforts in opening this knowledge. An important document in this way was written by (Triantafyllou & Smith, 1992). The current study of the DWC is highly based on computational tools. DWC models are highly non-linear and therefore, to solve their first principle model is a computationally challenging. For example, the hydraulic behavior of a DWC and its implications to the control is an open field of study.

#### 4.1.2.1 DWC configurations

There are two main groups for the classification of dividing wall columns: three product dividing wall columns and more than three products dividing wall columns. The last group is commonly known as Kaibel columns and has several difficulties being implemented industrially. As their internal parts are under heat transfer, metal dilatation and contraction generates mechanical stress in union sections that are an actual focus of study in engineering (Dejanović et al., 2010).

For three products dividing wall column, there are three configurations that can be used for the separation, see **Figure 4-9**. The first one refers to the totally coupled or conventional dividing wall column patented by first time by (Wright, 1949) in which, the feed, the sidestream product and the wall itself are located close to the middle part of the column, see **Figure 4-9a**. Side stripping and side rectifying dividing wall columns are shown in **Figure 4-9b** and **Figure 4-9c**, respectively. They were patented by (Monro, 1938) and are differenced because the wall is located at the top or the bottoms of the column. These two distinguished configurations require less energy for the separation than the conventional sequence, but they have less energy saving than the totally coupled dividing wall column (Asprion & Kaibel, 2010).

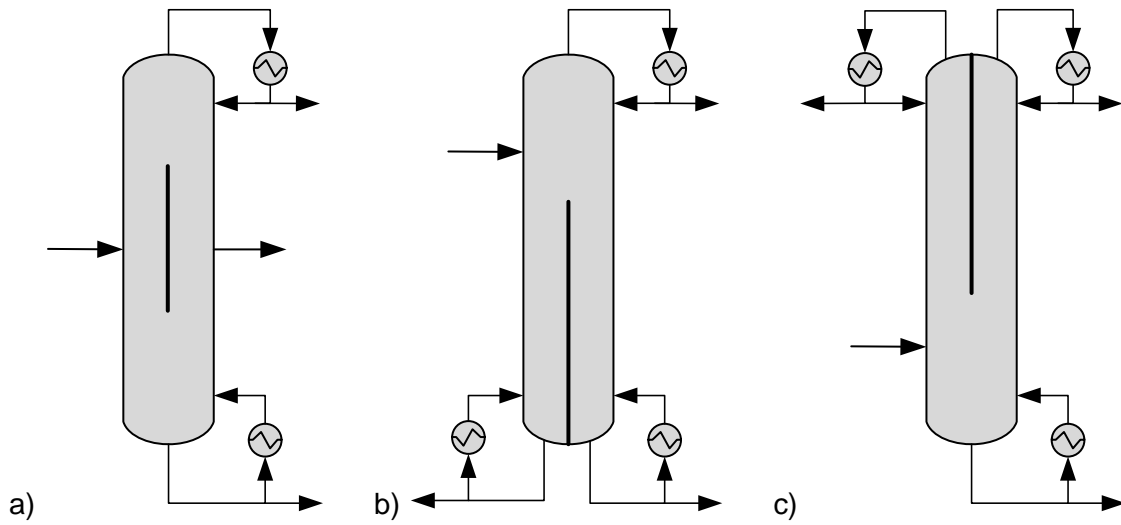


**Figure 4-9:** Three products dividing wall columns configurations. From (Yildirim, Kiss, & Kenig, 2011)

The configurations shown in **Figure 4-9** are not necessarily divided by the wall in two sections of equal semicircle area. In fact, it is possible to the wall to be located in a position near to the output streams position (**Figure 4-10a**) or near to the feed stream position. It is also possible to the wall to have a diagonal segment as is shown in **Figure 4-10b** and **Figure 4-10c**.

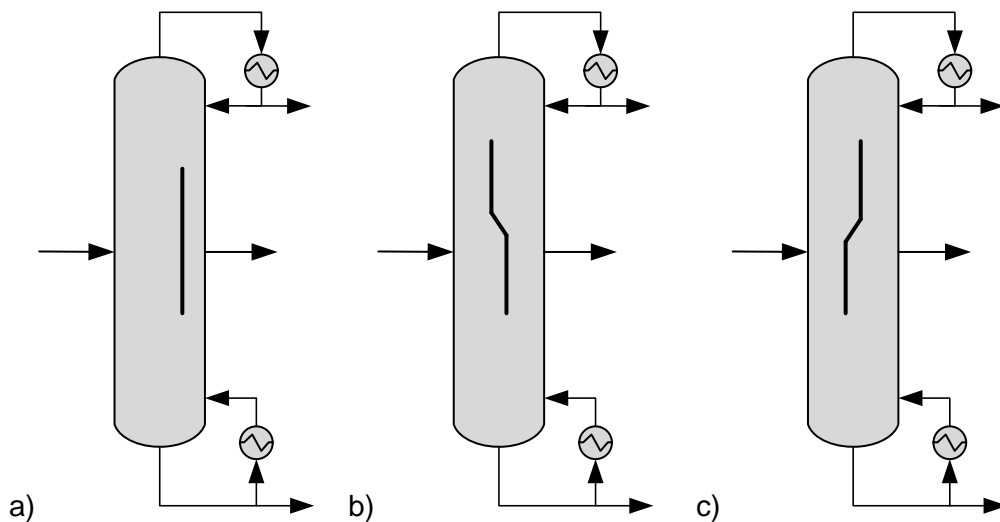


**Figure 4-10:** Possible adaptations of the dividing wall. From (Yildirim et al., 2011)

### 4.1.2.2 DWC design

First ideas with concerning to the design of the dividing wall distillation columns were discussed in the work of (Becker, Godorr, Ag, & Vaughan, 2001). This publication is related to the implementation of two columns for the separation of high value petrochemicals. Previously to this work, there were already some industrial dividing wall columns constructed by BASF but the knowledge about the design was not open. More recently, there have been a growing study of DWCs and other advanced distillation technologies that have been compiled in books as (Kiss, 2013) and articles as (Dejanović et al., 2010).

The design of dividing wall columns requires the use of adequate models and computational tools for the process analysis by simulation. In this way, three methods for the design of DWCs are reported by (Dejanović et al., 2010) as well as by (Kiss, 2013). The most simple method was reported by (Triantafyllou & Smith, 1992). In this called decomposition approach, the complex DWC system is studied as a sequence of conventional distillation columns. This has the advantage of working with less degrees of freedom in the simulation than if the DCW system were study as one single model. The method also has the advantage of making use of equations of Fenske, Underwood, Guilliland and Kirkbride, that are the base of a shortcut method (Triantafyllou & Smith, 1992). The second method is reported by (Halvorsen & Skogestad, 2003) and is based on a graphical approach for the determination of the minimum energy requirement represented as normalized vapor flow. The third design method is based in the calculation of detailed models as the shown in (Dejanović, Matijašević, & Olujić, 2011).

The success of the mentioned design methods requires the definition of appropriate initial values that approximate the convergence of the design model. (Becker et al., 2001) recommends a number of heuristics to achieve this objective:

- Design a two column sequence as base case.
- Use the number of stages for the DWC as 80% the number of required stages for the conventional sequence of two columns.  $N_{DWC} = 0,8 * (N1 + N2)$
- The wall must be between 33% and 66% of the DWC
- To fix the internal flows of the DWC as a percent of the total flow produced in the reboiler of the two column conventional sequence.  $Q_{DWC} = 0,7 * (Q1 + Q2)$
- Use the vapor split and liquid split as 0.5 initially.

### 4.1.2.3 DWC modeling, simulation and optimization

The actual commercial simulators do not have models for the direct simulation of dividing wall columns. From Aspen Plus 8.0 version, it is possible to model a thermodynamically equivalent Petlyuk arrangement, but this approximation does not take into account the effect of possible heat transfer across the wall. In Aspen Plus, DWC can also be simulated by means conventional models as RADFRAC. This has the advantage that the user has a detailed model for interpretation but, in disadvantage, more degrees of freedom must be specified manually, which makes the convergence difficult.

The number of distillation stages in a DWC is an integer variable and therefore the optimization of this kind of columns is a problem of the Mixed Integer Nonlinear Programming MINLP (Kiss, 2013). This model is not programmed in conventional simulators as Aspen Plus yet. Therefore, it is necessary to couple the simulator with a routine externally programmed in, for example, Matlab or other kind of mathematical tool.

### 4.1.3 Conventional extractive distillation sequence to E-DWC.

The conventional extractive distillation sequence can be thermally integrated eliminating the reboiler of the extractive column and substituting the required energy by means of the recovery column. To do this, the new arrangement should have the appearance shown in **Figure 4-11a**. A vapor side-stream originated from above the stripping recovery section is fed at the bottom of the extractive column. On the other hand, a liquid originated at the bottom of the extractive column is fed as side-stream feed in the same stage above the stripping recovery section. This arrangement is thermodynamically equivalent to the arrangement shown in **Figure 4-11b**. If the thermally coupled configuration is intensified in a single shell by means of a dividing wall in the upper section of the column, the result is the Extractive Dividing Wall Column shown in **Figure 4-11c**. As a consequence of the process intensification, a vapor split appears at the end of dividing wall. The split ratio is a new variable that must be specified between 0 and 1 and is of high relevance in the solution of the E-DWC model.

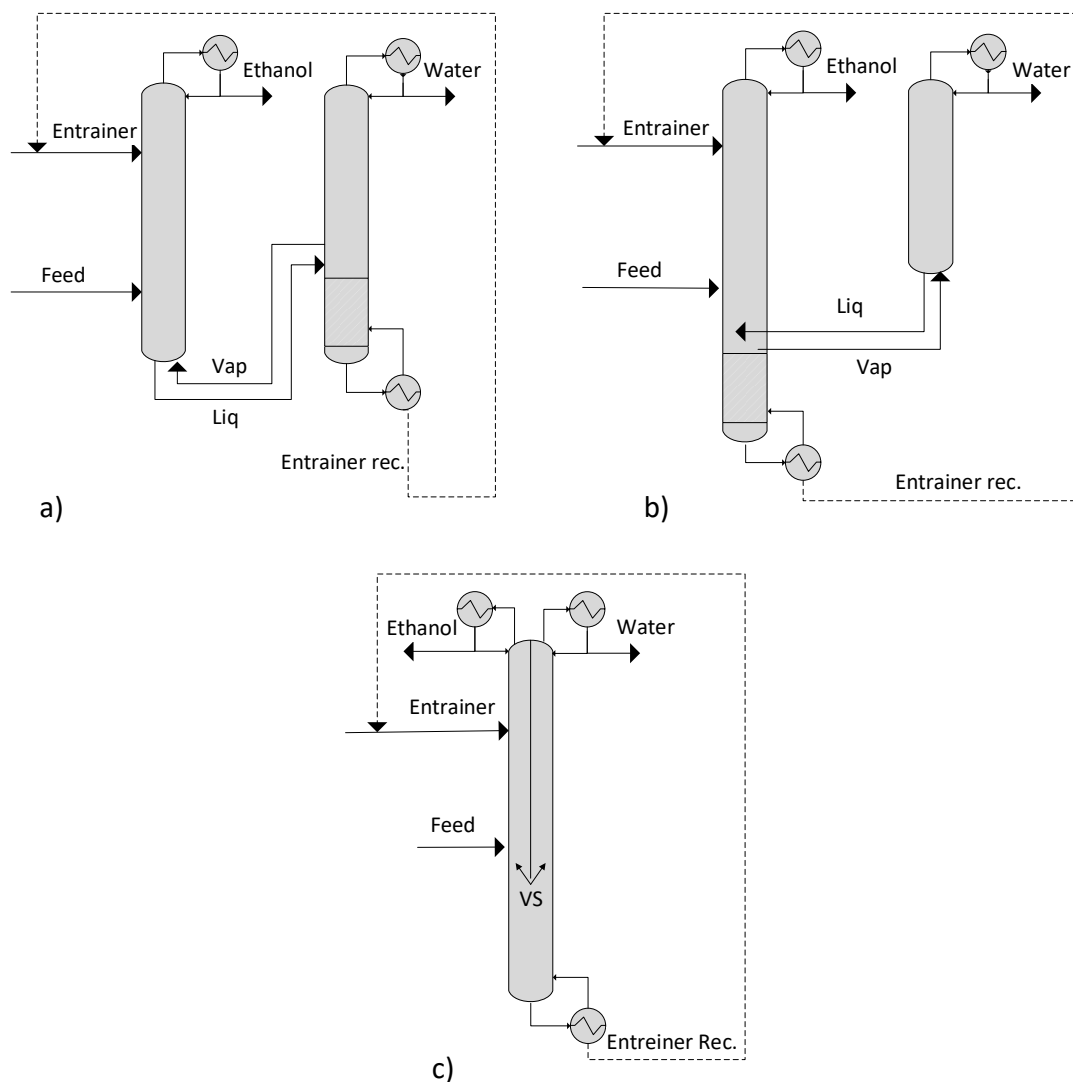


**Figure 4-11:** Thermally integration and intensification of an extractive distillation sequence.

#### 4.1.4 E-DWC modeling

E-DWC shown in **Figure 4-11c** can be modeled according to the decomposition approach by means of two column modules or three column modules, see **Figure 4-12**. In the two-columns simulation model of **Figure 4-12a**, the concentration and flows of the two lateral streams used should be specified in order to run the simulation. This specification of streams is not known during early stages of a design study, and therefore, an extra analysis should be made by the user in order to converge a solution. In addition, as the user changes some of the variables of the material streams in the model, the lateral streams need to be manually specified for each change. This is an additional effort because the global material balance does not commonly have a congruent result under these modifications.

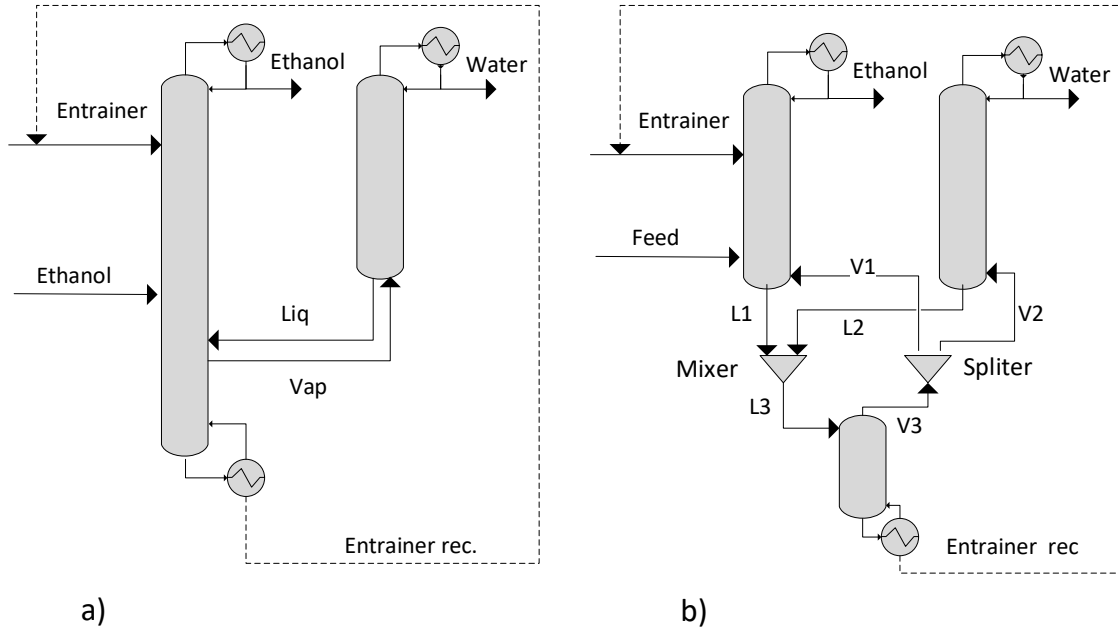


**Figure 4-12:** a) two modules model and b) three modules model

On the other hand, in the three-modules simulation model, see **Figure 4-12b**, the definition of the lateral streams is related to the rest of the submodels (three modules) by the use of a splitter. It defines the output streams of the splitter in terms of a splitting percentage of the inlet streams. This three-modules simulation model has an advantage in the way that if one material stream is changed in the global simulation, the splitting percentage value in the splitter modifies the lateral streams automatically, which is important for a sensitivity analysis of the variables affecting the column. In contrast, a more rigorous simulation of three modules implies the definition of the diameter of three modules, which needs to converge in one only expected physical diagram. This fact makes difficult the hydraulic simulation study of the column with the three modules model and therefore, a two modules model might be preferable in that case. One alternative can be to solve the three modules model and then use it for the solution of the two modules model.

#### 4.1.5 E-DWC conceptual study

From the previous chapter it was shown that the study of the equations representing the profiles of the different sections of the column is an important tool in the analysis of distillation columns. The identified sections in a conventional extractive distillation sequence and a E-DWC, according to the three modules model, are shown in **Figure 4-13**. In the non-conventional sequence, the extractive column or module has a rectifying section RS1, a

middle section MS1 and a stripping section SS1. The recovery module has only one rectifying section RS2 and the inferior module has one stripping section SS3. All the profile sections are represented by the same stripping, middle and rectifying equations that describe the conventional extractive sequence, see chapters 2 and 3. However, the equation that relates the boil-up ratio to the reflux ratio must be modified because of the presence of an additional reflux ratio in the global balance and because of the presence of the vapor splitter. In addition, equation relating the upper flow and the distillate flow (see equation (2.43)) also changes due to the additional reflux and vapor splitter, which affects the middle section profile.

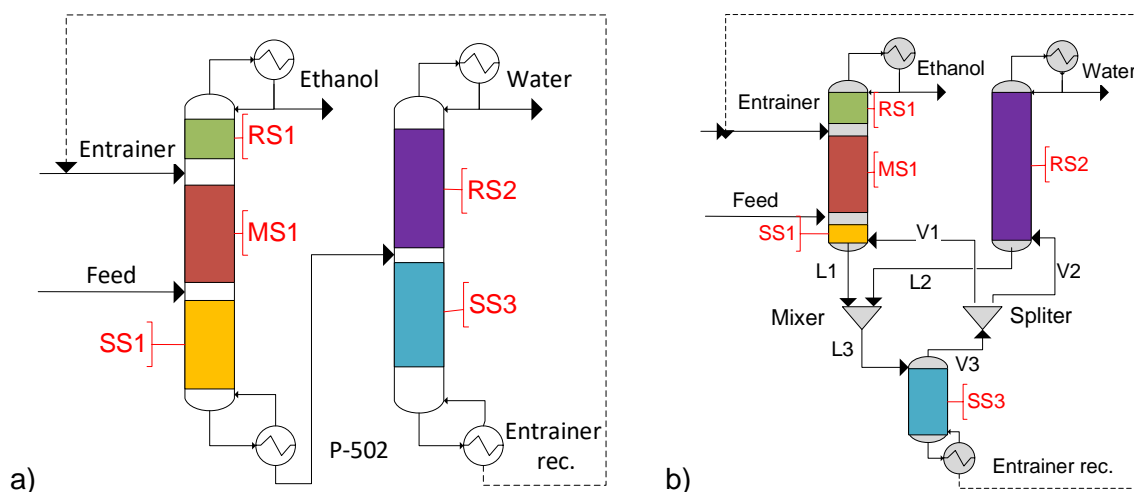


**Figure 4-13:** Profile sections in a) conventional extractive sequence and in b) E-DWC.

As the sections in **Figure 4-13** have the same equations of the conventional extractive sequence, the geometry of the column profiles should have the same behavior in the composition space. However, the position of the stable node should be different as a consequence of the dependence with the two reflux ratios.

It is important to note the existence of the stripping section SS1 in **Figure 4-13b**. Without this section it is not possible to find a balance line that could reach a low ethanol concentration in the recovery module, see **Figure 4-14**. For short stripping sections, the separation recovery of ethanol in the extractive module is low. As a consequence, an appreciable quantity of ethanol is transferred to the recovery module by means of the side vapor stream. A cost effective E-DWC should avoid this lost.

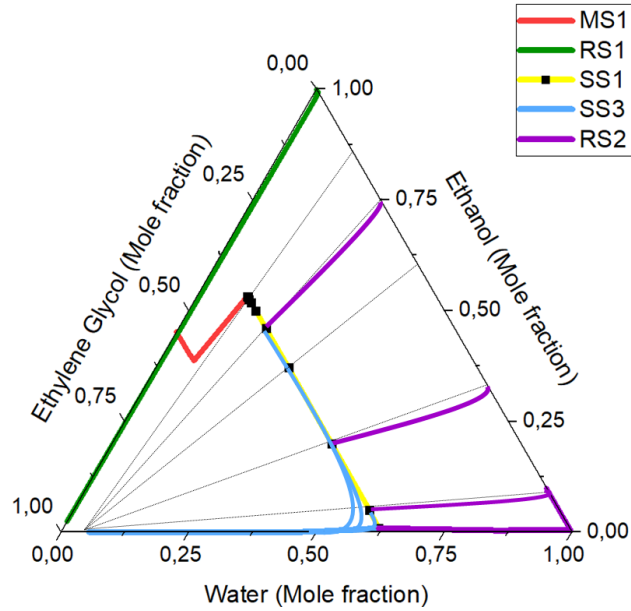


**Figure 4-14:** Qualitative E-DWC sections profiles for different number of stages in SS1.

**Figure 4-15 left** shows the effect of increasing the number of stages in an E-DWC working at relative low reflux ratio (reflux of the extractive module  $R_{EM} < 0,6$ ). For a SS1 section without stages, the global balance line starting from the bottoms composition gives an ethanol composition in the top of the recovery module that is over 0.25 mole fraction, see **Figure 4-15a left**. This mean a high quantity of ethanol is lost. By addition of one stage in this section, the ethanol composition in the top of the recovery module is reduced to almost 0.1 mole fraction **Figure 4-15b left**. If more stages are added, the distillate in the recovery module becomes richer in ethanol until it reaches a fixed point, see **Figure 4-15c left** and **Figure 4-15d left**.

The fixed point limits the minimum ethanol composition that can be obtained by addition of stages. If more SS1 stages are added to the profile shown in **Figure 4-15d left**, the composition of the side stream remains constant. This low composition is in line (same stage) with the maximum composition of the water profile shown in the stage 16 in **Figure 4-15d right**.



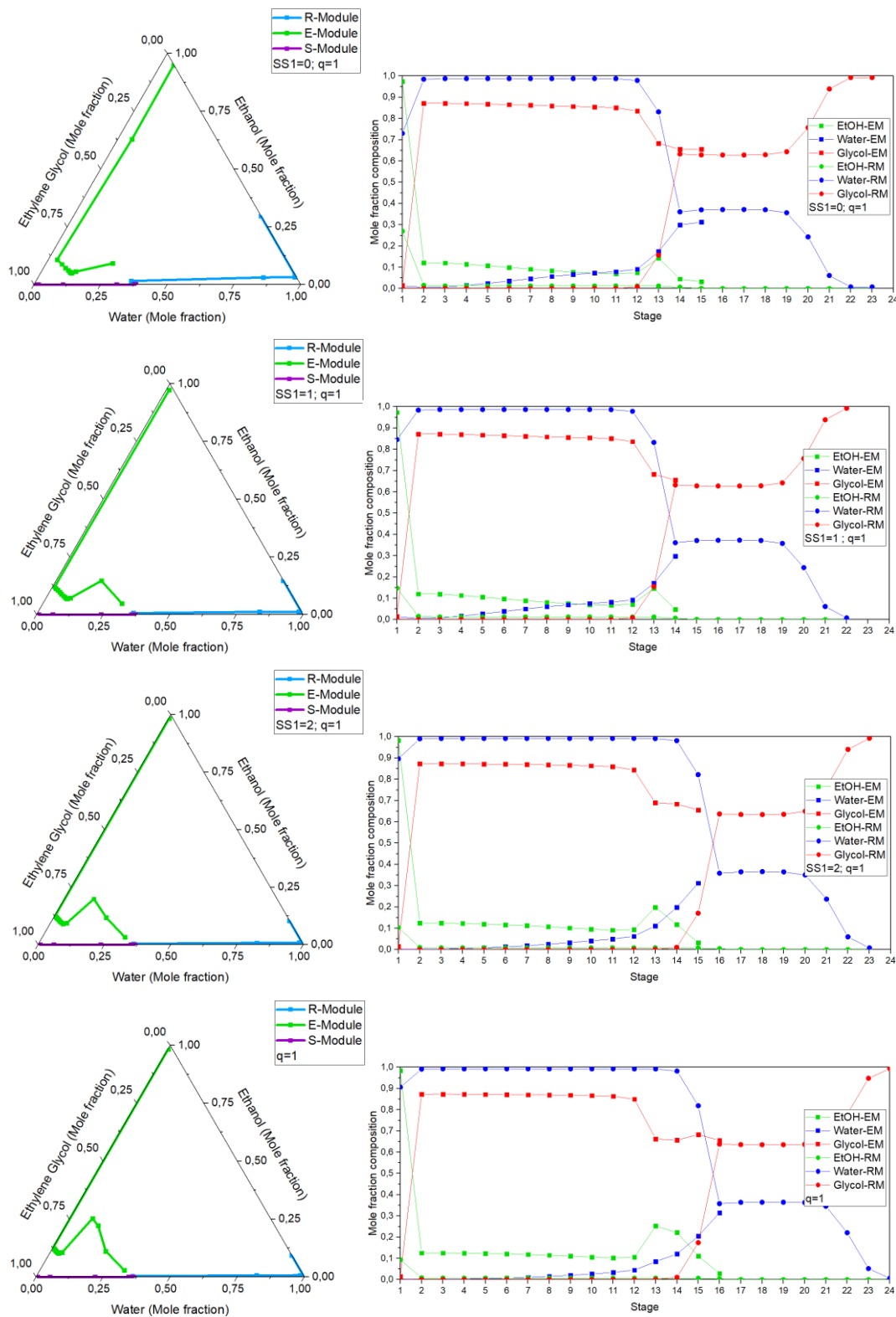
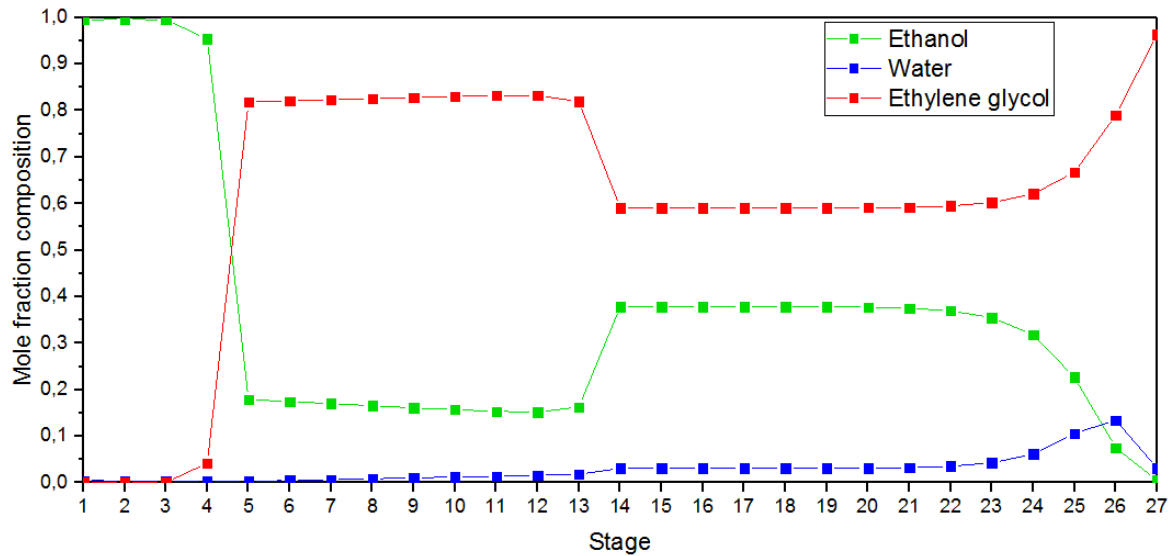


Figure 4-15: Liquid composition profiles of E-DWC for increasing number of SS1 stages.

**Figure 3-25** presents the liquid composition profiles of a conventional extractive distillation column in which the feed was saturated liquid. This profile evidences a complication in the separation using the DWC arrangement. If a side stream is taken out of the stage 26 (where the maximum water composition is located), the ethanol composition of that stage is necessarily above 0.12 mole fraction. A balance line from bottoms product composition that crosses the side stream composition will give a high ethanol composition in the water product stream. This separation is unfeasible from the economic point of view.



**Figure 4-16:** Liquid composition of an extractive column.

For cases as those shown in **Figure 3-25**, it is necessary to modify the ethanol profile in order to reduce its composition at the stage in which the water composition is the maximal. This is made by reducing the liquid remixing effect produced in the lower feed stage by means of preheating the feed. **Figure 4-17** shows the liquid composition profiles of an E-DWC when the lower feed is fed at different vapor fractions ( $q$ = quality).

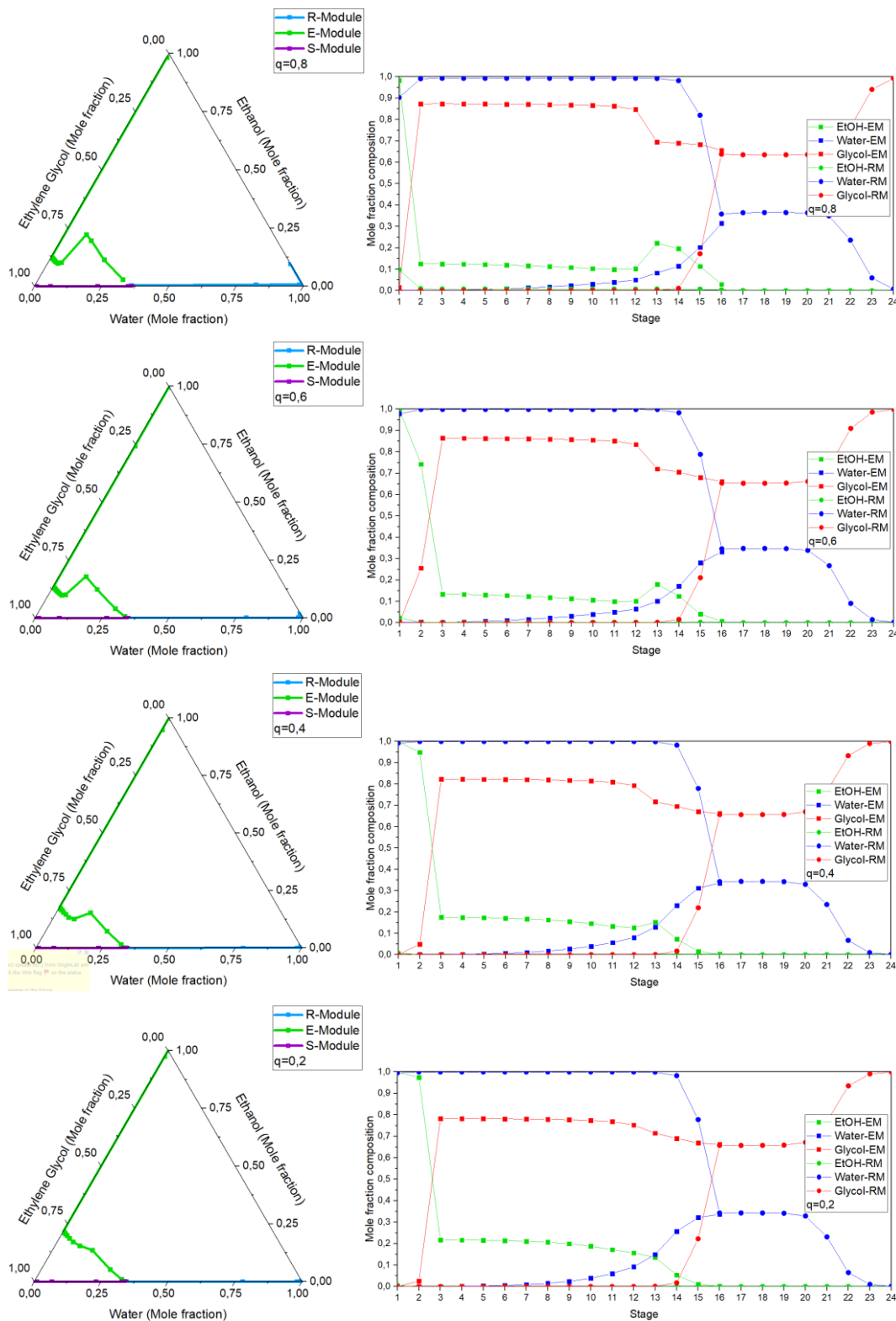
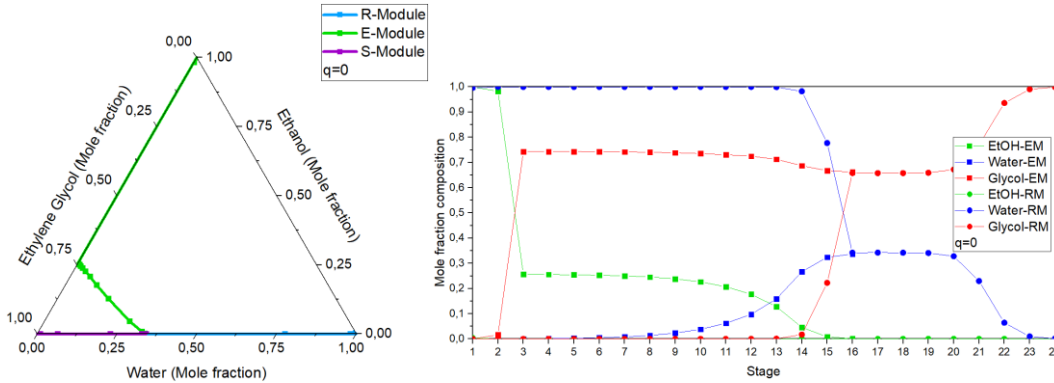


Figure 4-17: Effect of preheating the feed in the composition of the side stream.

If the lower feed of the E-DWC is fed as saturated vapor, the extractive module reaches a point of zero ethanol composition and the losses in the recovery module are minimized, see **Figure 4-18**. This column design is feasible for the separation. Note that according to the column profile, the design can be improved through the reduction of stages in the stripping module.



**Figure 4-18:** Liquid composition profile of an E-DWC for a feed condition of saturated vapor.

The energy requirements for the design in **Figure 4-18** are listed in **Table 3-6**. The preheating of the lower feed to vapor fraction 1 can be significantly reduced by taking into account the up-stream processing described in chapter one. It means, to use a partial cooler in the rectification column shown in **Figure 1-28**.

**Table 4-2:** E-DWC energy requirements.

<b>E-DWC</b>	<b>kJ/s</b>	<b>1785</b>
<b>Preheating Feed from 25°C to q=0</b>	kJ/s	1279
<b>Total energy</b>	kJ/s	3065
<b>Extractive column distillate flow</b>	kg/s	1,09
<b>Energy requirement</b>	kJ/kg	2820
<b>Energy requirement assuming preheating upstream</b>	kJ/kg	1638

## 4.2 Indirect Thermal Integration: Sequential Heat Exchangers

In the most general description, distillation is a separation process that generates at least two product streams of different composition from one or more liquid mixture streams. Both, feed streams as well as product streams, have a defined temperature and pressure. In contrast to mixing process, where the composition of the output streams is spontaneously formed from the input streams, distillation is not a spontaneous process. It means that heat and/or work must be consumed for the separation. Thermodynamically the separation work made by a distillation device can be analyzed in an analogous way to a Carnot machine, see **Figure 4-19a**. This hypothetical device acts between two energy reservoirs, one of high temperature  $T_1$  and the other one of low temperature  $T_2$ . The difference of temperature between reservoirs generates a heat transfer from  $T_1$  to  $T_2$ . The Carnot machine uses part of this energy flow to generate work.

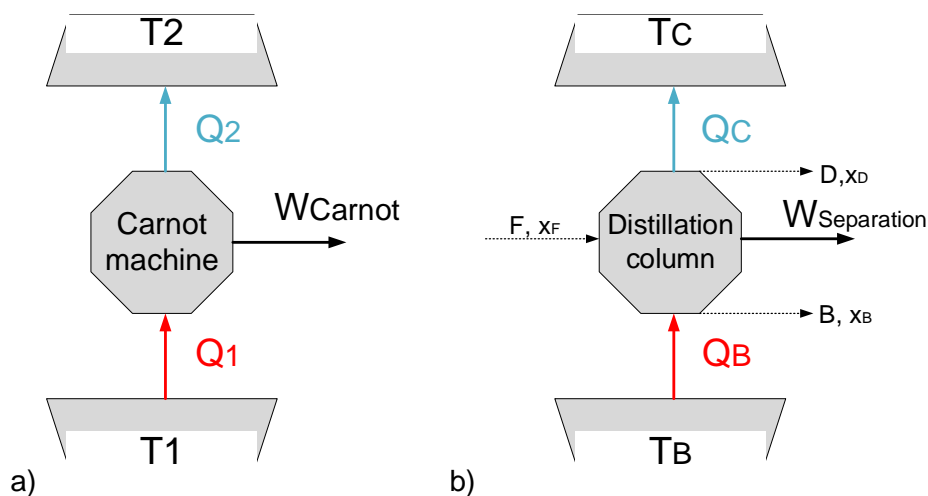


**Figure 4-19:** a) Carnot machine and b) distillation column analogy with a Carnot machine.

In analogy to the Carnot machine, the distillation device shown in **Figure 4-19b** has a high temperature reservoir  $T_B$  in the reboiler and a low temperature reservoir  $T_C$  in the condenser. Part of the energy supplied in the reboiler is used to generate a separation work. In a nonreversible case, this work (real work) is used for achieving the separation itself and to supply the energy requirements to overtake all possible irreversibilities of the phenomena happening inside the device. In a reversible column the work is used only for the separation (minimum distillation work) as the distillation column irreversibilities are reduced. The main

irreversibilities of the distillation columns are given by physical phenomena associated with the distillation itself. (King, 1979) lists the following irreversibilities in distillation:

- Irreversibility due to fluid flow
- Irreversibility due to heat transfer
- Irreversibility due to mass transfer
- Irreversibility due to chemical reactions

The phenomena cited can be driven by a pressure gradient, the temperature gradient and the chemical potential gradient.

Reducing the irreversibilities has positive impacts in the economic analysis of distillation systems. As irreversibilities are reduced, the work required for the separation is reduced to a minimum. This minimum separation work corresponds to a hypothetical distillation column with the following assumptions, see **Figure 4-20**:

- Infinity number of stages
- Heat is removed or supplied in each stage of the column
- The heat is supplied with an infinitesimal difference of temperature
- There are not heat losses
- There are not pressure losses.
- Each stage is in equilibrium condition
- The stages of feed as well as the reflux stages are also in equilibrium condition

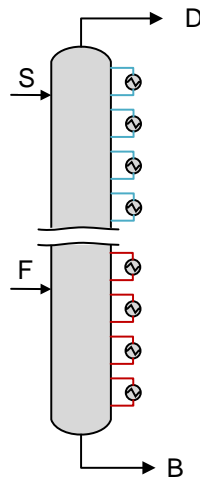


**Figure 4-20:** Reversible distillation column

## 4.2.1 Minimum and real separation work in distillation

The hypothetical case of the existence of an ideal distillation column is useful for the calculations of the minimum separation work which depends only on the composition, temperature and pressure of the feed streams and product streams. This work can be calculated from the material, energy and entropy balance of the reversible distillation column:

Material balances

$$F = D + B \quad (4.4)$$

$$F x_F = D x_D + B x_B \quad (4.5)$$

Energy balance

$$F h_F + \dot{Q}_{reb} = \dot{Q}_{cond} + D h_D + B h_B \quad (4.6)$$

Entropy balance

$$F s_F + \frac{\dot{Q}_{reb}}{T_{reb}} = \frac{\dot{Q}_{cond}}{T_{cond}} + D s_D + B s_B \quad (4.7)$$

Multiplying the entropy balance by a reference temperature  $T_0$  (ambient temperature):

$$F s_F T_0 + \frac{\dot{Q}_{reb}}{T_{reb}} T_0 = \frac{\dot{Q}_{cond}}{T_{cond}} T_0 + D s_D T_0 + B s_B T_0 \quad (4.8)$$

Adding the energy balance equation, it results in:

$$F s_F T_0 - F h_F + \frac{\dot{Q}_{reb}}{T_{reb}} T_0 - \dot{Q}_{reb} = \frac{\dot{Q}_{cond}}{T_{cond}} T_0 - \dot{Q}_{cond} + D s_D T_0 - D h_D + B s_B T_0 - B h_B \quad (4.9)$$

Rearranging:

$$\underbrace{\dot{Q}_{reb} \left(1 - \frac{T_0}{T_{reb}}\right) - \dot{Q}_{cond} \left(1 - \frac{T_0}{T_{cond}}\right)}_{W_{\text{equivalent of Carnot}} = W_{\text{min of separation}}} = \underbrace{D(h_D - s_D T_0) + B(h_B - s_B T_0) - F(h_F - s_F T_0)}_{\text{Exergy difference between input output streams}} \quad (4.10)$$

The minimum separation work represents the lowest energy limit that must be consumed for the separation. It is expressed in the left side of the equation (4.10). It can be noticed that the minimum separation work in equation (4.10) is given by the difference of exergy of the input material streams and output material streams. The minimum separation work is also equal to the increment of free energy of Gibbs of products with respect to feeds:

$$W_{\min \text{ of separation} | T} = \Delta G_{\text{separation}} = \underbrace{D(h_D - s_D T) + B(h_B - s_B T) - F(h_F - s_F T)}_{\text{Free energy of Gibbs increment of outputs with respect to input streams}} \quad (4.11)$$

Note that even when equations (4.10) and (4.11) are quite similar, they are not equal unless the temperature of the feeds is equal to  $T_0$ .

When a similar analysis is made for real distillation, the entropy balance must take into account the degradation of energy due to the irreversibilities of the process:

$$F s_F + \frac{\dot{Q}_{reb}}{T_{reb}} + \dot{S}_{irr} = \frac{\dot{Q}_{cond}}{T_{cond}} + D s_D + B s_B \quad (4.12)$$

With this balance the separation work in a real column is given by equation (4.13):

$$W_{\text{real of separation}} = \underbrace{D(h_D - s_D T_0) + B(h_B - s_B T_0) - F(h_F - s_F T_0)}_{W_{\min \text{ of separation}}} + \underbrace{T_0 \dot{S}_{irr}}_{\text{Degradation of energy due to process irreversibilities}} \quad (4.13)$$

## 4.2.2 Distillation column entropy mapping

From equation (4.10) and (4.13) the difference between the real separation work and the minimum separation work is the degradation of energy due to the irreversibilities of the process:  $T_0 \frac{ds_{irr}}{dt}$ . Main reasons for these irreversibilities were listed above and are significantly larger than the minimum work required for the separation. The term  $\frac{ds_{irr}}{dt}$  refers to the entropy generated in the process. This entropy generation depends on the trajectory followed by the process. Operation or design conditions can modify this trajectory and therefore, it is possible to optimize it in order to reduce the entropy generation (Mendoza, 2011). For analysis purposes, the quantification of the irreversibilities is preferable to be made taking as control volume small sections of the column and mapping the entropy production in each point of the column. Surely, the total entropy generation can be studied by calculating it for a global control



volume but it says not too much about the phenomena behind that generation. In contrast, entropy mapping has the advantages to identify the zones of more entropy generation and to associate those zones with the prevailing phenomena occurring at each point. **Figure 4-21** shows the entropy mapping of the extractive and recovery column for the design obtained in **Chapter 3**. For the extractive column, the most important contribution to the generated entropy is located in the upper feed, lower feed and in the reboiler. This entropy generation can be associated to the mixture in feed stages and heat transfer near to the reboiler. On the other hand, in the case of the recovery column, the entropy generation can be associated to the heat and mass transfer.

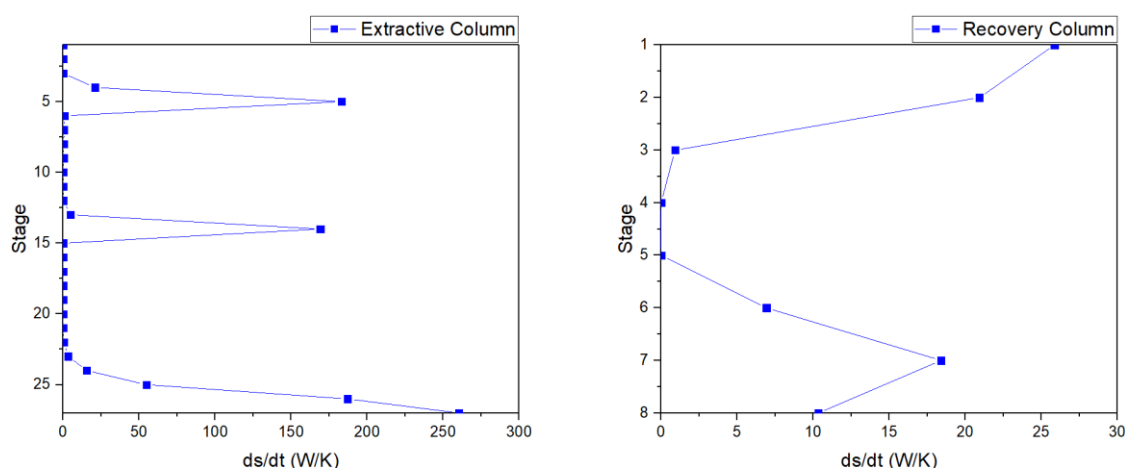


**Figure 4-21:** Entropy generation mapping of extractive and recovery column.

**Figure 4-21** shows the total entropy generated in each section of the extractive and recovery column. This total entropy is calculated through the entropy balance per section. The portion of entropy generated by heat and mass transfer between vapor and liquid can be calculated by means of the irreversible process thermodynamics as reported by (Mendoza, 2011). The author shows that the difference between the entropy generation in each column section and the entropy generated by heat and mass transfer is the entropy generated by mixture of internal streams and feed stages. The author also shows that the mass and heat transfer in liquid vapor zone dominates the irreversibilities in all column points with no feed streams and that the remixing irreversibilities dominate the entropy generation (or the exergy destruction) in feed points.

The entropy generation in a distillation column is influenced by variables like reflux ratio, the temperature of the feed, the temperature of the solvent and the solvent to feed ratio.

Parametric studies for extractive distillation column are reported in (Mendoza, 2011). Results showed that the solvent to feed flow ratio is the parameter that most affect the entropy generation in extractive column followed by the reflux ratio. Low solvent to feed ratio and low reflux ratio are recommended.

### 4.2.3 Distillation column targets

In addition to entropy mapping, distillation columns are analyzed in this document in terms of the energy targets. The scope of the energy targets analysis is to identify a column design modification with respect to energy consumption. The basis of analysis is the minimum thermodynamic condition introduced above and improved later in this chapter. This minimum thermodynamic condition is related to the hypothetical reversible column concept. For more real distillation columns, energy targets are studied based on the so called Practical Near-Minimum Thermodynamic Condition (PNMTC) (Dhole & Linnhoff, 1993). In order to develop this concept, it is convenient to return to the use of a temperature-enthalpy diagram (T-H) in the representation of a real column, **Figure 4-4a**. For the recovery column designed in **chapter 3**, a temperature enthalpy representation is shown in **Figure 4-22a**. a real column is also commonly represented in a stage-enthalpy diagram (S-H) as it is shown in **Figure 4-22b**.

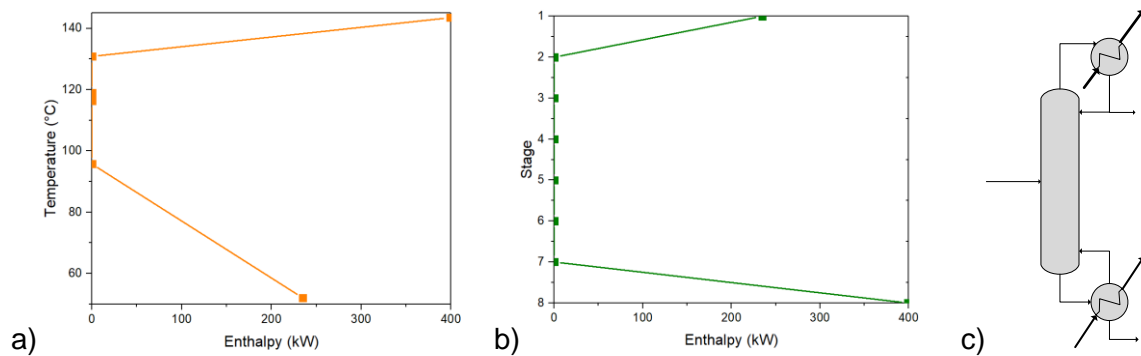


**Figure 4-22:** Box representation of the recovery distillation column designed in chapter 3.

In **Figure 4-22** the heat is transferred from and to the column only in the condenser and in the reboiler. This is not efficient and therefore it is preferable to distribute the heat transfer along the column stages with low temperature differences between the utilities and the column stages. A way to do this consists in adding side exchangers to the original distillation column. For example, if a side reboiler and a side condenser is added to the column represented in **Figure 4-22c**, it results in the S-H diagram shown in **Figure 4-23a**. Increasing

the number of reboilers, see **Figure 4-23b**, moves away the S-H profile until the limit condition PNMTCC shown in **Figure 4-23c**. The S-H profile at PNMTCC is known as the Column Grand Composite Curve (CGCC) which assumes an infinite number of stages and an infinite number of side exchangers.

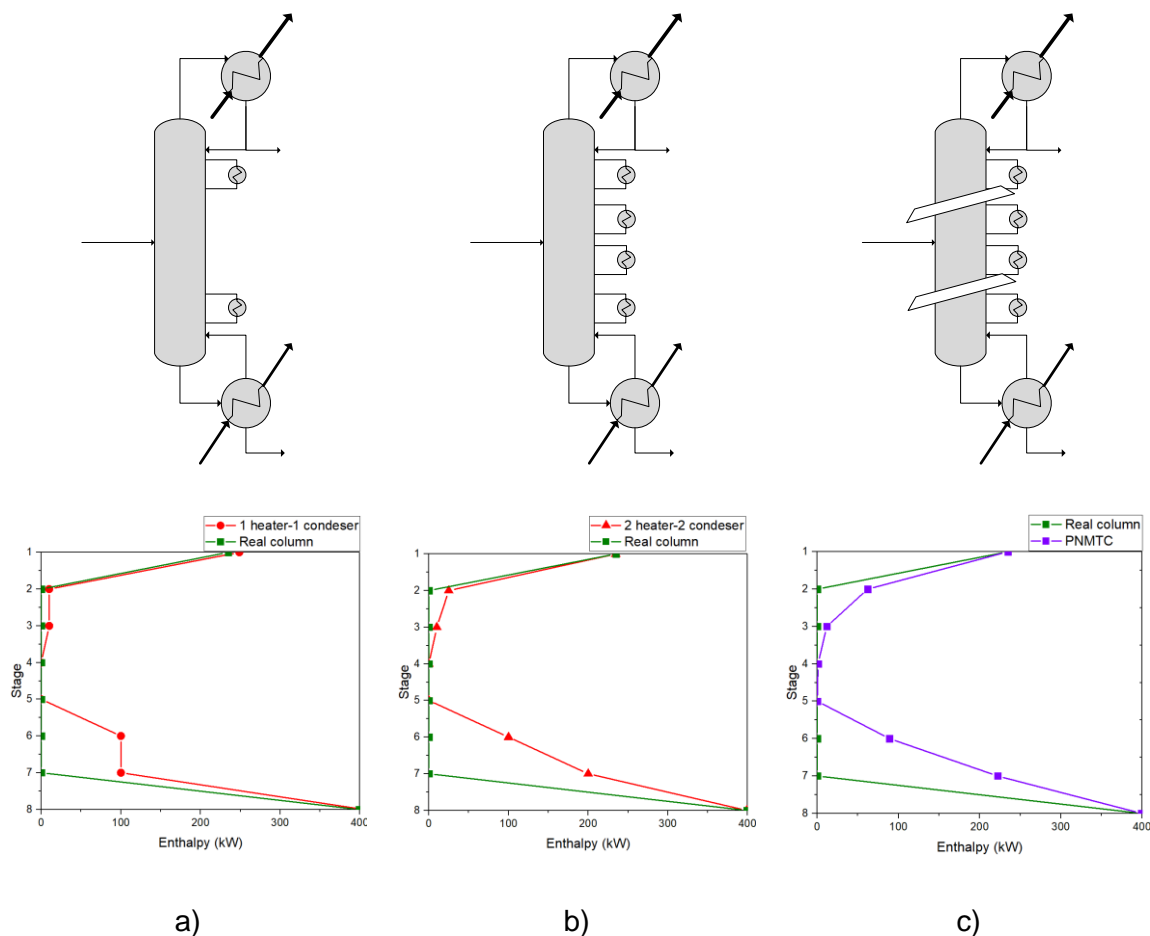


**Figure 4-23:** Approximation of a real distillation column to the PNMTCC by means of side columns and increasing of stages in a S-H diagram.

The PNMTCC can also be drawn in a T-H diagram as shown in **Figure 4-24a** for the recovery column and in **Figure 4-24b** for the extractive column. T-H diagram is not the best option for analysis of the grand composite curve as can be seen in these graphics, the stages overlap itself in the profile. Especially in the case of extractive column it is better to plot the grand composite curve in the S-H diagram, see **Figure 4-25**.

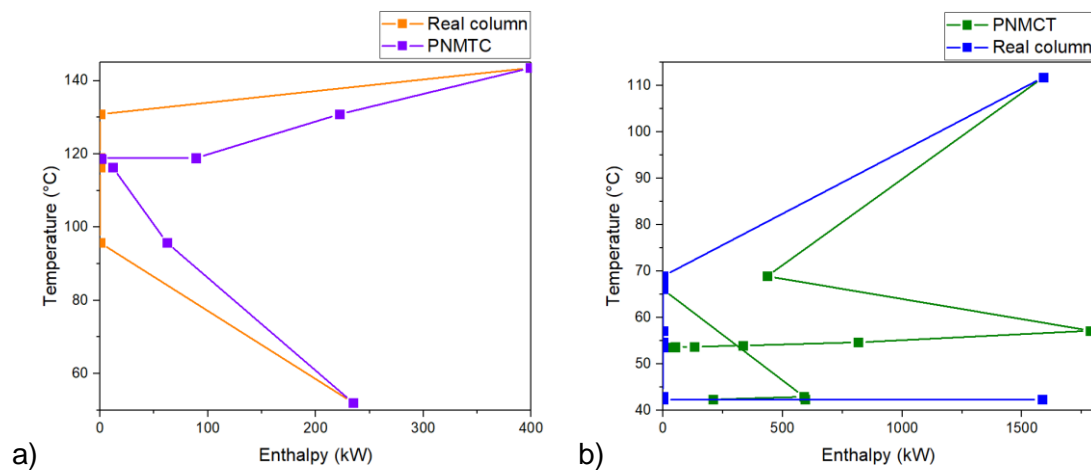


**Figure 4-24:** T-H grand composite curve for a) the recovery column and b) for the extractive column

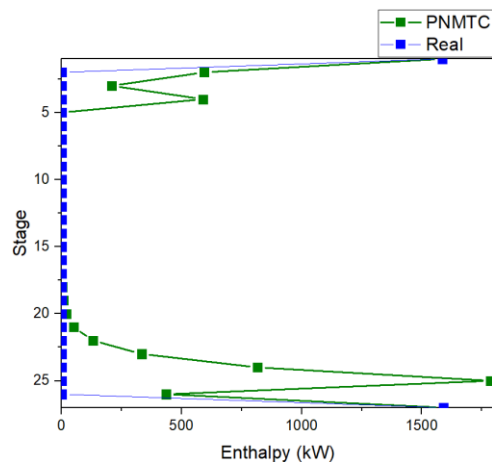


**Figure 4-25:** S-H grand composite curve for the extractive column designed in **Chapter 3**.

Grand composite curves shown are used to improve column design by means of modifications as for example:

- Reflux and pressure modifications
- Feed preheating or cooling
- Side condensing and side reboilers.

In next sections side condenser and side reboilers are of high interests to this study.

#### 4.2.4 Column Composite curves

Composite curves are well understood from the study of heat exchanger networks (Kemp, 2007). A composite curve shows graphically the heat loads and temperature change of multiple heat transfer streams in one single curve. For the case of distillation two kind of composite curves can be observed: a vapor curve formed from the loads and temperatures of the internal vapor streams in the column and a liquid curve formed from the loads and temperatures of the internal liquid streams in the column. **Figure 4-26** and **Figure 4-27** show this for the recovery and extractive columns designed in **Chapter 3**. The formed profiles are called Column Composite Curves (CCC) and can be plotted in the temperature-enthalpy diagram as well as in the stage-enthalpy coordinates. In the present document, these profiles are calculated based on the CGCC.

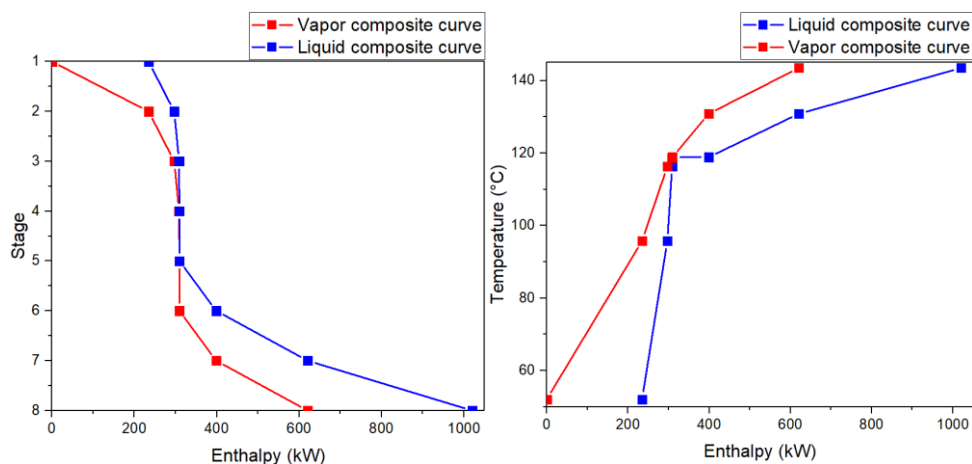


**Figure 4-26:** Column composite curves for the recovery column in **Chapter 3**.

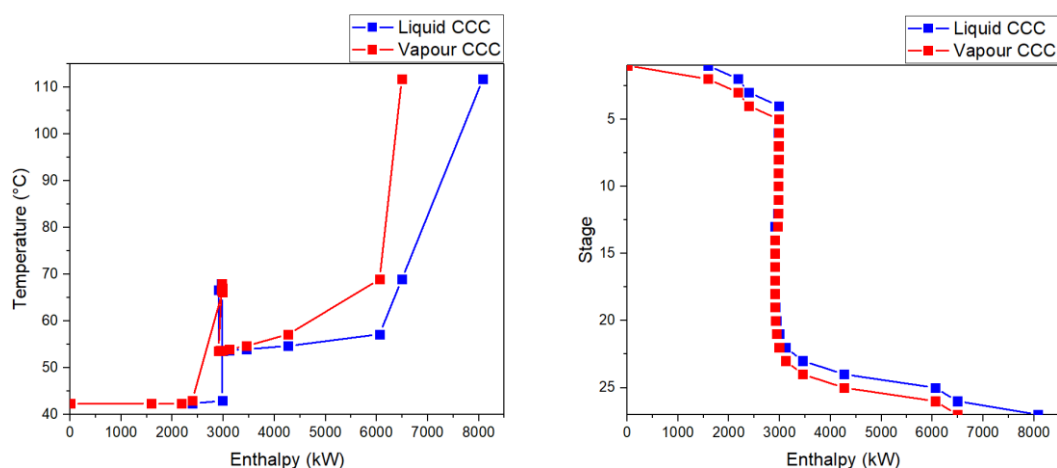


**Figure 4-27:** Column composite curves for the extractive column in **Chapter 3**.

### 4.2.5 The ideal distillation column model

This section refers to the ideal distillation concept reported by (Kaiser & Gourlia, 1985). The author parts from the characterization of a distillation column as follows:

- The feed has been adequate according to the column target analysis discussed previously
- Separation is obtained by means of counter flow between vapor and liquid streams
- Pressure is constant throughout.
- Heat transfer is allowed at any stage of the separation
- The light product is a dew point vapor
- The heavy component is a bubble point liquid
- Steady state and continuous process

Based on these characterizations an adiabatic and a diabatic distillation columns are shown in **Figure 4-28**. Notice that there is no difference between the material balance equation between the models but it is not the same for equilibrium equations. Also notice that in contrast to the adiabatic column, in the diabatic column there is heat exchange in all the stages.

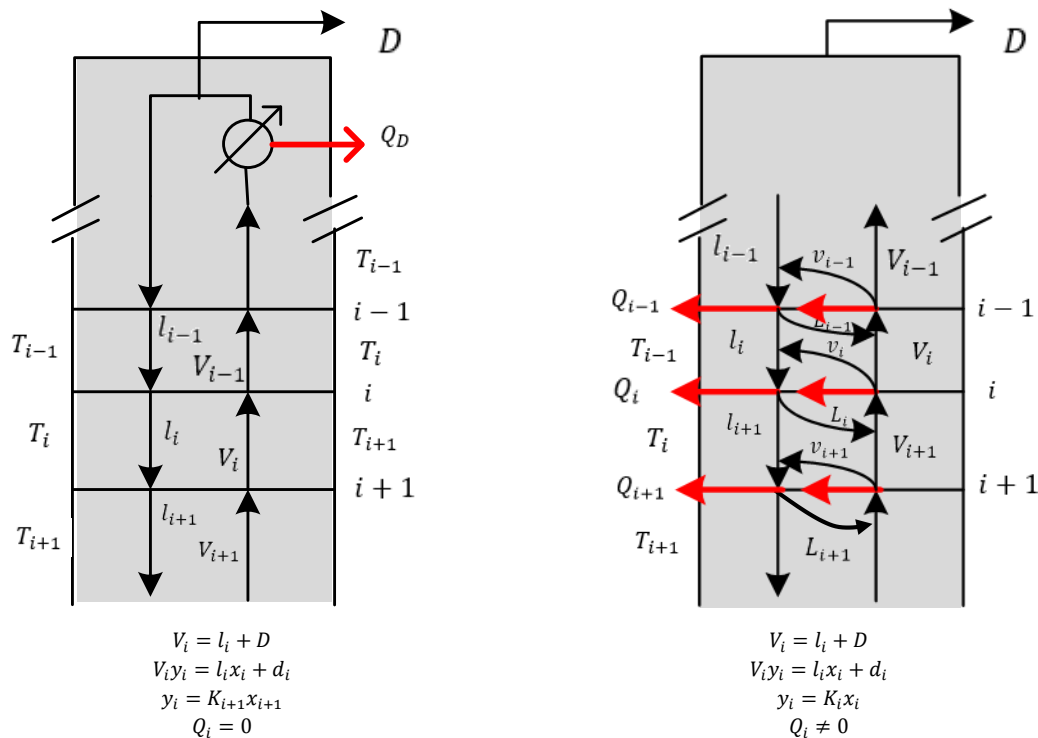


**Figure 4-28:** Adiabatic and diabatic distillation column characteristics. From (Kaiser & Gourlia, 1985)

In the adiabatic column the liquid  $l_i$  at  $T_i$  cannot be in equilibrium with the vapor  $V_i$  at temperature  $T_{i+1}$  and therefore when these two inlet streams are in contact there is a necessary mass transfer between liquid and vapor streams. On the other hand, in a diabatic column, there is a liquid stream  $l_i$  at  $T_i$  coming down from stage  $i - 1$  and is partially vaporized at stage  $i$  producing two equilibrium streams  $l_{i+1}$  and  $v_{i+1}$  at  $T_i$ . For this case  $v_{i+1}$  and  $V_{i+1}$  are at same composition and can be mixed before entering to the stage  $i$ . In the case of the liquid phase,  $L_i$  is mixed with  $l_i$  at same temperature and composition previously to enter to the stage  $i$ .

It can be noticed that the streams in the diabatic column inlet to the stages are in equilibrium and therefore there is not mass transfer between the inlet liquid and vapor streams. Therefore, there are no irreversibilities due to mass transfer. The mass transfer was replaced by heat transfer in each stage by means of lateral heat exchangers. If it is assumed that this heat transfer is made in absence of temperature difference, then the irreversibilities are avoided. The form to do this is with infinite number of heat exchangers in infinite number of stages.

From the point of view of the McCabe-Thiele diagram, see **Figure 4-29**, the diabatic composition profile corresponds to the composition of the equilibrium profile ((King, 1979) improves this idea). The McCabe-Thiele diagram is used here only to clarify that the columns with sequential exchangers even being finite have the need to increase the number of equilibrium stages. This is evidenced in **Figure 4-29a**. In this diagram, the operating line of the standard adiabatic column is shown by a straight line. In the case of a diabatic column (see **Figure 4-29b**), the operation line takes a curved shape almost parallel to the equilibrium isobaric of the system. The approach of this curve to the equilibrium isobaric is a measure of the reversibility of the studied process, being the overlap in the curves the condition of less exergy destruction. By counting the number of stages required for the distillation it is shown that, in order to achieve the same separation, the diabatic column requires a greater number of plates, and in the ideal case requires infinite number of plates.

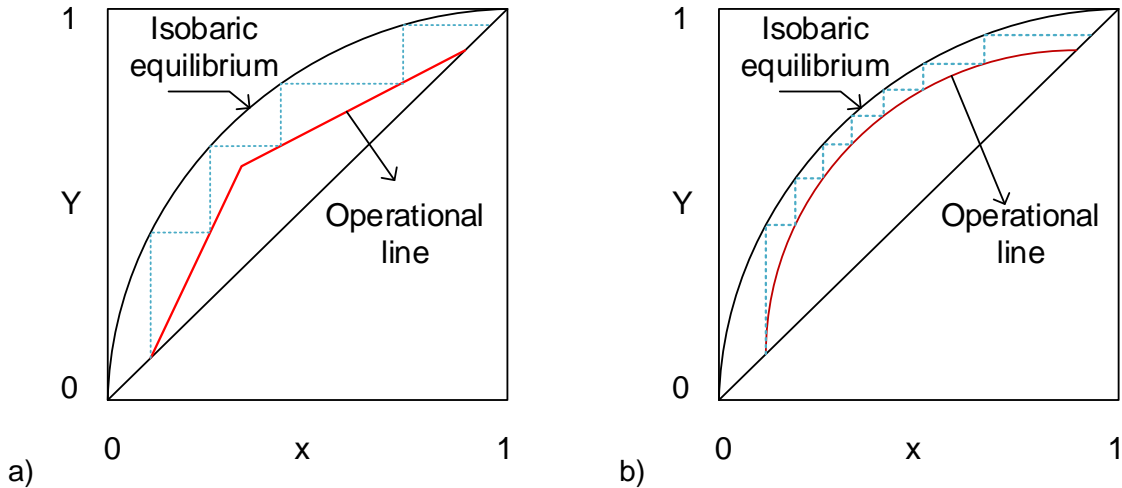


**Figure 4-29:** McCabe-Thiele diagram for a) an adiabatic column and b) a diabatic column.

#### 4.2.6 Partially reversible extractive distillation column

For extractive distillation column, a hypothetical ideal model is not clearly reported as in the case of simple distillation columns. In this section an ideal extractive distillation model is studied from the point of view of the pinch branches studied in previous chapters. First of all it is necessary to say that it is not possible to obtain a rigorously reversible extractive distillation model but only a partial reversible model. The reason for this is that extractive distillation uses a mass separation agent which generates dilution in the middle section of the extractive column. This dilution is itself an irreversible process and therefore extractive separation process is classified as only partially reversible process (King, 1979). The difficulty of making reversible a separation process with a mass agent is that in a reversible case the separation agent should be fed in each stage of the column. Even if it were practice, each entrainer feed should be saturated in the other components involved in the separation, which means that a reversible separation needs to be made previously to the feeding of the streams.

**Figure 4-30a** Shows three pinch branches of a extractive column. These branches concur to reversible trajectories of the stripping, middle and rectifying section of the extractive column. In order to find a column profile for the reversible extractive distillation, a column profile should be formed from sections of the pinch branches. **Figure 4-30b** shows a trajectory of composition for a column that concur with the pinch branches



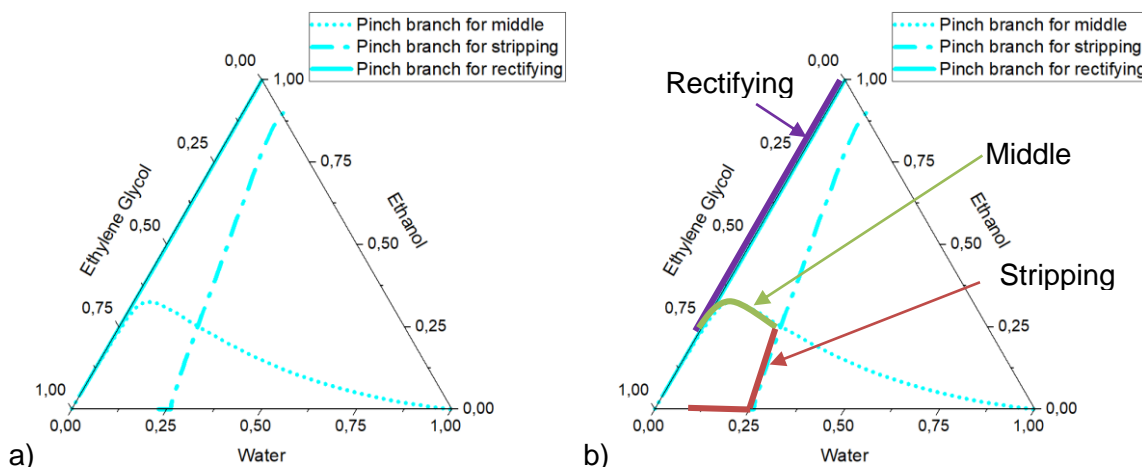


**Figure 4-30:** Reversible composition trajectories of an extractive distillation column.

However, as it was mentioned, due to dilution effects of the mass agent, the middle section composition profile do not follow a reversible trajectory as the shown in **Figure 4-30**. Instead of this it follows a partial reversible trajectory shown in **Figure 4-31** (In (Petlyuk, 2004) a similar geometry is present for Acetone-Water-Methanol case)

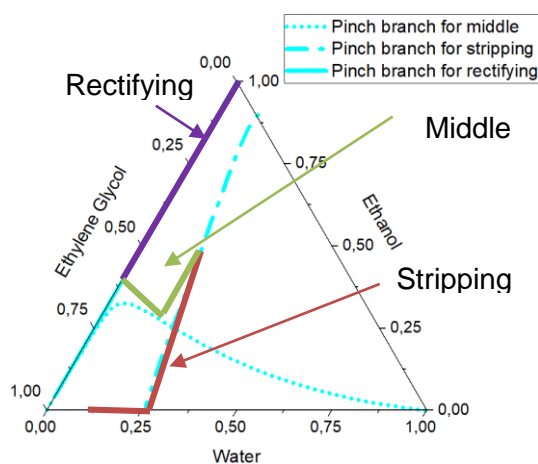


**Figure 4-31:** Partial reversible composition profile of an extractive distillation column.

On the other hand, it can be noticed that the stripping and rectifying column profiles in **Figure 4-31** do actually concur with the pinch branches. It means that even when the middle section profile has not a reversible behavior, the two other section are potentially reversible. Therefore, stripping section, and rectifying section in lesser extent, can be modified in order to reduce the irreversibilities present in an extractive distillation column. In order to explain this, **Figure 4-32** shows a typical composition profile of an extractive column as designed in

**Chapter 3.** At high reflux the column profile is away of the partial reversible profile, see **Figure 4-32a**. However, as the reflux is reduced to the minimum the profile approximates the ideal profile in the middle section as is shown in **Figure 4-32b**. This is analogous to the first case shown by (Dhole & Linnhoff, 1993) for binary distillation columns.

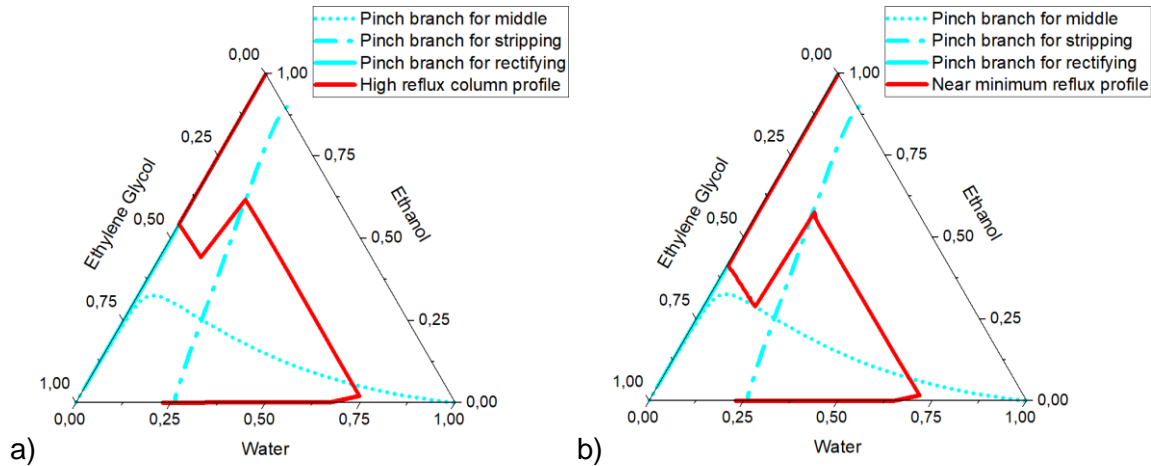


**Figure 4-32:** Effect of the reflux in the reduction of irreversibilities

Now, if side exchangers are added to the stripping section of the extractive column in analogous way as were added for binary mixtures in **Figure 4-23** then the stripping section profile approximates to the partial reversible profile, see **Figure 4-33**. This procedure with the analysis of the T-H diagrams can be applied to find opportunities of modifications of conventional as well as dividing wall extractive columns.

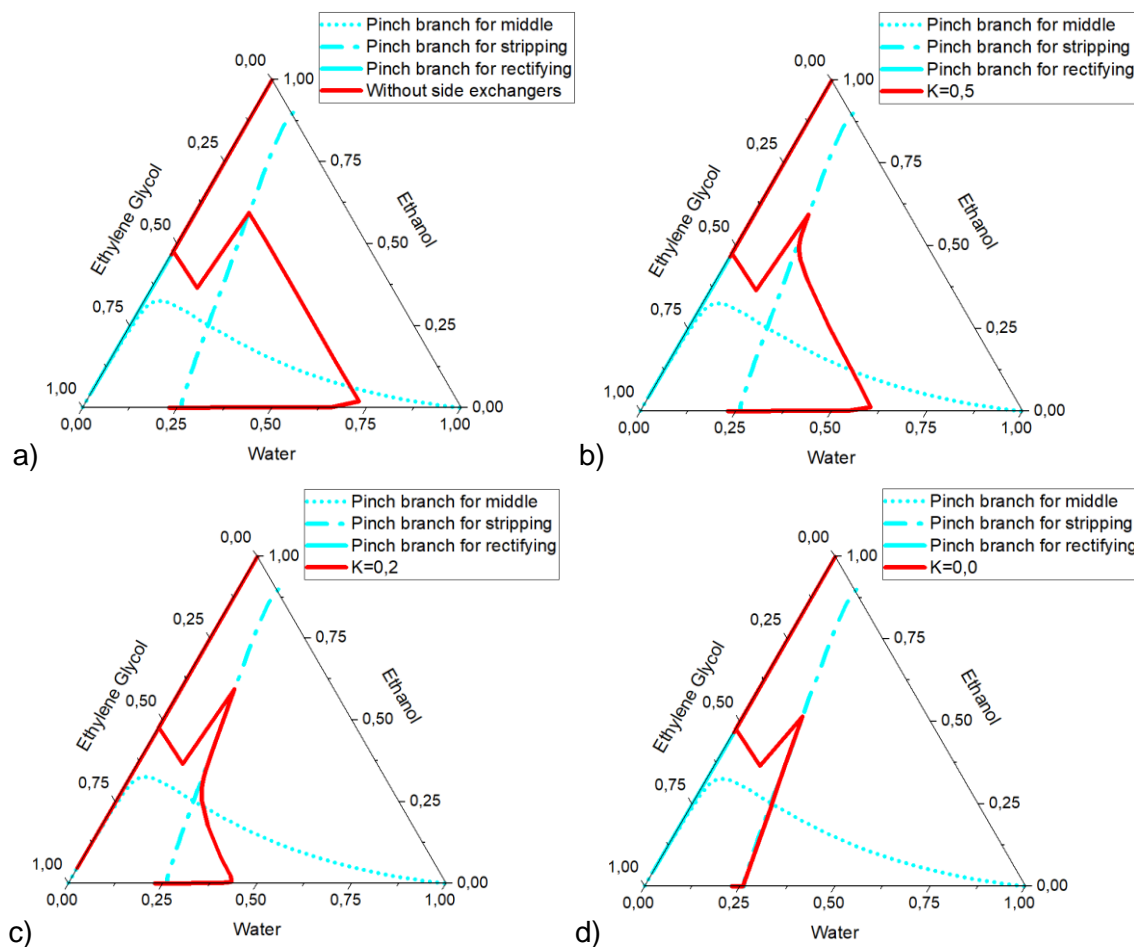


**Figure 4-33:** Effect of side exchangers in the extractive distillation column

#### 4.2.7 Extractive distillation column with sequential heat exchangers (SHE)

An SHE column is based on the idea of a diabatic column with a finite number of stages. The number of exchangers required in this case can range from one for each of the stages, to exchangers in only few stages. Choosing between the two cases is a decision based on a cost analysis. The greater the number of exchange stages, the greater the operational benefits of the column and, in turn, the greater the costs of its implementation. An optimization of the operational benefits versus the costs of implementation is required to define the number and position of exchange stages. In the particular case of the SHE column proposed in this document, three stages of exchange have been constructed at the upper end of the column and three at the lower end, see **Figure 4-34**. The position has been chosen based on an entropy minimization analysis and the temperature-enthalpy diagrams of the column for the

ethanol-water-ethylene glycol system (Mendoza, 2011). This SHE column is not totally diabatic, therefore, the use of reboiler and condenser exchange equipment is still required.

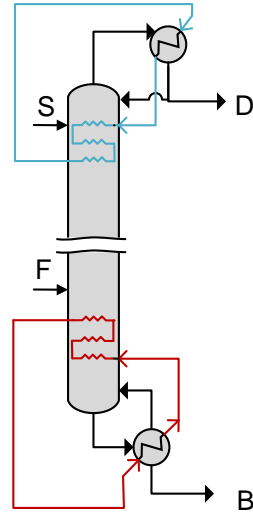


**Figure 4-34:** Extractive distillation column with sequential heat exchangers

In the design of SHE distillation columns, it is sought to influence irreversibilities related to the temperature gradient used for the separation. The higher the temperature gradient between the temperature service and the process, the greater the net consumption of separation work required. Reducing this gradient means providing the distillation column with a service temperature close to the specifications of each distillation stage. Graphically this can be seen **Figure 4-35**, where the lines of the heating and cooling services have a minimum temperature difference with respect to the profile of the column.

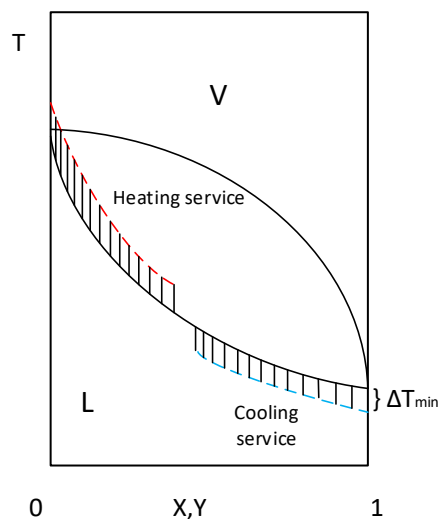


**Figure 4-35:** Temperature composition diagram for a distillation column where the temperature for heating and cooling is included stage by stage

## 4.2.8 SHE simulation study

In this section an extractive distillation column with sequential heat exchangers is compared with a conventional extractive distillation sequence or conventional ED. The number of stages for this design is restricted to 12 stages. The reason for do this is that the results obtained from the following study are going to be implemented in a pilot plant located in a laboratory with restriction of height. Specification for the simulation are shown in **Table 4-3**.

**Table 4-3:** Simulation specifications.

Specification	Conventional ED	SHE
<b>Absolute condenser pressure (bar)</b>	0,20265	0,20265
<b>Theoretical stages</b>	12	12
<b>Condenser stage</b>	1	1
<b>Upper feed</b>	3	3
<b>Lower feed</b>	8	8
<b>Reboiler</b>	12	12
<b>Entrainer to feed ratio (FU/FL)</b>		
<b>Reflux ratio</b>	0,5	0,5
<b>Distillate mole fractions</b>		
Ethanol	0,99472	0,99945
Water	0,00504	0,00522
Ethylene glycol	0,00023	0,0002
<b>Upper feed mole fractions</b>		
Ethanol	0,0	0,0
Water	0,001	0,001
Ethylene glycol	0,999	0,999
<b>Lower feed mole fractions</b>		
Ethanol	0,87	0,87
Water	0,13	0,13
Ethylene glycol	0,0	0,0
<b>Bottom mole fractions</b>		
Ethanol	0,004855	0,0049
Water	0,11236	0,1123
Ethylene glycol	0,8828	0,8828
<b>Upper feed quality</b>	1	1
<b>Upper feed temperature °C</b>	78	65
<b>Lower feed quality</b>	1	1
<b>Heat duty kJ/s</b>	8,4345	2,7794
<b>Distillate flow kg/h</b>	13,9888	13,9872
<b>Energy consumption</b>	2171	715,35

**Figure 4-36** shows the effect of use of internal heat exchangers in the extractive distillation column. As distillation is a separation process based on difference of volatilities the use of internal SHEs heat up the liquid mixture in the stage and therefore the vapor is enriched in the component of minimum boiling point. In **Figure 4-36.a** and **Figure 4-36b** this is noticed in the approximation of the stripping profile to the binary vertex glycol-water.

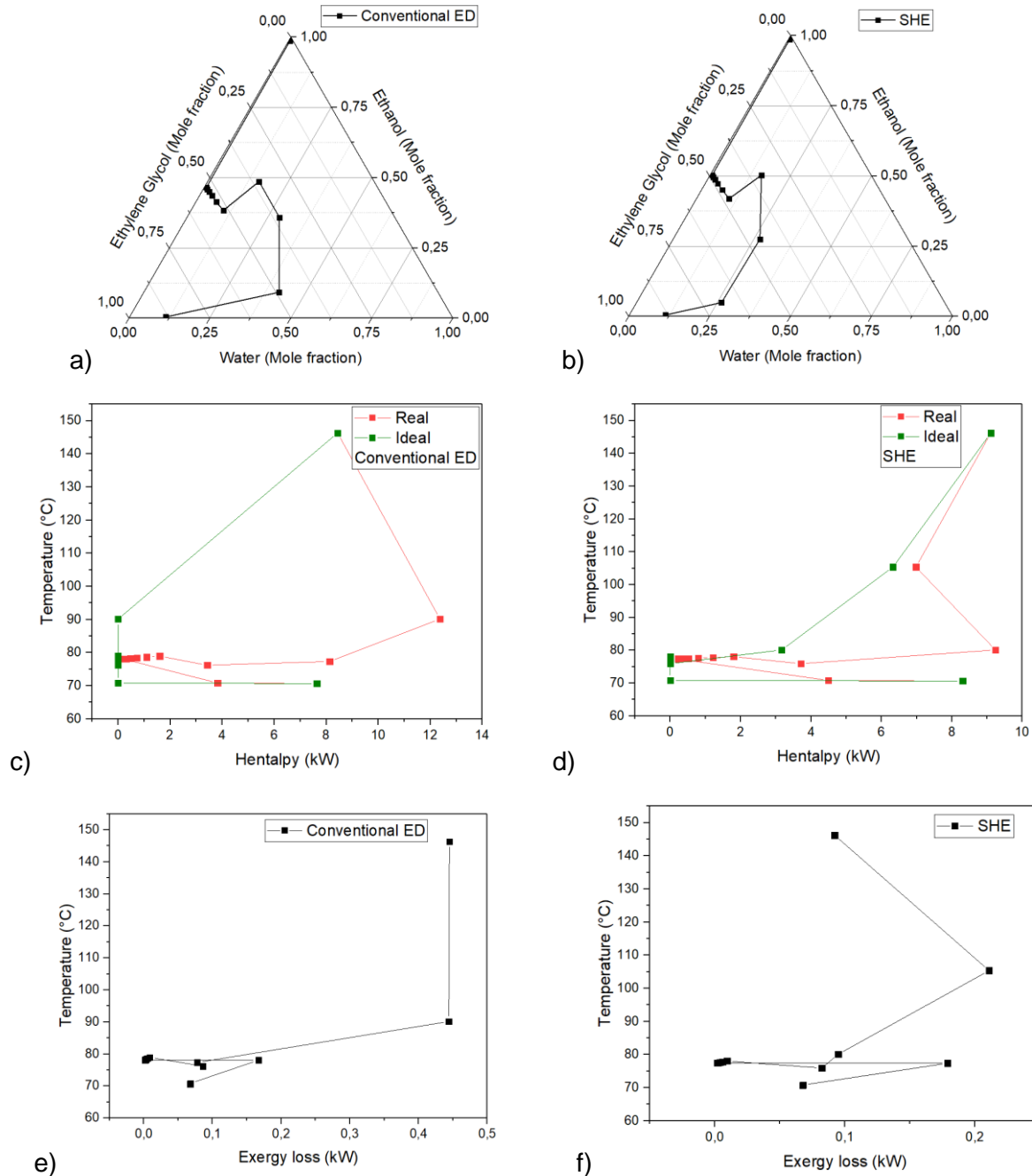


**Figure 4-36:** Column profiles, grand composite curves and loss entropy for a conventional distillation column and a column with SHE.

The heat transfer in the conventional extractive column is carried out only in the reboiler and in the condenser. However, the effect of the heat in the separation is notice stage by stage. It means that the reboiler should provide enough temperature vapor in order to mitigate the degradation of energy in the way. This degradation is shown to be mitigated comparing **Figure 4-36d** respect to **Figure 4-36c**. Note that the energy requirement decrease in quantity (first law of thermodynamics) and in quality (second law of thermodynamics). Internal SHE reduce the irreversibilities associated to the heat transfer in the stages of the column. This reduction is shown in **Figure 4-36e** and **Figure 4-36f**.

Because of the additional heat exchangers, the capital investment of a column with SHEs is increased. Therefore, the number of stages should be evaluated in terms of cost-benefit analysis. Once the number of cost effective is defined, the design problem consists in the determination of the stage or stages where indirect heat transfer is going to be made. This is a problem that can be solved by entropic optimization. For the extractive distillation of Ethanol-Water-Ethylene Glycol mixture, (Mendoza, 2011) has reported an optimal range of stages for the thermal integration that is located in stages near bottoms. Based on this results, a pilot plant column is described in the next chapter.

### 4.3 Conclusions

The literature review allowed to define the design variables of the non-conventional extractive dividing wall column studied in this thesis. The E-DWC is a particular case of the dividing wall distillation column but with significant changes. E-DWCs have two condensers and two feeds but only one reboiler. This changes the number of degrees of freedom for de design. In this chapter was concluded that the methodologies of the design applicable to conventional DWC are not pertinent for the E-DWC design.

E-DWC must have a stripping section in the extractive module of the column and low reflux ratios in order to connect the different section profiles.

The conceptual analysis made in this chapter allowed to identify that the quality of the lower feed of an E-DWC is an important variable for the feasibility of the separation. The quality of this feed can be increased in order to avoid loss of ethanol in mixture with water.

The energy required to bring the feed to the specified quality should be included in the total energy requirement. In cases where the E-DWC is in line with fractionation upstream

processes, the fractionation column should operate with a partial condenser and the distillate should be taken as vapor to feed the E-DWC.

A conceptual study of the indirect thermal integration was introduced. This allowed the comparison of an adiabatic column with a column with internal SHE or diabatic column. A reduction in energy consumption was observed. However, implementation of SHEs require of a total cost evaluation that will decide on its convenience.



## 5. Pilot plant non-conventional extractive distillation column

In this chapter, the pilot plant extractive distillation column using sequential heat exchangers (SHE column) is presented. The equipment of this plant is installed in the Chemical Engineering Laboratory building (Laboratorios de Ingeniería Química) of the Universidad Nacional de Colombia. The design, construction and start-up of the plant was sponsored by Colciencias in 2014 (convocatoria 700). The project was called “Non-conventional column to improve the energetic efficiency in distillation processes”. This project was presented as continuation of the results obtained in the doctoral thesis “Analysis and minimization of the entropy generated in an extractive distillation process for ethanol dehydration” written by Ph. D. Diego Mendoza (Mendoza, 2011).

In this document, an initial approach to the operation of a SHE column is given. The column is designed to be used as extractive column for the separation of ethanol-water mixtures using ethylene glycol as entrainer. The plant is still in construction and some issues detailed might change. In this chapter, the components of the column and its operation are detailed as stated in the first design.

### 5.1 Plant location

The plot plan of the Chemical Engineering Building (412) is shown in **Figure 5-1**. The dotted line limits the space that corresponds to the pilot plant. The location area of the SHE distillation column is shown in red. According with the most recent plans available in the pilot plant (López & Contreras, 2003), the red square is in the zones 15 and 16 of the key plan. Due to the constant renovation made in the pilot plant, the referenced plans are not actualized. Therefore, the direction of the laboratories is making a new sketch of the plant

plans. In this document, the reference to the existing plans (López & Contreras, 2003). is made.

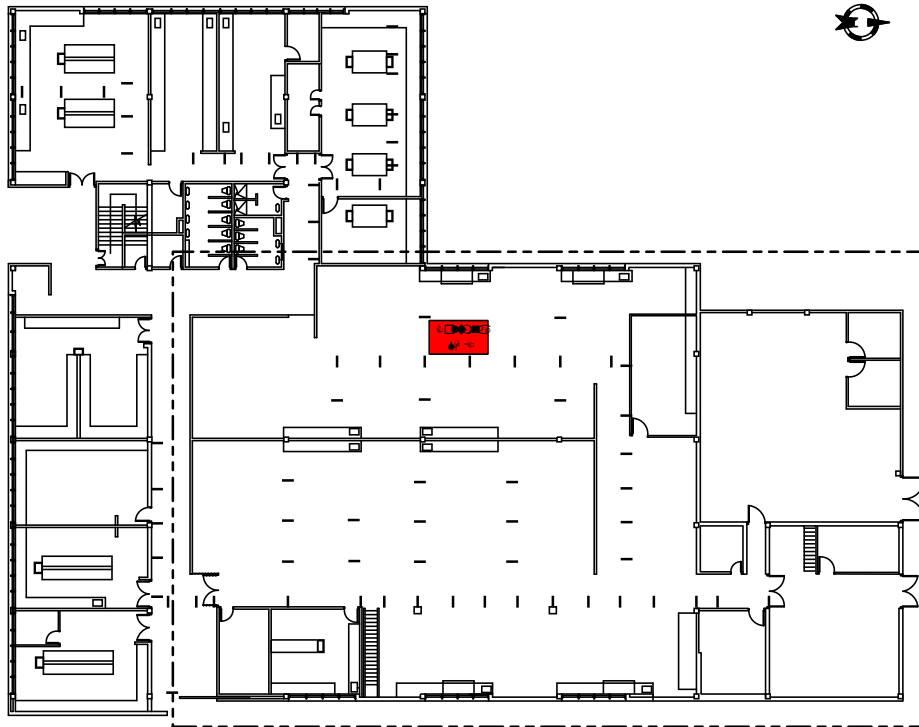


Figure 5-1: Plot plan of the Chemical Engineering Laboratory building 412

## 5.2 Basis of the design

### 5.2.1 Aim of the operation

The aim of the SHE extractive distillation system is to obtain ethanol with a composition above 99,5% v/v (resolution 0789 of 2016) or 99,7% v/v in the case of considering exportations to Europe (EN15376:2011). This means that the recovery of ethanol is higher than 99,8%. The feed stream has a flow of 20L/h with a composition near to the azeotrope ethanol-water at normal pressure. According with (Kiss & Ignat, 2013), an optimal value of the feed composition is 91.0 %wt. of ethanol (~80 %mole). The entrainer used is ethylene glycol with high purity (>99,9%). The expected flow of the distillate product is 18,5 L/h. The mass balance of the column with the given specifications is shown in **Table 5-1**. In this case, the recuperation of the 99,85% of ethanol was calculated with the regulation ASTM D4806, which states that the product concentration should be at least 99,7% v/v of ethanol. In the case of Colombia, lower concentrations (at least 99,5 % v/v) are accepted.

**Table 5-1:** Global mass balance of the extractive distillation separation system to obtain ethanol

Property	Units	Line			
		1	3	11	15
<b>Temperature</b>	°C	15	15	15	15
<b>Pressure</b>	kPa	74,66	74,66	74,66	74,66
	atm	0,736	0,736	0,736	0,736
<b>Total mass flow</b>	kg/h	22,5621	16,5147	15,0623	24,0145
Ethanol	kg/h	0,0000	15,0284	15,0047	0,0237
Water	kg/h	0,0066	1,4863	0,0576	1,4352
Ethylene glycol	kg/h	22,5555	0,0000	0,0000	22,5555
<b>Total mole flow</b>	kmol/h	0,3638	0,4087	0,3289	0,4436
Ethanol	kmol/h	0,0000	0,3262	0,3257	0,0005
Water	kmol/h	0,0004	0,0825	0,0032	0,0797
Ethylene glycol	kmol/h	0,3634	0,0000	0,0000	0,3634
<b>Total std. Vol. flow</b>	L/h	20	20	18,58	21,39
	L/min	0,33	0,33	0,310	0,357
Ethanol	L/h	0	18,98	18,95	0,03
Water	L/h	0,006	1,489	0,06	1,48
Ethylene glycol	L/h	20	0	0	20,32

Due to the column design seeks to apply an energy integration with heat exchanger, the operation of the column should allow the estimation of the energy consumption used in the separation. In the same way, it should allow the evaluation of the use of a feasible solvent to feed ratio under the specified operation conditions.

## 5.3 Process variables

### 5.3.1 Pressure

The operation pressure of an extractive distillation column is defined in the initial stages of the conceptual design of the column. This pressure has an influence on the basic design as well as on the detailed design. In the case of the SHE column, the pressure is 560 mmHg (0,74 atm 74,6 kPa), which corresponds to the atmospheric pressure in Bogotá. The pressure should not be initially considered an operation variable. However, the distillation columns might have unstable behavior and it is important to check the pressure drop between the extremes of the column to avoid hydraulic problems such as flooding.

### 5.3.2 Entrainer

The SHE distillation column was designed to operate with ethylene glycol as separation agent or entrainer. For the efficient use of this solvent, it is necessary to guarantee that its water content is less than 0.1% mole. Otherwise, the water entering to the column could evaporate and reduce the quality of the distillate product rich in ethanol.

On the other hand, (Meirelles et al., 1991) state that the operation temperature of an extractive distillation system using ethylene glycol should not be higher than 160°C. At higher temperatures the solvent degradation is very fast and would have a negative economic impact.

### 5.3.3 Heating utility

The heating utility used in the extractive distillation plant is steam generated in the boiler of the Chemical Engineering Plant. The boiler produces steam that reaches to the SHE equipment with a pressure between 75 to 100 psi. However, the jacket in the reboiler of the distillation column should operate at a lower pressure. This is controlled with the valve of the vapor inlet.

At the design pressure, the temperature of the liquid in the reboiler is calculated in 140°C. Heuristically, a temperature difference of at least 10°C is required. This means that the vapor pressure should be at least 150°C. According to the steam tables, the steam in the reboiler jacket should be at 69 psia (59 psig, manometric pressure). The steam should not be 5 psi above this pressure to avoid the solvent evaporation. In the case of the preheaters, the steam pressure should be below 15 psig, and should be controlled according to the temperature measurement in each line of inlet to the column.

Once the latent heat of the steam is transferred to the heat exchangers, the collected condensate volume should be measured to estimate the mass flow of steam used in the operation. This estimation is important to perform the energy balances on the system.

## 5.3.4 Temperature

### 5.3.4.1 Feed preheating

The ethanol-water mixture with composition near to the azeotrope (0,80 %mol of water) is heated in the equipment HE-4002 before entering to the column. This heating is made until a temperature near to the feed stage temperature according with the temperature column profile in stable state. If the feed enters to the column at a lower temperature, the energy in the reboiler should increase to overcome this effect. If the feed enters to the column at a temperature above the saturation temperature, the purity of the product is affected through the flash evaporation of the water when entering to the column.

### 5.3.4.2 Solvent preheating

The entrainer is heated in the equipment HE-4001 before entering to the SHE column. The temperature of the solvent should not exceed 100°C because it is feed in a stage of low temperature according with the temperature column profile. If this temperature is higher, an evaporation of the liquid in the feed stage would decrease que quality of the distillate product. If the temperature is lower, the energy requirement in the reboiler increases, and if the temperature is very low and the additional energy it is not properly supplied, the flooding of the column might happen. The recommended distillate temperature is round 71°C. If the column has a lower distillate temperature, it is possible that flooding has happened or that the steam flow in the reboiler is not enough to achieve the separation. If the distillate temperature is high, it can be reduced by changing the reflux ratio.

### 5.3.4.3 Reflux ratio

The liquid that enters to the column as reflux has been obtained as saturated liquid, and in some cases as subcooled liquid. Although the conditions of the distillate temperature are low considering the temperature column profile, its temperature might be higher than the reflux temperature. With the aim to promote the stability of the column and to avoid losing the obtained profile, it is necessary to enter the reflux at a temperature near to temperature in the first stage inside the column. For this reason, an equipment to preheat the reflux was added, HE-4006.

### 5.3.4.4 Distillate and bottoms flow

For security reasons, it is not convenient allow the distillate and bottoms of the column to be at temperatures higher than the ambient temperature. Therefore, the products are subcooled until 20°C before its storage in the product vessels TK-4003 and TK-4005.

## 5.4 Process flow diagram and description

The separation system consists in a double-feed continuous distillation column with sequential heat exchangers working at atmospheric pressure of Bogotá, see **Figure 5-2**

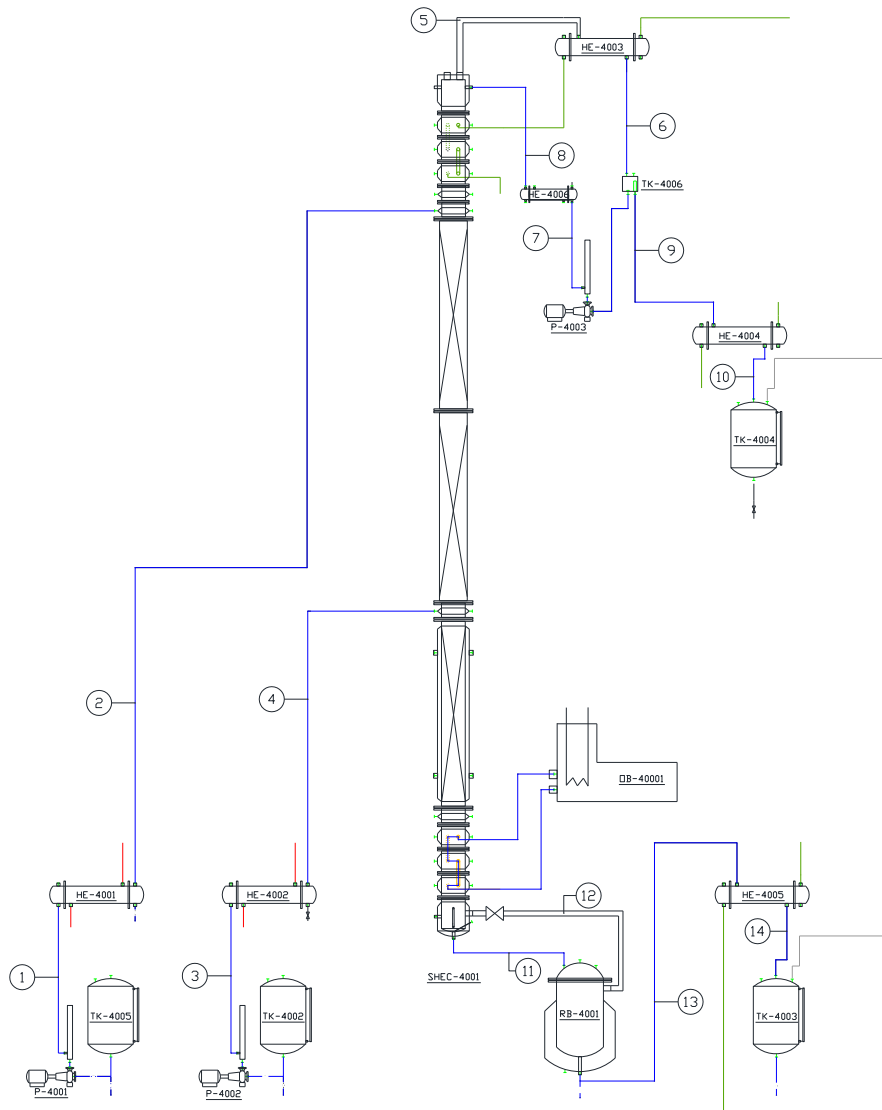


**Figure 5-2:** Process Flow Diagram showing the line numbering.

The chemical system to be separated is a binary mixture of ethanol and water, generally with a composition higher than 80 %mol of ethanol. This mixture is initially stored in the storage tank TK-4003. The feed is pumped by a piston pump P-4102 to the preheater HE-4002, in which is heated to a temperature near to the boiling point of the most volatile component in the mixture. Then, the mixture flows through the line 4 to the distillation column, in which an evaporation occurs. The two components of the feed are separated with help of the solvent that flows down inside the column. The feed is done in a middle stage of the column, as shown in the **Figure 5-2**.

The less volatile component of the mixture, the one with the highest boiling point, is collected as liquid in the column bottom. A part of this liquid is addressed to the reboiler HB-4001 and guided back to the column through the line 13. The circulation of the bottom liquid through the reboiler heats the liquid and produces a vapor phase. The vapor provides heat to the liquid in the bottom stages, so that the less volatile component is evaporated. Finally, the bottom product, which has reached the required specifications, is taken out of the system through the line 14. Due to the operation at vacuum, this product can be addressed to the storage tank of the bottom product TK-4003, after passing through a cooling operation in the heat exchanger HE-4005.

Simultaneously, the most volatile component of the feed mixture goes up to the top of the column in a vapor form. Then, it is led to the condenser HE-4003, in which it is cooled until a change of phase occurs. The condensed is sent to the tank TK-4005, where it is accumulated. A part of the liquid condensate, known as reflux, is recirculated to the top of the column through the pump P-4003 in the line 7. Once the condensate accumulated in the tank TK-4005 reaches the product specifications, it is taken out of the system through the line 10 and storage in the tank TK-4004 after being cooled in the heat exchanger HE-4004.

As explained in previous chapters, the operation of the column has a thermodynamic limitation called azeotropy. This limitation involves that the distillate product can't have a composition higher than the azeotropic composition, which for the case of ethanol-water is 90,3% at the atmospheric pressure of Bogotá. To overcome this limitation requires a more complex arrangement than the so far described. Some possibilities are the extractive distillation, the azeotropic distillation, and adsorption, among others.

In extractive distillation, the thermodynamic limitation is overcome through the addition of a mass separation agent in stages above the feed stage. For the ethanol-water mixture, the entrainer used is ethylene glycol, which is a liquid with a boiling point higher than that of the components in the mixture and does not form azeotropes with any of them.

The ethylene glycol is initially stored in the tank TK-4001. Then, the pump P-4001 takes it to the preheater HE-4001, in which it is heated until a temperature near 80°C. Once preheated, the entrainer flows through the line 2 to a stage near to the top of the column in which is fed. Due to its high boiling point, the solvent follows a down flow along the column until it is accumulated in the bottom of the column and in the reboiler. On its way, the ethylene glycol drags the water contained in the vapor mixture ascending along the column. The drag of water allows the concentration of the vapor rich in ethanol overcoming the thermodynamic limitation of the separation. Once the distillation specifications have been reached, the water is taken out of the mixture with the ethylene glycol in the bottoms product in the line 14.

## 5.5 Equipment

### 5.5.1 Storage tanks

The pilot plant of the separation system has four storage tanks for the feed, solvent, distillate product and bottom products. All the tanks have the following specifications: cylindrical vessels with a useful capacity of 20L each, 285 mm diameter, 370 mm height, built with a stainless steel, 316 schedule 12 (2.5 mm), spherical top with three unions of ½ NPT, and spherical bottom with one union of ½ NPT, cylinder with two unions of ½ NPT adapted for a level viewer and two brackets for the anchorage in stainless steel, schedule 12

Given the dimensions of the storage tanks and the feed and product flows, each tank has a storage capacity enough for one hour of continuous operation. The tanks have charging discharging valves to allow extending the operation time when necessary. The level control of the tanks should be done manually through the level viewer disposed in the body of the equipment, see **Figure 5-3**.



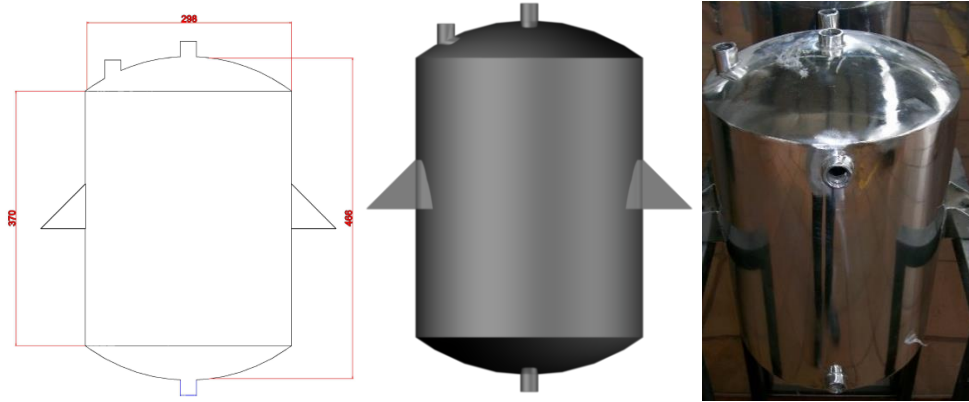


**Figure 5-3:** Storage tanks.

### 5.5.2 Preheaters

The preheater equipment are the preheater of the solvent HE-4001, the preheater of the feed HE-4002 and the preheater of the solvent HE-4006. The characteristics of these preheaters are: shell and tube heat exchangers with a shell of 4" diameter made of stainless steel, 304 schedule 10, and the tubes length is 400 mm, see **Figure 5-4**. In the extremes of the heat exchanger, it has two heads made of stainless steel schedule 10, 4" of diameter, 80 mm length, with two unions of  $\frac{1}{2}$  NPT each. The body of the heat exchanger has two unions of  $\frac{1}{2}$  NPT, coupling heads-heat exchanger through 9 mm thickness flanges and  $\frac{3}{8}$ " crews made of stainless steel.

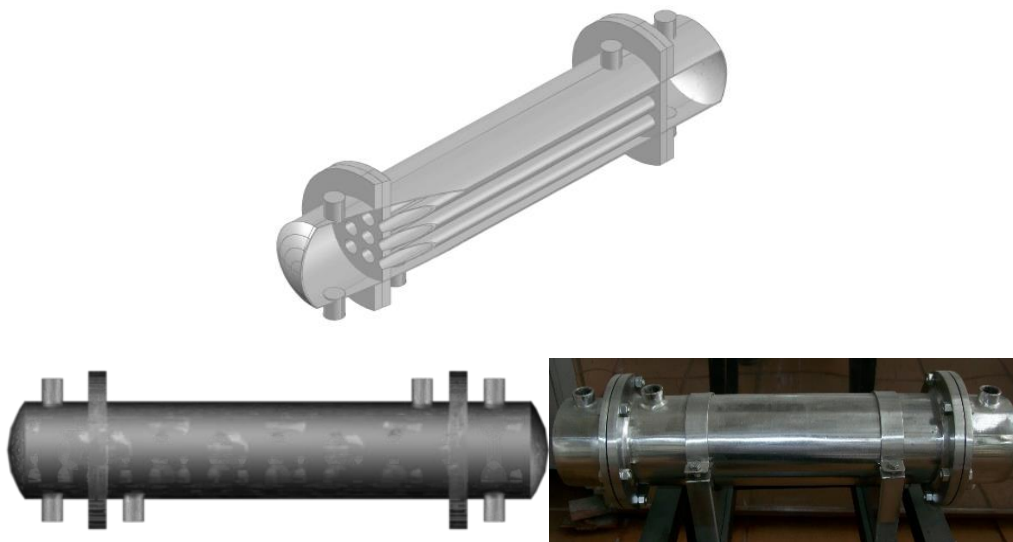


**Figure 5-4:** Preheaters.

### 5.5.3 Reboiler

The reboiler used in this plant is a jacketed reactor with useful capacity of approximate 20L and a heat transfer area to the jacket of 0,35 m<sup>2</sup>, see **Figure 5-5**. The jacket has temperature and pressure indicators. The reboiler has a 3" tube connected to the columns bottom, which drives the reflux vapor back to the column. In the top of the reboiler, there is a ½" pipeline used to canalize the bottom liquid from the column to the reboiler. In the bottom of the reboiler, there is a ½ pipeline used to canalize the bottom product from the reboiler to the storage tank. The jacket has a discharging tube for the condensed steam produced on it.

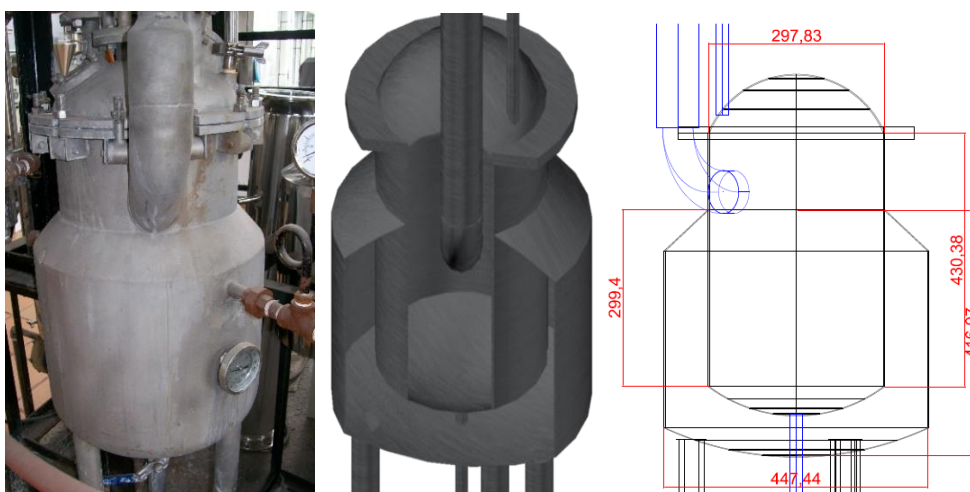


**Figure 5-5:** Reboiler of the SHE column.

### 5.5.4 Condenser

The product condenser is a heat exchanger with the following characteristics: stainless steel cylindrical shell, 304 schedule 10, nine stainless steel tubes, 304 schedule 10, with 1/2" diameter and 1000 mm length, two heads of stainless steel tube schedule 10, 4" diameter, 80 mm length with two unions of ½ NPT each, see **Figure 5-6**. The heat exchanger has three unions of ½ NPT, coupling heads-heat exchanger through 9 mm thickness flanges and 3/8" crews made of stainless steel.



**Figure 5-6:** Condenser of the SHE column.

### 5.5.5 Coolers

The plant has two coolers, one for the distillate product HE-4004 and the other for the bottom product HE-4005. The characteristics of these coolers are: shell and tube heat exchangers with a shell of 4" diameter made of stainless steel, 304 schedule 10, see **Figure 5-4**. Each heat exchanger has nine stainless steel tubes, 304 schedule 10, with ½" diameter and 400 mm length. In the extremes of the heat exchanger, it has two heads made of stainless steel, schedule 10, 4" of diameter, 80 mm length, with two unions of ½ NPT each. The body of the heat exchanger has two unions of ½ NPT, coupling heads-heat exchanger through 9 mm thickness flanges and 3/8" crews made of stainless steel.

### 5.5.6 Pumps

The plant has four dosing piston pumps of the serial PS1D025 of the Italian company SEKO S.P.A. These pumps are alternate volumetric pumps with the license plate shown in **Figure 5-7**.



**Figure 5-7:** License plate of the pumps.

The specifications of the code shown in the plate are summarized in **Table 5-2**.

**Table 5-2:** Specifications of the pumps

P	Model	Plunger Piston
S1	Type of mechanism	Piston
D	Displacement length	15 mm
025	Piston diameter	25 mm
A	Displacement index	58 displacement/min
21	Pump head materials	Pump head SS316 Piston: SS316 Piston seal: FPM Valves: SS316 Equipment: Standard

A4	Type of electric motor	0,18 kW (4 poles - 230/400 Vac - 50/60 Hz – three phase)
0	Displacement controller	Manual
0	Adaptations	Standard
0	Options	Standard

The flow rate of the pumps is 25 L/h and works at a maximal pressure of 20 bar. The connections to the charging and discharging pipelines are of 3/8". The main components of the pumps are shown in **Figure 5-8**.



**Figure 5-8:** Pump components.

It is recommended to watch the following video to become familiar with the dosing piston pumps used in the plant: <https://www.youtube.com/watch?v=vOHoLjafoW0>

The discharging pipeline of the pumps has a damper equipment that allows the stabilization of the flow through the formation of a liquid column. This equipment is shown in **Figure 5-9**. At the top part of this damper, there is a thread of 1/4" to introduce a manometer to measure the discharge pressure of the pump.

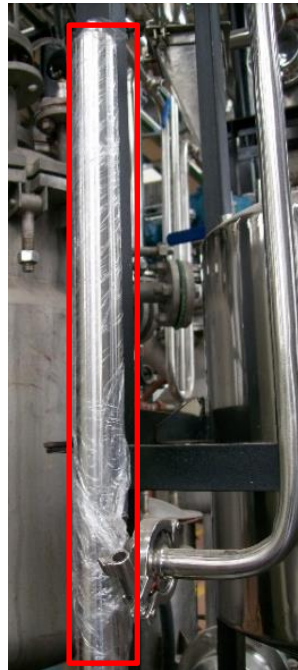


**Figure 5-9:** Damper equipment of pumps.

### 5.5.7 Control valves

The plant has three control valves for the vapor of the brand BELIMO LRB24-SR. These valves have a CV of 0,29 and can be used at a maximal temperature of 180°C. They are equal percentage valves of ½ NPT pipeline with a pneumatic actuator as shown in **Figure 5-10**.



**Figure 5-10:** Control valves for the vapor.

In addition, the plant has two control valves of ¼ NPT for the water. The valves are proportional and have an electric actuator. The reference of the valves is B211+TR24-3 of the brand BELIMO, as shown in **Figure 5-11**.

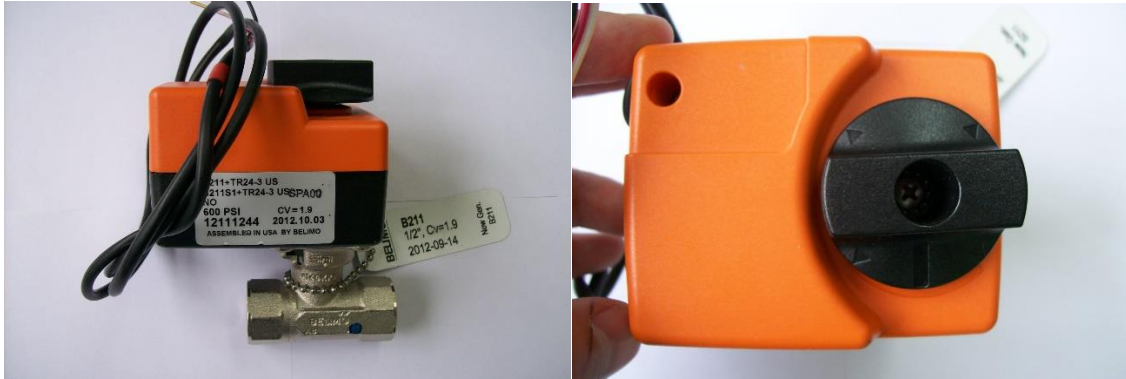


Figure 5-11: Control valves for the water.

### 5.5.8 Flow transmitter

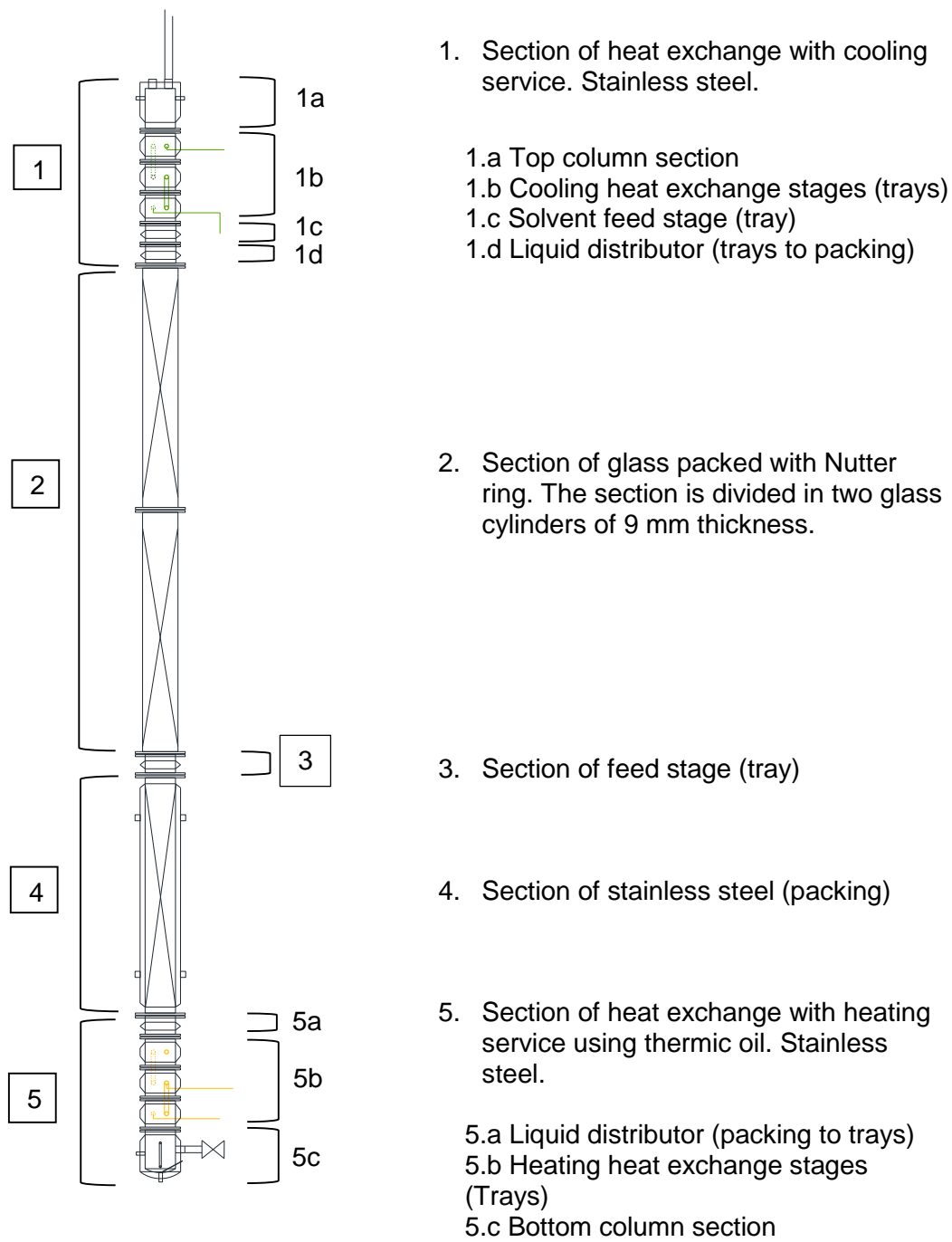
The plant has three transmitters with a  $\frac{1}{4}$ " connection to the process to measure the flow of the feeds. The maximal temperature that these transmitters can handle is  $80^{\circ}\text{C}$ , and the flow range is between 10 and 20L/h. A sample of the transmitters is shown in **Figure 5-12**.



Figure 5-12: Feed flow transmitter.

## 5.6 SHE Column

The sequential heat exchanger column scheme is shown in **Figure 5-13**. The description of each column part is given below.




**Figure 5-13:** Column with sequential heat exchangers SHEC-4001




## 5.6.1 Section of heat exchange with cooling service

The top section of the extractive SHE column has four subsections made of stainless steel 316. Each section is following described.

### 5.6.1.1 Top column section


	<p>The top part of the head of the column has 150 mm height and is made of stainless steel 316 of 6". The cylinder is covered by glass wool of 25 mm thickness. The cylinder has two unions of ½ NPT and the top has two ferules of 1-1/2 for the clamp. The head of the column is assembled to the body of the column through a screwed flange of 204 mm.</p>
-----------------------------------------------------------------------------------	----------------------------------------------------------------------------------------------------------------------------------------------------------------------------------------------------------------------------------------------------------------------------------------------------------------------------------------------------------------

### 5.6.1.2 Section of cooling heat exchange stages


	<p>This section has three modules made of stainless steel 316 with 152 mm (6") diameter, and height between 150 and 200 mm. Each module has a tubing serpentine of ¼ set in an equilibrium tray perforated with a square configuration. The tray has a down comer weir made of stainless Steel 316 with 1,5 mm thickness.</p> <p>The extremes of each module have stainless steel flanges of 205 mm diameter and 9 mm thickness.</p> <p>In each module, there is a place to take a sample of the vapor and liquid in the tubing of ¼.</p> <p>The modules are isolated with glass wool of 25 mm thickness and stainless-steel schedule 18 cover.</p>
-------------------------------------------------------------------------------------	-----------------------------------------------------------------------------------------------------------------------------------------------------------------------------------------------------------------------------------------------------------------------------------------------------------------------------------------------------------------------------------------------------------------------------------------------------------------------------------------------------------------------------------------------------------------------------------------------------------------------------------------------------



### 5.6.1.3 Solvent feed stage

	<p>The solvent feed tray has a cylinder made of stainless steel 316 and with a diameter of 152 mm (6") approximately.</p> <p>The module has flanges on its extremes used for the join with the other parts of the column. The flanges have a diameter of 205 mm approximately and 900 mm of thickness</p> <p>The section has two feed inlets made in tube of 1/4 NPT with ferule for a flange.</p>
-----------------------------------------------------------------------------------	----------------------------------------------------------------------------------------------------------------------------------------------------------------------------------------------------------------------------------------------------------------------------------------------------------------------------------------------------------------------------------------------------

### 5.6.1.4 Liquid distributor (trays to packing)

	<p>The section has a flange in the top part with a diameter of 205 mm approximately. In the bottom part has a 250 mm diameter flange for the join to the glass section.</p> <p>The section has a layette; which position can be adjusted on the superior flange. The base of the layette has tubes of 1/8" led to the inferior part and tubes of 1/4" led to the superior part. These tubes allow the flow of liquid and vapor through the tray, respectively.</p>
------------------------------------------------------------------------------------	--------------------------------------------------------------------------------------------------------------------------------------------------------------------------------------------------------------------------------------------------------------------------------------------------------------------------------------------------------------------------------------------------------------------------------------------------------------------

### 5.6.2 Section of glass (packing)



The SHE column has two glass sections with a thickness of 10 mm approximately. Each glass section has an internal diameter of approximately 157,4 mm and a height of 1220 mm. The extremes of each tube have flanges of 197,4 mm diameter and 10 mm thickness.

The glass sections are coupled through metallic flanges of a larger diameter, which are kept fastened to the tray through a blue plastic packing.



### 5.6.3 Section of feed stage



The main feed has a cylinder made of stainless steel 316 and a diameter of 152 mm (6"), approximately.

The module has flanges on its extremes, which are used to join it to the other parts of the column. The flanges have 205 mm of diameter, approximately, and 9 mm of thickness.

The section has two feed inlets made with tube of  $\frac{1}{4}$  NPT with ferule for flange.


### 5.6.4 Section of stainless steel (packing)

	<p>The SHE column has a stainless steel 316 column with 6" of diameter and 1000 mm of length. On its extremes the metallic column has stainless Steel flanges with 205 mm diameter and 9 mm thickness. The column has six unions of ½ NPT in the lateral side, three in each extreme. In addition, the column is isolated with glass wool with 25 mm of thickness inside a jacket made of stainless steel schedule 18.</p>
--	----------------------------------------------------------------------------------------------------------------------------------------------------------------------------------------------------------------------------------------------------------------------------------------------------------------------------------------------------------------------------------------------------------------------------

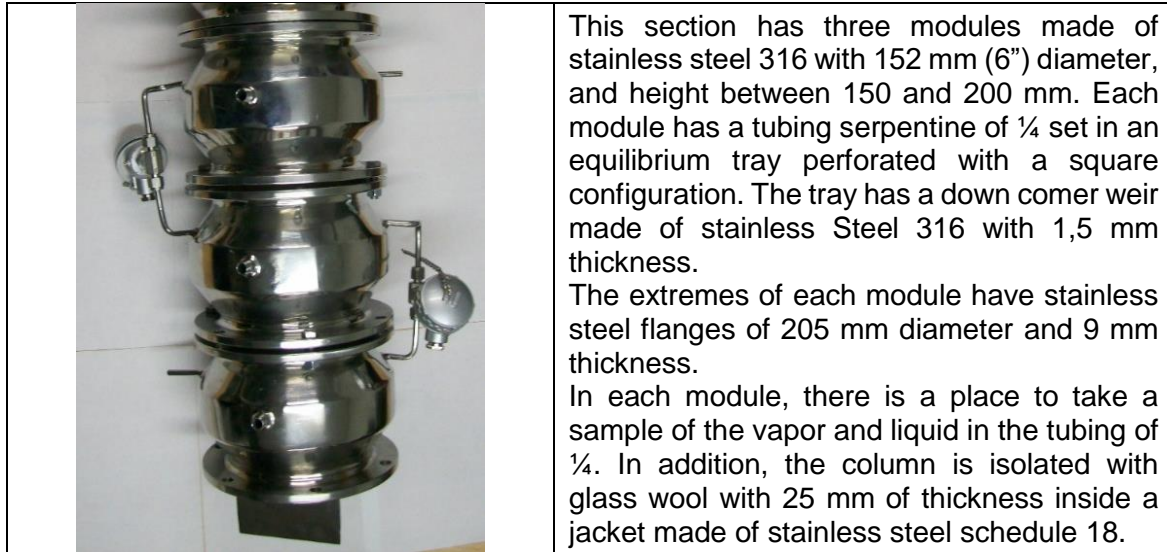
### 5.6.5 Section of heat exchange with heating service

In the bottom of the SHE extractive column, there are three heat exchange stages connected to a thermal oil bath. The liquid coming from the packed part of the column should be redistributed through a distributor that leads it to a down comer weir connected to the first heat exchange stage. This helps to control the liquid flow in the heat exchange stage. The parts of the bottoms heat exchange section are following described.

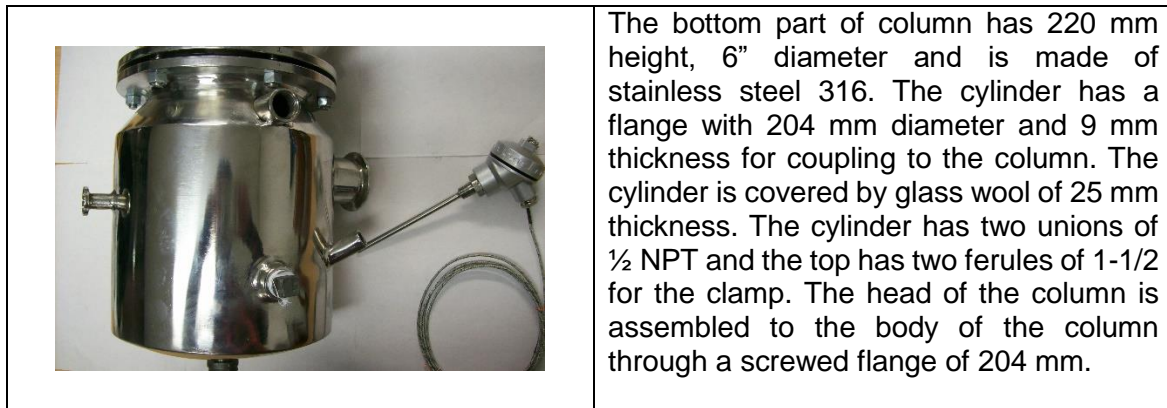
#### 5.6.5.1 Liquid distributor (packing to trays)

	<p>The liquid distributor packing to trays has the same specifications of the liquid distributor trays to packing. However, in this case, there is a down comer weir in the layette, which leads the liquid coming from the top part of the column to the subsequent heat exchange stages.</p>
-------------------------------------------------------------------------------------	------------------------------------------------------------------------------------------------------------------------------------------------------------------------------------------------------------------------------------------------------------------------------------------------

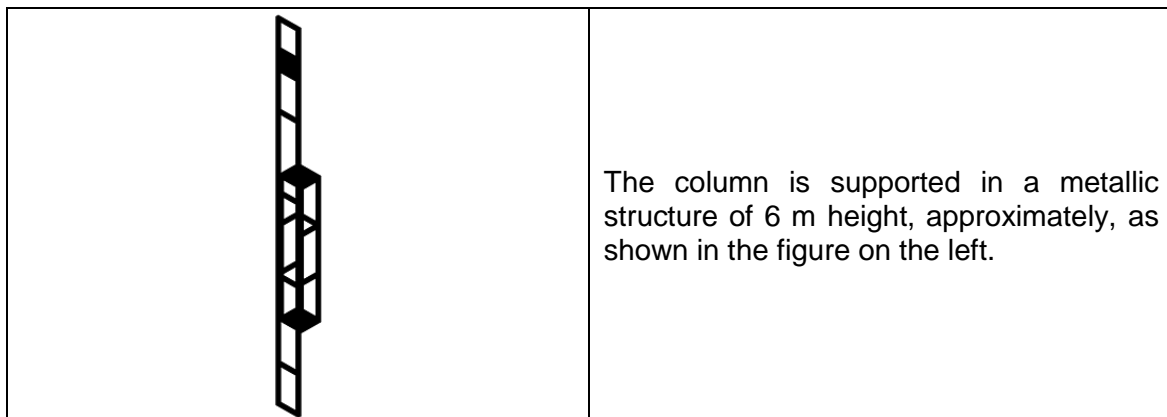
### 5.6.5.2 Section with heating heat exchange stages



### 5.6.5.3 Bottom column section



### 5.6.6 Column support



## 5.7 Auxiliary services

### 5.7.1 Cooling water

The cooling water is provided by the hydropneumatic water distribution DTI-LIQ-0201(López & Contreras, 2003), see **Figure 5-14**.

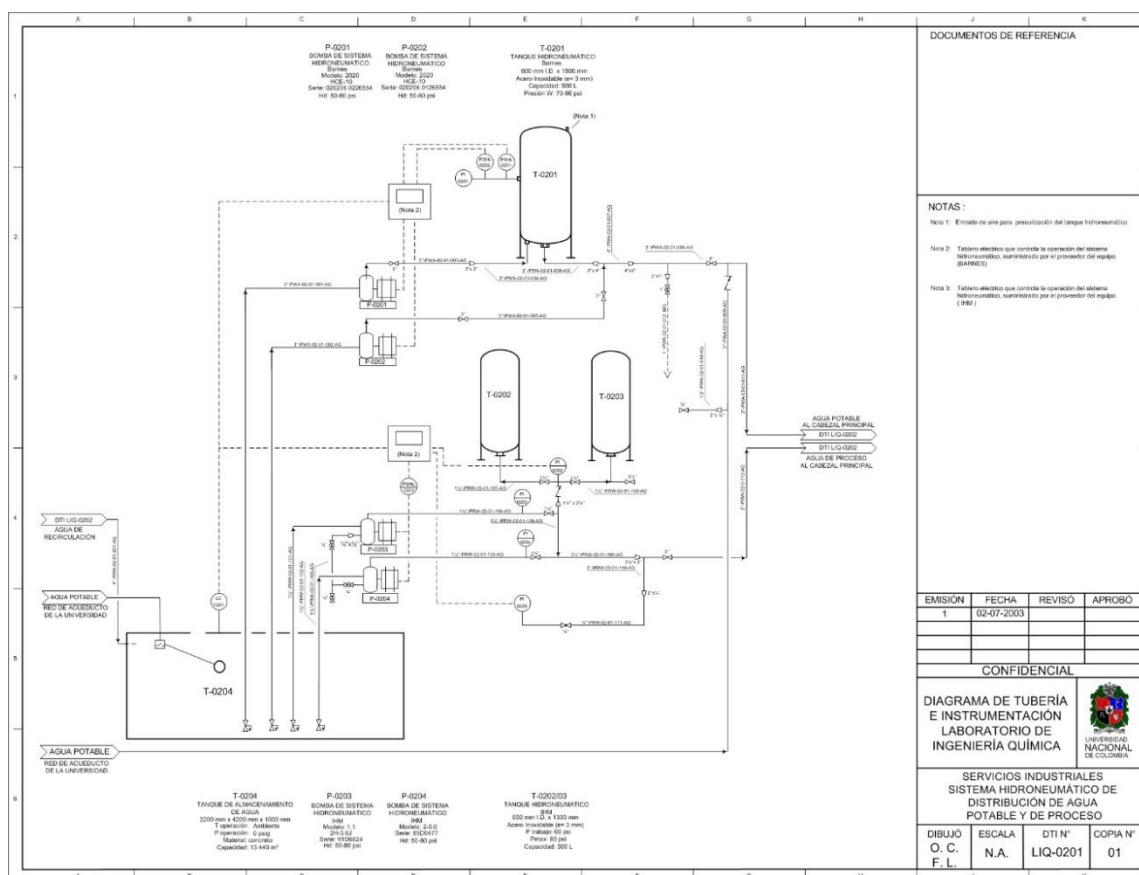


**Figure 5-14:** System of water supply of the pilot plant of the chemical engineering department UNAL. Taken from (López & Contreras, 2003).

The water line is distributed over the plant with a green pipeline. The water is used in the SHE extractive distillation plant as cooling service. The equipment using this service are the distillate product cooler HE-4004, the bottom product cooler HE-4005 and the column condenser HE-4003. The temperature of the cooling water is the ambient temperature of the Universidad Nacional de Colombia in Bogotá, which is in average 14°C, see **Figure 5-15**.



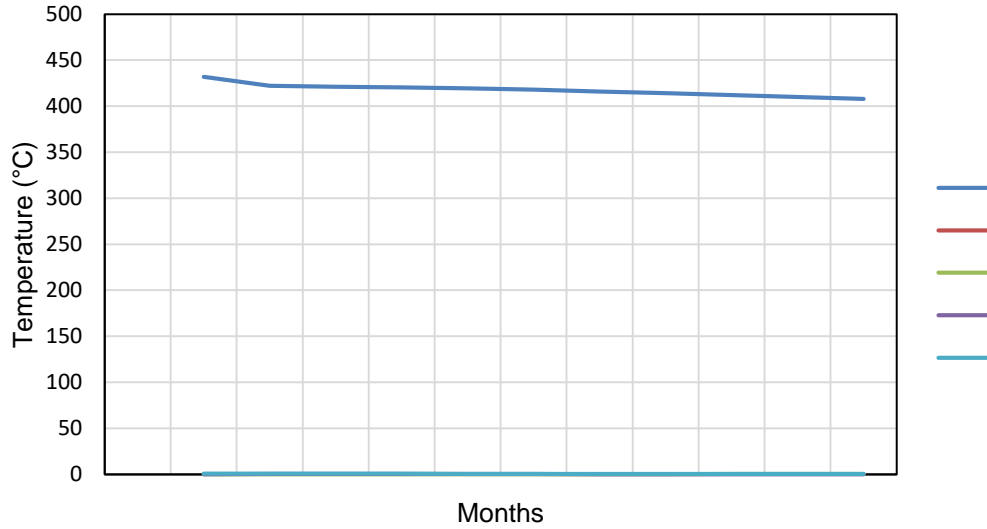


**Figure 5-15:** Ambient temperature in Bogotá. Adapted from (IDEAM, 2013)

### 5.7.2 Steam

The steam generation system of the chemical engineering plant has a boiler of the brand Tecknic serial No. 809 – M1493. It is a horizontal pirotubular boiler (gases through the tubes and water through the shell) with 50 B.H.P (Boiler Horse Power) capacity, which can operate with ACPM or gas. The boiler has a tank for condensate with moto pump for water injection. A photo of the boiler is given in **Figure 5-16** and the specifications of the boiler are presented in **Table 5-3**.



**Figure 5-16:** Boiler for steam generation in the pilot plant of the chemical engineering department UNAL.

**Table 5-3: Boiler specifications**

Capacity	50 B.H.P -1.673.000 BTU/h
Fuel	Dual (ACPM and/or Natural gas)
Working pressure	0 a 125 psi
Design pressure	150 psi
ACPM consumption	15 gallons/h
Natural gas consumption	54 m <sup>3</sup> /h of Hi:38.500 BTU/m <sup>3</sup>
Propane gas consumption	96 lb/h of Hi: 21.500 BTU/lb
Steam production	1.725 lb/h at 212 °F
Combustion burner	Forced shod according to norm UL& FM
Net weight	2750 kg
Weight with water to level	4350 kg
Type	Pirotubular, horizontal 2 steps
Transfer area	260 ft <sup>2</sup>
Body dimensions	135 cm diameter x 270 cm length
Base dimensions	220 cm length x 120 cm width
General dimensions	350 cm length x 175 cm width x 200 cm height
Electrical system	110 - 220 - 440 Volt
Operation	Automatic
Security control	Protection high low water level
	Protection maximal control of steam pressure
	Protection control of lame security
Additional equipment	Condensate tank with 60 gallons of capacity
	Moto pump for water feeding of 10 gal/min

The produced steam arrives the SHE extractive distillation plant through the pipeline 1"-VAP-03-02-434-AG-PE shown in the diagram DTI-0302 of the air and steam net in (López & Contreras, 2003). The vapor arrives at a pressure that oscillates between 75 and 100 psig, and it is used in the preheater of the solvent HE-4001, in the preheater of the feed HE-4002, in the preheater of the reflux HE-4006 and in the reboiler RB-4001. With the aim to take the maximal advantage of the heat of the steam, the pipeline following the heat exchangers have steam tramps, which hold the steam back and allow the flow of the condensate only.

### 5.7.3 Thermal oil

The SHE plant requires thermal oil for the runs with sequential heat exchangers in the column. Through these heat exchangers flows the thermal oil that can vary depending on the availability in plant. In the current arrangement the thermal oil used is a Chevron heat transfer oil grade 46, with the specifications shown in **Table 5-4**. The thermal oil is heater in a thermal bath as the one shown in **Figure 5-17**.

**Table 5-4:** Thermal oil specifications.

Grade	22	46
Product number	231706	231709
Number SDS/MSDS		
USA	4610MEX	37648
Colombia	33472	33472
El salvador	33473	33473
Gravity API	33,8	32,0
Kinematic viscosity		
cSt at 40°C	23,1	41,1
cSt at 100°C	4,47	6,32
Saybolt viscosity		
SUS a 100°F	120	212
SUS a 210°F	41,3	47,4
Viscosity index	104	101
Ignition point °C(°F)	210(410)	240(464)
Flash point, °C(°F)	229(444)	271(520)
Autoflash point °C(°F) ASTM E659	345(653)	359(678)
Runoff point, °C(°F)	-13(+9)	-15(+5)
Carbon residue Rasbottom re, wt%	0,04	0,04



**Figure 5-17:** Thermal bath with a maximal temperature of 170°C, flow of 15 L/min and pumping pressure of 0,35 bar.



## 5.8 Characteristics of the valves and valve diagram

Table 5-5: Ball valves

#	Tag	Size	Spec	Description	Line	#	Tag	Size	Spec	Description	Line #
1	HA-107	15	100HS01	BALL VALVE	1	31	HA-1003	15	100HS01	BALL VALVE	10
2	HA-102	15	100HS01	BALL VALVE	1	32	HA-1101	15	100HC01	BALL VALVE	11
3	HA-103	15	100HS01	BALL VALVE	1	33	HA-1202	8	100HS01	BALL VALVE	12
4	HA-104	15	100HS01	BALL VALVE	1	34	HA-1201	15	100HS01	BALL VALVE	12
5	HA-105	15	100HC01	BALL VALVE	1	35	HA-1401	15	100HS01	BALL VALVE	14
6	HA-106	15	100HS01	BALL VALVE	1	36	HA-1402	15	100HS01	BALL VALVE	14
7	HA-101	15	100HC01	BALL VALVE	1	37	HA-1501	15	100HC01	BALL VALVE	15
8	HA-201	15	100HC01	BALL VALVE	2	38	LS-008	8	100HS01	BALL VALVE	LS
9	HA-203	8	100HS01	BALL VALVE	2	39	LS-006	8	100HS01	BALL VALVE	LS
10	HA-202	8	100HS01	BALL VALVE	2	40	LS-007	8	100HS01	BALL VALVE	LS
11	HA-303	15	100HS01	BALL VALVE	3	41	LS-005	8	100HS01	BALL VALVE	LS
12	HA-304	15	100HS01	BALL VALVE	3	42	LS-003	8	100HS01	BALL VALVE	LS
13	HA-305	15	100HC01	BALL VALVE	3	43	LS-004	8	100HS01	BALL VALVE	LS
14	HA-306	15	100HS01	BALL VALVE	3	44	LS-002	8	100HS01	BALL VALVE	LS
15	HA-301	15	100HC01	BALL VALVE	3	45	LS-001	8	100HS01	BALL VALVE	LS
16	HA-302	15	100HC01	BALL VALVE	3	46	VS-007	8	100HS01	BALL VALVE	VS
17	HA-307	15	100HS01	BALL VALVE	3	47	VS-005	8	100HS01	BALL VALVE	VS
18	HA-402	8	100HS01	BALL VALVE	4	48	VS-008	8	100HS01	BALL VALVE	VS
19	HA-401	15	100HS01	BALL VALVE	4	49	VS-006	8	100HS01	BALL VALVE	VS
20	HA-403	8	100HS01	BALL VALVE	4	50	VS-004	8	100HS01	BALL VALVE	VS
21	HA-601	15	100HC01	BALL VALVE	6	51	VS-002	8	100HS01	BALL VALVE	VS
22	HA-602	15	100HC01	BALL VALVE	6	52	VS-003	8	100HS01	BALL VALVE	VS
23	HA-701	15	100HS01	BALL VALVE	7	53	VS-001	8	100HS01	BALL VALVE	VS
24	HA-702	15	100HC01	BALL VALVE	7	54	HA-W02	15	100HC01	BALL VALVE	W
25	HA-803	15	100HC01	BALL VALVE	8	55	HA-W03	15	100HC01	BALL VALVE	W
26	HA-801	15	100HC01	BALL VALVE	8	56	HA-W05	15	100HC01	BALL VALVE	W
27	HA-802	15	100H01	BALL VALVE	8	57	HA-W06	15	100HC01	BALL VALVE	W
28	HA-804	15	100HS01	BALL VALVE	8	58	HA-W04	15	100HC01	BALL VALVE	W
29	HA-1001	15	100HS01	BALL VALVE	10	59	HA-W08	15	100HC01	BALL VALVE	W
30	HA-1002	15	100HC01	BALL VALVE	10	60	HA-W09	15	100HC01	BALL VALVE	W
31	HA-1003	15	100HS01	BALL VALVE	10	61	HA-W07	15	100HC01	BALL VALVE	W
32	HA-1101	15	100HC01	BALL VALVE	11	62	HA-W11	15	100HC01	BALL VALVE	W
33	HA-1202	8	100HS01	BALL VALVE	12	63	HA-W10	15	100HC01	BALL VALVE	W
34	HA-1201	15	100HS01	BALL VALVE	12	64	HA-W12	15	100HC01	BALL VALVE	W
35	HA-1401	15	100HS01	BALL VALVE	14	65	HA-W13?	15	100HC01	BALL VALVE	W
36	HA-1402	15	100HS01	BALL VALVE	14	66	HA-W15	15	100HS01	BALL VALVE	W
37	HA-1501	15	100HC01	BALL VALVE	15	67	HA-W14	15	100HS01	BALL VALVE	W

#	Tag	Size	Spec	Description	Line	#	Tag	Size	Spec	Description	Line #
38	LS-008	8	100HS01	BALL VALVE	LS	68	HA-W01	15	100HS01	BALL VALVE	W
39	LS-006	8	100HS01	BALL VALVE	LS	69	HA-X02	15	100HC01	BALL VALVE	X
40	LS-007	8	100HS01	BALL VALVE	LS	70	HA-X01	15	100HC01	BALL VALVE	X
41	LS-005	8	100HS01	BALL VALVE	LS	71	HA-X03	15	100HC01	BALL VALVE	X

The globe valves of the plant are used mainly for the control of the vapor lines.

**Table 5-6:** Globe valves.

Tag	Size	Spec	Description
HA-V01	25	100HC01	GLOBE VALVE
HA-V02	25	100HC01	GLOBE VALVE
HA-V03	25	100HC01	GLOBE VALVE
HA-V04	25	100HC01	GLOBE VALVE
HA-V05	25	100HC01	GLOBE VALVE
HA-V06	25	100HC01	GLOBE VALVE
HA-V07	25	100HC01	GLOBE VALVE
HA-V08	25	100HC01	GLOBE VALVE
HA-V09	25	100HC01	GLOBE VALVE
HA-V10	25	100HC01	GLOBE VALVE
HA-V11	25	100HC01	GLOBE VALVE
HA-V12	25	100HC01	GLOBE VALVE
HA-V14	25	100HC01	GLOBE VALVE
HA-V15	25	100HC01	GLOBE VALVE
HA-V16	25	100HC01	GLOBE VALVE

## 5.9 Checking prior to the operation

### 5.9.1 Steps of the preliminary checking

**Table 5-7:** Check list prior to the operation

Activity	Check
Preparation of materials	
Check that the pumps and other equipment that use electricity are correctly installed and working.	
Check that there are no leaks on each of the lines of the system.	
Check the availability of the information about the calibration of the measurement instruments and that the instruments are ready to measure	
Load and check the availability of enough azeotropic ethanol and entrainer, through the level indicator of the tanks T-2901 and T-2902. In the case of there is not enough material, load the missing material.	
Check that all the auxiliary services (water, steam, electricity and thermal oil) required for the operation are available for the operation.	

Check that the column is empty and clean by draining the storage tanks of the anhydrous ethanol (T-2903 y T-2904) and the storage tanks of the used solvent (T-2905 y T-2906).	
ATTENTION! Check the joints of the hoses carrying the thermal oil and ensure that there are no leaks.	
Close all the drainage: valve in the bottom of the column, valves in the bottom of the tanks and the reboiler, and valves to take samples of the column.	
Check that the correct status and the location of the extinguishers, emergency washer and check possible risks.	

## 5.10 Detailed preliminary checking

In this section, the numbered items of the check list are detailed. It is recommended don't check any of the numbered items in the list without having carefully read this section. Some observations made here are based on previous experiences in the chemical engineering department (Gil, 2006).

### 5.10.1 Preparation of the materials

- Beaker for taking samples (10 mL)
- Computer
- Marker Sharpie
- Binnacle of the run
- Notebook
- Gloves to handle hot
- Pails 10-15L
- Drum of residues
- Drum of ethanol
- Drum of ethylene glycol
- Thermal oil
- Manual pump to transfer the liquids from the drums
- Soap and sponge to wash beakers
- Extinguisher

## **5.10.2 Checking of pumps and electrical equipment (Gil, 2006)**

### **5.10.2.1 Pumps prior to the operation**

- See the operation manual of the pumps provided by the producer.
- Check the correct installation of the pumps.
- Check the lubrication of the pumps.
- Check that the seals and the packings have been installed.
- Rotate the vacuum pumps checking possible vibrations and shooting due to high speed.

### **5.10.2.2 Pumps during the operation**

- Open completely the suction valves, purge the air trapped in the pipeline and in the pump, and fill them completely with liquid.
- Check the lubrication
- Turn on the pump and set it to the required speed. Immediately, observe the discharge pressure. If it does not increase, turn off the pump and find the failure. After making the correction, fill it again with liquid and turn it on again.
- When the discharge pressure has arrived the desired value, open the discharge valve to achieve the desired flow.
- Keep watching the pump regarding the temperature, pressure, vibration, lubrication and noise. If something abnormal happens, stop the equipment, correct and start again.
- Stop and clean the filter as many times as necessary.
- Check the seals and packings
- Check the alignment and reset it.
- Don't take out the provisional filter until it is completely clean. This indicates that the suction line is clean.
- The conventional packing should be changed after the initial proof.

### 5.10.3 Checking of the pipeline loop

The pilot plant has three sections of pipeline that are called loops here. Each of them are following described.

#### 5.10.3.1 Feed pipeline loop

The feed pipeline loop starts in the filling of the feed tanks TK-4001 and TK-4002. The feed is pumped from these tanks to the feed preheaters through the pump P-4101. The correct addressing of the feed flow to the column requires the checking of the opening of the valves shown with a blue circle in the **Figure 5-18**: valves HA-102 and HA-105. The other valves should remain closed

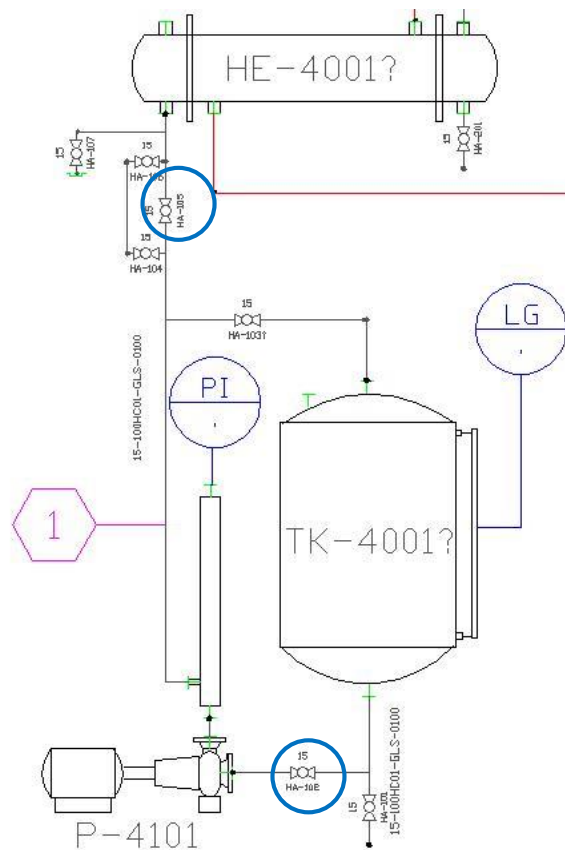


**Figure 5-18:** Feed storage pipeline loop.

### 5.10.3.2 Top pipeline loop

The top pipeline starts in the outlet at the heat of the SHE column. This vapor is condensed in the HE-4003 and is accumulated in the tank TK.4005. In the operation at total reflux, the valves shown in blue in **Figure 5-19** should be opened: valves HA-1001, HA-701 y HA-1002. At total reflux the valve HA-1003 (in red) should remain. In this way the flow continues due to the pumping from the accumulator tank TK-4005 to the reflux preheater HE-4006 through the pump P-4003. In the line 8, the rotameter is activated by holding closed the valve HA-801, while the valves HA-803 and HA-802 stayed closed.

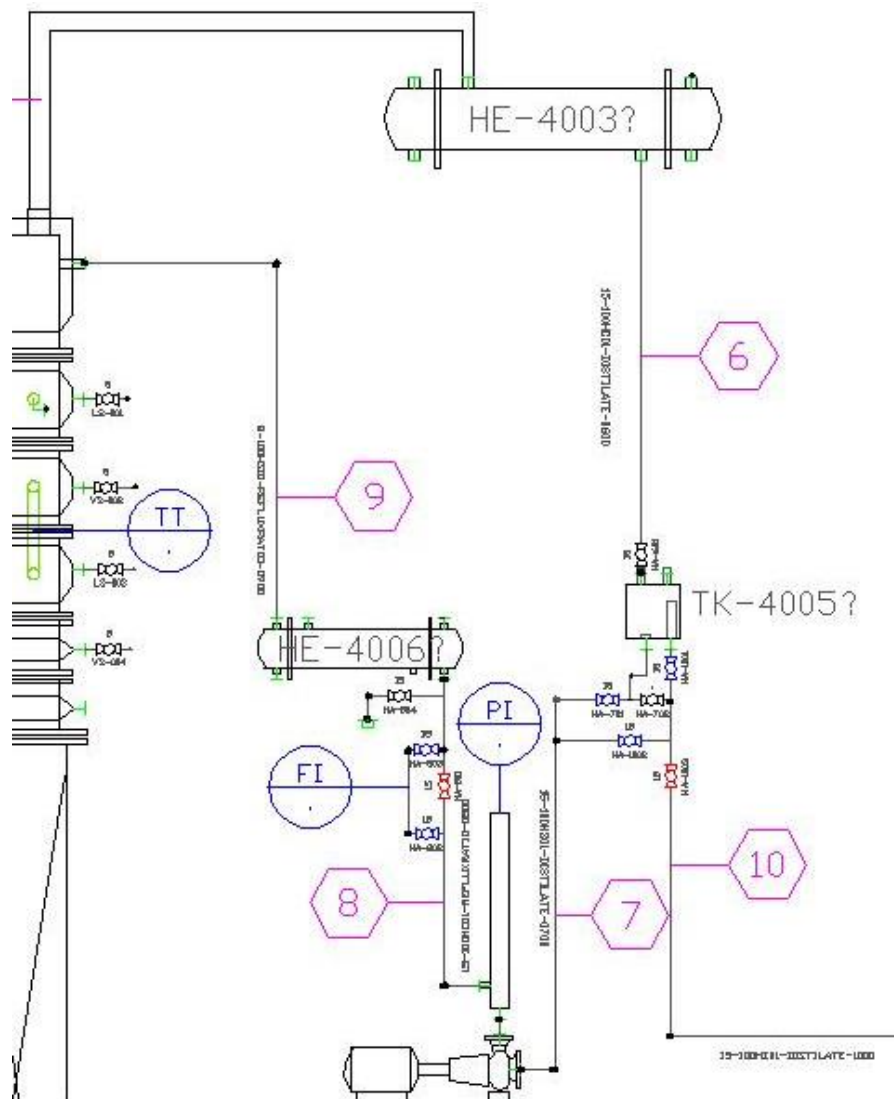


**Figure 5-19:** Top pipeline loop (red closed and blue opened).

### 5.10.3.3 Bottom pipeline loop

The bottom pipeline loop starts with the flow of liquid from the bottom of the SHE column to the reboiler RB-4001 through the opening of the valve HA-1201. Vapor from the reboiler is fed to the column through the valve HA-1301. This valve has a diameter of two inches and should be always opened while the reboiler is being heated. The loop has a security valve PSV, which is shown in **Figure 5-20**. If the reboiler has an overpressure, this valve would open to relieve the pressure, otherwise it remains closed. In the startup, the valve HA-1402 should stay closed. This valve is only opened when it is desired to obtain the product without cooling it in the equipment HE-4005.

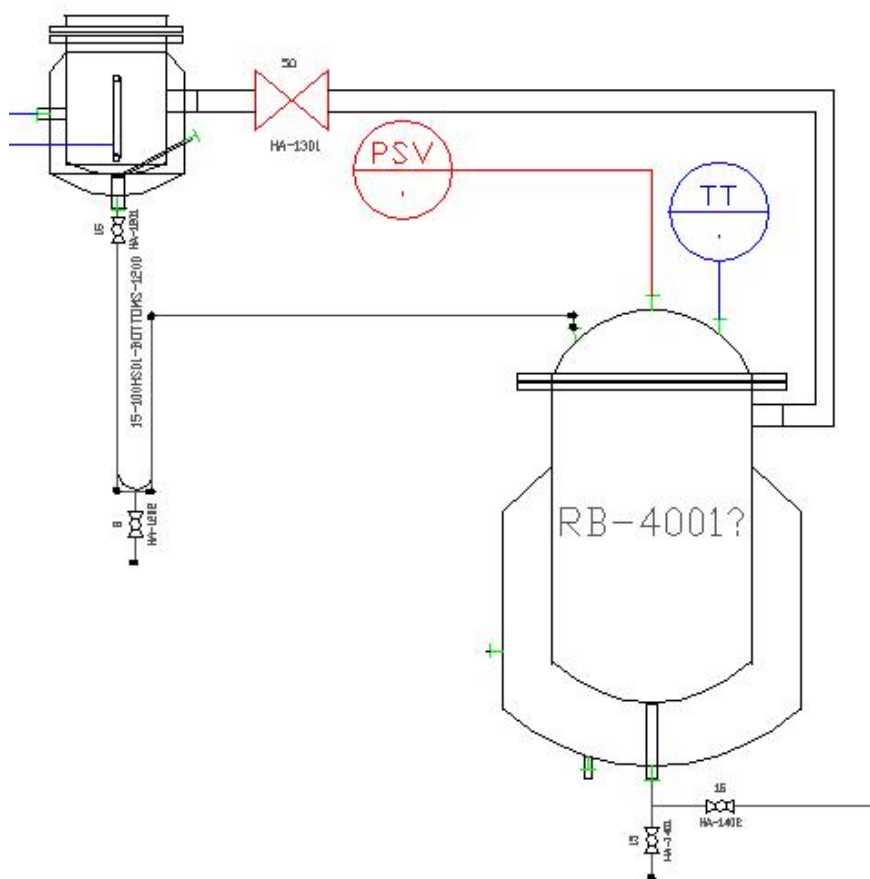


**Figure 5-20:** Bottom pipeline loop.

#### **5.10.4 Checking the measurement instruments**

- Check that the valves of the level indicator in all tanks are opened.
- Test and adjust all the security valves.
- After being installed, check all the transmission system of the thermocouples.
- Check the correct installation of the indicators of flow, pressure and temperature.
- Calibrate all the flow, pressure and temperature indicators.
- Calibrate or tare the feed tanks and product tanks to estimate the consumption and accumulation through change of level.
- Check the correct operation of the valves that give way to the rotameter and its corresponding control valves.

### **5.11 Conclusions**

The detailed sections of a constructed extractive distillation column with internal heat exchangers was presented. The pilot equipment shown can be used as an adiabatic column and as diabatic column. In the second case the transfer fluid can be a transfer oil or other fluid of high specific heat. The built equipment can be used to obtain hydraulic parameters for the improvement of diabatic column models. The column is operated in open loop.



## 6. Conclusions

There is a clear interest in the world for substituting the energy consumption obtained from fossil fuels. In this way, several policies have been agreed by the countries around the world. The policies have promoted investment in the development of alternative energy technologies. Renewable sources of energy have emerged with investments near to 300 thousand million in 2015. These technologies have advantages such as they can be produced at local level and therefore are a great opportunity for the governments to ensure their energy security. Renewables also have the advantage of generating new jobs. Only in the bioenergy source more than three millions of new jobs are estimated for year 2016.

In the transport sector biofuels are nowadays implemented in different countries as a mixture with liquid fossil fuels. Biomass for transport contributed with near to 0.8% of the total final energy consumption in the world. From this percentage, bioethanol is the mayor contributor with 74%, followed by biodiesel with 22%.

The bioethanol is used in mixture with gasoline for powering the transport of vehicles. As the local regulation for vehicle transport in each country becomes stronger, the bioethanol market increases. Main producers of bioethanol in the world are United States (~60%) and Brazil (~20%). The growth of the bioethanol market is limited by the availability of arable land. Even if 42% of the world arable land were dedicated to produce transport fuels, only 57% of the global petrol could be supply. This made necessary to improve the efficiency of energy crops. Sugar is the source of biofuel with the best yield per hectare.

Latin American countries have a combination of arable land availability and optimal climatology conditions for the growth of the energy crops. As an example, Colombia has 2.5 Mhe of area land for agriculture with climate conditions that makes the sugar crops to have the best productivity for bioethanol production. It is not clear how the bioethanol program was originated in Colombia but nowadays its installed capacity generates more

than 1.6 millions of ethanol liters per day in 40000 hectares. This production generates 7429 direct jobs and 14858 indirect jobs.

Sugarcane bioethanol is generated from the fermentation of subproducts of the sugar production. Cultures of fermentation are fractioned and then dehydrated. Several dehydration technologies have been proposed in the literature. The dehydration with molecular sieves is the less energy consuming technology followed by the extractive distillation. However, distillation based dehydration technologies have some advantages that are still appreciable by academy and industry mainly in Latin countries. In fact, there seem to be two tendencies in the world for the study of ethanol dehydration. Latin countries are leaders in the publication of documents related to extractive distillation and European countries in the study of adsorption technologies. This document thesis follows the Latin tendency.

Process design is may be the most interesting activity in the field of chemical engineering field. It is an activity that combines creativity and expertise. Because of its qualities some authors describe the conceptual designs as an uncompleted artwork. This presents a continuous challenge for chemical engineering students that can be approached by means of different alternatives as sequential engineering, reverse engineering, reengineering or concurrent engineering. For doing this is convenient to decompose the problem in different stages of design been two of most important the chemical reaction and the separation system.

The topic of this thesis is focused in the separation system or extractive distillation process. A conceptual design of this process requires of synthesis of a feasible separation sequence and an analysis respect to a defined criterion. The synthesis problem requires of 1) finding the optimum sequence of separations and the nature of each separator and 2) finding the optimal design values for each separator (sizes, operating conditions). It can be made by super structure optimization, evolutionary modification or systematic generation. As the extractive distillation was initially reported in patents, the evolutionary approach was applied here. The first synthesis problem of extractive distillation can be solved by energy integration. This integration can be of one of two types, direct or indirect. This was of great importance in the conceptual design development in this work.

Extractive distillation design deals with mixtures with azeotropes. The most general definition of azeotrope covers homogeneous azeotropes, heterogeneous azeotropes,

reactive azeotropes, minimum boiling point azeotropes, maximum boiling azeotropes among others. At least more than 9000 binary systems present azeotropes. Therefore, finding the cost effective separation sequences for this systems is a continuous interest area.

Azeotropy occurs due to molecular interaction of components in mixture. The nature of this phenomena is still studied. Thermodynamic description of the vapor and liquid phases in the composition of azeotrope are determinant for achieving a congruent design of an extractive distillation sequence. In this work, the NRTL model for the thermodynamic description of the ethanol-water system was compared with experimental data using a model that assumes ideal gas phase. The model parameters used adjusted with good prediction to the experimental data. Default thermodynamic model parameters predict with good performance the binary ethanol-water interactions but has not a good adjustment for the interactions with glycol. It is recommended to use the parameters reported by (Kamihama et al., 2012).

For the evaluation of the ternary interactions involved in the thermodynamic model, different isovolatility curve were draw. A growing tendency of the slope of the curves as they approximate to the ethanol vertices corroborates the good prediction of the ternary interactions.

Isovolatility, residue curve maps and column profile maps are important tools for the development of an extractive distillation sequence design based in conceptualization. Once this tools have been understood, the analysis of the separation by means of simulation is improved. These tools also bring information for the analysis of the nonconventional distillation technologies as extractive dividing wall columns.

A methodology for the conceptual design of extractive distillation was reported for Ethanol-Water-Ethylene Glycol mixtures. The followed methodology was supported by means of several graphical information obtained from the non-linear analysis of the mathematical model of the extractive distillation and of the thermodynamic behavior of the case of study. This analysis was replied for different pressure conditions. The results of the graphical analysis showed an observable the point of minimum solvent to feed flow ratio. They also showed minimum reflux ratio and maximum reflux ratio for the middle section of the extractive column. An interesting result obtained was the conclusion that the operative

reflux ratio is dominated by the profile of the rectifying section. The obtained parameters showed to be feasible by means of rigorous simulations in Aspen Plus.

A conceptual design of extractive dividing wall columns was proposed. A stripping section in the extractive module was observed to be important for the separation. The E-DWC design for the case of study is feasible only for low refluxes and qualities below 1 for the studied pressures. Equations of the sections of the E-DWC should be studied in more detail. Even when the equations reported for the conventional design can describe the E-DWC, the direction of the calculation of the solution of the equations makes difficult the convergence and interpretation of the results.

E-DWC as well as the internal use of SHEs showed to reduce the energy requirements for the separation. However, the use of these technologies can be limited by the availability of the internal elements that are required for their operation.

## References

- Ambrose, D., & Sprake, C. H. S. (1970). Thermodynamic properties oxygen compounds. - Vapour pressures temperatures of aliphatic of organic and normal alcohols, 631–645.
- Ambrose, D., Sprake, C. H. S., & Townsend, R. (1975). Thermodynamic properties of organic oxygen compounds Vapour pressures of methanol , and octan-1-ol from the normal boiling temperature to the critical temperature Values are given for methanol from 180 to 3300 kPa ( and these have been combined with those, 185–190.
- Ariel, C., & Alzate, C. (2009). Perspectivas de la producción de biocombustibles en Colombia : contextos latinoamericano y mundial. (Perspectives of biofuels production in Colombia : latinamerican and world Contexts, in spanish). *Revista de Ingeniería Uniandes*, 29, 109–120.
- ASOCAÑA. (2016a). *Aspectos generales del sector azucarero colombiano 2015-2016. (General aspects of the colombian sugar sector 2015-2016)*. Cali, Colombia.
- ASOCAÑA. (2016b). Proyectos de plantas productoras de etanol en Colombia. (Projects of bioethanol production plants in Colombia, in spanish). Retrieved from <http://www.fedebiocombustibles.com/nota-web-id-621.htm>
- Asprion, N., & Kaibel, G. (2010). Dividing wall columns: Fundamentals and recent advances. *Chemical Engineering and Processing: Process Intensification*, 49(2), 139–146. <https://doi.org/10.1016/j.cep.2010.01.013>
- Balat, M., Balat, H., & Öz, C. (2008). Progress in bioethanol processing. *Progress in Energy and Combustion Science*. <https://doi.org/10.1016/j.pecs.2007.11.001>
- Barnicki, S. D., Hoyme, C. A., & Sirola, J. J. (2006). Separation process synthesis. In *Kirk-Othmer Encyclopedia of Chemical Technology* (4th ed., pp. 923–962, vol. 21).
- Becker, H., Godorr, S., Ag, L., & Vaughan, J. (2001). Partitioned Distillation Columns, (January).
- Benedict, M., & Rubin, C. (1945). Extractive and Azeotropic Distillation I. Theoretical

- Aspects. *Trans IChemE*, 41, 353–370.
- Beneke, D. A., Peters, M., Glasser, D., & Hildebrandt, D. (2013). *Understanding Distillation Using Column Profile Maps*. USA: John Wiley & Sons.
- BEST. (2011). *Bioethanol for sustainable transport Results and recommendations from the European BEST project*. Stockholm.
- Biegler, I. ., Grossmann, I. E., & Westerberg, A. W. (1999). *Systematic methods of chemical process design*. United States: Prentice Hall.
- Black, C., & Ditsler, D. E. (1974). Dehydration of Aqueous Ethanol Mixtures by Extractive Distillation. *Extractive and Azeotropic Distillation*, 1–15. <https://doi.org/10.1021/ba-1972-0115.ch001>
- BP. (2016). *BP energy outlook 2016*. BP (Vol. 53). <https://doi.org/10.1017/CBO9781107415324.004>
- Caballero, J. A. (2008). Destilación con Acoplamiento Térmico. *Universidad de Alicante*, 1–16.
- Cardona, C. A., Sánchez, O. J., & Gutiérrez, L. F. (2010). *Process Synthesis for Fuel Ethanol Production* (First). United States: CRC Taylor and Francis Group.
- Carlberg, N. A., & Westerberg, A. W. (1989a). Temperature-Heat Diagrams for Complex Columns. 2. Underwood's Method for Side Strippers and Enrichers, 1379–1386.
- Carlberg, N. A., & Westerberg, A. W. (1989b). Temperature-Heat Diagrams for Complex Columns . 3 . Underwood ' s Method for the Petlyuk Configuration, (44), 1386–1397.
- Christiansen, A. C., Skogestad, S., & Lien, K. (1997). Complex distillation arrangements: Extending the petlyuk ideas. *Computers and Chemical Engineering*, 21(1), 1–6. [https://doi.org/10.1016/S0098-1354\(97\)87508-4](https://doi.org/10.1016/S0098-1354(97)87508-4)
- Clifton, J. R., Rossiter, W., & Brown, P. (1985). Degraded Aqueous Glycol Solutions: pH Values and the Effects of Common Ions on Suppressing pH Decreases. *Solar Energy Materials*, 12, 77–86.
- Company, P. P., Pahl, R. H., Ladisch, M. R., Dyck, K., Approach, N., Positive, G., ... Bascomb, P. E. (1985). United States Patent ( 19 ), (19).
- Congreso de Colombia. ley 693 de septiembre 19 del 2001. Por la cual se dictan normas sobre el uso de alcoholes carburantes, se crean estímulos para su producción, comercialización y consumo, y se dictan otras disposiciones. (By which regulations are passed on the use of fuel (2001).
- Creative Energy. (2008). *European roadmap for process intensification*.
- Dejanović, I., Matijašević, L., & Olujić, Ž. (2010). Dividing wall column—A breakthrough

- towards sustainable distilling. *Chemical Engineering and Processing: Process Intensification*, 49(6), 559–580. <https://doi.org/10.1016/j.cep.2010.04.001>
- Dejanović, I., Matijašević, L., & Olujić, Ž. (2011). An effective method for establishing the stage and reflux requirement of three-product dividing wall columns. *Chemical and Biochemical ...*, 25(2), 147–157.
- Dhillon, B. S. (1998). *Advanced Design Concepts for Engineers*. Pennsylvania, U.S.A: Technomic Publishing Company, Inc.
- Dhole, V. R., & Linnhoff, B. (1993). Distillation column targets. *Computers & Chemical Engineering*, 17(5–6), 549–560. [https://doi.org/10.1016/0098-1354\(93\)80043-M](https://doi.org/10.1016/0098-1354(93)80043-M)
- Doherty, M. F., & Knapp, J. P. (2004). Distillation, azeotropic and extractive. In *Kirk-Othmer Encyclopedia of Chemical Technology* (Vol. 8, pp. 786–852). <https://doi.org/10.1002/0471238961.0409192004150805.a01>
- Doherty, & Calderola. (1985). Design and Synthesis of Homogeneous Azeotropic Distillations . 3 . The Sequencing of Columns for Azeotropic and Extractive Distillations. *Industrial & Engineering Chemistry Fundamental*, 474–485.
- Doherty, & Malone. (2001). *Conceptual Design of Distillation Systems* (1st ed.). New York, US: McGraw-Hill.
- Doherty, & Perkins. (1978). On the dynamics of distillation processes—I. *Chemical Engineering Science*, 33(3), 281–301.
- Douglas, J. M. (1988). *Conceptual design of chemical processes*. United States: McGraw-Hill Chemical Engineering Series.
- Dyk, B. Van, & Nieuwoudt, I. (2000). Design of Solvents for Extractive Distillation, 1423–1429.
- EIA. (2016a). *International Energy Outlook 2016, IEO2016* (Vol. 484). Washington, DC: U.S. Energy Information Administration.
- EIA. (2016b). *International Energy Statistics*, U.S. Energy Information Administration. Retrieved July 6, 2017, from <http://www.eia.gov/cfapps/ipdbproject/iedindex3.cfm?tid=5&pid=62&aid=2&cid=regions&syid=2000&eyid=2013&unit=TBPD>
- FAO. (2008). *The state of food and agriculture 2008: Biofuels prospects, risks and opportunities*. Rome, Italy: Food and Agriculture Organization of the United Nations FAO.
- Fedebiocombustibles. (2016). Ethanol. Retrieved October 28, 2016, from <http://www.fedebiocombustibles.com/v3/main-pagina-id-4-titulo->

proceso\_de\_los\_biocombustibles.htm

- Foucher, E. R., Doherty, M. F., & Malone, M. F. (1991). Automatic Screening of Entrainers for Homogeneous Azeotropic Distillation. *Industrial and Engineering Chemistry Research*, 30(4), 760–772. <https://doi.org/10.1021/ie00052a021>
- Frolkova, A. K., & Raeva, V. M. (2010). Bioethanol Dehydration : State of the Art, 44(4), 545–556. <https://doi.org/10.1134/S0040579510040342>
- García, F., & Camacho, E. (2016). Tendencias recientes de la oferta y demanda de energía en Colombia. (Recent trends in energy supply and demand in Colombia, in spanish). *BBVA Research. Observatorio Economico de Colombia*.
- Gerbaud, V., & Rodriguez, I. (2014). Extractive Distillation. In *Distillation. Equipment and Processes* (pp. 201–245). New York, US: Elsevier.
- Gil. (2006). *Diseño, montaje y puesta en marcha de un sistema de destilación extractiva a nivel piloto para la producción de alcohol anhidro. (Design, assembly and start-up of a pilot-level extractive distillation system for the production of anhydrous alcohol, in spa*. Universidad Nacional de Colombia, sede Bogotá, Bogotá.
- Gil, I. D., García, L. C., & Rodríguez, G. (2014). Simulation of ethanol extractive distillation with mixed glycols as separating agent. *Brazilian Journal of Chemical Engineering*, 31(1), 259–270. <https://doi.org/10.1590/S0104-66322014000100024>
- Gil, Aguilar, & Caicedo. (2006). Producción de Alcohol Carburante por destilación azeotrópica homogénea con glicerina. *Ingeniería E Investigación*, vol 26(0120–5609), p.44-50.
- Gmehling, J., Kolbe, B., Kleiber, M., & Rarey, J. (2012). *Chemical Thermodynamics for Process Simulation*. Weinheim Germany: Wiley-VCH Verlag & Co.
- Guerrero, F. R. (2014). *Desarrollo y aplicación de un modelo computacional del arranque y operación de un proceso de adsorción por cambios oscilatorios de presión para la deshidratación de etanol azeotrópico*. Universidad Nacional de Colombia sede Bogotá.
- Halvorsen, I. J., & Skogestad, S. (2003). Minimum Energy Consumption in Multicomponent Distillation. 1. Vmin Diagram for a Two-Product Column. *Industrial & Engineering Chemistry Research*, 42, 596–604. <https://doi.org/10.1021/ie010863g>
- Hilmen, E.-K. (2000). Separation of Azeotropic Mixtures: Tools for Analysis and Studies on Batch Distillation Operation, (November), 1–298.
- Himmelblau, D., & Bischoff, K. (1968). *Process analysis and simulation*. New York, US: Wiley.



- IDEAM. (2013). *Estudio de la caracterización climática de Bogotá y la cuenca alta del río Tunjuelo*. Bogotá.
- IDEAM. (2015). *Tercer Comunicación Nacional de Cambio Climático de Colombia. Inventario Nacional de Gases de Efecto Invernadero (GEI) de Colombia. (Third National Communication on Climate Change in Colombia, in spanish)*. Bogotá, Colombia: Instituto de Hidrología Meteorología y Estudios Ambientales IDEAM.
- IEA. (2004). *Biofuels for transport: an international perspective*. Paris, France: International Energy Agency, IEA. <https://doi.org/10.1787/9789264015135-en>
- IEA. (2015). *World energy outlook factsheet: global energy trends to 2040*. Paris, France.
- IEEJ. (2015). *Asia/ World energy outlook 2015: Analyses of oil pricing and climate change measures under new circumstances*. Japan: The Institute of Energy Economics of Japan, IEEJ.
- IICA. (2007). *Atlas de la agroenergía y los biocombustibles en las Américas: Etanol. (Atlas of agroenergy and biofuels in the Americas: Ethanol, in spanish)*. San José, Costa Rica: Instituto Interamericano de Cooperación para la Agricultura, IICA.
- IPCC. (2015). *Climate change 2014: Synthesis report. A report of the Intergovernmental Panel on Climate Change*. Intergovernmental Panel on Climate Change, IPCC.
- IRENA. (2016). *The renewable route to sustainable transport: A working paper based on REMap*. Abu Dhabi: International Renewable Energy Agency, IRENA.
- Julka, V., & Doherty, M. F. (1990). Geometric behavior and minimum flows for nonideal multicomponent distillation, *45*(7), 1801–1822.
- Kaibel. (1987). Distillation Columns With Vertical Partitions. *Chem. Eng. Technol*, *10*, 92–98.
- Kaiser, V., & Gourelia, J. (1985). The ideal-column concept: Applying exergy to distillation, 45–53.
- Kamihama, N., Matsuda, H., Kurihara, K., Tochigi, K., & Oba, S. (2012). Isobaric Vapor–Liquid Equilibria for Ethanol + Water + Ethylene Glycol and Its Constituent Three Binary Systems. *Journal of Chemical & Engineering Data*, *57*(2), 339–344. <https://doi.org/10.1021/je2008704>
- Kemp, I. C. (2007). *Pinch Analysis and Process Integration. A user guide on process integration for efficient use of energy (Second)*. Burlington, MA, USA: Elsevier Ltd.
- King, J. (1979). *Procesos de separación*. España: Reverté.
- Kiss, A. (2013). *Advanced Distillation Technologies*. United Kingdom: John Wiley & Sons. <https://doi.org/10.1002/9781118543702>

- Kiss, A. a., Flores Landaeta, S. J., & Infante Ferreira, C. a. (2012). Towards energy efficient distillation technologies – Making the right choice. *Energy*, 47(1), 531–542. <https://doi.org/10.1016/j.energy.2012.09.038>
- Kiss, A. a., & Ignat, R. M. (2012). Innovative single step bioethanol dehydration in an extractive dividing-wall column. *Separation and Purification Technology*, 98, 290–297. <https://doi.org/10.1016/j.seppur.2012.06.029>
- Kiss, A. a., & Suszwalak, D. J.-. P. C. (2012). Enhanced bioethanol dehydration by extractive and azeotropic distillation in dividing-wall columns. *Separation and Purification Technology*, 86, 70–78. <https://doi.org/10.1016/j.seppur.2011.10.022>
- Kiss, & Ignat, R. M. (2013). Optimal Economic Design of an Extractive Distillation Process for Bioethanol Dehydration. *Energy Technology*, 1(2–3), 166–170. <https://doi.org/10.1002/ente.201200053>
- Knapp, J. P., & Doherty, M. F. (1994). Minimum Entrainer Flows for Extractive Distillation : a Bifurcation Theoretic Approach, 40(2).
- Knight. (1987). *Synthesis and Design of Homogeneous Azeotropic Distillation Sequences*. Massachusetts: University of Massachusetts.
- Knight, & Doherty, M. F. (1989). Optimal Design and Synthesis of Homogeneous Azeotropic Distillation Sequences. *Industrial & Engineering Chemistry Research*, 28, 564–572.
- Kretschmer, & Wiebe. (1949). Liquid-Vapor Equilibrium of Ethanol--Toluene. *Journal of American Chemical Society*, 71(5), 1793–1797.
- Lee, F., & Pahl, R. H. (1985). Solvent screening study and conceptual extractive distillation process to produce anhydrous ethanol from fermentation broth. *Industrial and Engineering Process Design and Development*, 24, 168–172.
- Li, J., Lei, Z., Ding, Z., Li, C., & Chen, B. (2005). Azeotropic Distillation: A Review of Mathematical Models. *Separation & Purification Reviews*, 34(1), 87–129. <https://doi.org/10.1081/SPM-200054984>
- Li, & Kraslawski, A. (2004). Conceptual process synthesis: Past and current trends. *Chemical Engineering and Processing: Process Intensification*, 43(5), 589–600. <https://doi.org/10.1016/j.cep.2003.05.002>
- López, F. J., & Contreras, O. A. (2003). *ELABORACIÓN DE LOS DOCUMENTOS TÉCNICOS DEL LABORATORIO DE INGENIERÍA QUÍMICA Y REPLANTEAMIENTO*. Unieversidad Nacional de Colombia.
- Macedo, I. C. (2007). Situação atual e perspectivas do etanol (Ethanol: current situation

- and outlook, in portuguese). *ESTUDOS AVANÇADOS*, 21(59), 157–165.
- MADS. (2016). Cambio Climatico. Retrieved from <http://www.minambiente.gov.co/index.php/cambio-climatico>
- Matsuyama, H., & Nishimura, H. (1977). Topological and themodynamic classification of ternary vapor-liquid equilibria. *J. Chem. Eng. Japan*, 10(3), 181–187. <https://doi.org/10.1252/jcej.10.181>
- Meirelles, A., Weiss, S., & Herfurth, H. (1991). Ethanol dehydration by extractive distillation. *Journal of Chemical Technology & Biotechnology*, 53(2), 181–188. <https://doi.org/10.1002/jctb.280530213>
- Mejia, S., Espinal, J., & Mondragón, F. (2006). Estudio del azeotropo etanol-agua. Caracterizaciónmolecular de dímeros de etanol, heterodímeros y heterotrímeros de etanol-agua. *Energética*, 36.
- Mejía, S. L. (2010). *La política de agrocombustibles y sus conflictos socioecológicos distributivos en Colombia (Agrofuel policy and its distributive socio-ecological conflicts in Colombia, in spanish)*. Universidad Nacional de Colombia sede Bogotá.
- Mendoza, D. (2011). *Análisis y minimización de la entropía generada en un proceso de destilación extractiva para la deshidratación de etanol*. Universidad Nacional de Colombia.
- MINIMINAS. (2009a). *Decreto 1135 del 2009*. Bogotá, Colombia: Ministerio de Minas y Energia.
- MINIMINAS. (2009b). *Politica de Biocombustibles - Minminas*. Bogotá, Colombia: Ministerio de Minas y Energia, MINIMINAS.
- MINTRANSPORTE. (2014). *Plan de Acción Sectorial de Mitigación (PAS). Sector Transporte*. Bogotá, Colombia: Ministerio de Transporte, Republica de Colombia.
- MINTRANSPORTE. (2015). *Transporte en cifras. Estadísticas 2015*. Bogotá, Colombia: Ministerio de Transporte, Republica de Colombia.
- Monro. (1938). U.S. 2,134,882.
- Nishida, N., Stephanopoulos, G., & Westerberg, A. W. (1981). A review of process synthesis. *AIChE Journal*, 27(3), 321–351. <https://doi.org/10.1002/aic.690270302>
- Oelz, S., Sims, R., & Kirchner, N. (2007). *Contribution of Renewables to Energy Security. Technology*. France: International Energy Agency, IEA.
- OICA. (2016). World Vehicles in Use - all vehicles. Retrieved November 1, 2016, from <http://www.oica.net/wp-content/uploads//total-inuse-2014.pdf>
- Olujić, Ž., Jödecke, M., Shilkin, a., Schuch, G., & Kaibel, B. (2009). Equipment

- improvement trends in distillation. *Chemical Engineering and Processing: Process Intensification*, 48(6), 1089–1104. <https://doi.org/10.1016/j.cep.2009.03.004>
- Petlyuk, F. B. (2004). *Distillation Theory and Its Application to Optimal Design of Separation Units*. USA: Cambridge University Press.
- Pla-Franco, J., Lladosa, E., Loras, S., & Montón, J. B. (2013). Phase equilibria for the ternary systems ethanol, water+ethylene glycol or + glycerol at 101.3kPa. *Fluid Phase Equilibria*, 341, 54–60. <https://doi.org/10.1016/j.fluid.2012.12.022>
- Prausnitz, J. M., & Anderson, R. (1961). Solvent Selectivity in Extractive Distillation of Hydrocarbons. *AIChE J.*, 7(1), 96–101.
- Rasmussen, S. C. (2012). *How glass changed the world. The history and chemistry of glass forms antiquity to the 13th century*. Heidelberg, New York. USA: SpringerBriefs in Molecular Science: History of Chemistry; Springer.
- REN21. (2013). *Renewables global futures report*. France: Renewable Energy Policy Network for the 21st Century, REN21.
- REN21. (2016). *Renewables 2016: global status report*. France: Renewable Energy Policy Network for the 21st Century, REN21.
- Renon, H., & Pruasnitz, J. M. (1968). Local compositions in thermodynamics excess functions for liquids mixtures. *AIChE J.*, 14(1), 116–128.
- RFA. (2016). *2016 Ethanol Industry Outlook*. Washington, DC: Renewable fuels Association, RFA.
- Rothman, H. (1983). *Energy From Alcohol: The Brazilian Experience*.
- Sánchez, C. A. (2011). Cálculo e interpretación de las trayectorias de puntos de composición constante (pinch) en columnas simples de destilación para mezclas azeotrópicas homogéneas. *EIA*, 77–92.
- Sanchez, C. A., Estupiñan, L., & Salazar, M. A. (2010). Herramientas para la caracterización termodinámica de sistemas ternarios en destilación. *Escuela de Ingeniería de Antioquia*, 13, 77–91.
- Sander, U., & Soukup, P. (1988). Design and operation of a pervaporation plant for ethanol dehydration, 36, 463–475.
- Schneible. (1922). *Absolute Alcohol*. U.S.
- Seader, J. D., Ernest, J., & Henley. (2006). *Separation process principles* (2nd ed.). United States: John Wiley & Sons.
- Seader, J. D., Hendley, E. J., & Roper, D. K. (2011). *Separation process principles: chemical and biochemical operations*. John Wiley & Sons.

- Smith, R. (2005). *Chemical Process Design and Integration* (Fisrt). England: John Wiley & Sons.
- Song, W., Huss, R. S., Doherty, M. F., & Malone, M. F. (1997). Discovery of a reactive azeotrope. *Nature*, *388*(6642), 561–563. <https://doi.org/10.1038/41515>
- Terranova, B. E., & Westerberg, A. W. (1989). Temperature-Heat Diagrams for Complex Columns . 1 . Intercooled / Interheated Distillation Columns, *V*(1985), 1374–1379.
- Thompson, R. W., & King, C. J. (1972). Systematic synthesis of separation schemes. *AIChE Journal*, *18*(5), 941–948. <https://doi.org/10.1002/aic.690180510>
- Triantafyllou, C., & Smith, R. (1992). THE DESIGN AND OPTIMISATION OF FULLY THERMALLY COUPLED DISTILLATION COLUMNS. *Trans IChEmE*, *70*(Part A), 118–132.
- U.S. Census Bureau. (2016). U.S. Census Bureau. Retrieved July 14, 2017, from [http://www.census.gov/population/international/data/worldpop/table\\_population.php](http://www.census.gov/population/international/data/worldpop/table_population.php)
- UPME. (2015a). Plan Energetico Nacional Colombia: Ideario Energético 2050. *Unidad de Planeación Minero Energética, Republica de Colombia*, 184.
- UPME. (2015b). *Proyección de demanda de combustibles en el sector transporte en Colombia: revisión Marzo de 2015. (Projection of demand for fuels in the transportation sector in Colombia: review March 2015, in spanish)*. Bogotá, Colombia: Unidad de Planeación Minero Energetica, UPME. Subdirección de demanda.
- UPME. (2016). Balance Energético Colombiano 1975 - 2015. Retrieved from <http://www1.upme.gov.co/balance-energetico-colombiano-1975-2015>
- Van Gerven, T., & Stankiewicz, A. (2009). Structure, Energy, Synergy, Time - The Fundamentals of Process Intensification. *Industrial & Engineering Chemistry Research*, *48*(5), 2465–2474. <https://doi.org/10.1021/ie801501y>
- Wade, J., & Merriman, R. (1911). nfluence of water on the boiling point of ethyl alcohol at pressures above and below the atmospheric pressure. *Journal of the Chemical Society, Transactions*, *99*, 997–1011.
- Washall, T. A. (1969). Separation of water from a single alkanol by extractive distillation with ethylene glycol. U.S.
- WEC. (2011a). *Global Transport Scenarios 2050*. London, UK: World Energy Council, WEC. <https://doi.org/10.1016/j.enpol.2011.05.049>
- WEC. (2011b). *Policies for the future: 2011 Assessment of country energy and climate policy*. London, UK: World Energy Council, WEC.

- WEC. (2016). *World energy trilemma 2016: Defining measures to accelerate the energy transition*. London, UK: World Energy Council, WEC in partnership with Oliver Wyman.
- Westerberg, A. W. (1981). Design research : both theory and strategy.
- Westerberg, A. W., & Wahnschafft, O. (1996). Synthesis of Distillation-based Separation Systems. *Advances in Chemical Engineering*, 23, 63–170.
- Wheeler, K. (2002). Technical Insights into Uninhibited Ethylene Glycol. *Process Cooling & Equipment. Heat Transfer Fluids*.
- Wright. (1949). U.S. Patent 2,471,134.
- Yildirim, Ö., Kiss, A. a., & Kenig, E. Y. (2011). Dividing wall columns in chemical process industry: A review on current activities. *Separation and Purification Technology*, 80(3), 403–417. <https://doi.org/10.1016/j.seppur.2011.05.009>

**Appendix A. Manual of operation of a  
distillation column with internal  
Sequential Heat Exchanger (SEH)**